The Analyst

A monthly international journal dealing with all branches of analytical chemistry

ROYAL SOCIETY OF CHEMISTRY

The Analyst

The Analytical Journal of The Royal Society of Chemistry

Information for Authors

Full details of how to submit material for publication in *The Analyst* are given in the Instructions to Authors in the January issue. Separate copies are available on request.

The Analyst publishes papers on all aspects of the theory and practice of analytical chemistry, fundamental and applied, inorganic and organic, including chemical, physical and biological methods. There is no page charge.

The following types of papers will be considered:

Full papers, describing original work.

Short papers, also describing original work, but shorter and of limited breadth of subject matter; there will be no difference in the quality of the work described in full and short papers.

Communications, which must be on an urgent matter and be of obvious scientific importance. Rapidity of publication is enhanced if diagrams are omitted, but tables and formulae can be included. Communications should not be simple claims for priority: this facility for rapid publication is intended for brief descriptions of work that has progressed to a stage at which it is likely to be valuable to workers faced with similar problems. A fuller paper may be offered subsequently, if justified by later work.

Reviews, which must be a critical evaluation of the existing state of knowledge on a particular facet of analytical chemistry.

Every paper (except Communications) will be submitted to at least two referees, by whose advice the Editorial Board of *The Analyst* will be guided as to its acceptance or rejection. Papers that are accepted must not be published elsewhere except by permission. Submission of a manuscript will be regarded as an undertaking that the same material is not being considered for publication by another journal.

Regional Advisory Editors. For the benefit of potential contributors outside the United Kingdom, a Panel of Regional Advisory Editors exists. Requests for help or advice on any matter related to the preparation of papers and their submission for publication in *The Analyst* can be sent to the nearest member of the Panel. Currently serving Regional Advisory Editors are listed in each issue of *The Analyst*.

Manuscripts (three copies typed in double spacing) should be addressed to:
The Editor, The Analyst,
Royal Society of Chemistry,
Burlington House,
Piccadilly,
LONDON W1V 0BN, UK

Particular attention should be paid to the use of standard methods of literature citation, including the journal abbreviations defined in Chemical Abstracts Service Source Index. Wherever possible, the nomenclature employed should follow IUPAC recommendations, and units and symbols should be those associated with SI.

All queries relating to the presentation and submission of papers, and any correspondence regarding accepted papers and proofs, should be directed to the Editor, *The Analyst* (address as above). Members of the Analytical Editorial Board (who may be contacted directly or via the Editorial Office) would welcome comments, suggestions and advice on general policy matters concerning *The Analyst*.

Fifty reprints of each published contribution are supplied free of charge, and further copies can be purchased.

JOURNAL OF ANALYTICAL ATOMIC SPECTROMETRY (JAAS)

An International Journal on the Development and Application of Spectrometric Techniques

Enhanced Sensitivity for the Determination of Endogenous Phylloquinone (Vitamin K₁) in Plasma Using High-performance Liquid Chromatography with Dual-electrode Electrochemical Detection

John P. Hart
Division of Cellular Biology, Kennedy Institute of Rheumatology, Bute Gardens, London W6 7DW, UK

and Martin J. Shearer and Patrick T. McCarthy
Department of Haematology, Guy's Hospital, London SE1 9RT, UK

High-performance liquid chromatography (HPLC) with dual-electrode electrochemical detection has been used, in the redox mode, to determine normal and sub-normal circulating plasma levels of phylloquinone (vitamin K_1) and concentrations down to 20 pg ml^{-1} have been measured in plasma. The coefficient of variation, for endogenous levels, was 10% (mean 330 pg ml^{-1}; $n = 6$). When compared with a single glassy carbon electrode, operated in the reductive mode, the sensitivity of the dual-electrode cell was greater by at least an order of magnitude. Thus the volume of plasma required for the assay could be reduced.

Keywords: *Phylloquinone (vitamin K_1) determination; dual-electrode electrochemical detection; high-performance liquid chromatography*

Recently, we have described an assay for the determination of normal circulating phylloquinone (vitamin K_1) levels in plasma using high-performance liquid chromatography (HPLC) with electrochemical detection (LCEC).[1] The detector consisted of a thin-layer cell containing a glassy carbon working electrode and was operated in the reductive mode. This method was about three times more sensitive than that developed by Shearer *et al.*[2] who employed HPLC with ultraviolet detection.

Our current studies required a method with even greater sensitivity, as we needed both to reduce the volume of plasma required for the assay and to determine sub-normal levels of vitamin K_1.

A relatively recent approach to improving the sensitivity, and selectivity, of LCEC is to use dual-electrode cells,[3] where the electrodes are arranged either in series,[4,5] or in parallel.[6,7] In the series configuration it has been shown that a product, formed by reduction at the first electrode, can be detected downstream at a second electrode by re-oxidation at a much lower working potential than by using reduction alone. In addition, there is no interference from oxygen at the detector electrode because the reduction reaction for this molecule is not reversible at the potentials applied.

Haroon and Hauschka[8] have shown that series dual-electrode LCEC may be used for the determination of phylloquinone and menaquinones (vitamins K_2) in biological materials. However, their studies were only preliminary and they did not extend their investigations to the determination of sub-normal plasma levels.

We have also investigated this technique, but we used our original apparatus and mobile phase, simply substituting the dual-electrode cell for the thin-layer cell. The purpose of this paper is to describe the optimisation of the conditions for the determination of vitamin K_1, by redox-mode LCEC, using a cell containing two porous graphite electrodes in series. The application of this technique to the determination of both normal and depressed circulating plasma levels of this vitamin is also described. The sensitivity achieved with the dual-electrode cell is compared with that of the thin-layer cell of our earlier method.[1]

Experimental

Chemicals and Reagents

All chemicals were of analytical-reagent grade, unless otherwise stated. Phylloquinone (an isomer mixture containing 70% *trans* and 30% *cis*) was obtained from Sigma Chemical Company. Solvents used for HPLC were of HPLC grade and obtained from Rathburn Chemicals.

The procedures used for the preparation of 95% methanol - 0.05 M acetate buffer (pH 3.0), which was used as the mobile phase and for preparing standard phylloquinone solutions, together with the deaeration procedure, have been described previously.[1]

Apparatus

LCEC was performed with a constant-flow reciprocating pump (Model 300 from Applied Chromatography Systems). In the reductive mode LCEC was performed with a Bioanalytical Systems electrochemical detection system; in the redox mode a Model 5100A Coulochem detector equipped with a dual-electrode cell (Model 5011) containing two porous graphite electrodes in series (Environmental Science Associates) was used.

Optimisation of the Conditions for LCEC

To optimise the applied potentials for LCEC, hydrodynamic voltammetry was performed by injecting fixed volumes of a standard vitamin K_1 solution and varying the applied potential in 50-mV steps. For detection in the redox mode two voltammograms were constructed: the first was obtained by keeping the potential of the downstream electrode constant at +0.2 V and varying the potential of the upstream electrode between −0.5 and −1.5 V; the second was obtained by keeping the upstream electrode constant at −1.3 V and varying the potential of the downstream electrode between −0.3 and +0.5 V.

Method for the determination of vitamin K₁ in plasma by redox-mode LCEC

Generally, about 3 ml of plasma were extracted for the assay of vitamin K_1 in the normal subjects and about 5 ml for the osteoporotic patients with a fractured neck of femur. These plasma samples were extracted with hexane and further purified by semi-preparative HPLC as described previously.[1,2] The residues from the second purification step, involving normal-phase HPLC, were dissolved in 70 µl of mobile phase with the aid of a vortex mixer; usually, 30 µl of these solutions were injected into a Spherisorb (5 µM) octyl column (25 cm × 5 mm i.d.). The flow-rate was 1 ml min^{-1} and the applied
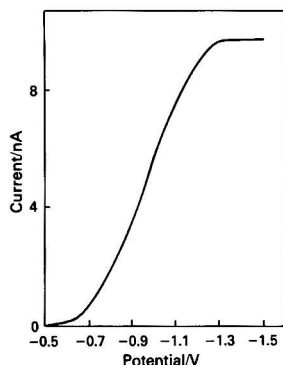
Fig. 1. Cathodic hydrodynamic voltammogram for 1-ng injections of phylloquinone. Downstream electrode held constant at $+0.2$ V
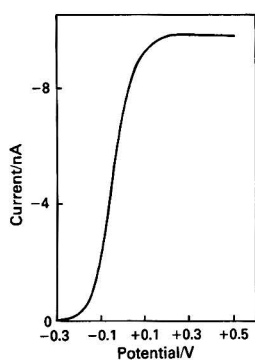
Fig. 2. Anodic hydrodynamic voltammogram for 1-ng injections of phylloquinone. Upstream electrode held constant at -1.3 V

potentials were -1.3 V at the upstream electrode and 0 V at the downstream electrode.

Calibration, effect of dissolved oxygen and precision in redox-mode LCEC

Calibration graphs were constructed by injecting between 50 pg and 1 ng of vitamin K_1 dissolved in the mobile phase. Peak heights were measured from the chromatograms and graphs of peak height *versus* amount injected were constructed. This procedure was performed both without deaeration and with deaeration by the method previously described.[1]

To determine the precision of the assay six 3-ml aliquots of plasma were taken from the same normal subject (female, aged 53 years); these were extracted and measured by the method described above.

Results and Discussion

Optimisation of Redox-mode LCEC Conditions

The principle of operation of the series dual-electrode cell, for redox-mode detection of vitamin K_1, is as follows: the first electrode (upstream electrode) is held at a potential where the quinone form of the vitamin is reduced to the hydroquinone form; this is then detected at the second electrode (downstream electrode) where the hydroquinone is reoxidised to the quinone.[8]

In order to determine the optimum potentials to apply to the two electrodes, two hydrodynamic voltammograms were constructed (Figs. 1 and 2).

It is apparent from these voltammograms that the maximum current occurred at a potential of -1.3 V at the upstream electrode and $+0.2$ V at the downstream electrode. However, when these conditions were used for the analysis of some plasma samples an interfering pre-peak overlapped with the vitamin K_1 peak. This interference could be reduced significantly by simply decreasing the applied potential of the downstream electrode below $+0.2$ V. The results shown in Table 1 were with an applied potential of 0 V, although in more recent studies potentials of 0 to $+0.1$ V have been found suitable (results not given).

When the redox-mode LCEC system was being used on a routine basis it was found beneficial to leave the mobile phase recycling overnight with the detector set at the operating potentials. This procedure eliminated the time required to stabilise when first activating the electrochemical detector and also reduced the risk of losing sensitivity.

Occasionally, the sensitivity decreased to an unacceptable level; this may have been due to adsorption of the hydroquinone form of vitamin K_1 and/or co-extracted plasma compounds, on to the surface of the electrodes. However, the sensitivity could often be restored by recycling the mobile phase overnight with the downstream and upstream electrodes set at -0.5 and $+1.3$ V, respectively. If this procedure was unsuccessful, the cell was detached from the HPLC system and treated by one, or both, of the following procedures: in the first the cell was flushed sequentially by means of a syringe, with water, 6 M nitric acid, water and finally methanol; in the second, the cell was flushed sequentially with water, tetrahydrofuran, 2 M sodium hydroxide solution, water and finally methanol.

Calibration, Effect of Dissolved Oxygen and Precision in Redox-mode LCEC

The calibration graph of peak height *versus* mass of vitamin K_1 injected was linear in the range 50 pg–1 ng; there was no change in the slope of the graph when the mobile phase was deaerated. Therefore, all subsequent investigations were carried out without deaerating the mobile phase.

The coefficient of variation for six plasma samples, taken from the same normal subject, was 10% and the mean value was 330 pg ml^{-1}; this was not included in the results given in Table 1.

Comparison of the Sensitivities of a Single Glassy Carbon Electrode Cell (TL5) and a Dual Porous Graphite Electrode Cell

When compared with a single glassy carbon electrode cell, operated in the reductive mode, the peak height obtained with a dual-electrode cell was greater by at least an order of magnitude (Fig. 3). This is perhaps not surprising as the surface areas of the porous graphite electrodes are both greater than that of the glassy carbon electrode; therefore, higher concentrations of vitamin K_1 would be expected to be electrolysed.

It should be mentioned that the detection system, incorporating the TL5 cell, provides current ranges below that used in our investigations, *i.e.*, 5 nA; however, these ranges could not be used for the assay, to amplify further the vitamin K_1 signal, because the base line was found to drift too rapidly; there was also interference from oxygen that was present in the injected sample.

Determination of Normal and Sub-normal Circulating Vitamin K_1 Levels by Redox-mode LCEC

Fig. 4 shows the chromatograms obtained with the dual-electrode cell for a normal subject and an osteoporotic patient with a fractured neck of femur. In both cases well defined

Table 1. Endogenous plasma levels of phylloquinone in normal subjects and osteoporotic patients with a fractured neck of femur

	Normal subjects				Osteoporotic subjects		
Subject's initials	Age	Sex	Phylloquinone plasma concentration/ pg ml^{-1}	Subject's initials	Age	Sex	Phylloquinone plasma concentration/ pg ml^{-1}
P.F.	51	F	950	L.W.	69	F	70
A.S.	57	F	460	M.M.	81	F	30
J.C.	59	M	430	D.M.	64	F	70
M.C.	64	F	130	I.B.	75	F	140
B.C.	64	F	80	B.J.	83	F	110
A.G.	53	F	90	W.B.	75	F	110
F.M.	69	M	330	L.T.	88	F	70
B.S.	54	F	120	B.C.	63	F	20
H.K.	69	M	240	S.W.	80	M	80
F.R.	69	M	580	J.F.	81	F	60
L.M.	65	F	430	E.C.	81	F	80
B.P.	62	F	530	E.L.	72	F	250
B.D.	62	F	210	E.H.	80	F	40
J.O.	72	M	520	M.T.	74	F	40
J.M.	81	F	540	E.H.	79	F	80
				E.W.	86	F	310
Mean			376	Mean			98
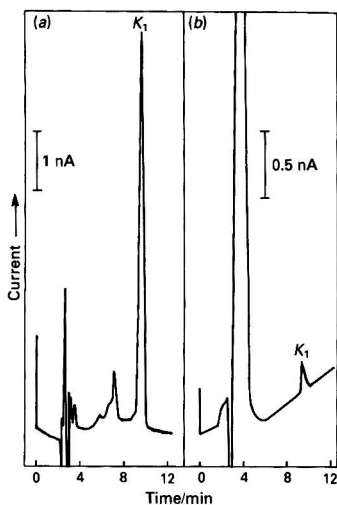
Fig. 3. Chromatograms obtained for 1-ng injections of phylloquinone using LCEC in: (a) redox mode; and (b) reductive mode

Fig. 4. Chromatograms of plasma samples obtained by LCEC in the redox mode for: (a) a normal subject (endogenous concentration of 240 ng ml^{-1} in plasma); and (b) a patient with osteoporosis and fractured neck of femur (endogenous concentration of 60 pg ml^{-1} in plasma)

peaks were obtained; the injected volumes were equivalent to only 1.3 and 1.8 ml of plasma, respectively.

The limit of detection of this method is obviously a function of both plasma volume and vitamin K_1 concentration. Under the conditions described earlier, for this particular study, down to 50 pg of vitamin K_1 could be measured; therefore, an injected sample containing the vitamin K_1 from 2.5 ml of plasma was required to measure 20 pg ml^{-1}.

The results obtained for circulating vitamin K_1 levels in the osteoporotic patients, and the age matched normals, are summarised in Table 1; these results and their possible clinical significance have been discussed elsewhere.[9,10] We are also investigating vitamin K_1 levels in other disorders of bone and envisage that this work will be reported at a later date. However, it is clear that the technique described in this paper can be applied to other nutritional aspects of vitamin K_1, particularly where low plasma levels may occur.

References

1. Hart, J. P., Shearer, M. J., McCarthy, P. T., and Rahim, S., *Analyst*, 1984, **109**, 477.
2. Shearer, M. J., Barkhan, P., Rahim, S., and Stimmler, L., *Lancet*, 1982, **ii**, 460.
3. Johnson, D. C., Ryan, M. D., and Wilson, G. S., *Anal. Chem.*, 1984, **56**, 7R.

4. MacCrehan, W. A., and Durst, R. A., *Anal. Chem.*, 1981, **53**, 1700.
5. Roston, D. A., and Kissinger, P. T., *Anal. Chem.*, 1982, **54**, 429.
6. Lunte, C. E., and Kissinger, P. T., *Anal. Chem.*, 1983, **55**, 1458.
7. Yamamoto, T., Shimizu, H., Kato, T., and Nagatsu, T., *Anal. Biochem.*, 1984, **142**, 395.
8. Haroon, Y., and Hauschka, P. V., *J. Chromatogr. Sci.*, 1984, **22**, 89.
9. Hart, J. P., Catterall, A., Dodds, R. A., Klenerman, L., Shearer, M. J., Bitensky, L., and Chayen, J., *Lancet*, 1984, ii, 283.
10. Hart, J. P., Yaakub, R., Shearer, M. J., Klenerman, L., Catterall, A., Reeve, J., Sambrook, P. N., Bitensky, L., and Chayen, J., *Clin. Sci.*, 1985, **68**, 29P.

High-performance Liquid Chromatographic Assay of Carbenicillin, Ticarcillin and Sulbenicillin in Serum and Urine Using Pre-column Reaction with 1,2,4-Triazole and Mercury(II) Chloride

Jun Haginaka* and Junko Wakai

Faculty of Pharmaceutical Sciences, Mukogawa Women's University, 4–16 Edagawa-cho, Nishinomiya 663, Japan

A high-performance liquid chromatographic method has been developed for the assays of carbenicillin (CBPC), ticarcillin (TIPC) and sulbenicillin (SBPC) in serum and urine. These penicillins were reacted with 2 M 1,2,4-triazole and 10^{-3} M mercury(II) chloride in solution (pH 9.0) at 60 °C for 10 min. The resulting products were separated on a C_{18} column using a mobile phase containing tetrabutylammonium bromide and sodium thiosulphate, and were detected at between 327 and 331 nm. The method has been applied to the assays of these penicillins in serum and urine samples, which were ultra-filtered with a YMT membrane, or filtered with an acrylate copolymer membrane. The procedure permits the accurate determination of penicillin concentrations in serum down to 0.05 µg ml^{-1} for SBPC and 0.1 µg ml^{-1} for CBPC and TIPC, and is specific to intact penicillins without interference from corresponding penicilloic acids.

Keywords: *Carbenicillin assay; ticarcillin assay; sulbenicillin assay; pre-column derivatisation; high-performance liquid chromatography*

Carbenicillin (CBPC), ticarcillin (TIPC) and sulbenicillin (SBPC) are semi-synthetic penicillins that are active against *Pseudomonas aeruginosa*. However, the high-performance liquid chromatographic (HPLC) method[1,2] so far employed for the assay of TIPC in body fluids requires a tedious extraction procedure and has a detection limit as high as 1 µg ml^{-1}; and the method[3] previously reported for the assays of CBPC and SBPC in urine requires a long run time and is insensitive. A number of HPLC methods[1–22] have been developed for the assay of penicillins in body fluids. Ultraviolet (UV) detection around 220 nm has been commonly employed for the assays of these antibiotics. However, detection at this wavelength lacks both sensitivity and selectivity. Therefore some pre-column[12,23–25] and post-column[6,7,12,25,26] derivatisation methods have been investigated in order to enhance the detectability and selectivity of the determination of these drugs.

Recently, Rogers *et al.*[24,25] reported a pre-column derivatisation procedure for naturally occurring penicillins using

the reaction with imidazole and mercury(II) chloride followed by reversed-phase chromatography of the resulting mercury(II)-stabilised penicillenic acids on a C_{18} column. However, the procedure is at a disadvantage in that it requires a long reaction time (50 min) and the detection limit is as high as 0.5 µg ml^{-1}.

Previously,[27] we observed that the reaction rate of penicillins with 1,2,4,-triazole and mercury(II) chloride was faster than that with imidazole and mercury(II) chloride, and described a spectrophotometric method for the determination of penicillins based on UV absorbance of the reaction products with the former reagent. This work describes an HPLC method for the assay of CBPC, TIPC and SBPC in serum and urine using a pre-column reaction with 1,2,4-triazole and mercury(II) chloride.

Experimental

Materials and Reagents

De-ionised, glass-distilled water was used for the preparation of reagent solutions and HPLC eluents. Disodium CBPC, TIPC and SBPC were kindly donated by Beecham Yakuhin (Tokyo, Japan) and Takeda Chemical Industries (Osaka, Japan). The structures and abbreviations of penicillins used in this study are illustrated in Fig. 1. Human control sera were purchased from Hyland Diagnostics (Round Lake, IL, USA). 1,2,4-Triazole and other chemicals of analytical-reagent grade and acetonitrile of HPLC grade were purchased from Nakarai Chemicals (Kyoto, Japan), and used without further purification.

The 2 M 1,2,4-triazole solution containing 10^{-3} M mercury(II) chloride, was prepared as follows: dissolve 13.81 g of 1,2,4-triazole in 60 ml of distilled water, add 10 ml of a solution of mercury(II) chloride (0.27 g dissolved in 100 ml of water), adjust to pH 9.0 ± 0.05 by the addition of saturated sodium hydroxide solution, and dilute to 100 ml with water.

The 0.0004 M phosphate buffer solution was prepared by dissolving 14.32 g of $Na_2HPO_4.12H_2O$ and 6.240 g of $NaH_2PO_4.2H_2O$ in 1 l of water, and diluting 100-fold.

Apparatus

For the examination of pre-column reaction conditions and the assays of penicillins, the following equipment was used: a
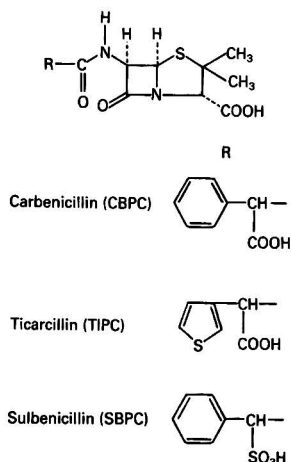
Fig. 1. Structure of penicillins

---

* To whom correspondence should be addressed.

JASCO BIP-I pump for delivering eluent; a JASCO Model VL-614 loop injector for the introduction of sample solutions; a Shimadzu C-R3A integrator for the determination of peak areas; a JASCO UVIDEC-100-V spectrophotometer, equipped with an 8-μl flow cell, as the detector; a home-made column packed with Develosil ODS-5 (5-μm particle size, Nomura Chemicals, Seto, Japan) in a 150 × 4.6 mm i.d. stainless-steel column; a JASCO TU-310 thermostatically controlled column oven, to maintain the column temperature at 40 °C; a thermostated water-bath, to examine pre-column reaction conditions; and an Horiba (Kyoto, Japan) Model F-8 pH meter, to measure pH values.

Pre-column Derivatisation Procedure

For serum samples, a penicillin standard was dissolved in human control serum. To a 200-μl aliquot of the serum samples, 200 μl of 10 M urea solution were added, and the mixture was ultra-filtered using an Amicon MPS-1 micropartition system with Amicon YMT membranes at 1500g for 10 min at ambient temperature. To a 200-μl aliquot of the ultra-filtrate, 200 μl of 2 M 1,2,4-triazole reagent [pH 9.0 containing the mercury(II) chloride] were added. The solution was sealed in a screw-topped vial and allowed to stand in a water-bath at 60 °C for 10 min. The vial was removed and immediately cooled to room temperature. A 30–90-μl portion of the solution was injected on to an HPLC column.

For urine samples, a penicillin standard was dissolved in human control urine. The urine sample, diluted 10-fold with water, was filtered with a 0.45-μm acrylate copolymer membrane (Showa Denko, Tokyo). To a 200-μl aliquot of the filtrate, 200 μl of 2 M 1,2,4-triazole reagent (pH 9.0) were added. The solution was treated in the same way as the serum samples (described above); a 30–60-μl portion of the solution was then injected on to the HPLC column.

HPLC Conditions

For the assays of CBPC and TIPC, the HPLC conditions used were as follows. A mobile phase of 0.0001 M phosphate buffer [containing 0.005 M tetrabutylammonium bromide (TBAB) and sodium thiosulphate] - acetonitrile (1.8 + 1 V/V) was used at a flow-rate of 1.0 ml min⁻¹. All separations were carried out at 40 °C, and detections at 328 nm for CBPC and 327 nm for TIPC.

For the assays of SBPC, a mobile phase of 0.01 M NaH₂PO₄ (containing 0.005 M TBAB and sodium thiosulphate) - acetonitrile (1.8 + 1 V/V) was used at a flow-rate of 1.0 ml min⁻¹. Separations were performed at ambient temperature and detections at 331 nm.

Assay of TIPC in Serum

TIPC (3 g) was administered intravenously at a constant rate for 1 h to a healthy male volunteer. Blood samples were collected at 0.5, 1, 1.5, 2, 4, 6 and 8 h after initiation of the infusion. The serum layer was obtained and stored at −80 °C until required for assay. The serum samples, except for those collected at 6 and 8 h, were diluted 10- or 20-fold with control sera, and assayed according to the procedures described above.

Results and Discussion

HPLC Conditions

The reaction products of CBPC, TIPC and SBPC with 1,2,4-triazole and mercury(II) chloride were stabilised in a mobile phase containing either EDTA or sodium thiosulphate. As revealed by Rogers et al.[24,25] the absence of these reagents resulted in very broad, asymmetrical peaks. The presence of EDTA in a mobile phase resulted in broad peaks

and a narrow range of linear response against injection volumes, compared with results using sodium thiosulphate. Thus, the pre-column reaction conditions were examined in a mobile phase containing sodium thiosulphate as described below.

When the mobile phase did not contain an ion-pairing agent (TBAB), the retention times of the reaction products were markedly shortened, resulting in poor separation from the background peaks. The peak shapes of derivatised CBPC and TIPC were improved by elevating the column temperature to 40 °C.

Pre-column Reaction Conditions

The effects of the concentration of 1,2,4-triazole and mercury(II) chloride, pH of the reagent solution and the reaction temperature on the formation of UV-absorbing products from CBPC, TIPC and SBPC were examined in order to establish the pre-column reaction conditions for the assays of these penicillins.

In a previous paper,[28] we described an HPLC method using the pre-column reaction with 1,2,4-triazole for the determination of sulbactam in plasma and urine. At first the pre-treatment procedures for the assays of penicillins were based on those for the assays of sulbactam; but the reactions of penicillins in serum samples with a 1,2,4-triazole reagent, following the deproteinisation of serum proteins with acetonitrile, gave a response which was only 40% of those in aqueous solutions. In addition, other deproteinising agents examined (methanol, ethanol, acetone and trichloroacetic acid) were also unsuitable for the present purpose. However, ultra-filtration, after denaturation of the serum proteins with urea, gave a total recovery above 80%. The urine samples were diluted 10-fold with water as reported previously.[28]

The serum and urine sample solutions (1 part) were treated by the pre-treatment procedures described above and reacted with a 1,2,4-triazole reagent (1 part). A 30-μl portion of the reaction solution was accurately withdrawn at pre-determined intervals and subjected to HPLC under the conditions described under Experimental. The peak areas were plotted against the reaction times. Fig. 2 shows the time courses of the formation of UV-absorbing products from CBPC, TIPC and SBPC reacted with a 2 M 1,2,4-triazole reagent (pH 9.0) in the pre-treated serum samples at 60 °C. A maximum and constant response was obtained at a reaction time of 10 min (or more). Thus, the pre-column reaction conditions described under Experimental were selected for the assays of these penicillins in serum. Similar results were also obtained for the reaction of these penicillins in urine samples and so the same pre-column reaction conditions were adopted.
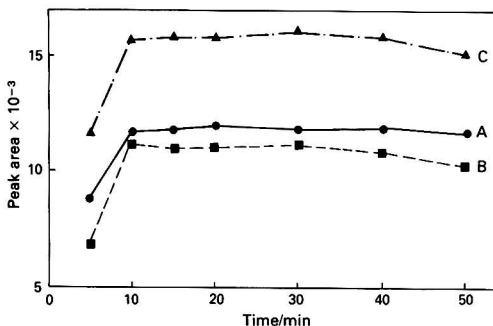
Fig. 2. Effect of reaction time on the pre-column derivatisation of (A) carbenicillin, (B) ticarcillin and (C) sulbenicillin in serum samples. Each penicillin (1.0 μg ml⁻¹) in control serum was ultra-filtered and reacted with 2 M 1,2,4-triazole reagent at 60 °C. Injection volume, 30 μl; sensitivity, 0.004 a.u.f.s.; other chromatographic conditions, as described under Experimental
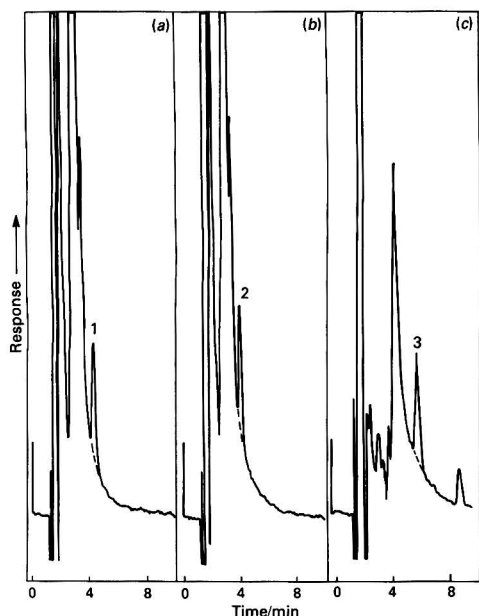
Fig. 3. Chromatograms of derivatised (*a*) carbenicillin, (*b*) ticarcillin and (*c*) sulbenicillin in control serum. Each penicillin $(1.0 \, \mu g \, ml^{-1})$ in control serum was ultra-filtered after denaturation of serum proteins, and reacted with 2 M 1,2,4-triazole reagent at 60 °C for 10 min. 1, Carbenicillin; 2, ticarcillin; 3, sulbenicillin. Injection volume, 30 μl; sensitivity, 0.004 a.u.f.s.; other chromatographic conditions, as described under Experimental. Broken line indicates serum blank
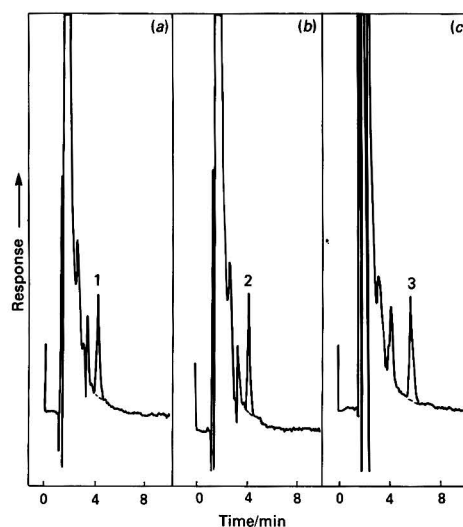
Fig. 4. Chromatograms of derivatised (*a*) carbenicillin, (*b*) ticarcillin and (*c*) sulbenicillin in control urine. Each penicillin $(5.0 \, \mu g \, ml^{-1})$ in control urine was diluted 10-fold, and reacted with 2 M 1,2,4-triazole reagent at 60 °C for 10 min. (*a*)–(*c*) as in Fig. 3. Injection volume, 30 μl; sensitivity, 0.004 a.u.f.s.; other chromatographic conditions, as described under Experimental. Broken line indicates urine blank

Table 1. Recovery of carbenicillin, ticarcillin and sulbenicillin from serum

| | | Penicillin | | | | | |
| | | Carbenicillin | | Ticarcillin | | Sulbenicillin | |
Parameter							
Concentration/μg ml^{-1}		0.5	5.0	0.5	5.0	0.5	5.0
Recovery, %		99.3	96.6	81.7	85.3	93.3	95.1
CV*, %		5.41	0.52	3.99	1.44	1.01	2.94

* CV = coefficient of variation of five analyses.

Table 2. Recovery of carbenicillin, ticarcillin and sulbenicillin from urine

| | | Penicillin | | | | | |
| | | Carbenicillin | | Ticarcillin | | Sulbenicillin | |
Parameter							
Concentration/μg ml^{-1}		5.0	50.0	5.0	50.0	5.0	50.0
Recovery, %		95.0	102	101	104	88.0	92.1
CV*, %		6.59	5.25	2.97	5.80	4.21	1.80

* CV = coefficient of variation of five analyses.

Table 3. Precision of penicillin assay in serum and urine. Control serum and urine spiked at penicillin concentrations of 1.0 and 5.0 μg ml^{-1} were treated according to the procedures described under Experimental

| | | | Penicillin | | |
Sample			Carbenicillin	Ticarcillin	Sulbenicillin
Serum					
Within-day CV*, %			8.45	5.73	6.23
Between-day CV, %			6.56	9.26	2.92
Urine					
Within-day CV, %			6.62	5.97	1.54
Between-day CV, %			6.56	2.00	0.53

* CV = coefficient of variation of three analyses.

HPLC Assay

The serum and urine samples spiked with CBPC, TIPC or SBPC were treated according to the optimum pre-column reaction conditions and a 30-μl portion of the treated serum or urine sample was subjected to HPLC under the optimum conditions. Figs. 3 and 4 show that the derivatised CBPC, TIPC and SBPC were completely separated from ordinary components of serum and urine within 5 min (CBPC and TIPC) or 7 min (SBPC) after injection. The limit of accurate determination was as low as 0.05 μg ml⁻¹ for SBPC and 0.1 μg ml⁻¹ for TIPC and CBPC in serum samples, and 0.5 μg ml⁻¹ for SBPC and 1.0 μg ml⁻¹ for TIPC and CBPC in neat urine samples. The calibration graphs (which were constructed by plotting peak area *versus* penicillin concentration) for SBPC concentrations between 0.05 and 5.0 μg ml⁻¹ and CBPC and TIPC concentrations between 0.1 and 5.0 μg ml⁻¹ in serum and diluted urine samples, were linear with a correlation coefficient of 0.999 (or more), and passed through the origin.

The presence of corresponding penicilloic acids (in equimolar concentrations to parent penicillins) did not interfere in the assays of CBPC, TIPC and SBPC.

Recovery and Precision

Tables 1 and 2 show the total recoveries of CBPC, TIPC and SBPC from spiked serum and urine samples, respectively, and the coefficients of variation.

Table 3 shows the within- and between-day precision of the assays of these penicillins in serum and urine.

Assay of TIPC in Serum

The serum levels of ticarcillin, after intravenous infusion to a healthy male volunteer, were determined by the proposed method. Fig. 5 shows a semi-logarithmic plot of the time course data. The pharmacokinetic behaviour obtained is consistent with that reported previously.[29]
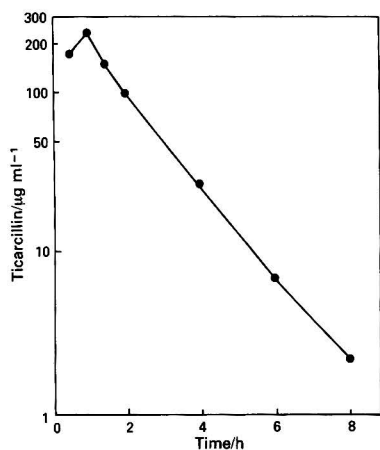
Conclusion

The reaction of CBPC, TIPC and SBPC with 1,2,4-triazole and mercury(II) chloride yielded products having UV absorption maxima between 327 and 331 nm. An HPLC method has been developed that utilises this reaction as a pre-column derivatisation procedure for the determination of these penicillins in serum and urine. The proposed method is rapid, sensitive, accurate and precise, compared with the one reported previously. This method is effective for the determination of CBPC, TIPC and SBPC in clinical studies, and could also be applicable to the assay of other penicillins after slight modification.

References

1. Kwan, R. H., MacLeod, S. M., Spino, M., Teare, F. W., *J. Pharm. Sci.*, 1982, **71**, 1118.
2. Arabind, M. K., Miceli, J. N., and Kauffman, R. E., *J. Liq. Chromatogr.*, 1984, **7**, 2887.
3. Yamaoka, K., Narita, S., Nakagawa, T., and Uno, T., *J. Chromatogr.*, 1979, **168**, 187.
4. Vree, T. B., Hekster, Y. A., Baars, A. M., and Van der Kleijn, E., *J. Chromatogr.*, 1978, **145**, 496.
5. Lee, T. L., D'arconte, L., and Brooks, M. A., *J. Pharm. Sci.*, 1979, **68**, 454.
6. Westerlund, D., Carlqvist, J., and Theodorsen, A., *Acta Pharm. Sue.*, 1979, **16**, 187.
7. Carlqvist, J., and Westerlund, D., *J. Chromatogr.*, 1979, **164**, 373.
8. Thijssen, H. H. W., *J. Chromatogr.*, 1980, **183**, 339.
9. Uno, T., Masada, M., Yamaoka, K., and Nakagawa, T., *Chem. Pharm. Bull.*, 1981, **29**, 1957.
10. Foulstone, M., and Reading, C., *Antimicrob. Agents Chemother.*, 1982, **22**, 753.
11. Borner, K., Lode, H., and Elvers, A., *Antimicrob. Agents Chemother.*, 1982, **22**, 949.
12. Miyazaki, K., Ohtani, K., Sunada, K., and Arita, T., *J. Chromatogr.*, 1983, **276**, 478.
13. Lee, T. L., and Brooks, M. A., *J. Chromatogr.*, 1984, **306**, 429.
14. Lindberg, R. L. P., Huupponen, R. K., and Huovinen, P., *Antimicrob. Agents Chemother.*, 1984, **26**, 300.
15. Fasching, C. E., and Peterson, L. R., *J. Liq. Chromatogr.*, 1983, **6**, 2513.
16. Fiore, D., Auger, F. A., Drusano, G. L., Dandu, V. R., and Lesko, L. J., *Antimicrob. Agents Chemother.*, 1984, **26**, 775.
17. Weber, A., Opheim, K. E., Wong, K., and Smith, A. L., *Antimicrob. Agents Chemother.*, 1983, **24**, 750.
18. Hinderling, P. H., Gundert-Remy, U., Forster, D., and Gau, W., *J. Pharmacokin. Biopharm.*, 1983, **11**, 5.
19. Westerlund, D., Pettersson, B., and Carlqvist, J., *J. Pharm. Sci.*, 1982, **71**, 1148.
20. Brisson, A. M., and Fourtillan, J. B., *Antimicrob. Agents Chemother.*, 1982, **21**, 664.
21. Meulemans, A., Mohler, J., Decazes, J. M., Dousset, I., and Modai, A., *J. Liq. Chromatogr.*, 1983, **6**, 575.
22. Jung, D., and Mahajan, N. K., *Clin. Chem.*, 1984, **30**, 122.
23. Lam, S., and Grushka, E., *J. Liq. Chromatogr.*, 1978, **1**, 33.
24. Rogers, M. E., Adlard, M. W., Saunders, G., and Holt, G., *J. Liq. Chromatogr.*, 1983, **6**, 2019.
25. Rogers, M. E., Adlard, M. W., Saunders, G., and Holt, G. *J. Chromatogr.*, 1984, **297**, 385.
26. Rogers, M. E., Adlard, M. W., Saunders, G., and Holt, G., *J. Chromatogr.*, 1983, **257**, 91.
27. Haginaka, J., Wakai, J., Yasuda, H., and Uno, T., *Anal. Sci.*, 1985, **1**, 73.
28. Haginaka, J., Wakai, J., Yasuda, H., Uno, T., and Nakagawa, T., *J. Chromatogr.*, 1985, **341**, 115.
29. Ueda, Y., *Chemotherapy (Tokyo)*, 1977, **25**, 2389.

Fig. 5. Semi-logarithmic graph of serum concentration of ticarcillin. A healthy male volunteer was given ticarcillin (3 g) by intravenous infusion

Sensitive Ascorbic Acid Assay for the Analysis of Pharmaceutical Products and Fruit Juices

Warren L. Baker* and Trevor Lowe
Swinburne Institute of Technology, John Street, Hawthorn 3122, Melbourne, Australia

A simple method has been developed for the determination of ascorbic acid concentrations in pharmaceutical products and fruit juices. The procedure is based on the rapid reduction of copper(II) ion in the presence of ascorbic acid. The copper(I) ion is measured by reaction with neocuproine. The method was used to determine between 2 and 20 µg of ascorbic acid. Results of determinations of ascorbic acid using this procedure were comparable to those using dichlorophenolindophenol titration.

Keywords: *Ascorbic acid determination; neocuproine; copper(II) ion reduction; pharmaceuticals; fruit juices*

Ascorbic acid concentrations are frequently determined by 2,6-dichlorophenolindophenol (DCPIP) titrations[1] or the official pharmacopoeial methods.[2] Results are obtained rapidly but the methods are not particularly specific for ascorbic acid or very sensitive. If used with beverages or fruit, the colouring matter may interfere with the determination of the end-point. High-performance liquid chromatography[3] and fluorimetry[4] have been used to increase the analytical sensitivity for ascorbic acid and the fluorimetric assay has been automated,[5] but specialised equipment is required for these procedures. It was proposed to investigate the stability of ascorbic acid preparations under commercial conditions. A sensitive analytical method was required that was simple, capable of use with a large number of samples (and possibly automation) and that would provide results quickly. The above methods did not completely satisfy these criteria so a procedure was developed based on the reducing effect of ascorbic acid on copper(II) ion and the chelating ability of neocuproine (2,9-dimethyl-1,10-phenanthroline) with copper(I) ion to provide a coloured solution.

Experimental

Apparatus

A Varian-Techtron 635 recording spectrophotometer was used to measure absorbance at 450 nm. A Metrohm AG396 pH meter was used for pH measurements.

Solutions

Colour reagent was prepared by mixing 96 cm³ of 0.05 mol l⁻¹ phosphate buffer (pH 7), 20 cm³ of (0.25 mg cm⁻³) neocuproine solution in ethanol - distilled water (1 + 1) and 4 cm³ of 4 mmol l⁻¹ copper sulphate solution in distilled water. The absorbance of a freshly prepared solution was approximately 0.02 and increased slowly to about 0.075 over a 24-h period. This effect was controlled in blanks as required.

Analytical Procedures

An Eppendorf micropipette was used to deliver 0.1 cm³ of ascorbic acid solution (10–200 µg cm⁻³ of ascorbic acid) into tubes containing 3 cm³ of colour reagent and the tubes were mixed thoroughly after each addition. The colour that developed was read at 450 nm 1 h after the addition of ascorbic acid solution. Ascorbic acid solutions were usually prepared in a mixture of 60 cm³ of glacial acetic acid and 30 g of metaphosphoric acid with 900 cm³ of distilled water (AA -

MPA), but this solvent was diluted with an equal volume of water (AA - MPA - H₂O) in some experiments. Five per cent. trichloroacetic acid (TCA) was also used as a solvent for ascorbic acid. Neocuproine and copper sulphate concentrations and the buffer for colour reagent were also varied as described in the text.

A DCPIP titration was used for comparative purposes to determine the amount of ascorbic acid in pharmaceutical products, orange and lemon juice and commercial fruit beverages.

The presence of sulphydryl groups in solutions to be analysed was examined using Ellman's reagent[6] after dilution with 0.05 mol l⁻¹ phosphate buffer (pH 7).

Fruit Juices, Beverages and Pharmaceutical Preparations

The juices of fruit or fruit beverages were mixed with an equal volume of AA - MPA, clarified with diatomaceous earth, filtered on a Büchner funnel and 5 cm³ of the filtrate analysed using a DCPIP titration. Further dilutions were made for neocuproine analysis.

Pharmaceutical products were dissolved in AA - MPA at a concentration of 1 mg cm⁻³ of ascorbic acid on the basis of declared amounts. A 5-cm³ volume was taken for DCPIP titration and a further dilution made in AA - MPA to contain 100 µg cm⁻³ of ascorbic acid (declared) and 0.1 cm³ was used for neocuproine analysis as described above.

Results

Concentration of Neocuproine and Copper Ion

Colour developed strongly as the amount of neocuproine in the reaction mixture was increased to 0.125 mg (Fig. 1). The increase in sensitivity that occurred at higher neocuproine concentrations was inadequate to justify additional neocuproine in the reaction mixture. A solution of 0.25 mg cm⁻³ of neocuproine was used as the copper(I) ion chelating agent in the preparation of the colour reagent. Neocuproine solutions were found to be stable for many weeks at room temperature.

Absorbance values obtained using 10 µg of ascorbic acid were constant as the amount of copper ion was increased from 0.4 to 3.2 µmol. This indicates an excess of the oxidation catalyst.

Stability of Colour

The reaction occurred immediately on addition of ascorbic acid to the colour reagent and the absorbance at 450 nm was stable for at least 1 h. This permitted absorbance readings to be taken as convenient.

---

* To whom correspondence should be addressed.
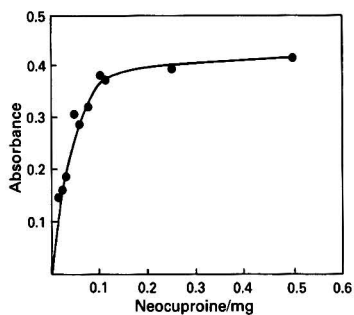
Fig. 1. Effect of amount of neocuproine on the development of colour with ascorbic acid. Ascorbic acid, at a concentration of 1 μmol cm^{-3}, was prepared in AA - MPA solvent and 0.1 cm^3 was added to 3 cm^3 of colour reagent containing a mass of neocuproine as indicated

Fig. 3. Stability of ascorbic acid solutions kept in A, AA - MPA, AA - MPA - H$_2$O or 5% TCA; and B, 0.05 mol l^{-1} phosphate buffer (pH 7) at room temperature. Solution (0.1 cm^3) containing 100 μg cm^{-3} of ascorbic acid was added to 3 cm^3 of colour reagent as described in the text

Fig. 2. Calibration graph of ascorbic acid in the range of 2–20 μg. Ascorbic acid solutions (0.1 cm^3) in the concentration range 20–200 μg cm^{-3} were added to 3 cm^3 of colour reagent as described in the text

Table 1. Effect of variation of conditions on absorbance. All absorbance readings taken 1 h after the addition of 0.1 cm^3 of solution containing 10 μg of ascorbic acid. N-Ethylmaleimide (NEM) and iodoacetic (IAA) added at a level of 2.5 μmol, cysteine (CySH) and cystine (CySSCy) at 0.2 μmol and sodium dodecylsulphate (SDS) at 20 mg

System	Absorbance, %
Buffer (pH 4)	93.7
Buffer (pH 4.5)	95.5
Buffer (pH 5)	110
Buffer (pH 6)	96.5
Buffer (pH 7)	100
Buffer (pH 8)	108
Buffer (pH 7), ascorbic acid in 5% TCA	102
Buffer (pH 7) + NEM	101.4
Buffer (pH 7) + IAA	102.4
Buffer (pH 7) + SDS	103.8
Buffer (pH 7) + CySH	260
Buffer (pH 7) + CySSCy	102

Table 2. Comparison of results obtained by neocuproine and DCPIP analysis

No.	Preparation	Declared concentration	Assay result Neocuproine method	Assay result DCPIP method
1	Tablet	50 mg	42.6	44.9
2			45.9	45.7
3			49.8	50.7
4			38.9	39.9
5			42.4	44.7
6		250 mg	218	217.5
7			217.5	218
8			222.5	220.4
9			215	210.5
10			212.5	212.3
11			247.1	247.6
12	Multi-vitamin capsule	75 mg	75.6	74.2
13	Commercial fruit juice	40 mg per 100 cm^{-3}	56.4	58.2
14			59.4	54.6
15			40	41.6
16	Commecial fruit juice concentrate	160 mg per 100 cm^{-3}	156	166
17	Orange	Unknown (100 cm^{-3})	45	39.2
18	Orange		43	47.5
19	Lemon		45	43.5

Concentration Range and Calibration Graph

At pH 7 the absorbance was proportional to the amount of ascorbic acid within the range 2–20 µg (Fig. 2). Above this level there was regular deviation from Beer's law as the ascorbic acid level increased to 50 µg. Most analyses were performed on solutions containing approximately 10 µg per 0.1 cm³ (100 µg cm⁻³) of ascorbic acid.

Stability of Ascorbic Acid

Sixty-seven per cent. of the copper-reducing activity of a solution of ascorbic acid (100 µg cm⁻³), held at pH 7, disappeared within 2 h (Fig. 3). When ascorbic acid was prepared in either AA - MPA, AA - MPA - H_2O or 5% TCA the reducing activity was stable for 2 h but it decreased steadily after that time. AA - MPA was used as the solvent for ascorbic acid when possible, but AA - MPA - H_2O was used to prepare standards for fruit juices. TCA is considered to be a suitable solvent if deproteinisation is required.

Variation in Reaction Conditions

Minor variations were noted when the colour reagent was prepared with phosphate buffers between pH 6 and 8 (Table 1). The absorbance values were lowered slightly when acetate buffer (pH 4) was used in the colour mixture.

Interfering Compounds

Any compound that reduces copper(II) to copper(I) interferes with the reaction. Cysteine (0.2 µmol) interfered to an extent of 160% but the disulphide cystine did not interfere. The sulphydryl group reagents N-ethylmaleimide and iodoacetic acid and the protein denaturant sodium dodecylsulphate also showed little interference.

Precision

The mean of 30 analyses of a solution of ascorbic acid at a concentration of 10 µg per 0.1 cm³ assayed at its prepared value with a standard deviation of 0.7%. This level of precision is adequate for quality control purposes as might be required for the analysis of pharmaceutical preparations and fruit juices.

Comparative Results

DCPIP titration and neocuproine analysis of several preparations generally gave concordant results (Table 2). The Student t value for these results was 0.29 (18 degrees of freedom), which indicates that there was no difference between the two sets of results at the 5% level of significance. Some commercial fruit beverages contained ascorbic acid levels considerably in excess of the declared concentrations. In many instances the assay results for the pharmaceutical preparations were outside the British Pharmacopoeial limits for ascorbic acid preparations, but this was obviously due to lack of control over storage. On the assumption that there was complete oxidation of the detected sulphydryl groups in diluted juice samples by copper(II), the maximum possible error from this source was found to be less than 3%.

Discussion

The salient features of the proposed procedure using neocuproine for the determination of ascorbic acid are simplicity and excellent precision and sensitivity. The rate of development and stability of the colour make the procedure ideal for handling large numbers of samples and there is potential for automation as only one colour reagent is required. The sensitivity range of the assay is of the same order as the method using α,α'-dipyridyl to chelate iron(II) ion[7] and it should be possible to adapt the procedure for use with small volumes and micro-scale equipment.

The major use, so far, has been for the rapid analysis of pharmaceutical preparations and the determination of concentrations of ascorbic acid in fruit juices and fruit beverages. The dilution of these latter preparations eliminated colour interference, whereas the end-point was sometimes difficult to detect using DCPIP titration. Some preliminary experiments have suggested that neocuproine may be used for determining plasma and erythrocyte concentrations of ascorbic acid, particularly as the preparation of samples in 5% TCA did not affect colour development at pH 7. However, the presence and effect of other copper(II) reducing substances in tissue and blood preparations requires further investigation before the reaction can be reliably used for this purpose.

References

1. Roe, J. H., *Methods Biochem. Anal.*, 1954, **1**, 115.
2. "British Pharmacopoeia 1981," HM Stationery Office, London, 1981, p. 39.
3. Williams, R. C., Baker, D. R., and Schmidt, J. A., *J. Chromatogr. Sci.*, 1973, **11**, 618.
4. Deutsch, M. J., and Weeks, C. E., *J. Assoc. Off. Anal. Chem.*, 1965, **48**, 1248.
5. Roy, R. B., Conetta, A., and Salpeter, J., *J. Assoc. Off. Anal. Chem.*, 1976, **59**, 1244.
6. Ellman, G. L., *Arch. Biochem. Biophys.*, 1959, **82**, 70.
7. Maickel, R. P., *Anal. Biochem.*, 1960, **1**, 498.

Sensitive Method for the Measurement of Alcohol Dehydrogenase Activity in Human Serum by Differential-pulse Polarography

Sadallah T. Sulaiman
Department of Chemistry, College of Science, University of Mosul, Mosul, Iraq

and Maysoon M. N. M. Saleem
Department of Biochemistry, College of Medicine, University of Mosul, Mosul, Iraq

A method is described for the measurement of alcohol dehydrogenase (E.C. 1.1.1.1) (ADH) activity in human serum using differential-pulse polarography, based on the measurement of the reduction of nicotinamide adenine dinucleotide (NAD+) in the presence of an excess of ethanol substrate. This method is both sensitive and rapid.

Keywords: *Alcohol dehydrogenase activity; differential-pulse polarography; human serum*

Alcohol dehydrogenase [ADH, alcohol:NAD+ (nicotinamide adenine dinucleotide) oxidoreductase, E.C. 1.1.1.1] is the principal enzyme involved in the hepatic metabolism of ethanol[1] and is considered to be almost exclusively confined to the livers of humans and animals.[1,2] It has been known for a long time that ADH activity in serum from healthy livers is undetectable, whereas some activity can be detected in liver diseases.[3]

The relative insensitivity of the conventional ADH assay,[4] which is based on optical measurement of the rate of NADH formation, is inherent in the enzyme and is related primarily to its low molecular activity.[1] Because of this, the assay cannot be used as a standard method for the detection of liver malfunctions. Tamaoki *et al.*[5] used a semisynthetic thio analogue of NAD+ for routine ADH activity measurements, and it was found that with this modified coenzyme, ADH exhibits considerably higher activity towards ethanol than NAD+.

In addition, performing the conventional ADH assay at elevated temperatures was found to enhance the activity of minute amounts of the enzyme normally present in serum at a detectable level.[6]

As yet, ADH activity assay has not been introduced into clinical practice; the limited sensitivity of the current photometric methods,[3–6] due to the low molar absorptivity of NADH,[2] does not allow the determination of ADH activity in normal sera or in the early stages of liver disease. Therefore, the development of a highly sensitive and rapid analytical technique for the determination of ADH activity may help in the diagnosis of liver disease.[7–9]

Recently we reported a sensitive differential-pulse method for ADH activity measurement based on a recycling process[10] and measurement of the polarographic reduction of *p*-nitroso-*N,N*-dimethylaniline (NDMA). Because nitroso compounds are generally poisonous and require careful handling, we have introduced a new differential-pulse polarographic (DPP) method for ADH activity measurement, which is a modification of the method described by Schimasue *et al.*[3] and Dalziel[4] in which they measured, spectrophotometrically, the rate of reduction of NAD+ to NADH. In this way ADH activity can be measured in the serum of a normal individual.

Experimental

Reagents

All chemicals were of purum grade from Fluka AG (Buchs, Switzerland).

Nicotinamide adenine dinucleotide (NAD), 1 mg *per* 10 ml. Prepared freshly daily.

Glycine (0.1 M) - *sodium hydroxide buffer, pH 10.*

Pyrazole, 0.1 M.

Phosphate buffer, 0.1 M. Sodium dihydrogen phosphate buffer was prepared and adjusted to pH 8 using sodium hydroxide.

Butanol, 200 mM. Prepared in doubly distilled water.

Sample Preparation

Liver tissue from rats was removed immediately after decapitation of the animals, cut into small pieces, collected on filter-paper, weighed and homogenised ice cold with an equal volume of distilled water.[3] The homogenate was centrifuged to give a clear or barely opalescent supernatant. The supernatant was collected and used as the solution for ADH activity measurement after the appropriate dilution. Samples of human serum were obtained from routine clinical assays.

Apparatus

All experiments were performed using a Metrohm Polarecord Model E 506 with an E 505 polarography unit. A three-electrode system was used: the working electrode was a dropping-mercury electrode (DME); the reference electrode was a Ag - AgCl electrode with a ceramic liquid junction; and the counter electrode was a platinum wire.

Recommended Procedure

The differential-pulse mode was used with a 100-mV pulse, a 1-s drop time and a 3 mV s^{-1} scan rate. The polarographic cell was thermostated at 30 °C. The solution was de-aerated by passing through it a slow stream of helium for 15 min to remove the dissolved oxygen.

For polarographic measurement the sample cuvette contained 4.0 ml of 0.1 M glycine buffer (pH 10.0), 0.5 ml of 135 μM NAD and 0.1 ml of sample in a final volume of 5.1 ml, so that the total volume was always constant. The differential-pulse polarogram was recorded, and reaction was initiated by the addition of 0.5 ml of ethanol; the polarogram was again recorded. The activity of the enzyme was determined during the first 1–3 min. One unit of ADH activity was equal to the rate of formation of 1 μM of NADH per minute under the assay conditions, or the rate of decomposition of 1 μM of NAD+ per minute. Activity is expressed in units per litre of serum, and in units per milligram fresh mass of liver tissue.

Results and Discussion

It has previously been found that NAD+ gives a well defined major differential-pulse peak at −0.8 V *vs.* Ag - AgCl in Britton - Robinson buffer at pH 7.5.[11] In this study the differential-pulse polarographic behaviour of NAD+ was

studied in different media containing a buffer (glycine or phosphate) and an alcohol (ethanol or butanol) in order to optimise the conditions for measuring the alcohol dehydrogenase activity in rat liver and human serum. Table 1 illustrates the effect of the buffer and alcohol on the ADH activity of pooled human serum. The results show that the highest activity of ADH was obtained with a glycine buffer and ethanol. Therefore, optimum conditions were then determined for the DPP of NAD+ in these media and were found to be a pulse amplitude of 100 mV and a drop time of 1 s. A well defined peak was observed at 0.8 V vs. Ag - AgCl as shown in Fig. 1(a).

Using serial dilutions of standard NAD+ solution a calibration graph was obtained in glycine containing ethanol (19.6 mM).

The alcohol dehydrogenase activity was then determined in rat liver and human serum by measuring the rate of decomposition of NAD+ to NADH from the polarographic reduction peak of NAD+ after addition of the enzyme [Fig. 1(b) and (c)].

Optimum Concentration of NAD+ and Ethanol

To determine the optimum concentration of NAD and ethanol a series of experiments was carried out in which their concentrations were varied. The highest activity was obtained with 13.2 μM NAD and 19.6 mM ethanol; higher concentrations did not cause any effect as shown in Tables 2 and 3, so these concentrations were considered optimum at 30 °C.

The method of measuring the enzyme activity by DPP was accurate when the activity was determined using optimum concentrations of reaction components. The precision of the method was tested six times using rat liver tissue; the activity

was found to be 6.8 ± 0.5 U mg^{-1} of fresh wet liver tissue (in terms of coefficient of variation, CV = 7.3%, n = 6).

The activity of another sample of rat liver extract was 37.3 U mg^{-1}, which decreased with time to 3 U mg^{-1} after 11 min.

Inhibition by Pyrazole

Pyrazole is generally a specific potent inhibitor of ADH activity except for π-ADH[12] (π-alcohol dehydrogenase). Thus on the addition of this compound to a cuvette containing the reaction mixture and serum, the rate of formation of NADH decreased or stopped completely owing to the presence of ADH alone. The result for a diseased state of human serum shows the decrease of total ADH activity from 77 to 12 U l^{-1} after the addition of 0.5 ml of 0.1 M pyrazole over 1–3 min. This represents the pyrazole-insensitive alcohol dehydrogenase activity (PI-ADH), which was 15% of the total enzyme activity. The PI-ADH activity of another sample of pooled human serum was 26% of the total enzyme activity. This inhibition of the enzyme activity is due to the presence of π-ADH, which is insensitive to pyrazole. However, there is evidence to suggest that it might be the π-ADH isoenzyme in the serum that is responsible for the pyrazole-insensitive portion of the total enzyme activity as recently,[12] the serum of some individuals has been found to contain a fraction whose ADH activity is not inhibited by pyrazole.

ADH Activity of Human Serum

The total ADH activities of nine healthy human serum samples were found to be in the range from 18 to 36 U l^{-1} over a period of 1–3 min as shown in Table 4; the mean of the nine results ($\pm$ s.d.) was 26.5 ± 6.2 U l^{-1}. The mean activity for two pathological cases of jaundice was 130.7 ± 3.3 and for two

Table 1. Effect of buffer and alcohol on ADH activity

	ADH activity/U l^{-1}			
Sample No.	Glycine with ethanol	Glycine with butanol	Phosphate with ethanol	Phosphate with butanol
1*	57	29	32	26
2†	176	115	55	52
3*	47	29	30	25

* The ADH activity was measured in pooled human serum from normal individuals.
† Diseased liver state.

Table 2. Effect of NAD concentration on ADH activity

NAD/μM	ADH activity*/U l^{-1}
2.6	45
6.9	60
13.2	61.5
19	61.3
24	60.5
33.7	61

* The enzyme activity was measured in pooled human serum, at 30 °C, in glycine - NaOH buffer, pH 10.

Table 3. Effect of ethanol concentration on ADH activity

Ethanol/mM	ADH activity*/U l^{-1}
10	60
19.6	72.5
28	72.3
35.7	72.0
50	72.1

* The ADH activity was measured in pooled human serum.
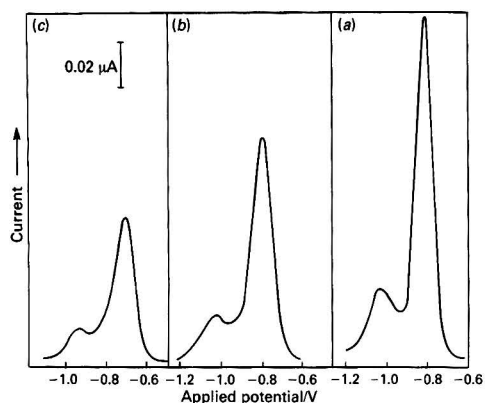
Fig. 1. Differential-pulse polarograms of 13.2 μM NAD+ at pH 10 in the presence of different concentrations of ADH: (a) 0 μg l^{-1} and (b) 57 μg l^{-1} (normal human serum); and (c) 176 μg l^{-1} (diseased human serum)

cases of obstructive jaundice 165 ± 5.0 U l^{-1}. Khayrollah *et al.*[9] found that the mean ($\pm$ s.d.) of serum enzyme activity for 36 patients suffering from obstructive jaundice, Gilbert's ascites and other liver diseases was 2.14 ± 0.39 times the upper normal values.

Table 4. ADH activity measured in nine healthy individuals

	ADH activity/U l^{-1}	
Sample No.	This method	Recycling method
1	26	21.7
2	35	
3	28	
4	21	
5	23	
6	36	38
7	18	
8	32	
9	20	24

Conclusion

With the aid of differential-pulse polarography, the ADH activity can be measured in normal human serum and rat liver tissue with a high degree of sensitivity and accuracy.

References

1. Bränden, C. I., Jörnvall, H., Eklund, H., and Furugren, B., *in* Boyer, P. D., *Editor*, "The Enzymes," Third Edition, Volume 11, Academic Press, New York, 1975, p. 103.
2. Pietruszko, R., *in*, Majchrowicz, E., *Editor*, "Biochemical Pharmacology of Ethanol," Volume 56, Plenum Press, New York, 1975, p. 1.
3. Schimasue, A., Murakami, M., and Tsunokura, T., *Hiroshima J. Med. Sci.*, 1972, **21**, 131.
4. Dalziel, K., *Acta Chim. Scand.*, 1957, **11**, 397.
5. Tamaoki, H., Mizushima, H., Takei, S., Minato, S., and Nakanishi, K., *Ann. Sankyo Res. Lab.*, 1973, **25**, 85.
6. Carter, E. A., and Isselbacher, K. J., *Proc. Soc. Exp. Biol. Med.*, 1977, **155**, 290.
7. Skurský, L., Kovář, J., and Štachová, M., *Anal. Biochem.*, 1979, **99**, 65.
8. Kovář, J., Neubauerová, J., and Broinek, P., *Čas. Lêk. Čêsk.*, 1980, **119**, 929.
9. Khayrollah, A., Al Tamer, Y. Y., Taka, M., and Skursky, L., *Ann. Clin. Biochem.*, 1982, **19**, 35.
10. Sulaiman, S. T., and Saleem, M. M. N. M., *Fresenius Z. Anal. Chem.*, 1984, **317**, 750.
11. Hameed, Y., *MSc Thesis*, University of Mosul, 1982.
12. Skursky, L., and Khayrollah, A., *Drug Alcohol Dependence*, 1980, **6**, 187.

Determination of Nickel in Human Nails by Adsorption Differential-pulse Voltammetry

Bente Gammelgaard and Jan Rud Andersen
Royal Danish School of Pharmacy, Department of Chemistry AD, 2 Universitetsparken, DK-2100 Copenhagen Ø, Denmark

A procedure is described for the determination of nickel in human nails, which consists in a simple wet digestion followed by quantitation by adsorption differential-pulse voltammetry. This procedure produced more reliable results for low nickel levels than atomic-absorption spectrometry; for unexposed individuals, mean values for nickel in finger- and toenails were found to be 2.14 ± 1.20 µg g^{-1} and 0.78 ± 0.42 µg g^{-1}, respectively.

Keywords: *Nickel determination; adsorption voltammetry; stripping voltammetry; wet digestion; finger- and toenail analysis*

Nickel is used for a wide variety of purposes in modern industry and, because it is a constituent of stainless steel, virtually every individual in the industrialised part of the world is in daily contact with the metal. Nickel is an allergenic and in some of its compounds a carcinogenic element,[1] hence the need for reliable analytical procedures for monitoring nickel in human tissues and body fluids has been emphasised during recent years.[2]

A number of investigations have been carried out on the uptake and excretion of nickel in individuals who are occupationally exposed to the metal, the general method being the measurement of blood or urine levels over a period of time.[3-6] The normal levels of nickel in body fluids are reasonably well established,[7,8] thus rendering it possible to establish whether the levels in people exposed to the metal are elevated.[9]

As an alternative to blood and urine analysis, the possibility of using nail analysis should be pursued as this type of analysis has several advantages. Firstly, the normal nickel levels in nails appear to be in the µg g^{-1} region,[10-12] which is three orders of magnitude higher than the levels in blood or urine. This allows the analysis of very small samples and reduces the risk of contamination to a minor problem compared with blood or urine samples. Secondly, the sampling procedure is simpler: urine samples should be from 24-h pools in order to obtain meaningful results; this is inconvenient for the individual involved. In addition, collecting blood samples requires medical assistance: there are no such restraints on nail sampling. Thirdly, there are no storage problems with nails during the period between sampling and analysis and finally, the decomposition of nails demands less powerful destruction methods than do blood or urine.

The purpose of this work is to define a normal range of nickel in human nails as determined by the voltammetric method described by Pihlar *et al.*[13] The method involves a constant potential pre-concentration of the analyte at the electrode - solution interface. The actual species accumulated is the Ni^{2+} - bisdimethylglyoximate [Ni(DMG)$_2$], formed in the electrochemical cell by the addition of dimethylglyoxime. After the concentration step, a cathodic differential-pulse scan reduces the chelate. The technique is known as adsorption differential-pulse voltammetry (ADPV).

In contrast to conventional anodic-stripping voltammetry the reduction of Ni(DMG)$_2$ is performed by a cathodic scan, implying that no interference from common amalgam-forming metals will occur.[13] The only possible interferent is cobalt, which forms a complex with DMG and accumulates at the electrode surface in a similar way to nickel. However, the potential for reduction of Co(DMG)$_2$ is 0.15 V more negative

than for Ni(DMG)$_2$ and interference is only a problem when cobalt is present in much larger amounts than nickel. This is not so for nails or for almost any other material of biological origin.

Experimental

Apparatus

A PAR Model 264 polarographic analyser, a PAR Model 303 standard mercury-drop electrode and a Kipp & Zonen Model B90 X - Y recorder were used. Instrument settings were as follows: drop size, medium; purge time, 4 min; initial potential, -0.7 V *vs.* Ag - AgCl; final potential, -1.30 V; pulse amplitude, 50 mV; clock time, 0.5 s; scan rate, 5 mV s^{-1}; adsorption time, 120 s; equilibration time, 30 s.

Reagents

The dimethylglyoxime used was of analytical-reagent grade, further purified by recrystallisation from 96% ethanol. All other chemicals, including the electrode mercury were of Suprapur grade (Merck, Darmstadt, FRG). Water was purified with a Milli-Q system (Millipore Corp., Bedford, MA, USA). Standard solutions were prepared from a certified 1 g l^{-1} nickel stock solution (Titrisol, Merck, Darmstadt, FRG).

Procedures

All glassware, plastic containers, utensils, etc., were soaked for several days in 7 M HNO$_3$ and then rinsed with Milli-Q water before use.

Finger- and toenails were cut with a common nail cutting instrument (Trim cutter, Basset Corp., Derby, CT, USA) in amounts ranging from 11.3 to 57.6 mg directly into 5-ml calibrated borosilicate glass flasks, and 1 ml of concentrated HNO$_3$ and 0.1 ml of concentrated H$_2$SO$_4$ were added. The flasks were subsequently placed in a sand-bath and heated to 170 °C overnight. This resulted in clear solutions with virtually no HNO$_3$ present. Finally, the solutions were neutralised with 0.6 ml of 25% ammonia solution and made up to volume with water. Reagent blanks were subjected to the same procedure. A 1-ml aliquot of digested solution was mixed in the electrochemical cell with 1 ml of ammonia buffer (pH 9.2), 10 µl of 0.1 M dimethylglyoxime in ethanol and 8 ml of water and was analysed after deaeration with purified nitrogen by means of ADPV. Three standard additions were used for the quantitation. The analyses were carried out in a normal

Table 1. Nickel in nails from unexposed subjects (1–5) ($\mu g\ g^{-1}$)

Sample	Subject				
	1	2	3	4	5
Left hand	3.38	5.08	1.57		
Left hand 2 weeks later ..		3.06			
Right hand	1.40	3.06	1.96		
Right hand 2 weeks later		1.64			
Left foot	0.75	1.31			
Left foot 8 weeks later ..	0.24				
Right foot	1.04	0.55			
Pooled nails from both hands			1.87	2.85	
			1.22	1.19	
Broken off nail	0.65				1.00
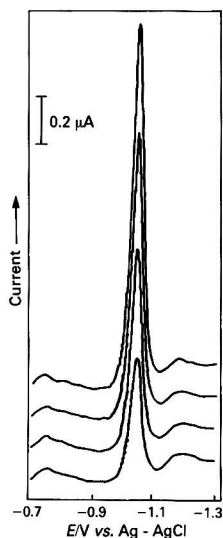
Fig. 1. Recorder traces of nickel in a digested nail sample. Three standard additions of 5 ng each yield a nickel concentration of 0.726 $\mu g\ l^{-1}$ ($r = 0.999\ 97$)

Table 2. Recovery of nickel added to reagent blanks and subjected to the digestion procedure

Amount added/ng	Amount found/ng	Recovery, %
10	9.96	99.6
20	20.51	102.6
30	30.61	102.0
40	39.56	98.9

Table 3. Determination of nickel in nails by ADPV and AAS

ADPV/$\mu g\ g^{-1}$	AAS*/$\mu g\ g^{-1}$	Deviation, %
1.96	2.08	3.0
1.31	1.48	6.1
3.06	3.86	11.6
1.64	1.63	0.3
1.19	1.34	5.9
0.248	0.392	22.5

* A Perkin-Elmer Zeeman 5000 spectrophotometer was used. The temperature programme was a slightly modified version of the one used in reference 15.

laboratory, but as many operations as possible took place in a laminar air flow clean-bench. The mercury-drop electrode was placed inside the clean-bench.

Results and Discussion

The results from the nail analyses are given in Table 1 and a typical voltammogram is shown in Fig. 1. Unless otherwise stated, the values originate from a pool of nails from the same hand or foot. The individuals donating the nails were not occupationally exposed to nickel. A blank value of 2.74 ± 0.60 ng per digestion has been subtracted from the results.

Over-all means of $2.14 \pm 1.20\ \mu g\ g^{-1}$ ($n = 14$, range 0.65–5.08 $\mu g\ g^{-1}$) for fingernails and $0.78 \pm 0.42\ \mu g\ g^{-1}$ ($n = 5$, range 0.24–1.31 $\mu g\ g^{-1}$) for toenails were obtained. This is in close agreement with results reported previously for fingernail analysis.[10–12]

Using ADPV Ostapzuk et al.[12] obtained a value of $0.240 \pm 0.020\ \mu g\ g^{-1}$ ($n = 2$), for nickel in toenails but it is not clear whether the nails analysed were obtained from one or two people. In any event, our results showed a wider variation for nickel in toenails than those of Ostapzuk et al.[12]

As seen from Table 1, there is a significant difference between the nickel levels in toe- and fingernails, which was also observed by Ostapzuk et al.; however, we did not find any dependence of the nickel levels in fingernails handedness in our admittedly limited number of samples. Subjects 1 and 2 showed the highest nickel content in their left-hand nails. Subject 2 was left-handed, subject 1 was not. Another feature that emerges from the results in Table 1 is the variation in the nickel content of nails with time. This has not to our knowledge been observed before, but further work is needed to establish the validity of the observation.

In sampling the nails it is of utmost importance that the cutting tool does not compromise the samples by contamination with nickel. We tested our nail cutter for release of ionic nickel by means of the dimethylglyoxime test: a piece of filter-paper was wetted with ammonia buffer (pH 9.2) and a few drops of 0.1 M dimethylglyoxime in 96% ethanol were added, the filter-paper was then rubbed against the specimen to be tested; with our nail cutter no reddening of the paper was observed, i.e., no nickel ions were released. As the dimethylglyoxime test cannot detect minute amounts of Ni^{2+}, we analysed, in addition, two fingernails that had been broken off without the use of the cutting instrument. The results are given in Table 1 and it is seen that the nickel content is lower in the broken off nails indicating some contamination from the cutter. The toenails, in contrast, were all cut off and had low nickel contents indicating no contamination from the nail cutter. Consequently, we believe that our samples are uncontaminated, and that the low values found for the broken off nails are due to individual variations between nails. This is corroborated by the fact that none of the broken off nails came from thumbs, which are known to be higher in nickel than other fingernails,[12,14] and that all of the pooled fingernail samples included thumbnails.

The precision of the voltammetric procedure was about 2.5%. A digested solution in the sub ng g^{-1} region whose concentration was measured three times, showed a mean of 0.201 ng g^{-1} with a standard deviation of 0.005 ng g^{-1} (range 0.196–0.206 ng g^{-1}). It was difficult to establish the accuracy of the method owing to the lack of a suitable reference material. Instead, a recovery experiment was carried out by adding standards to reagent blanks. The results are given in Table 2. It appears that the recovery is satisfactory, as the deviation from the true value does not exceed 2.6% in the concentration area of interest, i.e., concentrations in the ng g^{-1} region.

Some of the results were checked with an atomic-absorption spectrophotometric method (AAS) using Zeeman background correction. The results are given in Table 3. The differences between results obtained by ADPV and AAS ranged between 0.3 and 22.5%, the latter observed when the nickel concentration was very low. Further, the results found by AAS tended to be higher than those obtained by ADPV. The AAS method has a detection limit of 0.1 $\mu g\ l^{-1}$, for an

injection of 100 µl,[16] while the detection limit of ADPV is a 100-fold lower.[13] This implies that reagent blanks cannot be quantitated by AAS and that AAS-results in the sub-ng g^{-1} area are questionable. As a consequence samples that have low concentrations of nickel should be analysed by ADPV.

It can be concluded that the proposed procedure, based on a simple wet digestion followed by quantitation by ADPV, is a convenient, dependable and precise method for the determination of nickel in human nails yielding results that are in agreement with literature values. A study, utilising the procedure with the purpose of assessing whether the analysis of nails is an appropriate indication of the exposure to nickel, is in progress, and will be reported elsewhere.

References

1. Nriagu, J. O., *Editor*, "Nickel in the Environment," Wiley, New York, 1980.
2. Brown, S. S., Nomoto, S., Stoeppler, M., and Sunderman, F. W., *Pure Appl. Chem.*, 1981, **53**, 773.
3. Hassler, E., Lind, B., Nilsson, B., and Piscator, M., *Ann. Clin. Lab. Sci.*, 1983, **13**, 217.
4. Bernacki, E. J., Zygowicz, E., and Sunderman, F. W., *Ann. Clin. Lab. Sci.*, 1980, **10**, 33.
5. Høgetveit, A. Ch., Barton, R. Th., and Kostøl, C. O., *Ann. Occup. Hyg.*, 1978, **21**, 113.
6. Rahkonen, E., Junttila, M.-L., Kalliomäki, P. L., Olkinouora, M., Koponen, M., and Kalliomäki, K., *Int. Arch. Occup. Environ. Health*, 1983, **52**, 243.
7. Stoeppler, M., *in* Nriagu, J. O., *Editor*, "Nickel in the Environment," Wiley, New York, 1980, p. 661.
8. Sunderman, F. W., *Pure Appl. Chem.*, 1980, **52**, 527.
9. Sunderman, F. W., *Ann. Clin. Lab. Sci.*, 1977, **7**, 377.
10. Alder, J. F., and Batoreau, M. C. C., *Anal. Chim. Acta*, 1983, **155**, 199.
11. Lindemayr, H., *Hautarzt*, 1984, **35**, 292.
12. Ostapczuk, P., Valenta, P., Stoeppler, M., and Nürnberg, H. W., *in* Brown, S. S., and Savory, J., *Editors*, "Chemical Toxicology and Clinical Chemistry of Metals," Academic Press, London, 1983, p. 61.
13. Pihlar, B., Valenta, P., and Nürnberg, H. W., *Fresenius Z. Anal. Chem.*, 1981, **307**, 337.
14. Gammelgaard, B., *PhD Thesis*, Royal Danish School of Pharmacy, Copenhagen, Denmark, 1985, in preparation.
15. Molin Christensen, J., and Kirchoff, M., *in* Brown, S. S., and Sunderman, F. W., *Editors*, "Progress in Nickel Toxicology," Blackwell, Oxford, 1985, p. 125.
16. "Analytical Methods for Atomic Absorption Spectrophotometry," Perkin-Elmer Corporation, CT, USA, January 1982, p. 12.3.

Amperometric Flow Injection Determination of Ethylenediaminetetraacetic Acid (EDTA) at an Electrochemically Pre-treated Glassy Carbon Electrode

Arnold G. Fogg
Chemistry Department, Loughborough University of Technology, Loughborough, Leicestershire LE11 3TU, UK

Miguel A. Fernández-Arciniega
Departamento de Química Analítica, Universidad Autonoma, 28034 Madrid, Spain

and Rosa M. Alonso
Departamento de Química, Universidad del Pais Vasco, Bilbao, Spain

Ethylenediaminetetraacetic acid (EDTA) is determined in 0.1 M sulphuric acid by flow injection analysis using amperometric detection at a glassy carbon electrode held at 1.25 V *versus* S.C.E. The signal at the glassy carbon electrode is increased about eight-fold by pre-treating the electrode by holding it first at 2.0 V for 2 min and then at −0.50 V for 2 min whilst eluent is flowing. Calibration graphs are rectilinear in the range 0.01 to 10 μg ml⁻¹ of the disodium salt.

Keywords: *Flow injection analysis; EDTA determination; glassy carbon electrode; electrochemical pre-treatment*

The disodium salt of ethylenediaminetetraacetic acid (EDTA) is used widely throughout industry owing to its outstanding complexing properties.[1] The anodic voltammetric behaviour of EDTA has been studied by several workers at platinum electrodes,[2-5] paraffin-impregnated graphite electrodes[6] and glassy carbon electrodes.[7] The rectilinearity of the calibration graphs is reported either to be poor, or to be good over only a very narrow range, thus limiting severely any proposed methods based on amperometric detection.

In recent studies in this laboratory EDTA was found to interfere in the oxidative determination of sulphite at a glassy carbon electrode.[8] Using a newly polished glassy carbon electrode, minor interference to the sulphite signal by EDTA present in the pharmaceutical samples being analysed was observed. Subsequently, the sulphite signal was shown to be improved by electrochemically pre-treating the electrode but this pre-treatment increased the EDTA signal even more substantially and made its interference intolerable. Studies of the amperometric determination of EDTA at a glassy carbon electrode are described here. The effect of various electrochemical pre-treatments on the signal size has been investigated and an improved amperometric flow injection method is recommended.

Experimental

A single-channel flow injection system was used.[9] Eluent, 0.1 M sulphuric acid in the final recommended procedure, was pumped through the system by means of an Ismatec Mini-S pump. Injections were made with a Rheodyne low pressure sample injection valve (5020) fitted with a 75-μl sample loop and connected to a laboratory-built amperometric detector by means of 1 m of 0.58-mm bore PTFE tubing. The amperometric detector,[9] which holds a Metrohm glassy carbon electrode in the wall-jet configuration, is used partly immersed in electrolyte of the same composition as the eluent. The platinum counter and saturated calomel reference electrodes are placed in this electrolyte to complete the three-electrode system. The potential of the glassy carbon electrode was maintained at the required potential by means of a PAR 174A polarographic analyser (Princeton Applied Research). Signals

were recorded on a Houston Instruments Omnigraphic 2000 x - y - t recorder. A single glassy carbon electrode was used to obtain the results given here.

Reagents

Sulphuric acid, 0.1 M (*eluent*). Add 5.6 ml of concentrated sulphuric acid to about 800 ml of water and dilute to 1 l.

Standard disodium ethylenediaminetetraacetate dihydrate solution, 100 μg ml⁻¹. Dissolve 0.100 g of disodium ethylenediaminetetraacetate dihydrate in water and dilute to 1 l. More dilute solutions are prepared from this.
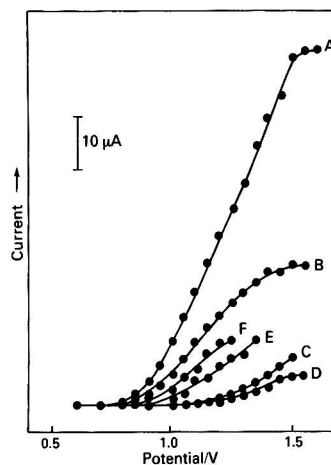
Fig. 1. Hydrodynamic voltammograms for EDTA in various media after electrochemical pre-treatment of the glassy carbon electrode. A, 0.1 M sulphuric acid; B–F, Britton - Robinson buffer (B pH 3, C pH 5, D pH 7, E pH 9 and F pH 11)

Results

Effect of pH on the Hydrodynamic Voltammograms for the Oxidation of EDTA at the Glassy Carbon Electrode

The oxidation of EDTA was studied in 0.1 M sulphuric acid and in Britton - Robinson buffers of pH 3, 5, 7, 9 and 11. A flow-rate of 5.5 ml min⁻¹ was used in these experiments. Studies in neutral or alkaline solution showed very little response from EDTA. In an attempt to obtain a greater response, electrochemical pre-treatment was tried using the method described by Engstrom et al.,[10,11] viz. polishing the electrode for 1 min with very fine alumina (0.015–0.3 μm) followed by pre-treatment for 5 min at +1.75 V and then for 1 min at −1.00 V. In acidic solution this produced a better response but in neutral and alkaline solutions, although an increase in response was observed, the reproducibility of the signal was very poor. This latter situation was improved by conditioning the electrode on-line in 0.1 M sulphuric acid and then switching to the buffer solution to be studied.

Hydrodynamic voltammograms at different pH values were obtained in this way, polishing the electrode and conditioning it in 0.1 M sulphuric acid before making the study at each new pH value. The hydrodynamic voltammograms are shown in Fig. 1. Clearly, the most satisfactory signals were obtained in 0.1 M sulphuric acid and this medium was used in all subsequent studies. The least response was obtained at near-neutral pH 5 and at pH 7 with some slight increase in response being apparent again in alkaline conditions, i.e., pH 9 and 11.

Optimisation of the Electrochemical Pre-treatment

Injections of 75 μl of a 100 μg ml⁻¹ solution of EDTA into 0.1 M sulphuric acid eluent were made in these studies. Measurements were made at 1.25 V, as at higher potentials the background current increased markedly and difficulties were experienced in measuring the low concentrations of EDTA that might need to be determined in the final method.
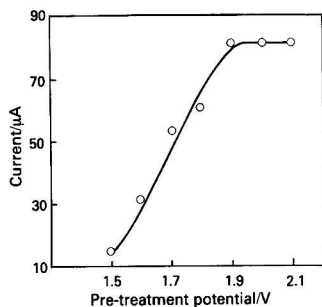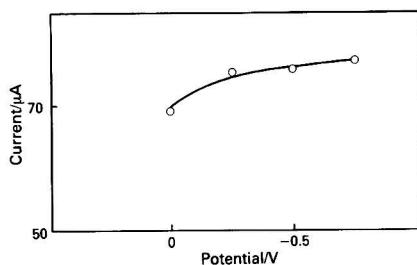
The effect of the positive potential used in the pre-treatment was studied first. At each potential the electrode was polished with alumina and then pre-treated at the chosen positive potential for 2 min and then at −0.50 V for 1 min. The potential of the electrode was then adjusted to 1.25 V, the base line was allowed to stabilise for 3 min and the signals were recorded on injecting EDTA. Conditioning potentials from 1.5 to 2.1 V were studied and the results are shown in Fig. 2. An increase in signal up to a conditioning potential of 1.9 V is clearly seen; the signal remained at a steady maximum value from 1.9 to 2.1 V and a conditioning potential of 2.0 V was used in all subsequent experiments.

The effect of the negative potential used in the pre-treatment was studied next. In this experiment at each potential studied the electrode was polished with alumina and was then electrochemically pre-treated for 2 min at +2.0 V and then at various potentials from 0 to −0.6 V for 1 min. The effect of omitting the negative potential pre-treatment was also studied. The results are shown in Fig. 3. Clearly, the effect of the pre-treatment at this second potential is not as marked as that at the more positive potential. Nevertheless, a slight increase in signal is observed when the second potential pre-treatment is used and the use of a pre-treatment of −0.5 V for 1 min was adopted. The maximum signal obtained in this study of the effect of the negative potential used was slightly lower than that obtained in the other studies. The reason for this is not known.

The optimum time of pre-treating the electrode at +2.0 V was next studied using a 1-min pre-treatment at −0.5 V. The results shown in Fig. 4 indicate a sharp increase in signal up to 1 min, above which a constant signal was obtained; a 2-min pre-treatment at 2.0 V is recommended. Using this 2-min pre-treatment at 2.0 V, the effect of the length of time the electrode is held at −0.50 V was next studied (Fig. 5). With a minimum 1-min pre-treatment time a constant maximum

Fig. 2. Effect of positive potential pre-treatment. Current, 10.1 μA when no positive potential pre-treatment was applied

Fig. 3. Effect of negative potential pre-treatment. Current, 65.2 μA when no negative potential pre-treatment was applied
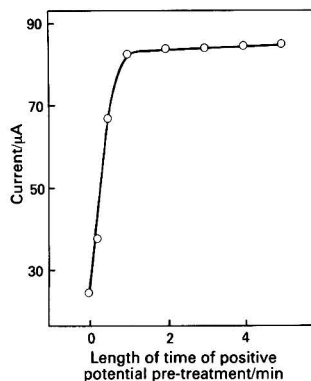
Fig. 4. Effect of the length of time of positive potential pre-treatment
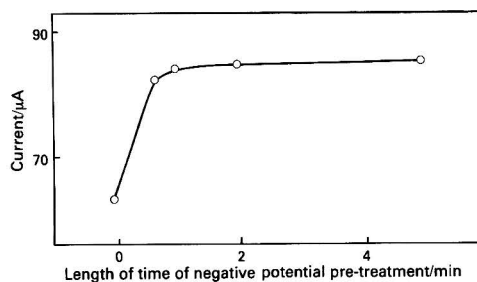
Fig. 5. Effect of the length of time of negative potential pre-treatment

1203

Table 1. Effect of flow-rate

Flow-rate/ml min^{-1}	..	..	1.7	2.6	4.1	4.9	5.8	7.0
Current/µA	..	..	41.6	52.8	61.6	69.6	72.8	72.0
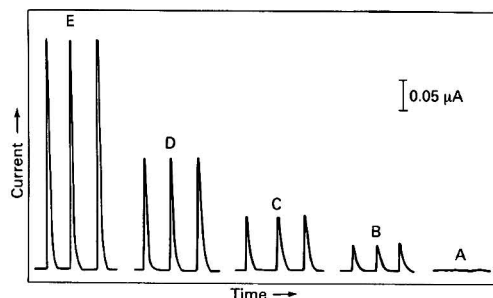
Fig. 6. Signals obtained for constructing a calibration graph for determining EDTA after electrochemical pre-treatment of the electrode. EDTA (disodium salt) concentration: A, 0; B, 0.1; C, 0.2; D, 0.4; and E, 0.8 µg ml^{-1}

signal was obtained, but a 2-min pre-treatment time was adopted subsequently.

The electrochemical pre-treatment of the glassy carbon electrode in a flowing stream of 0.1 M sulphuric acid after polishing is recommended as 2 min at 2.0 V followed by 2 min at −0.5 V.

Effect of Flow-rate

The effect of flow-rate on the signal using the optimised conditioning technique is shown in Table 1. The signal changes relatively little at flow-rates above about 5.5 ml min^{-1}. A flow-rate of 6.0 ml min^{-1} was chosen for the final method.

Calibration Graphs and Precision

Calibration graphs were rectilinear from 0.01 to 10 µg ml^{-1} using the recommended technique including the recommended electrochemical pre-treatment of the electrode. Calibration graphs obtained with an untreated electrode were also rectilinear up to about 10 µg ml^{-1}, but the detection limit was only about 0.1 µg ml^{-1}. Typical signals obtained with the pre-treated electrode in the range 0–0.8 µg ml^{-1} of the disodium salt are shown in Fig. 6. The coefficient of variation at the 0.8 µg ml^{-1} level was 1.8% (ten injections). After considerable use, some decrease in the signal was observed; the electrode was then cleaned, pre-treated again and re-calibrated.

Discussion

A technique has been optimised for pre-treating a glassy carbon electrode that can be used for the oxidative determination of EDTA. This has allowed a satisfactory flow injection method of determining EDTA to be developed.

Electrochemical or chemical pre-treatment of carbon electrode surfaces improves the electrode performance in many applications by increasing the electron transfer rate and producing a more reversible electrode reaction. Better shaped and more reproducible voltammograms are obtained. Treatment is believed to result in an increase in the number of surface quinone and carbonyl groups that seem to catalyse the oxidation or reduction of the species of interest in solution. Bleadel and Jenkins[12] showed that alternate treatment at 1.35 and −1.35 V lowered the potential at which NADH is oxidised and improved the shape of the voltammogram at a rotating glassy carbon electrode. Electrochemical pre-treatment of

carbon fibre electrodes is particularly important in neuro-scientific studies to separate the ascorbic acid and catechol-amine peaks.[13] Van Rooijen and Poppe[14] have discussed the electrochemical reactivation of solid electrodes used in electrochemical detection for high-performance liquid chromatography (HPLC) and flow injection analysis (FIA). Particularly good examples of the effect of electrochemical pre-treatment are given by Engstrom and co-workers[10,11] who studied hydroquinone, hexacyanoferrate(II) and hydrazine oxidation at glassy carbon electrodes. Treatment involved periods at high positive (1.5 V) potentials and then at negative potentials. For hydroquinone, positive potential pre-treatment alone was sufficient to produce a good voltammo-gram. For hexacyanoferrate(II), positive potential pre-treatment alone reduced the signal whereas using both potential pre-treatments an excellent signal was obtained. The most marked change occurred with hydrazine: positive potential pre-treatment increased an almost non-existent signal markedly and this was improved further by using both potentials. Ravichandran and Baldwin[15] have observed similar effects with hydrazine derivatives.

The oxidation studies described here illustrate well the gains that can be made from electrochemical pre-treatment of glassy carbon electrodes. Clearly, the possibility of electrochemical pre-treatment should be borne in mind when developing high-performance liquid chromatography - electrochemical detection and flow injection amperometric methods, and other voltammetric methods.

This method appears to be suitable for the determination of EDTA added as a stabiliser to pharmaceutical and other products, providing that other constituents do not interfere. The method clearly could be adapted for use with HPLC and for determining EDTA in a variety of commercial products including washing powders.

The effect of the presence of large amounts of metal ions has not been studied extensively but the addition of 200 µg ml^{-1} of magnesium or zinc sulphate heptahydrates did not interfere with the determination of 2 µg ml^{-1} of disodium ethylene-diaminetetraacetate dihydrate in 0.1 M sulphuric acid. Relatively few metal ions are complexed extensively by EDTA at pH 1, but in applications where strongly complexed metals are present the effect on the signal should be studied. Kinetic processes affect the polarographic reduction of cadmium in the presence of EDTA at pH values where complex formation occurs, and similar processes could possibly affect the present amperometric signals.

The oxidation mechanism has not been studied in detail here. Previous workers[7] indicate that carbon dioxide is produced first and then formaldehyde and various amines. It was considered whether the carbon–carbon bond in the ethylenediamine moiety might be split but nitrilotriacetic acid is oxidised at 1.25 V giving a peak about a quarter the size of that of EDTA, and ethylene glycol is not oxidised. Thus it seems unlikely that the carbon–carbon bond is split in the oxidation of EDTA at glassy carbon. Clearly, methods of analysis can be developed for the determination of EDTA analogues.

References

1. "Kirk-Othmer Encyclopoedia of Chemical Technology," Third Edition, Wiley, New York, 1984.
2. Kopecka, L., *Chem. Listy*, 1956, **50**, 1084.
3. Usatenko, Y. I., and Vitkina, A. M., *Nauchn. Dokl. Vyssh. Shk. Khim. Khim. Tekhnol.*, 1958, 502.
4. Reishakhrit, L. S., Martynova, V. N., and Tichnova, Z. I., *Vestn. Leningr. Univ.*, 1965, **20**, 146.

5. Štulík, K., and Vydra, F., *J. Electroanal. Chem.*, 1968, **16**, 385.
6. Terenteva, E. A., and Bernkaya, B. V., *Zh. Anal. Khim.*, 1966, **21**, 870.
7. Petak, P., and Vydra, F., *J. Electroanal. Chem.*, 1971, **33**, 161.
8. Fogg, A. G., Fernández-Arciniega, M. A., and Alonso, R. M., *Analyst*, 1985, **110**, 851.
9. Fogg, A. G., and Summan, A. M., *Analyst*, 1984, **109**, 1029.
10. Engstrom, R. C., *Anal. Chem.*, 1982, **54**, 2310.
11. Engstrom, R. C., and Strasser, V. A., *Anal. Chem.*, 1984, **56**, 136.
12. Blaedel, W. J., and Jenkins, R. A., *Anal. Chem.*, 1975, **47**, 1337.
13. Gonon, F. G., Fombarlet, C. M., Buda, M. J., and Pujol, J. F., *Anal. Chem.*, 1981, **53**, 1386.
14. Van Rooijen, H. W., and Poppe, H., *Anal. Chim. Acta*, 1981, **130**, 9.
15. Ravichandran, K., and Baldwin, R. P., *Anal. Chem.*, 1983, **55**, 1782.

Semi-micro Determination of Fluorine in Organic Compounds by Oxygen Silica-flask Combustion and Gran-type Potentiometric Titration of Fluoride with Lanthanum Nitrate

Gareth J. Davies and Michael A. Leonard
Department of Analytical Chemistry, The Queen's University of Belfast, Belfast BT9 5AG, UK

A sufficient amount of organofluorine compound to yield about 7 mg of fluoride was burned in a 2-l silica flask filled with oxygen. After absorption of the combustion gases in water the solution was adjusted to pH 4.6 and titrated in a polythene beaker with 0.02 M lanthanum nitrate solution using a fluoride ion-selective electrode as an indicator and a calomel electrode as a reference. Use of a calibration graph based on sodium fluoride and Gran-type evaluation of the potentiometric data gave accurate results with a coefficient of variation of 0.17%.

Keywords: *Organofluorine determination; flask combustion; fluoride electrode; Gran plot*

The determination of fluorine in organic compounds by oxygen flask combustion[1–5,18] is beset with many difficulties, namely the high strength of the carbon–fluorine bond,[4–15] the high volatility of highly fluorinated compounds,[6,16,17,22] interaction of hot hydrofluoric acid vapour with aluminoborosilicate glass[8,13,14,16,19–22] and the poor precision of the usual visual fluoride titrations, which makes the detection of small losses uncertain. During the course of an investigation of a photometric fluoride titration[23] the senior author was struck by the magnificent and easily obtained precision of the potentiometric titration of fluoride with lanthanum nitrate using a fluoride electrode,[24–29] which he had included for comparison. At the same time other work in the department[36] was showing the very precise nature of Gran-type silver halide titrations; therefore, it was decided to combine these two methods with a silica-flask combustion, hopefully to produce a very precise method for organofluorine determination. After one minor setback our hopes were amply fulfilled.

Theory

A solution resulting from oxygen flask combustion of a paper-wrapped organic compound contains much dissolved carbon dioxide. With increase in pH the fraction present as carbonate increases and causes high results in the lanthanum titration owing to precipitation of lanthanum carbonate. At low pH values fluoride is present largely as undissociated hydrofluoric acid yielding low results.[26] Examination of the dissociation equilibria of the carbonic acid and hydrofluoric acid systems shows that a good compromise pH where the fraction of fluoride F^-/ C_F = the fraction of carbonic acid $[H_2CO_3]/C_{CO_3} = 0.98$, is given by the equation

$$\frac{K_{a(HF)}}{[H^+] + K_{a(HF)}} = \frac{[H^+]^2}{[H^+]^2 + K_{a1}[H^+] + K_{a1}K_{a2}}$$

from which an optimum pH of 4.76 is obtained. [$K_{a(HF)} = 6.8 \times 10^{-4}$; $K_{a1(H_2CO_3)} = 4.45 \times 10^{-7}$; and $K_{a2(HCO_3^-)} = 4.69 \times 10^{-11}$].

Gran Function for the Fluoride - Lanthanum Titration

This has been treated by several workers[30–35] but for completeness a short version is given here. For the reaction

$$3F^- + La^{3+} \rightleftharpoons LaF_3 \downarrow$$
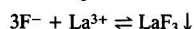
consider the titration of V_o cm^3 of fluoride solution of initial concentration C_{F_o} with lanthanum nitrate solution of concentration C_{La} using the fluoride electrode to monitor the titration. Then

$$C_{F_o}V_o = 3C_{La}V_e$$

where V_e is the equivalence-point volume. Neglecting the contribution to soluble fluoride of the lanthanum fluoride precipitate, before the equivalence point and after the addition of V cm^3 of lanthanum ($V < V_e$)

$$C_F = \frac{3C_{La}(V_e - V)}{V_o + V}$$

or

$$C_F(V_o + V) = 3C_{La}(V_e - V) \quad \ldots \quad \ldots \quad (1)$$

After the equivalence point ($V > V_e$)

$$C_F^3 = \frac{K_{sp}(V_o + V)}{C_{La}(V - V_e)}$$

or

$$(V_o + V)C_F^{-3} = \frac{(V - V_e)C_{La}}{K_{sp}} \quad \ldots \quad \ldots \quad (2)$$

where K_{sp} is the solubility product of lanthanum fluoride. C_F must now be related to potential readings taken during the course of the titration. The relevant Nernst equation may be written as follows:

$$E = a - 2.303\frac{RT}{F}\log C_F$$

where $a = (2.303\ RT/F) \log K_F^o$ and represents the sum of various fixed potentials in the system. Hence

$$E = 2.303\frac{RT}{F}\log\frac{K_F^o}{C_F}$$

and at 25 °C we may write

$$C_F = K_F^o \times 10^{-16.9E} \quad \ldots \quad \ldots \quad \ldots \quad (3)$$

Combining equations (1) and (3) gives

$$K_F^o \times 10^{-16.9E}(V_o + V) = 3C_{La}(V_e - V)$$

which can be rearranged to give

$$f_1 = \frac{3C_{La}(V_e - V)}{K_F^o} = 10^{-16.9E}(V_o + V)$$

from which a plot of $10^{-16.9E}(V_o + V)$ against V will yield a straight line that cuts the volume axis at V_e. Similarly, combining equations (2) and (3) we obtain

$$\frac{V_o + V}{(K_F^o)^3 \times 10^{-50.8E}} = \frac{(V - V_e)C_{La}}{K_{sp}}$$

which may be arranged to give

$$f_2 = \frac{C_{La}(K_F^o)^3(V - V_e)}{K_{sp}} = 10^{50.8E}(V_o + V)$$

Hence a plot of $10^{50.8E}(V_o + V)$ against V will yield a straight line that cuts the volume axis at V_e.

In practice we used only the before-equivalence function f_1 because ripening of the precipitate after equivalence caused a slow potential drift.

Experimental

Apparatus

A 16-year-old Orion fluoride ISE Model 94–09 was used as the indicator and an EIL calomel as the reference electrode. A Philips PW 9415 ion-selective digital meter was used to measure the potential difference. The pH was measured using separate glass and calomel electrodes in the usual way. Combustions were performed in a 2-dm³ conical silica flask with a B24 top made to order from Thermal Syndicate Ltd. The B24 stopper was fitted with a stout tungsten rod and platinum gauze of appropriate size; a 1-dm³ flask would be suitable. A 10-cm³ microburette with magnifying reader was used to dispense the titrant and a programmable calculator employed for linear regression analysis.

Reagents

Doubly distilled water was used throughout.

Lanthanum nitrate solution, 0.02 M. Dissolve 17.3208 g of BDH GPR-grade La(NO₃)₃.6H₂O in water and dilute to 2 dm³.

Sodium fluoride solution, 0.0200 M. Dry BDH analytical-reagent grade sodium fluoride in an oven at 110 °C for 2 h. Dissolve 1.6788 g in water and dilute to 2 dm³. Store in a plastic bottle.

pH-adjustment solutions. Prepare 1, 0.1 and 0.01 M hydrochloric acid and sodium hydroxide solutions and store in suitable dropping bottles.

Preliminary Experimental Work

Before performing any organic compound analyses some preliminary studies were carried out to see if the above theoretical treatment occurred in practice. To this end solutions containing 7.60 mg of fluoride (20.00 cm³ of 0.0200 M) plus an equimolar amount of hydrogen carbonate were titrated as described in the basic method at a variety of pH values between 4 and 8. The true equivalence point was taken to be the mean of six parallel titrations of 7.60 mg of fluoride with no addition of hydrogen carbonate. The results were as follows: $V_e = 6.58 \pm 0.02$ cm³; coefficient of variation, 0.33%. Table 1 shows the results of the carbonate - pH study.

Fig. 1 shows the Gran plots at pH values of 4.0, 4.6 and 7.0. Equivalence-point values show the trend expected from theory. A pH of 4.6 was chosen for all subsequent analyses; at this pH the equivalence point was slightly sensitive to the hydrogen carbonate to fluoride ratio but insensitive to the area of paper burned in the flask.

Organofluorine Analysis

Weigh a sufficient amount of compound to yield about 7 mg of fluoride in a 3 × 3 cm square of Whatman No. 1 filter-paper. Burn in the oxygen flask over 20 cm³ of water in the usual way, then transfer the solution quantitatively, using three 5-cm³ rinsings, into a 150-cm³ plastic beaker. Adjust the pH to 4.6, mark the liquid level on the beaker, insert the electrodes and titrate potentiometrically with lanthanum nitrate solution using 0.2-cm³ increments. Obtain V_o by adding water to the beaker from a 50-cm³ burette. Plot a graph of $10^{-16.9E}(V_o + V)$ using linear-regression analysis to obtain the line of best fit and the x-axis intersection. Construct a calibration graph by pipetting in turn 5.00, 10.00, 15.00, 20.00 and 25.00 cm³ of 0.0200 M sodium fluoride (1.90, 3.80, 5.70, 7.60 and 9.50 mg of fluoride), plus water to bring the volume to at least 20 cm³, into the combustion flask. Burn a 3-cm square paper in the flask, then treat the resulting solution as above.

Results

Six replicate determinations on about 50 mg of MAR-grade 4-fluorobenzoic acid (%F = 13.56) gave a mean of 13.57 ± 0.02% at the 95% confidence level with a standard deviation of 0.02% and a coefficient of variation of 0.17%. Five determinations on approximately 16-mg amounts of MAR trifluoroacetanilide (%F = 30.13) gave a mean of 30.14 ± 0.05%, a standard deviation of 0.04% and a coefficient of variation of 0.14%. Hence the determined means equalled the true values with very high certainty.

Discussion

Before the final method was developed a set of seven replicate analyses of about 50 mg of 4-fluorobenzoic acid in which the titrations were carried out in a 150-cm³ Pyrex beaker gave a mean of 13.35 ± 0.08% and a standard deviation of 0.09%. The mean is very significantly different from the true value of 13.56%; hence Pyrex equipment should not be used for the combustion or for the titration.
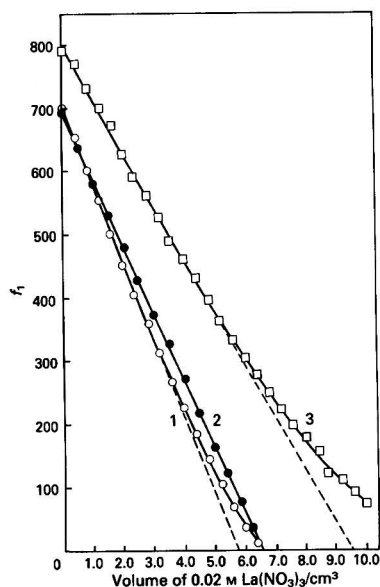
Fig. 1. Gran plots for the titration of 4×10^{-4} mol (7.60 mg) of fluoride and 4×10^{-4} mol of hydrogen carbonate with 0.02 M lanthanum nitrate at 1, pH 4.0; 2, pH 4.6; and 3, pH 7.0. Initial volume 40 cm³. $f_1 = 10^{-16.9E}(V_o + V)$

Table 1. Results of carbonate - pH study

pH	4.0	4.2	4.6	4.8	5.0	5.2	5.4	6.0	7.0
V_e	5.72	6.28	6.56	6.54	6.62	6.53	6.63	7.11	9.54

As this work constituted an MSc project, time was, regretfully, not available to examine a wide range of fluorine compounds but for suitable materials the method is undoubtedly very precise even in the hands of an inexperienced but very competent student and the results inspire confidence. The method would be useful for investigating the complete decomposition of $-CF_3$ or perfluorocyclohexane-type compounds and assessing the value of combustion aids.

References

1. Schöniger, W., *Mikrochim. Acta*, 1955, 123.
2. Macdonald, A. M. G., *Analyst*, 1961, **86**, 3.
3. Meslans, M., *Bull. Soc. Chim. (Paris)*, 1893, **9**, 109.
4. Schöniger, W., *Mikrochim. Acta*, 1956, 872.
5. Soep, H., *Nature (London)*, 1961, **192**, 67.
6. Rittner, R. C., and Ma, T. S., *Mikrochim. Acta*, 1972, 404.
7. Mazor, L., "Analytical Chemistry of Organic Halogen Compounds," Pergamon Press, Oxford, 1975, p. 21.
8. Rogers, R. N., and Yasuda, S. K., *Anal. Chem.*, 1959, **31**, 616.
9. Ferrari, H. J., Geronimo, F. C., and Brancone, L. M., *Microchem. J.*, 1961, **5**, 617.
10. Senkowski, B. Z., Wollish, E. G., and Shafer, E. G. E., *Anal. Chem.*, 1959, **31**, 1574.
11. Belcher, R., Leonard, M. A., and West, T. S., *J. Chem. Soc.*, 1959, 3577.
12. Steyermark, A., Kaup, R. R., Petras, D. A., and Bass, E. A., *Microchem. J.*, 1959, **3**, 523.
13. Light, T. S., and Manion, R. F., *Anal. Chem.*, 1969, **41**, 107.
14. Shearer, D. A., and Morris, G. F., *Microchem. J.*, 1970, **15**, 199.
15. Macdonald, A. M. G., *in* Riley, C. N., *Editor* "Advances in Analytical Chemistry and Instrumentation," Volume 4, pp. 100–103.
16. Fernandopulle, M. E., and Macdonald, A. M. G., *Microchem. J.*, 1966, **11**, 41.
17. Kirsten, W. J., *Microchem. J.*, 1963, **7**, 34.
18. Macdonald, A. M. G., *Pure Appl. Chem.*, 1976, **45**, 31.
19. Johnson, C. A., and Leonard, M. A., *Analyst*, 1961, **86**, 101.
20. Olsen, E. C., and Shaw, S. R., *Microchem. J.*, 1961, **5**, 101.
21. Burroughs, J. E., Kator, W. G., and Attla, A. I., *Anal. Chem.*, 1968, **40**, 657.
22. Ma, T. S., and Rittner, R. C., "Modern Organic Elemental Analysis," Marcel Dekker, New York, 1979, p. 158.
23. Asea, P. E. A., and Leonard, M. A., *Analyst*, 1984, **109**, 395.
24. Frant, M. S., and Ross, J. W., *Science*, 1966, **154**, 1553.
25. Lingane, J. J., *Anal. Chem.*, 1967, **39**, 881.
26. Francis, H. J., Deonarine, J. H., and Persing, D. D., *Microchem. J.*, 1969, **14**, 580.
27. Anfält, T., and Jagner, D., *Anal. Chim. Acta*, 1970, **50**, 23.
28. Lingane, J. J., *Anal. Chem.*, 1968, **40**, 935.
29. Eriksson, T., and Johansson, G., *Anal. Chim. Acta*, 1970, **52**, 465.
30. Gran, G., *Analyst*, 1952, **77**, 661.
31. Anfält, T., Dyrssen, D., and Jagner, D., *Anal. Chim. Acta*, 1968, **43**, 487.
32. Eriksson, T., *Anal. Chim. Acta*, 1972, **58**, 437.
33. Burden, S. L., and Euler, D. E., *Anal. Chem.*, 1975, **47**, 793.
34. Jagner, D., and Aren, K., *Anal. Chim. Acta*, 1976, **52**, 491.
35. Svehla, G., "Automatic Potentiometric Titrations," Pergamon Press, Oxford, 1978, p. 187.
36. Maitin, B., *PhD Thesis*, "Simultaneous Determination of Halogens," Queen's University, Belfast, 1982, p. 73.

Ionic Polymerisation as a Means of End-point Indication in Non-aqueous Thermometric Titrimetry

Part XII.* Acetals and Cyclic Ethers as End-point Indicators in the Titration of Organic Bases

Edward J. Greenhow and Mina Kashanipour
Analytical Chemistry Group, Department of Chemistry, Birkbeck College, University of London, Christopher Ingold Laboratories, 20 Gordon Street, London WC1E 6BT, UK

Dimethoxymethane, 1,3,5-trioxane, 1,3-dioxolane and alicyclic ethers with three- to seven-membered rings were evaluated as thermometric end-point indicators in the non-aqueous titration of weak organic bases including some basic drugs, in the free form and as hydrochlorides, phosphate and tartrate, with perchloric acid in acetic acid.

All the indicators except the three and four-membered-ring cyclic ethers give sharp end-point inflections in titrations of quinuclidine and 8-hydroxyquinoline, but for caffeine only the acetal indicators are satisfactory. Relative standard deviations obtained in replicate determinations of 0.1-mequiv. amounts range from 0.10 to 0.66%, with sample and titrant delivery errors making a significant contribution.

In the drug titrations, the acetal indicators give the sharpest end-point inflections for chloroquine phosphate. Only 1,3-dioxolane is a suitable indicator for the adrenaline hydrogen tartrate titration. The perchloric acid titrant is effective only in the presence of acetic anhydride, when it functions as acetyl perchlorate. Boron trifluoride etherate in 1,4-dioxane can also be used as the titrant/catalyst but is less effective in terms of end-point sharpness.

Keywords: *Non-aqueous catalytic thermometric titrimetry; ring-opening cationic polymerisation; acetals; cyclic ethers; basic drugs*

It was shown in Part I[1] that the rapid rise in temperature resulting from the exothermic cationic polymerisations of α-methylstyrene and isobutyl vinyl ether, catalysed at ambient temperature by perchloric acid in acetic acid and boron trifluoride etherate in 1,4-dioxane, respectively, can be used to indicate the end-point in the titration of organic bases with these catalyst solutions. More recently, it has been shown[2] that the presence of acetic anhydride in the solvent system improves the sharpness of the end-point inflection.

Other substances known to undergo cationic polymerisation reactions readily when perchloric acid and boron trifluoride etherate in non-aqueous solution are employed as catalysts include the cyclic acetals 1,3,5-trioxane (I) and 1,3-dioxolane
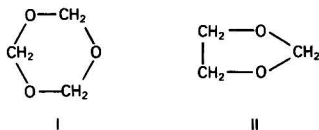
(II), and also the cyclic ethers oxetane (trimethylene ether) and tetrahydrofuran.[3,4]

Polymerisation is initiated by the addition of a cation or Lewis acid to the ring oxygen, followed by the fission of the ring C–O bond. According to Jaacks and Kern,[5] catalyst efficiency in the ring-opening cationic polymerisation of 1,3,5-trioxane in cyclohexane at 60 °C, in terms of conversion in a given reaction time, decreases in the following order: $CH_3CO^+ClO_4^- > FeCl_3 > SnCl_4 > BF_3 \cdot OEt_2 > SbCl_5 \gg H_2SO_4$.

It has been shown conclusively[6-9] that the most efficient of these catalysts, acetyl perchlorate, is formed when acetic

anhydride is added to perchloric acid in acetic acid solution, according to the following equation:

$$HClO_4 + (CH_3CO)_2O \rightleftharpoons CH_3CO^+ClO_4^- + CH_3COOH \quad (1)$$
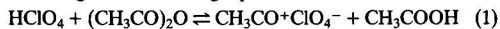
and the reaction proceeds rapidly to the right.[6]

In this study, 0.1 M perchloric acid in acetic acid is used as the titrant/catalyst to evaluate the efficiency of cyclic, and linear, acetals and cyclic ethers as end-point indicators in the catalytic thermometric titration of nitrogen bases, including the very weak base caffeine ($pK_b = 13.39$) and some basic drug substances in their free form and as hydrochlorides, phosphate and tartrate. It has been shown[11] that it is not necessary to add mercury(II) acetate in the catalytic thermometric of base hydrochlorides because HCl does not interfere with end-point detection. The titrations are carried out in the presence and absence of acetic anhydride to establish whether the acetyl perchlorate formed is more effective than perchloric acid as the catalyst. Boron trifluoride etherate in 1,4-dioxane was also evaluated as a titrant/catalyst.

Experimental

Reagents

Perchloric acid (71.0–73.0%), acetic anhydride, acetic acid, formic acid (98–100%), toluene, 1,4-dioxane and 8-hydroxyquinoline were analytical-reagent grade materials. Boron trifluoride etherate, dimethoxymethane (99%), 1,3,5-trioxane (98%), 1,3-dioxolane (99.5%), 1,2-epoxybutane (99%), oxetane (trimethylene oxide) (97%), tetrahydrofuran (THF), tetrahydropyran (THP) (98%), oxepane (hexamethylene oxide), quinuclidine (99%), caffeine (99%) and adrenaline hydrogen tartrate (98.5%) were of laboratory-reagent grade. The commercial drug substances diazepam, chlordiazepoxide hydrochloride (librium hydrochloride), Tetracycline Hydrochloride BP and Chloroquine Phosphate BP were gifts.

A 0.1 M solution of perchloric acid in dry acetic acid was prepared from 71.0–73.0% perchloric acid, acetic acid and acetic anhydride by the method of Belcher *et al.*[10] A 0.1 M

---

solution of boron trifluoride etherate in 1,4-dioxane was prepared from redistilled $BF_3.OEt_2$ and 1,4-dioxane dried over a 4A molecular sieve.

Apparatus

Details of the automatic titration apparatus, in which titrant is introduced by means of a motor driven syringe and the temperature is measured by means of a thermistor, and recorded on a potentiometric chart recorder, were given elsewhere.[11] The titration vessel was a Dewar beaker (14 ml) and solutions were stirred with a magnetic stirrer.

Procedure

Prepare 0.1 or 0.05 M solutions of the bases and base hydrochlorides, phosphate and tartrate in toluene, acetic acid, acetic acid + formic acid or acetic anhydride as convenient. Add to 1 ml of the sample solution acetic anhydride and indicator reagent in amounts depending on the indicator reagent. Prepare the solution of the 1,3,5-trioxane in acetic anhydride separately and allow it to attain ambient temperature before adding it to the sample solution. Add titrant at the rate of about 0.2 ml min^{-1}. It is convenient to operate the chart recorder over the 0–100-mV range when the bridge circuit described in Part I[1] is used. Measure the "maximum" temperature attained with a 0–120 °C thermometer, 30 s after completion of the titration.

The end-point of the titration is located on the titration graph as the point where the tangent to the main heat rise leaves the curve at its lower temperature end,[12] as shown in Fig. 1.

Results and Discussion

In Figs. 1, 2 and 3 are shown the titration curves obtained when quinuclidine, 8-hydroxyquinoline and caffeine are titrated with the 0.1 M perchloric acid reagent, using di-methoxymethane, 1,3,5-trioxane, 1,3-dioxolane, THF, THP and oxepane as thermometric indicators. Additionally, in Fig. 2 is shown the titration curve for 8-hydroxyquinoline when oxetane is the indicator. No end-point inflections were obtained using the three-membered ring cyclic ether 1,2-epoxybutane as the indicator reagent and these titration curves have not been included in Figs. 1–3.

Quinuclidine, 8-hydroxyquinoline and caffeine were chosen for evaluating the indicator reagents as being representative of a reactive aliphatic tertiary amine, an aromatic heterocyclic amine and a very weak base ($pK_b = 13.39$), respectively.

In the titrand solution, the solvent system consisted of (a) the solvent used to prepare the 0.1 M sample solutions, namely acetic anhydride for the quinuclidine, toluene for the 8-hydroxyquinoline and acetic acid for the caffeine solution, (b) the thermometric indicator and (c) acetic anhydride. Acetic anhydride was included in the solvent system when it was established that in its absence the end-point inflection was poor or non-existent. The effect of acetic anhydride on end-point sharpness is shown in Fig. 4 for blank titrations and in Fig. 5 for titrations of 8-hydroxyquinoline. Only with 1,3-dioxolane as the indicator was it found possible to obtain a measurable end-point in the absence of acetic anhydride, and even with this indicator the end-point was much less sharp than when some acetic anhydride was present. The high reactivity of the 1,3-dioxolane made it necessary to use a relatively small amount of acetic anhydride to obtain efficient titrations, because with high proportions of acetic anhydride, e.g., equal volumes of 1,3-dioxolane and acetic anhydride, it was necessary to have very efficient, rapid stirring to prevent the indicator reaction from occurring prematurely.

The end-point inflection obtained with oxetane indicator in the titration of 8-hydroxyquinoline was not distinct (Fig. 2, E)
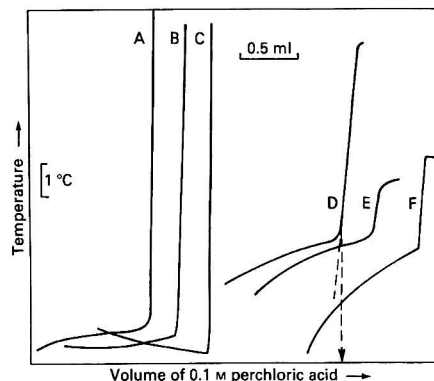
Fig. 1. Catalytic thermometric titration of quinuclidine with 0.1 M perchloric acid in acetic acid. Sample, 11.14 mg of quinuclidine in 1 ml of acetic anhydride. Indicator, ml (acetic anhydride, ml): A, dimethoxymethane, 2(3); B, 1,3,5-trioxane, 2(4); C, 1,3-dioxolane, 3.5(0.5); D, oxepane, 2(3); E, THF, 2(3); and F, THP, 2(3). Arrow shows end-point in D
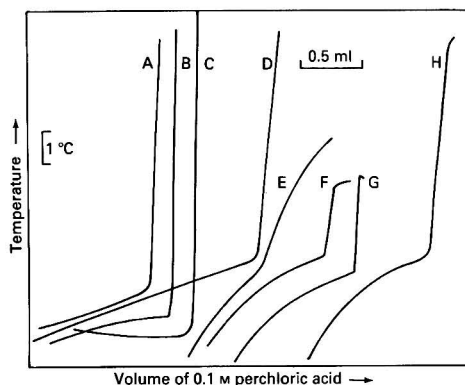
Fig. 2. Catalytic thermometric titration of 8-hydroxyquinoline with 0.1 M perchloric acid in acetic acid. Sample, 14.52 mg of 8-hydroxyquinoline in toluene. Indicator, ml (acetic anhydride, ml): A, 1,3,5-trioxane, 2(5); B, dimethoxymethane, 2(3); C, 1,3-dioxolane, 3.5(0.5); D 1,3,5-trioxane, 2(5) (sample, 29.04 mg in 2 ml of toluene); E, oxetane, 1(3.5) (sample, 7.26 mg in 0.5 ml of toluene); F, THF, 2(3); G, THP, 2(3); H, oxepane, 2(3)
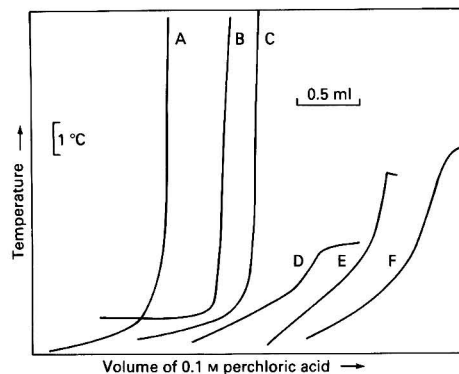
Fig. 3. Catalytic thermometric titration of caffeine with 0.1 perchloric acid in acetic acid. Sample: 19.42 mg of caffeine in 1 ml of acetic acid. Indicator, ml (acetic anhydride, ml): A, dimethoxymethane, 2(3); B, 1,3,5-trioxane, 2(4); C, 1,3-dioxolane, 3.5(1); D, THF, 2(3); E, THP, 2(3); F, oxepane, 2(4)

Table 1. Results for precision from the thermometric titration of organic bases with 0.1 M perchloric acid, using acetals and cyclic ethers as indicator reagents

Compound	Amount/mg	Indicator reagent*/ml	Solvent†/ml	Mean titre‡/ml	Standard deviation/ml	Relative standard deviation, %	Mean maximum temperature§/°C
Quinuclidine	11.14	M, 2	A, 4	1.021	0.00098	0.096	70
	11.14	T, 2 g	A, 5	1.020	0.0067	0.66	75
	11.14	D, 3.5	A, 1.5	0.9894	0.0050	0.51	103
	11.14	F, 2	A, 4	1.016	0.0066	0.65	22.5
	11.14	O, 2	A, 4	1.033	0.0041	0.40	24
8-Hydroxyquinoline . .	14.52	M, 2	A, 3; T, 1	1.044	0.0041	0.39	70
	14.52	T, 2 g	A, 4; T, 1	1.028	0.0042	0.41	60
	14.52	D, 3.5	A, 0.5; T, 1	1.037	0.0022	0.21	59
	14.52	F, 2	A, 3; T, 1	1.034	0.0047	0.45	25
	14.52	P, 2	A, 3; T, 1	1.013	0.0061	0.60	25
	14.52	O, 2	A, 3; T, 1	1.055	0.0066	0.63	30
Caffeine	19.42	M, 2	A, 3; Ac, 1	0.984	0.0043	0.44	71
	19.42	T, 2 g	A, 5; Ac, 1	1.082	0.0064	0.59	87
	19.42	D, 3.5	A, 1.5; Ac, 1	1.007	0.0042	0.42	76
	19.42	F, 2	A, 3; Ac, 1	0.929	0.0029	0.31	24
	19.42	P, 2	A, 3; Ac, 1	0.966	0.0061	0.63	25
	19.42	O, 2	A, 4; Ac, 1	0.941	0.0055	0.58	28

* M = dimethoxymethane; T = 1,3,5-trioxane; D = 1,3-dioxolane; F = THF; P = THP; O = oxepane.

† A = acetic anhydride; T = toluene; Ac = acetic acid.

‡ Four determinations.

§ 30 s after completion of titration (ambient temperature 19–20 °C).
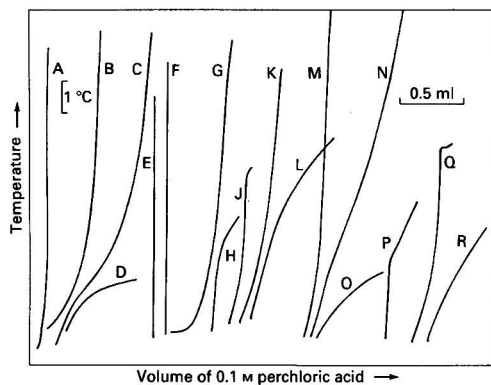
Fig. 4. Effect of acetic anhydride on end-point sharpness in blank titrations with 0.1 M perchloric acid in acetic acid. Indicator, ml (acetic anhydride, ml): A, dimethoxymethane, 2(4); B, dimethoxymethane, 4(2); C, dimethoxymethane, 4(0.5); D, dimethoxymethane, 4(0); E, 1,3-dioxolane, 2(3); F, 1,3-dioxolane, 2(2); G, 1,3-dioxolane4(0); H, THF, 2(4); J, THF, 4(3); K, THF, 4(1); L, THF, 4(0); M, oxepane, 2(3); N, oxepane, 4(0.5); O, oxepane, 4(0); P, THP, 2(3); Q, THP, 4(0.5); and R, THP, 4(0)

Fig. 5. Effect of acetic anhydride on end-point sharpness in the titration of 8-hydroxyquinoline with 0.1 M perchloric acid in acetic acid. Sample: 14.52 mg of 8-hydroxyquinoline in toluene. Indicator, ml (acetic anhydride, ml): A, 1,3-dioxolane, 3.5(0.5); B, 1,3-dioxolane, 4(0); C, 1,3,5-trioxane, 2(5); D, 1,3,5-trioxane, 2(0.5) (+3.5 ml of toluene); E, 1,3,5-trioxane, 2(0) (+4 ml of toluene); F, THF, 2(3); G, THF, 4(0); H, THP, 2(3); J, THP, 4(0.5)

and no further titrations were carried out with this reagent. Apparently, only cyclic ethers with five-membered rings or larger appear to undergo reaction suitable for end-point indication.

The need for acetic anhydride in these titrations with perchloric acid confirms the earlier views[6–9] that acetyl perchlorate is formed readily when perchloric acid in acetic acid is mixed with acetic anhydride, as it is known that acetyl perchlorate is a very effective catalyst for ring-opening polymerisations.[5]

The "maximum" temperatures that occur during the indicator reactions are noted in Table 1. It can be seen that these range from 60 to 103 °C for the acetal reagents but are much lower for the cyclic ethers, usually only 4 or 5 °C above ambient for THF and THP and up to 13 °C above ambient for

oxepane. The shape of the cyclic ether titration curves suggests that the reaction is inhibited soon after its initiation.

Figs. 1–3 show that both the acetal indicators and THF, THP and oxepane give satisfactory end-point inflections for quinuclidine and 8-hydroxyquinoline but only the acetals are suitable for the determination of the very weak base caffeine.

A 0.1 M solution of boron trifluoride etherate in 1,4-dioxane was evaluated as a titrant for quinuclidine, 8-hydroxyquinoline and caffeine, using the acetals as indicator reagents. In all instances, very rounded end-point "inflections" were obtained, and the blank titration curves, also showing rounded end-point inflections, gave significant titration values. This confirmed that the boron trifluoride reagent is much less efficient than acetyl perchlorate as a catalyst for the acetal polymerisations, and it was not evaluated further as a titrant.

The precision values, reported as relative standard deviations, obtained for four replicate titrations of the three
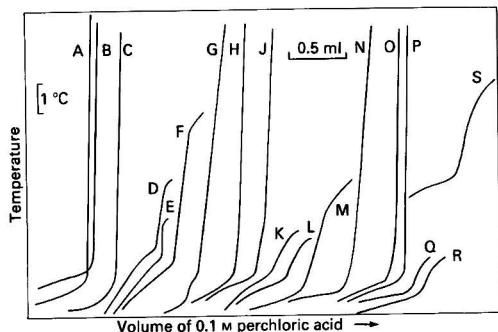
Fig. 6. Catalytic thermometric titration of diazepam, librium hydrochloride and tetracycline hydrochloride with 0.1 M perchloric acid in acetic acid. Samples: I, 14.22 mg of diazepam in 1 ml of Ac₂O (A–F); II, 16.81 mg of librium hydrochloride in 2 ml of AcOH (G–M); and III, 24.07 mg of tetracycline hydrochloride in 2 ml of AcOH (N–S). Indicator, ml (acetic anhydride, ml): A, 1,3,5-trioxane, 2 g (4); B, dimethoxymethane, 2(3); C, 1,3-dioxolane, 3.5(0.5); D, THF, 2(3); E, THP; 2(3); F, oxepane, 2(4); G, 1,3,5-trioxane, 2 g (4); H, dimethoxymethane, 2(3); J, dimethoxymethane, 3.5(0.5); K, THF, 2(3); L, THP, 2(3); M, oxepane, 2(4); N, 1,3,5-trioxane, 2 g (4); O, dimethoxymethane, 2(3); P, D 1,3-dioxolane, 3.5(0.5); Q, THF, 2(3); R, THP, 2(3); S, oxepane, 2(4)
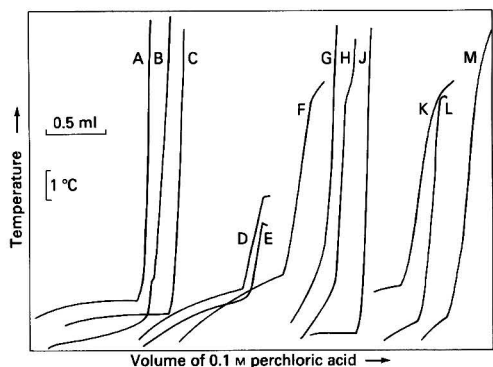
Fig. 7. Catalytic thermometric titration of chloroquine phosphate and adrenaline hydrogen tartrate with 0.1 M perchloric acid in acetic acid. Samples: I, 25.88 mg of chloroquine phosphate in 1 ml of AcOH (A–F); II, 16.66 mg of adrenaline hydrogen tartrate in 0.5 ml of AcOH + 0.5 ml of HCO₂H (G–M). Indicator, ml (acetic anhydride, ml): A, dimethoxymethane, 2(3); B, 1,3,5-trioxane, 2 g (4); C, 1,3-dioxolane, 3.5(0.5); D, THF, 2(3); E, THP, 2(3); F, oxepane, 2(4); G, dimethoxymethane, 2(3); H, 1,3,5-trioxane, 2 g (4); J, 1,3-dioxolane, 3.5(0.5); K, THF, 2(3); L, THP, 2(3); and M, oxepane, 2(4)

representative bases as their 0.1 M solutions, using the different thermometric indicators, are given in Table 1, and range from 0.096 to 0.66%. The lowest value, for quinuclidine, was obtained with the dimethoxymethane indicator reagent but, in general, there seems to be little difference among the six indicator systems evaluated.

The contribution of sampling error was calculated for the three sample solutions, all of which were delivered from the same 1-ml pipette, by weighing to four decimal places four replicates of the delivered 1-ml solutions. The relative standard deviations were 0.09, 0.22 and 0.18% for the quinuclidene, 8-hydroxyquinoline and caffeine solutions, respectively. The differences are probably due to the different surface tensions of the sample solvents—acetic anhydride, toluene and acetic acid. The titrant error was determined by weighing the amount of titrant delivered by the motorised syringe in 6 min, a time corresponding to an average titrant volume of 1 ml. The relative standard deviation of four

replicate determinations was 0.13%. Hence, the sample and titrant-delivery errors make a significant contribution to the over-all precision value.

Titration of Drug Substances

The indicator reagents were evaluated for the catalytic thermometric titration of five drug substances: diazepam, librium hydrochloride, tetracycline hydrochloride, chloroquine phosphate and adrenaline hydrogen tartrate, in addition to caffeine. Each of the drug substances was prepared as a 0.05 M solution in a convenient solvent. The titration curves are shown in Figs. 6 and 7. It can be seen that satisfactorily sharp end-point inflections are obtained with all six indicators in the titrations of diazepam (Fig. 6, A–F) and chloroquine phosphate (Fig. 7, A–F) but the acetals show significantly greater temperature rises. With the latter compound two of its basic functions were determined, as distinct from only one basic function in the titration of the other drug substances. In the titration of adrenaline hydrogen tartrate (Fig. 7, G–M) premature indicator reactions occurred with the dimethoxymethane and 1,3,5-trioxane indicators, but a sharp end-point inflection was obtained with the 1,3-dioxolane reagent. The cyclic ethers gave poor end-point inflections and the titration values were sub-stoicheiometric, suggesting that some acetylation of the amino group of adrenaline had occurred. It is probably significant that the 1,3-dioxolane solvent system contains only a relatively small amount of acetic anhydride (8.3% V/V at the end-point), and this may account for the absence of premature acetylation during the titration when this indicator reagent is used. In the titrations of librium and tetracycline hydrochlorides the most satisfactory end-points were obtained with the 1,3-dioxolane and dimethoxymethane indicators.

Conclusions

This investigation has shown that the three acetals and the cyclic ethers with five-, six- and seven-membered rings are satisfactory as end-point indicators in the acetous perchloric acid in the titration of weak nitrogen bases in the presence of acetic anhydride, but only the acetals give satisfactory end-point inflections in the titration of very weak bases, represented by caffeine. The precisions obtained in replicate titrations are, in general, better than those achieved with alternative indicator systems for the non-aqueous titration of bases.

The significant contribution of sampling and titrant-delivery errors to these precision values suggests that if these errors are reduced to better than 0.1%, then over-all errors of better than 0.2% might be achieved by this catalytic thermometric method. It should be noted that these precision values are obtained with 11- to 19-mg amounts of sample requiring about 1 ml of 0.1 M titrant, whereas the non-aqueous titration of basic drugs described in assays in the pharmacopoeias normally uses about 20 ml of 0.1 M titrant for up to 500 mg of sample.

References

1. Greenhow, E. J., and Spencer, L. E., *Analyst*, 1973, **98**, 81.
2. Greenhow, E. J., and Vinas, P., *Talanta*, 1984, **31**, 611.
3. Vogl, O., and Tsukamoto, A., *in* Jenkins, A. D., *Editor*, "Progress in Polymer Science," Volume 3, Pergamon Press, Oxford, 1971, Chapter 4, p. 240.

4. Meerwein, H., Delfs, D., and Morschel, H., *Angew. Chem.*, 1960, **72**, 927.

5. Jaacks, V., and Kern, W., *Makromol. Chem.*, 1963, **62**, 1.

6. Sorokin, E. S., Geidel'man, N. I., and Bytenskii, V. Ya., *Zh. Prikl. Khim.* (*Leningrad*), 1970, **43**, 1595.

7. Bytenskii, V. Ya., Sorokin, E. S., and Shtamm, N. B., *Zh. Prikl. Khim.* (*Leningrad*), 1975, **48**, 249.

8. Boubli, B. J., *Boll. Chim. Farm.*, 1955, **94**, 186.

9. Avedikian, A. M., and Commeyras, A., *Bull. Soc. Chim. Fr.*, 1970, 1258.

10. Belcher, R., Nutten, A. J., and Macdonald, A. M. G., "Quantitative Inorganic Analysis," Third Edition, Butterworths, London, 1970.

11. Greenhow, E. J., and Spencer, L. E., *Analyst*, 1973, **98**, 98.

12. Vaughan, G. A., and Swithenbank, J. J., *Analyst*, 1970, **95**, 890.

NOTE—References 1 and 11 are to Parts I and III of this series, respectively.

Determination of Free Acid in the Presence of Hydrolysable Cations by Titration

E. H. Rudolf von Barsewisch
The Council for Mineral Technology, Private Bag X3015, Randburg, 2125, South Africa
and Robert A. Hasty
Department of Chemistry, University of the Witwatersrand, 1 Jan Smuts Avenue, Johannesburg, 2001, South Africa

A simple method is described for the determination of free acid in process solutions containing iron(III), aluminium(III), iron(II) and manganese(II). The solutions analysed are those resulting from the leaching of Witwatersrand gold and uranium ores with sulphuric acid. The method involves titrating the sample solution with sodium hydroxide solution to the hydrogen sulphate end-point, the detection of which is facilitated by the use of the first derivative of the pH response.

Preliminary results have indicated that the method is accurate and free of interferences from aluminium(III) (up to 2 g l^{-1}), iron(II) (up to 2 g l^{-1}) or manganese(II) (up to 5 g l^{-1}). The hydrolysis of iron(III) at a concentration of 5 g l^{-1} reduced the magnitude of the signal, which made detection of the end-point difficult. This problem was overcome by the addition of a neutral salt, *e.g.*, sodium sulphate.

The derivative method, which is applicable to all strong mineral acids in the presence of sulphate anions, has been compared with the potassium oxalate method and has been found to be more accurate, even though it is subject to errors caused by the differentiating circuit.

Keywords: *Free acid determination; hydrolysable cations; derivative techniques; titration*

The determination of free acid concentrations has been studied,[1-11] but no universal method has yet been developed as in all instances the hydrolyses of certain cations, *e.g.*, iron(III), have been found to interfere in the determination to some extent. During a neutralisation reaction, the hydrolysable cations react to form basic salts, liberating extra protons in the process. Because these protons are indistinguishable from the free acid protons, the values determined for the free acid content are anomalously high. The free acid concentration is defined as the acid concentration that would be determined if the hydrolysis of the cations could be suppressed completely.

A knowledge of the exact free acid content is very important in the treatment of nuclear fuels, for example in the extraction of uranium and the treatment of uranium solutions, but existing analytical methods for the determination of free acid are unreliable for solutions in which the ratio of the analyte to the interferents is low. This problem arises in the treatment of Witwatersrand uranium leach liquors, 1 l of which can contain up to 5 g of iron(III), 2 g of aluminium(III), 2 g of iron(II) and 5 g of manganese(II).[1] The combined concentration of the main interferents, iron(III) and aluminium(III), may be twenty times higher than the concentration of free acid, which can be as low as 0.01 M.

Complexing agents can be used to mask the hydrolysable cations, which is the approach most commonly used. Theoretical considerations indicate that complexing agents such as oxalate or ethylenediaminetetraacetate (EDTA) should effectively mask the interferents at pH 5,[12-14] but experiments have shown[1-11] that the results obtained by such methods are inaccurate. As the complexometric approach has failed, it was decided that in this investigation the competing reactions of the proton and the hydrolysable cation should be studied by conventional neutralisation titration, and as it has been shown that the use of mathematical derivative techniques enhance the resolution of the signal,[15] it was decided that derivative techniques would be used.

Experimental

Apparatus and Operating Conditions

A continuous titrator was assembled that consisted of a reaction vessel, a Gilson Minipuls II peristaltic pump, a depulser, a reagent reservoir and a stirrer. Base (0.1 M sodium hydroxide solution) was added to the stirred sample solution (10–30 ml) at a flow-rate of 1.0 ml min^{-1}. The pH response obtained from a Schott N 60 EE combination electrode was amplified by a Radiometer PHM 84 pH meter. The signal was transformed by a specially constructed electronic circuit (a "compensated differentiator" using an operational amplifier) that produced an output voltage that was proportional to the first derivative of the input signal. This derivative was then recorded on a Rikadenki R 11 chart recorder. A detailed description of the apparatus and the differentiator has been reported elsewhere.[16]

Standard Solutions

Standard solutions of the metal ions were prepared with a known amount of sulphuric acid. The iron(III) standard solution was prepared from the nitrate salt (Merck, pro analysi) and the other standards were prepared from sulphate salts (analytical-reagent grade or Merck, pro analysi). The metal ion content was known but the absolute concentration of the acid in the standard solutions was not. The presence of an excess of acid or base in the standard metal solution was ignored as the excess of acid was determined together with the free acid concentration during the subsequent determination. The samples were analysed without pre-treatment or dilution, and no replicate experiments were performed in this preliminary study. The sulphuric acid and sodium hydroxide solution were standardised against sodium carbonate and potassium hydrogen phthalate solutions (all of analytical-reagent grade). De-ionised water was used throughout.

Results and Discussion

Free acid protons originate from strong mineral acids; acid dissociation constants of some mineral acids are listed in Table 1. The second dissociation of sulphuric acid has a pK_a of 1.8, which means that at pH 1.8, HSO_4^- and SO_4^{2-} are present in equal proportions. The hydrogen sulphate - sulphate couple consumes free protons and, in acidic sulphate solutions, most protons are bound in the form of hydrogen sulphate.

In the determination of free acid, the most serious interferences are from iron(III) and aluminium(III). These cations are Lewis acids and can produce protons according to the reaction expressed in equation (1):

$$M(H_2O)_n^{z+} \rightleftharpoons M(H_2O)_{n-1}(OH)^{(z-1)+} + H^+_{(aq.)} \cdot \cdot \quad (1)$$
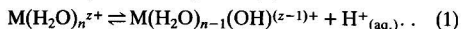
where M represents the metal ion with charge z and the coordination number n. The hydrated cation is a masked acid, and is a source of protons. During a neutralisation reaction, protons are split from the hydration shell resulting in the formation of a basic hydroxide. The pH value at which the hydrolysis becomes significant can be found via the hydrolysis constant, K_h, which is defined as

$$K_h = \{[M(H_2O)_{n-1}(OH)^{(z-1)+}] [H^+]\}/[M(H_2O)_n^{z+}] \quad \cdot \cdot \quad (2)$$

The values of hydrolysis constants of the major interferents are given in Table 2. It can be seen that the most severe interferent is iron(III), which is 50% hydrolysed at pH 2.2. The hydrolysis constants of other interferents have pK_h values greater than 5.0 and, hence, only interfere above pH 3. The hydrogen sulphate (pK_a ca. 1.8) and, indirectly, the free proton, react with the base before iron(III) hydrolyses (pK_h ca. 2.2).

In this study, iron(III) nitrate samples in 0.0250 M sulphuric acid were titrated with sodium hydroxide solution. The reaction was monitored continuously and the response of the curve for pH *versus* titrant volume was analysed. A very small inflection was found, followed by a broad plateau caused by the hydrolysis of iron(III). This inflection was in the correct region for the hydrogen sulphate equivalence point. Subsequently, the derivative of the pH response was recorded instead of the original pH response. In the derivative mode, the small inflection gave rise to a peak with a signal of 35 mV or less, compared with a signal of 10 V for the peak subsequent to the complete hydrolysis of iron(III). The titrations were stopped after the first peak had been recorded, and consequently the pH value of the solution was never greater than 2.5 so that hydrolysis of iron(III) was avoided.

The inflection was assigned to the hydrogen sulphate endpoint, and determinations of the concentration of free acid based on this end-point were found to be systematically high. Also, the detection of the end-point became more difficult as the concentration of iron(III) in 0.0250 M sulphuric acid increased. Typical results are shown in Fig. 1. The addition of neutral sodium sulphate to the sample effectively reversed the hydrolysis such that the results of the titration approached the known molarity of the sulphuric acid as shown in Table 3. The peak corresponding to the hydrogen sulphate end-point became more distinct, *i.e.*, the signal to noise ratio improved, with increasing ratios of sulphate to interferent. In the presence of an excess of sulphate, there was little interference from iron(III).

Solutions containing aluminium(III), iron(II) or manganese(II) were analysed in a similar manner. These cations were found to interfere to some extent, although their interference in the presence of iron(III) is negligible on theoretical grounds. The effect of these cations was, therefore, ignored in subsequent determinations.

Sample solutions containing aluminium(III) as the interferent, hydrochloric acid and sodium sulphate were analysed for their free acid content, and the results were found to be identical (within experimental error) with those for sample solutions containing sulphuric acid as the mineral acid.

Finally, the results obtained by the derivative method and the potassium oxalate method, as recommended by Solomons,[1] were compared. These samples were synthetic leach liquors containing sulphuric acid. No additional sulphate was added to the test solutions under comparison as it was desired to apply the derivative method to the untreated sample solution. The addition of sulphate in excess of that supplied by the sulphuric acid would improve the signal to noise ratio and is currently under investigation. The derivative method was found to be more accurate in all situations where the end-point could be distinguished. As can be seen from Table 4, the correct concentration of free acid can be determined by the derivative method without interference from iron(III), whereas the oxalate method is prone to systematic error. Although the possible presence of free acid in the metal salt was initially ignored, Table 4 shows that there was no excess of acid or base present in the iron(III) nitrate salt, which was used to prepare the standard solutions. Although the iron(III) nitrate concen-

Table 1. Dissociation constants[12] of some strong mineral acids

Mineral acid			pK_a
HCl	..	..	<0
HNO_3	..	..	<0
H_2SO_4	..	..	−3
HSO_4^-	..	..	1.8

Table 2. First hydrolysis constants of selected hydrolysable cations

Metal ion				pK_h
Fe(III)	..	..	..	2.2*
Al(III)	..	..	..	5.0*
Fe(II) ..	..	..	..	≥5.5†
UO_2^{2+}	..	..	..	5.8*
Mn(II)	..	..	..	≥8.5†

* Results from reference 4.
† Extrapolated from the data of Solomons[1] and Kolthoff *et al.*[17]
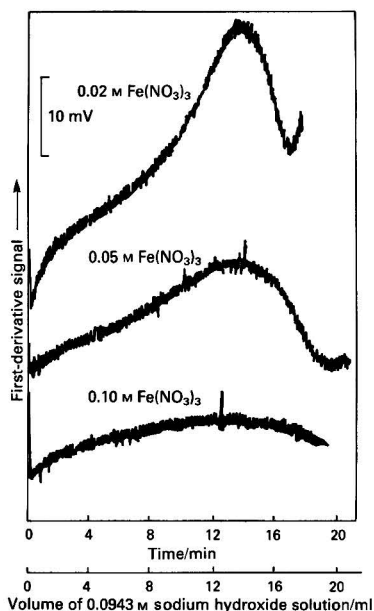
Fig. 1. First-derivative signal of the hydrogen sulphate end-point of sulphuric acid on titration with sodium hydroxide in the presence of iron(III) nitrate. Conditions: titrant flow-rate, 1.0 ml min⁻¹; titrant, 0.0943 M sodium hydroxide solution; sample volume, 20 ml

Table 3. Analysis of 20.0 ml of 0.0250 M sulphuric acid in the presence of various amounts of iron(III). The sulphate to iron(III) ratio was increased by the addition of solid sodium sulphate. The acid solution contained 0.001 mol of H^+ and 0.0005 mol of SO_4^{2-}

Amount of SO_4^{2-}/mol	Observed acid concentration/M		
	0.0002 mol Fe(III)	0.0005 mol Fe(III)	0.0010 mol Fe(III)
0.0005	0.032	0.032	0.031*
0.0026	0.025	0.030	0.030*
0.0111	0.025	0.025	0.030*
0.0234	N.d.†	N.d.	0.025
0.0269	N.d.	N.d.	0.024

* End-point almost indistinguishable.
† N.d. = not determined.

Table 4. Comparison of the derivative method with the potassium oxalate method for the determination of free acid in the presence of iron(III) nitrate

Acid concentration/ mol l⁻¹	Iron(III) concentration/ mol l⁻¹	Observed acid concentration/ mol l⁻¹	
		Oxalate method	Derivative method
0.025	0.02	0.031	0.026
	0.05	0.033	0.027
	0.10	0.030	I.d.*
0.050	0.02	0.058	0.049
	0.05	0.058	0.049
	0.10	0.058	I.d.
0.075	0.02	0.082	0.075
	0.05	0.082	0.075
	0.10	0.081	0.075

* I.d., indistinct, *i.e.*, the end-point could not be determined because the peak maximum was too shallow.

tration was increased by a factor of five, there was no systematic increase in the observed acid concentration by either method. The derivative method, therefore, has considerable utility in establishing the neutrality of salts of hydrolysable cations. However, the results obtained in this study were subject to an error originating in the design of the compensated differentiator. The design of the differentiator that was used allowed slowly changing signals to be differentiated accurately. Rapidly changing signals, *e.g.*, those due to changes in pH in the titration of a strong acid with a base in the absence of any buffer, gave rise to an error of undetermined magnitude in the derivative. The limits of the method can be determined only if the electronic differentiator can be improved, as outlined previously,[16] or if alternative methods, *e.g.*, numerical differentiation, are used for the determination of the derivative.

Conclusions

The application of derivative techniques to conventional titrations improves the resolution of the signals. Standard text books[18,19] advise that the determination of "mixed acids" is possible only if the dissociation constants are separated by at least three orders of magnitude. The use of derivative methods makes it possible for the concentration of the first of two very closely related species to be measured without interference by the second species.

References

1. Solomons, M., Report 2039, National Institute for Metallurgy, Randburg, 1980, 26 pp.
2. Mayankutty, P. C., Ravi, S., and Nadkarni, M. N., *J. Radioanal. Chem.*, 1982, **68**, 145.
3. Booman, G. L., Elliott, M. C., Kimball, R. B., Cartan, F. O., and Rein, J. E., *Anal. Chem.*, 1958, **30**, 284.
4. Baumann, E. W., and Torrey, B. H., *Anal. Chem.*, 1984, **56**, 682.
5. Damien, N., and Cauchetier, P., *Anal. Chim. Acta*, 1968, **41**, 483.
6. Ahrland, S., *Acta Chem. Scand.*, 1960, **14**, 2035.
7. Pakalns, P., *Anal. Chim. Acta*, 1981, **127**, 263.
8. Schmid, E. R., and Jünger, E., *Fresenius Z. Anal. Chem.*, 1971, **257**, 112.
9. Blaedel, W. J., and Panos, J. J., *Anal. Chem.*, 1950, **22**, 910.
10. Tomasevic, M., *Hem. Ind.*, 1973, **27**, 399.
11. Moeken, H. H. P., and van Neste, W. A. H., *Anal. Chim. Acta*, 1967, **39**, 264.
12. Ringbom, A., *in* Elving, P. J., and Kolthoff, I. M., *Editors*, "Chemical Analysis," Volume XVI, Interscience, New York, 1963, 395 pp.
13. Martell, A. E., and Smith, R. M., "Critical Stability Constants," Volume 1, Plenum Press, New York, 1974, p. 204.
14. Martell, A. E., and Smith, R. M., "Critical Stability Constants," Volume 3, Plenum Press, New York, 1977, p. 92.
15. O'Haver, T. C., *Anal. Proc.*, 1982, **19**, 22.
16. von Barsewisch, E. H. R., and Hasty, R. A., Report M194, Council for Mineral Technology, Randburg, 1985.
17. Kolthoff, I. M., Sandell, E. B., Meehan, E. J., and Bruckenstein, S., "Quantitative Chemical Analysis," Fourth Edition, Macmillan, London, 1969, p. 252.
18. Blaedel, W. J., and Meloche, V. W., "Elementary Quantitative Analysis—Theory and Practice," Second Edition, Harper and Row, New York, 1963, p. 361.
19. Skoog, D. A., and West, D. M., "Fundamentals of Analytical Chemistry," Fourth Edition, Saunders College Publishing, Philadelphia, 1982, p. 231.

Study of Interferences in the Determination of Lead by Hydride Generation - Direct Flame Atomic-absorption Spectrometry when Oxidising Agents are Employed to Increase the Sensitivity

Juan R. Castillo, Jose M. Mir, Jesus Val, Maria P. Colón and Carmen Martínez
Department of Analytical Chemistry, Faculty of Sciences, University of Zaragoza, Zaragoza, Spain

The greatest sensitivity in the determination of lead by hydride generation - direct flame AAS is obtained in the presence of ammonium persulphate (0.012 µg). A complete interference study is reported, comparing the results obtained when hydrogen peroxide and ammonium persulphate are employed. The oxidation to a metastable tetravalent state of lead by the prior action of the oxidising agent is considered to be the mechanism by which the atomic-absorption signal in increased.

Keywords: *Covalent hydrides; lead determination; flame atomic-absorption spectrometry; interferences*

Several papers have been published on the determination of As, Bi, Sb, Sn, Ge, Se, Te and Pb by their conversion into gaseous hydrides followed by atomisation by various means (silica tube, electrothermal or direct flame).[1] Recently, indium has also been determined by these combined techniques.[2]

Thompson and Thomerson[3] generated lead hydride in different media and in the presence of H_2O_2 or $K_2Cr_2O_7$ as oxidising agents. They obtained poor results for the production of lead hydride from 0.2 M HCl with 1% *m/V* $NaBH_4$. Fleming and Ide[4] carried out the generation of lead hydride in the presence of $K_2Cr_2O_7$ and tartaric acid. This was the first time both an oxidising agent and $NaBH_4$ were used to improve the efficiency of production of lead hydride. Iron enhances the lead signal considerably in this process, and nickel and copper interfere. The detection limit was 7 µg ml^{-1}.

Vijan and Wood[5] converted lead into its hydride by reacting the sample, containing 0.7% *V/V* of nitric acid or 1% *V/V* of perchloric acid, with 12% *V/V* hydrogen peroxide solution and 4% *V/V* $NaBH_4$ solution. The atomisation was carried out in an electrically heated silica tube; copper and iron were found to cause interferences, which were reduced by addition of citric acid and potassium cyanide solution. This method has been applied to the determination of lead in steel and drinking water.[6]

Jin *et al.*[7] studied the influence of organic chelating agents on the use of $K_2Cr_2O_7$ as an oxidising agent. In the presence of malic acid the minimum detectable concentration of lead was 1.5 ng ml^{-1} when the atomisation was carried out in a nitrogen-supported hydrogen diffusion flame.

In a previous paper[8] we have reported a complete study of the optimum media (acidity, volume and concentration of $NaBH_4$), the nature and type of the oxidising agent ($K_2Cr_2O_7$, Ce^{4+}, MnO_4^-, H_2O_2, $S_2O_8^{2-}$) and instrumental parameters for converting lead into its hydride followed by direct atomisation in an air - acetylene flame without using a carrier gas.

There is an exponential relationship between the atomic-absorption signal obtained and the E° value of the oxidising agents.[8] The following results were obtained: with $K_2Cr_2O_7$, characteristic mass 4.96 µg, sensitivity 0.001; with $KMnO_4$, characteristic mass 4.37 µg, sensitivity 0.001; with $Ce(SO_4)_2$, characteristic mass 1.96 µg, sensitivity 0.013; with H_2O_2, characteristic mass 0.46 µg, sensitivity 0.018; and with $Na_2S_2O_8$, characteristic mass 0.012 µg, sensitivity 0.365. The characteristic mass is defined as the total amount of Pb giving 1% absorption and the sensitivity as the slope of the calibration graph.

The interferences in hydride generation - AAS depend on the media, oxidising agent, chelating agent and atomisation

system used. Fleming and Ide[4] found that Ni, Fe and Cu enhance the AA signal considerably. Vijan and Wood[5] concluded that Al, Zn, As, Ni, Sn and Mn do not interfere at levels up to 10 µg ml^{-1}, K, Mg, Ca, PO_4^{3-}, SO_4^{2-} and Cl$^-$ up to 100 µg ml^{-1} and Cu, Fe and EDTA interfere seriously. Schmidt[6] found that Al, Ba, Ca, Co, Cu, Cr, Fe^{2+}, Fe^{3+}, Mn, Ni, Sr and Zn, do not interfere at levels up to 5 µg ml^{-1} for 50 µg of lead, and Ca, Mg and K up to 1000 µg ml^{-1} for 100 µg ml^{-1} of lead. Only Cu interferes seriously and Ni and Fe do not interfere.

In this paper we report a complete study of interferences when H_2O_2 or $S_2O_8^{2-}$ is used as the oxidising agent. A chelating agent was not used; the hydride generation system used has been fully described previously[9–12] and the lead hydride was atomised directly in the air - acetylene flame of a conventional spectrophotometer (Perkin-Elmer 3030) without any modification.

Experimental

Apparatus

A Perkin-Elmer 3030 atomic-absorption spectrophotometer equipped with a lead hollow-cathode lamp (217 nm) and a deuterium arc lamp as background corrector was used. The hydride generation system was constructed by ourselves.[9–12] A Beckman 150 pH meter was utilised. Glass material was previously washed with nitric acid to prevent trace contamination.

Reagents

All reagents were of analytical-reagent grade.

$NaBH_4$ solution, 4% *m/V*. Prepared by Knechtel and Fraser's method.[13]

Buffer solution, HCl - KCl (pH 1).

Stock solution, 1000 µg ml^{-1}. A stock solution of Pb^{2+}, Cu^{2+}, Ni^{2+}, Fe^{3+}, Co^{2+}, Sr^{2+}, Mg^{2+}, Na^+, Ca^{2+}, Cd^{2+}, Ba^{2+}, Al^{3+}, Zn^{2+}, Zr^{4+}, Bi^{2+}, As^{3+}, Se^{4+}, V^{5+}, K^+, Cr^{3+}, La^{3+}, Ce^{4+}, UO_2^{2+}, NH_4^+, Sb^{3+}, Cl$^-$, NO_3^-, I$^-$, PO_4^{3-} and EDTA was prepared.

Hydrogen peroxide solution, 6% *V/V*.

Procedure

Aliquots containing different concentrations of lead, oxidising agent, interfering species and buffer solution are placed in the reaction vessel, which is then closed. The 4% $NaBH_4$ solution is injected through a septum membrane 40 s after mixing the solutions. The positive pressure of hydrogen generated and the aspiration process sweep the gas phase generated into the

air - acetylene flame. The atomic-absorption signal is completely developed in 20 s. This signal is compared with the signals obtained without the interferent species under the same conditions (five times).

Results and Discussion

In hydride generation - AAS the atomic-absorption signal depends very critically on the acid medium, volume and concentration of $NaBH_4$ solution, the instrumental system for generating the hydride, carrier system into the atomiser and the atomisation system used.

The interferences in hydride generation - AAS are many and can be subdivided into three types.

(a) The background absorption is not considered generally as an interference. However, there is an important effect of variation on the atomisation conditions when the gas phase, with hydrogen, is released to the flame, viz., the flame transparency decreases and a non-specific absorption signal is obtained. The use of a background correction system avoids this effect.

(b) Valency state: As(III) and -(V), Sb(III) and -(V), Se(IV) and -(VI) and Te(IV) and -(VI) give different signals. It is necessary to know the valency state of the sample in order to prepare the calibration graph. This effect could be used to speciate the different species by simply changing the acid concentration, e.g., it is possible to determine total As from 50% HCl and only As^{3+} from 5% HCl.

(c) Inter-element effects are the most important, but they fall into two categories, transition elements and other hydride-forming elements. The mechanisms of interference are totally different.[14]

The inter-element effects, which suppress or enhance the true signal, are the most important. This interference process can act in two ways: prior consumption of reducing agent, and retention or decomposition of the hydride by the metallic elements formed during the reduction process.

On the other hand, the possibility of organic binding within the sample should always be borne in mind when environmental and biological samples are to be analysed, or when the sample solution contains organic and inorganic ligands that can form complexes with the analyte.

The necessity for the presence of an oxidising agent (H_2O_2 or better $S_2O_8^{2-}$) introduces other possibilities. The action of foreign ions can be different in the presence of H_2O_2 and $S_2O_8^{2-}$, and the interference mechanism can also be different. On the other hand, it is necessary to consider that the hydride generation system used does not have a stirrer or carrier gas. There have been few interference studies relating to lead hydride generation, and there have been no studies of lead hydride generation under these conditions. Only interferences from Ni, Cu, Fe and EDTA have been described and, in some instances with contradictions. Fleming and Ide[4] stated that only copper interefered seriously.

Table 1 shows the effect of several cationic species on the atomic absorption of lead atomised from its gaseous hydrides in the presence of H_2O_2. In each instance the concentration of interfering ion was increased until a change in effect was noted.

Under the conditions of lead hydride generation and atomisation used, only Ca^{2+}, K^+, Na^+, Mn^{2+}, NH_4^+ and Mg^{2+} do not interfere. Cu^{2+}, Ni^{2+}, Se^{4+}, Fe^{3+}, V^{5+}, Co^{2+}, As^{3+}, UO^{2+}, Bi^{3+}, Ce^{4+}, Ag^+, Cd^{2+}, Zr^{4+}, Sr^{2+}, Sn^{4+}, Sb^{3+}, La^{3+} and Hg^{2+} decrease the atomic-absorption signal of lead more than 10%, from a [Pb^{2+}] to [interferent] ratio of 1 : 0.016

Table 1. Study of cationic interferences in the determination of lead by hydride generation direct flame AAS when H_2O_2 is used as an oxidant. 30 µg of Pb^{2+} present in a total volume of 10 ml at pH 1 (HCl buffer), 4 ml of 4% $NaBH_4$ solution injected

Ion studied			[Pb^{2+}]/ [interfering ion]	Variation of AA signal in the presence of interfering ion, %
Cu^{2+}	..	..	1 : 0.016	−31
Ni^{2+}	..	..	1 : 0.016	−44
Se^{4+}	..	..	1 : 0.016	−74
Fe^{3+}	..	..	1 : 0.016	+17
V^{5+}	..	..	1 : 0.016	+160
Co^{2+}	..	..	1 : 0.16	−24
As^{3+}	..	..	1 : 0.16	−32
UO^{2+}	..	..	1 : 0.33	−12
Bi^{3+}	..	..	1 : 0.33	−25
Ce^{4+}	..	..	1 : 1.6	−49
Ag^+	..	..	1 : 1.6	−91
Cd^{2+}	..	..	1 : 3.3	−33
Zr^{4+}	..	..	1 : 3.3	−52
Ca^{2+}	..	..	1 : 16.6	−4
Sr^{2+}	..	..	1 : 16.6	−23
Sn^{4+}	..	..	1 : 16.6	−68
Na^+	..	..	1 : 33.3	−1
Mn^{2+}	..	..	1 : 33.3	−2
NH_4^+	..	..	1 : 33.3	−6
Mg^{2+}	..	..	1 : 33.3	−9
Sb^{3+}	..	..	1 : 33.3	−16
La^{3+}	..	..	1 : 33.3	−23
Cr^{3+}	..	..	1 : 33.3	−39
Hg^{2+}	..	..	1 : 33.3	−57

Fig. 1. Variation of the atomic absorption of lead hydride when the reaction time between Pb^{2+} and the hydrogen peroxide solution is increased. Injection time, 2 s; total sample volume, 10 ml; volume of buffer, 1.7 ml; volume of 6% m/V H_2O_2, 2 ml; and volume of 4% m/V $NaBH_4$, 4 ml

Table 2. Study of anionic and chelating agent interferences in the determination of lead by hydride generation - direct flame AAS when H_2O_2 was used as an oxidant. 30 µg of Pb^{2+} present in a total volume of 10 ml at pH 1 (HCl - KCl buffer), 4 ml of 4% Na BH_4 solution injected

Species studied			[Pb^{2+}]/ [interfering anion]	Variation of AA signal in the presence of the interfering ion, %
Hydrogen sulphites	..		1 : 1	−100
EDTA	..	..	1 : 1	−80
Phosphates	..	..	1 : 1.16	−100
Iodides	..	..	1 : 3.3	−100
Nitrates	..	..	1 : 33.3	0
Fluorides	..	..	1 : 33.3	−3
Borates	..	..	1 : 33.3	−9
Sulphates	..	..	1 : 33.3	−22
Oxalates	..	..	1 : 33.3	−100
Citrates	..	..	1 : 33.3	−100

Table 3. Study of cationic interferences in the determination of lead by hydride generation - direct flame AAS when persulphate was used as an oxidant. 1 µg of Pb^{2+} present in a total volume of 10 ml at pH 6, 4 ml of 4% $NaBH_4$ solution injected

Ion studied			$[Pb^{2+}]/$ [interfering ion]	Variation of AA signal in the presence of the interfering ion, %
Cr^{6+}	..	..	1:1	−25
Cu^{2+}	..	..	1:1	−54
Fe^{3+}	..	..	1:1	−55
Ni^{2+}	..	..	1:5	−12
Zn^{2+}	..	..	1:5	−12
Cd^{2+}	..	..	1:5	−17
Mn^{2+}	..	..	1:33.3	−5
Ca^{2+}	..	..	1:100	−1
Mg^{2+}	..	..	1:100	−22
Na^+	..	..	1:100	−39

Table 4. Study of anionic and chelating agent interferences in the determination of lead by hydride generation - direct flame AAS when persulphate was used as an oxidant. 1 µg of Pb^{2+} present in a total volume of 10 ml at pH 6, 4 ml of 4% solution injected

Species studied			$[Pb^{2+}]/$ [interfering anion]	Variation of AA signal in the presence of the interfering ion, %
EDTA	..	..	1:1	−100
Citrate	..	..	1:100	−13
Borate	..	..	1:100	−18
Oxalate	..	..	1:1000	−6
Sulphates	..	..	1:1000	−9
Fluorides	..	..	1:1000	−7
Phosphates	..	..	1:1000	−44

to 1:33.33. Some of these interferences can be avoided using a more concentrated $NaBH_4$ solution (As^{3+}, UO_2^{+}, Bi^{3+}, Ce^{4+}, Sr^{2+}, Sb^{3+}, Cr^{3+} and La^{3+}). Especially interesting is the effect of iron and vanadium, which increase the lead atomic-absorption signal by 17 and 160%, respectively, when a $[Pb^{2+}]$ to [interferent] ratio of 1:0.016 is used.

The effect of oxidising agents on lead hydride generation has been attributed to the oxidation of lead to a metastable tetravalent state before conversion into plumbane (PbH_4).[5] Experiments carried out in this work appear to confirm this conclusion. If the injection of $NaBH_4$ solution is delayed a few seconds after mixing the solution containing Pb^{2+} and the oxidising agent, the atomic-absorption signal for lead is increased (see Fig. 1).

When the $NaBH_4$ solution is injected 40 s after mixing the solution of Pb^{2+} and the oxidising agent, the maximum atomic absorption is attained. This fact could be explained by considering that 40 s is the optimum time to reach the maximum amount of lead in solution in the tetravalent metastable form and from this time the signal decreases owing to the low stability of that valence state.

The presence of Fe^{3+}, or more significantly V^{5+}, catalyses this oxidation to the metastable tetravalent state and then the kinetics of the reduction process are more complete and faster. In fact, in the presence of Fe^{3+} or V^{5+}, the atomic-absorption signal of lead, as the hydride, is at a maximum immediately after mixing the Pb^{2+} solution and the oxidising agent.

From the results shown in Table 2, it is possible to differentiate two interference mechanisms when an anion or chelating agent is present. The first type is related to the reducing character of the anion or chelating agent (hydrogen sulphites, iodides or organic matter), which produces the reduction of the hydrogen peroxide, avoiding the subsequent oxidation of lead to the metastable tetravalent state. Moreover, it is necessary to consider the chelating action of agents as phosphates, EDTA, oxalates and citrates, which avoid both the oxidation of lead to the tetravalent state and its reduction to plumbane.

There are some significant differences when persulphate or hydrogen peroxide is used as the oxidising agent. A higher sensitivity is attained if persulphate is used, as shown in the interference study.

Se^{4+}, Co^{2+}, As^{3+}, UO_2^{2+}, Bi^{3+}, Zr^{4+}, Sr^{2+}, Sb^{3+}, La^{3+}, Ce^{3+}, Ag^+, Cr^{3+} and Hg^{2+} do not interfere when persulphate is used and the interferences from Cu^{2+}, Ni^{2+} and Cd^{2+} are minimised (Table 3). The positive effect of Fe^{3+} and V^{5+} is not observed. On the contrary, the presence of iron produces a suppressing effect on the signal when persulphate is used. The causes of the interferences of Mg and Na, which do not occur when hydrogen peroxide is used, are not clear.

When both anionic interferences and interferences from chelating agents are studied, the differences using hydrogen peroxide or ammonium persulphate are also very significant, except for the total suppressing effect of EDTA. Hydrogen sulphites and iodides do not cause any effect, and the suppressing effect of phosphates, borates, sulphates, oxalates and citrates are minimised (Table 4).

In conclusion, in the determination of lead by hydride generation - direct flame atomic-absorption spectrometry, using $NaBH_4$ solution as a reducing agent, it appears to be necessary to use an oxidising agent in order to increase the sensitivity and avoid some interferences. The results improve as the oxidising power increases.

References

1. Godden, R. G., and Thomerson, D. R., *Analyst*, 1980, **105**, 1137.
2. Busheina, I. S., and Headridge, J. B., *Talanta*, 1982, **29**, 519.
3. Thompson, K. C., and Thomerson, D. R., *Analyst*, 1974, **99**, 595.
4. Fleming, H. D., and Ide, R. G., *Anal. Chim. Acta*, 1976, **83**, 67.
5. Vijan, P. N., and Wood, G. R., *Analyst*, 1976, **101**, 966.
6. Schmidt, R. S., *At. Spectrosc.*, 1976, **2**, 5.
7. Jin, K., Taga, M., Yoshida, H., and Hikime, S., *Bunseki Kagaku*, 1978, **27**, 759.
8. Castillo, J. R., Mir, J. M., Martínez, C., Val, J., and Colon, P., *Mikrochim. Acta.*, in the press.
9. Castillo, J. R., Lanaja, J., and Aznárez, J., *Analyst*, 1982, **107**, 89.
10. Castillo, J. R., Lanaja, J., and Martínez, M. C., and Aznárez, J., *Analyst*, 1982, **107**, 1488.
11. Castillo, J. R., and Martínez, C., *At. Spectrosc.*, 1983, **4**, 63.
12. Castillo, J. R., Martínez, C., and Belarra, M. A., paper presented at the VIIIth International Spectroscopy Symposium, Amsterdam, 1983.
13. Knechtel, J. R., and Fraser, J. L., *Analyst*, 1978, **103**, 105.
14. Welz, B., and Melcher, M., *At. Absorpt. Newsl.*, 1980, **1**, 145.

Determination of Tellurium and Lead at Picogram Levels by Candoluminescence Spectrometry

Zuhair M. Kassir* and Mansour B. Taher

Department of Chemistry, College of Science, University of Basrah, Basrah, Iraq

Tellurium and lead are determined by candoluminescence using the coated-rod technique. Tellurium is found to give its maximum luminescence from magnesium oxide coated on calcium oxide - calcium sulphate rods with an emission peak at 470 nm. Perchloric acid is used as a coactivator. A number of parameters were studied and optimised and a linear calibration graph was obtained for the range 0–12 ng using 2 µl of sample. The detection limit was 25 pg µl^{-1} with a relative standard deviation of 7.0%. Lead gave a stronger luminescence in a calcium fluoride matrix compared with a calcium oxide - calcium sulphate matrix. Hydrochloric acid was used as coactivator. A linear calibration graph was obtained in the range 0–100 ng using a 1-µl sample volume. The detection limit was 6 pg µl^{-1} with a relative standard deviation of 5.0%. A number of interfering elements were studied for their effect on both elements.

Keywords: *Tellurium determination; lead determination; candoluminescence spectrometry*

Candoluminescence spectrometry has been used for the determination of a number of elements at trace levels.[1,2] In a recent publication by Kassir *et al.*,[2] a method of coating matrices on calcium oxide - calcium sulphate rods was described. This technique widens the scope of using new matrices and activators in candoluminescence. In this work the candoluminescence of tellurium in a magnesium oxide matrix with perchloric acid as a coactivator is reported. Lead has also been studied in a new matrix, *i.e.*, calcium fluoride, and the results have been compared with a calcium oxide - calcium sulphate matrix, used by Karpel.[3]

Experimental

Instrumentation

A Beckman DU-2 spectrophotometer fitted with a spectral energy recorder and flame attachment was used. The flame compartment of an EEL Model 140 atomic-absorption spectrophotometer was positioned in such a way that the luminescence from the burner was received by the entrance slit of the spectrophotometer. Details of this set-up have been described previously.[4] An acetylene - dinitrogen oxide burner, with 5-cm slot, was adapted to a hydrogen flame. A specially designed rod holder, which has been described already,[2] was used with the burner.

Reagents and Solutions

Water. Distilled water was passed over a mixed-bed ion exchanger and stored in a polyethylene bottle.

Telluric stock solution. The correct amount of telluric acid of analytical-reagent grade was dissolved in water to give a 1000 p.p.m. tellurium stock solution.

Lead stock solution. Lead nitrate, of analytical-reagent grade, was used to prepare a 1000 p.p.m. lead solution.

All other solutions were prepared from analytical-reagent grade reagents.

Gases. Hydrogen and argon gases of high purity (99%) were used in this study.

Preparation of Rods

Large numbers of rods were prepared from calcium oxide and calcium carbonate paste according to the procedure described by Dhaher and Kassir.[4] Coated rods were prepared by dipping the uniformly wet tip of each rod into a slurry of the matrix to be studied for 5 s, then withdrawing and placing them in a rod rack before drying at 110 °C for 30 min. Dried rods are stored in a desiccator.[2]

Procedures

Determination of tellurium in magnesium oxide

Inject 2 µl of tellurium solution prepared with 3.5 N perchloric acid on to the tip of a rod coated with magnesium oxide. Fix the rod in position and expose it to a cool hydrogen flame (H$_2$ - Ar, 1.5 + 15) and measure the emission from the rod tip after 60 s at 470 nm. Five measurements are taken on separate rods for each concentration and the average emission is reported. A blank rod is always examined for background corrections.

Lead in calcium fluoride

Dry a batch of coated rods in an oven for 30 min at 110 °C and leave them to cool in a desiccator. Expose a rod to a hydrogen flame (H$_2$ - Ar, 1.5 + 10) for 90 s, withdraw the rod and cool it for 20 s and inject 1 µl of lead solution, 0.1 N in hydrochloric acid, and re-insert into the same position in the flame and record the emitted luminescence at 385 nm. The average reading from five different rods is taken for each concentration.

Determination of lead in a calcium oxide - calcium sulphate matrix

Use the prepared dry rods directly. Pipette 1 µl of lead solution prepared with 1 N hydrochloric acid on to the tip of the calcium oxide - calcium sulphate rod and introduce it into the flame (H$_2$ - Ar, 1 + 10). The emission is recorded at 385 nm.

Results and Discussion

Matrices

Because the coating method offers a simple way of examining and choosing matrices for a specific activator, the candoluminescence of tellurium was examined using a number of matrices coated on calcium oxide - calcium sulphate rods. Matrices tested were BeO, CaWO$_4$, MgO, CaF$_2$, Y$_2$O$_3$, Gd$_2$O$_3$, Al$_2$O$_3$ and uncoated rods, *i.e.*, CaO - CaSO$_4$. MgO proved to be the best matrix; the other matrices either showed very weak luminescence or no luminescence at all. Therefore, MgO was chosen for the study of the candoluminescence of tellurium.

The same matrices were examined for the luminescence of lead; only CaO - CaSO$_4$ and CaF$_2$ gave strong emission for lead. Both matrices were used in a comparative study for sensitivity.

Spectra

The spectrum of tellurium in magnesium oxide showed a broad peak at 470 nm. Lead in calcium fluoride gave a broad peak similar to that in calcium oxide - calcium sulphate with a maximum at 385 nm, which agrees with the wavelength reported by Karpel.[3]

Gas Ratio

The cool flame used in this study was obtained by diluting hydrogen with argon. The argon gas replaced nitrogen gas in this study to reduce the quenching effect due to the N_2 molecule. To find the optimum ratio of H_2 to Ar, which gives the maximum luminescence for tellurium and lead in the matrices studied, a number of flow-rates of hydrogen were chosen and the flow-rate of argon was changed; the emission from the rod was then recorded. Fig. 1 shows the results obtained for tellurium in MgO where the maximum emission is at the ratio 1.5 : 15 (H_2 - Ar). The ratio of gases for lead in CaF_2 is 1.5 : 10 and for lead in CaO - $CaSO_4$ 1 : 10. All values are in arbitrary units.

Volume of Sample

The volume of the sample introduced on to the tip of the rod was investigated by pipetting different volumes of activator, keeping the amount of activator constant. The results
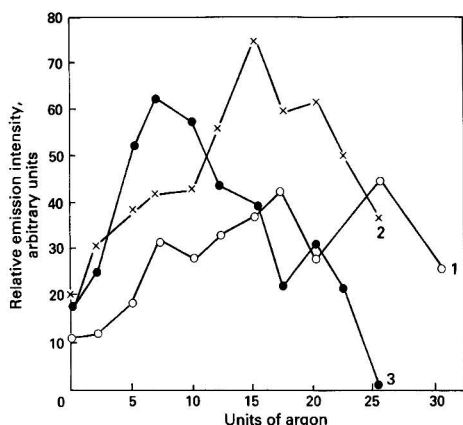
Fig. 1. Effect of H_2 to Ar ratio on the luminescence of tellurium in magnesium oxide: H_2 (in arbitrary units): 1, 2.0; 2, 1.5; and 3, 2.0
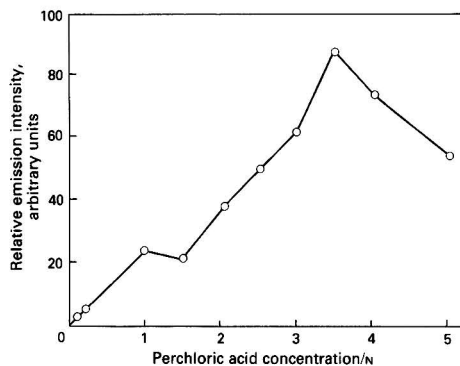
Fig. 2. Effect of perchloric acid concentration on the luminescence of 50 ng of tellurium

obtained showed that 2 μl was the optimum volume for maximum luminescence of tellurium and 1 μl for lead in both CaF_2 and CaO - $CaSO_4$.

Effect of Coactivator

A number of acids were examined for their effect on the luminescence of tellurium in MgO and the results are summarised in Table 1. Perchloric acid gave the greatest enhancement at 3.5 N as is shown in Fig. 2. $MgCl_2$ showed an enhancement effect on the luminescence of tellurium, but not as marked as that of hydrochloric acid, which suggests that both the acid radical and the hydrogen ion participate in the enhancement effect.

The same acids were tested for their effect on the luminescence of lead in CaF_2 and CaO - $CaSO_4$ matrices; all acids depressed the luminescence of lead except hydrochloric acid, which showed an enhancement effect using 0.1 N HCl for lead in CaF_2 of about 120% and 1 N HCl for lead in CaO - $CaSO_4$ where the enhancement was about 140%.
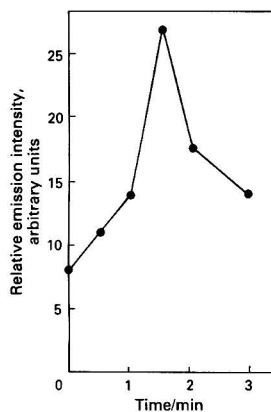
Fig. 3. Effect of pre-heating time on the luminescence of 100 ng of lead in calcium fluoride

Table 1. Effect of enhancing agents on the luminescence of tellurium in a magnesium oxide matrix

Reagent				Concentration for maximum emission/N	Relative emission intensity
HCl	..	..	..	2.2	18
H_2SO_4	..	..	..	3.0	16
$HClO_4$	..	..	..	3.5	90
HNO_3	..	..	..	0.2	9
$MgCl_2$	..	..	..	2.0	40

Table 2. Effect of interfering ions on the luminescence of tellurium

Ion			Percentage increase or decrease in the relative emission intensity		
			One-fold m/m	Two-fold m/m	Five-fold m/m
Cd^{2+}	..	..	−25.2	−33.1	−19.1
Cu^{2+}	..	..	−32.2	−19.0	−26.1
Pb^{2+}	..	..	−8.5	−25.2	−54.5
Mn^{2+}	..	..	−21.2	−55.4	−71.5
Ni^{2+}	..	..	−16.3	−20.0	−42.0
As^{3+}	..	..	−50.0	−60.5	−64.2
Cr^{3+}	..	..	−42.0	−26.6	−10.0
Co^{3+}	..	..	−46.2	−33.6	−64.5
Fe^{3+}	..	..	−44.0	−56.7	−86.0
Sb^{3+}	..	..	−20.1	−63.7	−60.3
Se^{4+}	..	..	+2.5	−5.2	−31.2
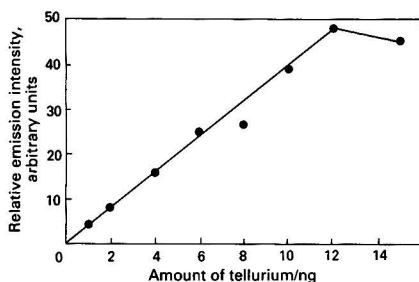
Fig. 4. Calibration graph for tellurium
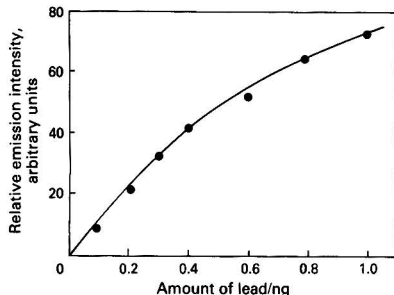
Fig. 5. Calibration graph for lead in a calcium fluoride matrix

Table 3. Effect of interfering ions on the luminescence of lead in a calcium fluoride matrix

Ion	Percentage increase or decrease in the relative emission intensity			
	One-fold m/m	Two-fold m/m	Five-fold m/m	Ten-fold m/m
K^+	−3	−8	−10	−5
Ag^+	−23	−38	−61	−85
Cu^{2+}	−41	−63	−78	−86
Ni^{2+}	−5	−63	−80	−90
Cd^{2+}	−88	−46	−35	−60
Zn^{2+}	−28	−70	−66	−65
Mn^{2+}	−15	−60	−53	−73
Al^{3+}	0	−50	−71	−80
Dy^{3+}	+7	−4	−13	−7
Sb^{3+}	−65	−68	−92	−96
As^{3+}	−63	−35	−15	−70
Pr^{3+}	−89	−63	−76	−94
Cr^{3+}	−51	−74	−89	−94
Br^-	−34	+4	−50	−55
F^-	−70	−50	−40	−70
I^-	−5	−43	−28	−70

fluoride was 6 pg μl^{-1} with a 5% r.s.d. (5 ng of Pb taken); and 200 pg μl^{-1} on calcium oxide - calcium sulphate with an 11% r.s.d. (10 ng of Pb taken). Ten rods were used for each study.

Interferences

Tellurium

The interfering effect of a number of cations on the candoluminescence emission of tellurium were studied at one-, two- and five-fold m/m excesses, using 10 ng of tellurium. As is shown in Table 2 most cations studied depressed the emission intensity of tellurium. Similarly, the effect of a number of anions was studied whilst studying coactivators and it was found that Cl^-, SO_4^{2-} and ClO_4^- enhanced the emission and NO_3^- depressed it by half.

Lead

A number of cations and anions were tested for their interfering effect on the candoluminescence of lead on a calcium fluoride matrix at one-, two-, five- and ten-fold m/m excesses and the results are summarised in Table 3; most ions exerted some degree of depression.

Rod Pre-treatment

Pre-treatment of rods is sometimes required for maximum emission, and better reproducibility for certain activators.[1,4] Rods coated with MgO for the determination of tellurium required no pre-treatment except for drying in an oven at 110 °C for 30 min before use. The same treatment was required for CaO - CaSO₄ rods when they were used for the study of lead. The determination of lead in CaF_2 required pre-heating of the coated rod by exposing each rod to the flame for 90 s (Fig. 3) followed by a 20-s cooling period before introduction to the lead solution (1 μl). The rod was re-introduced into the flame for measurement of emission. This treatment gave maximum emission and an improved reproducibility.

Calibration Graphs

The candoluminescence of tellurium on magnesium oxide with 3.5 N $HClO_4$ as the coactivator, measured under optimum conditions, gave a linear calibration graph between 0 and 12 ng (Fig. 4) although deviating from linearity above 12 ng. The conditions for the determination were as follows: sample volume, 2 μl; slit width, 1.5 mm; wavelength, 470 nm; flame ratio, 1.5 : 15 units (H_2 - Ar).

Lead on calcium fluoride gave a linear relationship between the luminescence and the amount of lead in the range 0–100 ng. Fig. 5 shows a calibration for a small concentration range of lead under the following conditions: sample volume, 1 μl; slit width, 0.5 mm; wavelength, 385 nm; HCl, 0.1 N; flame, 1.5 : 10 (H_2 - Ar); and sensitivity, 100 mV.

Lead also showed a linear relationship when CaO - CaSO₄ was used as a matrix, the range of linearity being in the range 0–50 ng under the following conditions: sample volume, 1 μl; slit width 1.5 mm; wavelength, 385 nm; HCl 1.0 N; flame, 1 : 10 (H_2 - Ar) and sensitivity, 10 mV.

Detection Limit and Reproducibility

The detection limit[5] of tellurium on magnesium oxide was 25 pg μl^{-1}, with a relative standard deviation (r.s.d.) of 7% (10 ng of Te taken). The detection limit of lead on calcium

Conclusion

The study showed that tellurium can be determined by candoluminescence using magnesium oxide as a matrix with a very low detection limit, *i.e.*, at the picogram level. The study on lead revealed that calcium fluoride acts as a very sensitive matrix for lead, where lead gives a luminescence in calcium fluoride ten times stronger than that obtained from a calcium oxide - calcium sulphate matrix. The detection limit was also at the picogram level.

References

1. Belcher, R., Nasser, T. A. K., Shahidullah, M., and Townshend, A., *Am. Lab.*, 1977, **43**, 61.
2. Kassir, Z. M., Al-Muaibed, A. M., Kareem, A. H., and Nasser, T. A. K., *Anal. Chim. Acta*, 1984, **160**, 235.
3. Karpel, S., *PhD Thesis*, University of Birmingham, UK, 1976.
4. Dhaher, S. M., and Kassir, Z. M., *Anal. Chem.*, 1980, **52**, 459.
5. Willard, H. H., Merritt, L. L., and Dean, J. A., "Instrumental Methods of Analysis," Van Nostrand, New York, 1974.

A Designed Experiment for the Examination of Techniques Used in the Analysis of Near infrared Spectra

Part 1. Analysis of Spectral Structure

Ian A. Cowe, James W. McNicol and D. Clifford Cuthbertson
Scottish Crop Research Institute, Pentlandfield, Roslin, Midlothian EH25 9RF, UK

To assess the effectiveness of several statistical techniques to detect the known structure of sample spectra, a factorially designed experiment was carried out using mixtures of four pure chemicals. Analyses of the variation between spectra as expressed by correlation graphs and principal components are shown to be powerful techniques for relating the spectra of constituents to those of samples. A method of interpreting correlation graphs is proposed that identifies the existence of dominant effects such as particle size variation. For these samples, a standardisation algorithm was shown to reduce interference effects due to particle size and to allow easier interpretation of both correlation graphs and principal components.

Keywords: *Near-infrared reflectance; graphical analysis; principal components; particle size*

Although near-infrared reflectance (NIR) analysis has been used successfully on a number of agricultural products to determine their composition, many of the factors determining the success of any particular application are still not fully understood. This is partly because the technique has been developed with an emphasis on solving practical problems with immediate commercial potential, such as the rapid measurement of protein and moisture in cereals,[1,2] oil in oilseeds[3] and fat in meat,[4] rather than as the result of any systematic study of the chemical, physical or statistical problems involved.

A number of workers have identified overtone and combination bands in the near-infrared region that relate to fundamental absorption effects from specific molecular groups,[5,6] but the statistical strategies used to select terms for a regression model have not always included these points in the spectrum. The complexity of biological material makes it very difficult to determine which of many potential interference effects may be significant in any calibration. In addition, the use of reflectance measurements means that control of particle size between samples is important, as differences in the general level of absorbance between samples of different particle size obscure the smaller changes in absorption due to variation in the concentration of any constituent. As a consequence, apparent absorption (log 1/reflectance) values at any single wavelength rarely correlate highly with concentration. Multiple linear regression can relate measurements at several points in the spectrum to the concentration of any constituent, but in doing so may also incorporate regression terms to compensate for effects introduced by particle size. Under these conditions, it is difficult to determine whether the success or failure of any calibration attempt is due to the nature of the material or to the techniques used to derive the regression model.

One way to resolve some of these uncertainties is to test wavelength selection strategies using a set of synthetic samples where the number of absorbance effects is limited and where the exact composition of each sample is known. Using samples that match these criteria, it is also possible to examine how the spectra of samples relate to those of constituents.

In this paper, the relationships between the spectra of samples and those of constituents are examined using a number of graphical representations of statistical treatments of the data.

Materials and Methods

Samples

Sixty-four samples were created by adding small amounts of each of three constituents, AnalaR-grade sucrose, arginine hydrochloride and benzoic acid, to a filler, sodium hydrogen carbonate. These four chemicals were chosen because they are all white crystalline powders that can be mixed easily. While the filler lacks any obvious absorption effects in the NIR spectrum, the other constituents all have clearly defined absorbance bands that can be used as "markers" to identify their presence in samples.

For each sample, the three constituents were present in a factorial arrangement of four concentration levels, 1.0, 2.0, 3.0 and 4.0 g, arranged so that the 64 samples included all possible combinations of these levels. Each sample was made up to a constant mass of 40 g using the filler. The mass of the filler thus varied between 28.0 and 37.0 g and was therefore the major ingredient of each sample.

As a consequence of this experimental design, the three constituents all have correlation values of zero with each other and of −0.53 with the filler. This avoids one of the problems found in material of biological origin where, as many of the constituents are highly correlated with each other, difficulties arise in identifying effects specific to any single constituent.

Further, as the concentrations of the three constituents were relatively low, their absorbance bands should be difficult to identify in the spectra of the samples. These spectra were therefore analogous to those of many agricultural products where the dominant absorption effects from starch mask weaker effects from constituents such as protein. Although these samples lack the complex structure inherent in biological material they still provide a challenge to the techniques used in NIR analysis.

Spectroscopy

All samples were scanned using a Neotec 6350 Research Composition Analyser. Spectra were recorded as log $1/R$, at 2-nm intervals from 1100 to 2500 nm; R, the reflectance value, is defined as

$$R = I_s/I_0$$

where I_s is the intensity of light reflected from the sample and I_0 is the intensity of light reflected from an internal ceramic standard.

This instrument operates in the single-beam mode recording five scans per second. To reduce the effect of instrument noise, all spectra were calculated as the average of 50 scans, and were smoothed using a five-point moving average algorithm. After smoothing, only wavelengths within the range 1120 to 2480 nm were considered, thus minimising any errors associated with the smoothing and any edge effects from the optics.

Statistical Methods for the Analysis of Spectral Structure

Previous attempts to relate the structure of spectra to the composition of samples have concentrated on constructing spectra by combining in various proportions the spectra of known constituents.[7] The proportions that generate the spectrum with the greatest similarity to the sample spectrum can then be compared with reference analytical values.

If the opposite approach is adopted, the composition of samples may be inferred by deriving spectral analogues, graphical representations of functions of the data that can be shown to resemble the spectra of constituents. The simplest of these analogues are the mean and standard deviation spectra, which are produced by calculating, for all samples, the mean and standard deviation of spectral values at each wavelength. Similarly, for each constituent, a correlation graph can be created by calculating the correlation between the spectral values at each wavelength and the concentration of the constituent, and plotting these correlations against wavelength.

In addition, the total variation found in sample spectra can be partitioned into principal components, which provide a further representation of the data and which can be plotted and visually evaluated. Principal component analysis is a standard statistical technique that can be used to incorporate all spectral values into a regression model and simultaneously allows a visual examination of the inherent structure of the data. A detailed explanation of the application of principal components to near-infrared reflectance analysis has been given earlier[9] but the most important points can be summarised as follows:

1. Principal components, unlike reflectance values, are uncorrelated variables.
2. Principal component variables are weighted averages of the original apparent absorption values, where the squared weights are constrained to sum to unity. Thus the relative importance of any point in the spectrum to a specific component is described by the weight at that point. For each component the weights may be plotted against the wavelengths to produce a spectral analogue that describes the structure of the variation for that component.
3. The products of the deviations of reflectance values from their means times the weighting coefficients may be summed across the spectrum to give a principal component score, which may be used in regression models to predict the composition of a sample.
4. In our experience, the number of principal components needed to express almost all the spectral variation rarely exceeds six.

Thus the use of principal component analysis permits both a visual inspection of features found in spectral data and the derivation of statistical models that describe the behaviour of the spectra in terms of composition.

In summary, therefore, for each set of samples it is possible to derive spectral analogues that relate to the mean, the variance, partitions of the total spectral variation (principal components) and the relationship between the spectral values and the concentration of constituents (correlation graphs).

These graphical representations form the basis of our analysis of spectral structure.

Standardisation of Spectra

As this experiment used samples created by mixing four ingredients, each with a different particle size distribution, a strong particle size influence was expected in the sample spectra. While multiple linear regression appears to compensate for the effect of particle size variation in NIR analyses, this effect does inhibit clear interpretation of the influences of individual absorbing constituents. Murray and Hall[10] have suggested a standardisation algorithm that partially compensates for particle size variation. The algorithm can be defined as follows.

Let y_{iw} denote the spectral value of the ith sample at wavelength w. Then the corresponding standardised value is defined by the following equation:

$$y_{iw}(\text{adj}) = y_{iw} [(a_m + b_m w)/(a_i + b_i w)]$$

where $a_i + b_i w$ is the estimated regression line of the ith sample spectral values on the wavelengths and $a_m + b_m w$ is the estimated regression line of the mean sample spectral values on the wavelengths.

Unsatisfactory adjustments occur, however, when $a_i + b_i w$ is close to zero. This problem can be avoided by offsetting all spectral values by a positive amount k, deriving the adjusted values by the above equation, then subtracting k from each adjusted value. For the results here k was set to a value of 1.00.

This algorithm has been applied to all the sample spectra, and analyses of the resulting standardised data are presented together with the analyses of the raw data.

Statistical Definitions

As many of the results presented here use the correlation coefficient (r) to describe relationships between variables, subscripts have been added to help identify the variables involved. Thus, r_{cc} is the correlation between constituent concentrations; r_{ce} is the correlation between constituent concentration and the energy values (log $1/R$) at a single wavelength; r_{cs} is the correlation between constituent concentration and the scores on a principal component; and r_{cp} is the correlation between the constituent concentration and particle size.

Results

Spectra of the four pure chemicals used in preparing the samples are shown in Fig. 1. While the filler lacks any clearly defined absorbance bands, the other constituents all have bands that can serve as markers. For arginine hydrochloride,
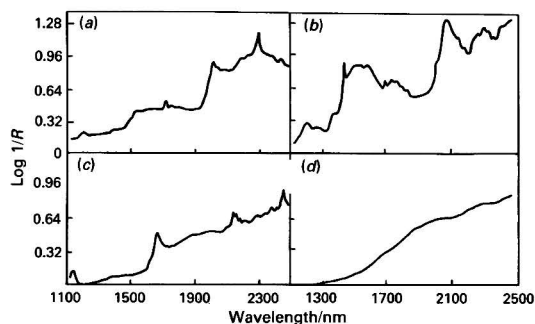

Fig. 1. NIR spectra of the four constituents used in the samples. (a) Arginine hydrochloride; (b) sucrose; (c) benzoic acid; and (d) sodium hydrogen carbonate
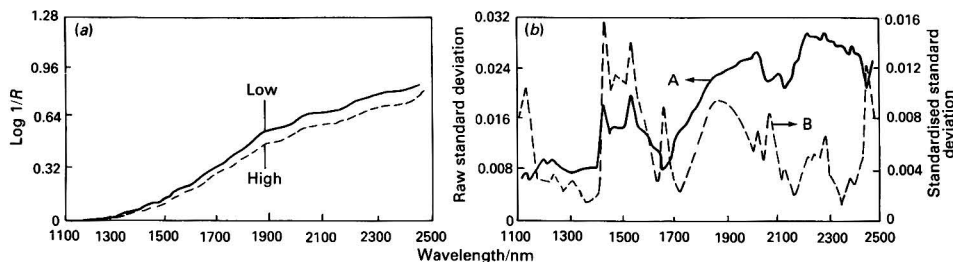
Fig. 2. (*a*) Spectra of the two samples with extremes of concentration of active constituents. (*b*) Standard deviation spectra for: A, raw standard deviation data; and B, standardised standard deviation data
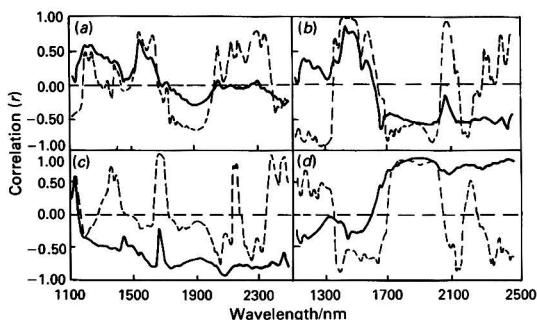

Fig. 3. Correlations of the sample absorption values with the concentration of each of the four constituents: (*a*) arginine hydrochloride; (*b*) sucrose; (*c*) benzoic acid; and (*d*) sodium hydrogen carbonate. Solid lines, raw data; broken lines, standardised data

bands at 1540, 1708, 2000 and 2288 nm were chosen, and for benzoic acid 1136, 1664, 2138, 2288 and 2456 nm. While both these constituents have isolated and well defined bands, the spectrum of sucrose is more complex. The dominant feature in the lower half of the spectrum is an area of high absorbance caused by three overlapping bands at 1438, 1524 and 1582 nm. In the top half, a very strong band at 2076 nm and a smaller band at 2316 nm complete a distinctive spectral pattern.

These characteristic patterns of spectral absorption provided references against which either the spectra of samples or of derived spectral analogues were compared.

Analysis of Mean and Standard Deviation Spectra

Fig. 2(*a*) shows spectra from the two samples that exhibited the extremes of concentration for all the constituents. Visual examination of these spectra reveals little information that can be related to the spectra of constituents. The mean spectrum lies between these two extremes and also provides little information relating to composition. However, the standard deviation spectra for both raw and standardised data [Fig. 2(*b*)] do exhibit features relating to those found in the spectra of constituents. For the raw data, peaks (local maxima) in variation occur where absorbance bands for arginine hydrochloride (1202, 1542 and 2000 nm), sucrose (1202 and 1440 nm) and benzoic acid (1136 nm) were observed. Local minima coincide with bands observed for benzoic acid (1660, 2138 and 2452 nm). It is interesting to note that the broad band at 2076 nm associated with sucrose does not feature in the raw standard deviation plot.

Standardisation of the data had three main effects on the standard deviation spectrum for the tendency: a general increase in variation in the upper half of the spectrum is removed, the influence of peaks corresponding to absorbance bands associated with benzoic acid now appear as peaks. The broad peak around 1888 nm does not match any band detected in the three constituents but may relate to the filler.

Analysis of Correlation Graphs

Interpretation

Fig. 3 shows the correlation graphs for both raw and standardised data for each of the four constituents. Before considering the relationship between the concentration of each constituent and the apparent absorption expressed in these graphs, it is necessary to define how the graphs should be evaluated.

If we accept that absorbance bands increase in intensity as the number of chemical bonds vibrating at the relevant frequency increases, then it follows that an absorbance band found only in one constituent should, if considered in isolation, cause the correlation between spectral values and concentration of the constituent of interest (r_{ce}) to be positive. However, some correlation graphs reveal areas of negative correlation at points in the spectrum where absorbance bands for this constituent are known to occur. This apparent contradiction can be explained if we consider how other constituents interact with the constituent of interest and how general effects such as particle size modify correlation values.

Where absorbance bands from two constituents coincide, this will modify r_{ce} by a factor that describes the relationship between the concentrations of the two constituents (r_{cc}) as determined by the inherent chemical nature of the samples. If r_{cc} is positive, then we have two effects acting in the same direction and r_{ce} may well be increased. If, on the other hand, r_{cc} is negative, then the effects act in opposition and r_{ce} will be reduced at that point in the spectrum. In practice, effects of absorbance bands from several constituents may be found at any point in the NIR spectrum.

In addition, we must also consider how variation in particle size affects spectral values. In the reflectance mode, larger particles cause greater absorbance effects, while reducing the particle size of a sample causes attenuation of absorption bands. Where constituents exhibit different particle size distributions, or vary in hardness and hence affect the milling properties of samples, then the final distribution of particles in the sample will depend upon the proportion of each constituent.

If the concentration of a constituent of interest is positively correlated with particle size (r_{cp}) then the graph of correlation values (r_{ce}) will generally be positive with local maxima matching absorbance bands associated with the constituent of interest. Local minima will match absorbance bands from constituents where r_{cp} is negative.

Where, for the constituent of interest, r_{cp} is negative then the graph will generally be negative with areas in the spectrum

relating to bands in that constituent appearing as local maxima. If this negative correlation (r_{cp}) is strong, then r_{ce} may not even attain positive values. Absorbance bands from other constituents will cause the negative base line effect of particle size to be increased or decreased depending upon the relationship between the other constituents and particle size.

In summary, for most NIR applications, we expect to find that correlation graphs exhibit a base line effect relating to particle size variation on which are superimposed effects due to absorbance bands. Where bands relate to the constituent of interest, deviations from this artificial base line should always be positive; where they relate to other constituents, the deviations may be either positive or negative, reflecting the inherent relationship between this other constituent and particle size.

Arginine hydrochloride

The raw correlation graph [Fig. 3(a)] exhibits local maxima (1200, 1540, 1708 and 2288 nm) at points in the spectrum where absorbance bands for this constituent were observed. Local minima appear to be associated with absorbance bands for benzoic acid (1132, 2184 and 2454 nm) and sucrose (1438 and 2072 nm). For standardised data, these features are considerably enhanced and additional points in the spectrum are revealed that match other absorbance bands.

Sucrose

For sucrose [Fig. 3(b)], high positive correlations are found in the lower half of the spectrum, while in the upper half all correlations are negative. In the upper half there are local maxima matching sucrose absorbance bands (1726, 2076, 2316 and 2422 nm). If the graph is interpreted in terms of a particle size interference effect, then these peaks are consistent with the expected absorption effects where particle size variation is presenting an offset base line.

In the lower half of the spectrum, peaks can be detected that match absorbance bands from sucrose (1372, 1438, 1726, 2316 and 2422 nm). The other constituents appear to have little influence, only minor effects relating to arginine hydrochloride being observed (1542 and 2380 nm).

When the data are standardised, the picture is considerably clarified. Peaks in the correlation graph relating to sucrose are now generally positively correlated, while troughs are found that coincide with absorbance bands for arginine hydrochloride (1712, 1748 and 2286 nm) and benzoic acid (2210 nm). In this instance, standardisation appears to have removed most of the interference from particle size variation and in doing so exposes the absorption effects from all constituents.

Benzoic acid

For benzoic acid [Fig. 3(c)], the effects of particle size variation are more pronounced than those observed for the other constituents. With raw data, an almost uniformly high negative correlation exists between spectral values and the level of benzoic acid in the samples. Only at 1134 nm can an area of high positive correlation be observed that matches an absorbance band for benzoic acid. Other dominant features in this graph are local maxima at 1662 and 2454 nm, which also match bands from benzoic acid. If we regard the over-all high negative correlations as a base line effect relating to particle size, then these effects are consistent with absorption effects from benzoic acid acting in an opposite direction to particle size effects. Minor effects relating to sucrose (1436, 2076 and 2314 nm) can also be observed but no effects from arginine hydrochloride are visible.

After standardisation, all correlations with absorption effects relating to benzoic acid become high and positive (1136, 1660, 2140, 2156, 2380 and 2454 nm) while troughs match effects from sucrose (1194, 1380, 1440, 2312 and 2422 nm) and arginine hydrochloride (1542 nm).

Sodium hydrogen carbonate

The absence of clear absorbance bands in the filler should result in a correlation graph characterised either by localised effects from the other three constituents or by general effects relating directly to the level of filler. Both these phenomena can be observed [Fig. 3(d)]. Areas of high positive correlation do not match absorption effects found in any of the constituents, and the uniformly high nature of these correlations again suggests a base line effect due to particle size. Acting against this effect are local minima relating to absorbance bands for sucrose. In the lower half of the spectrum these effects dominate. It is also of interest to note that the correlation graphs for sucrose and sodium hydrogen carbonate appear to be closely related, correlations (r_{ce}) at any wavelength being approximately equal but of opposite sign.

Standardisation enables additional effects from all three constituents to be identified. However, in both raw and standardised correlation plots, the area from 1700 to 2000 nm appears to relate solely to the level of filler in the samples.

Principal Components

Raw spectra

The first six principal components derived for raw data are shown in Fig. 4. These account for 99.94% of the total spectral variation. The percentage variation accounted for by each component and the correlation of scores with the concentration of each constituent (r_{cs}) are shown in Table 1.

The shape of the first principal component shows a general increase in weighting across the spectrum consistent with effects expected from particle size variation. Given that this component accounts for the vast majority of the spectral variation (85.51%), and that scores for this component are negatively correlated with all three constituents and highly positively correlated with the filler, then interpretation of this component as representing the effects of particle size variation is entirely consistent with conclusions drawn from the correlation graphs.

The second component accounts for almost all the remaining variation in the spectra (11.06%). This component may be interpreted as a comparison of the effects due to sucrose and arginine hydrochloride with those of benzoic acid and the filler. Absorbance effects due to sucrose and arginine hydrochloride are associated with relatively large positive
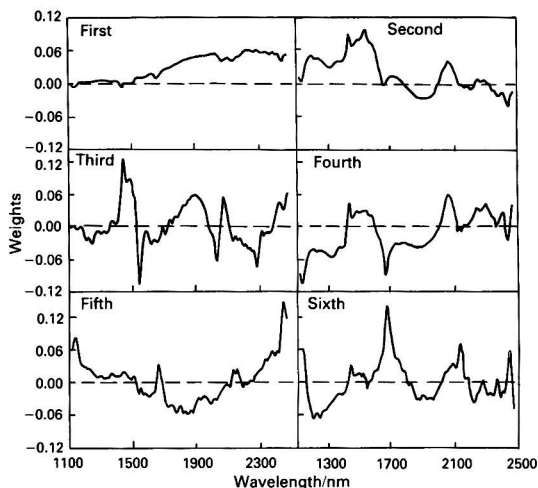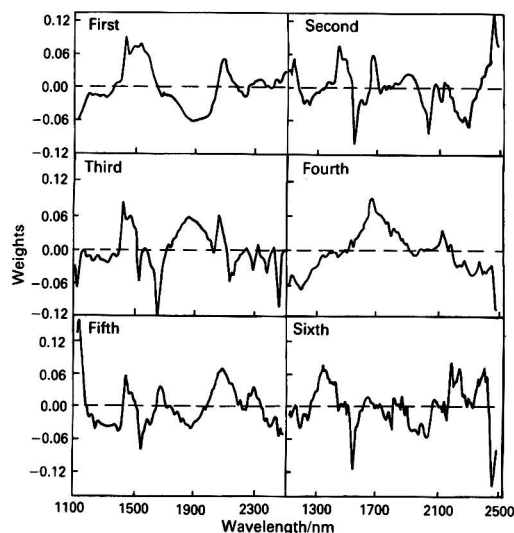

Fig. 4. First six principal components for the raw data

Table 1. Correlations between scores on each component and concentration of each constituent, and percentage variation expressed by each component

| | Arginine hydrochloride | Sucrose | Benzoic acid | Filler | Variation, % | | |
					Raw	Standardised	Adjusted
Raw:							
1	−0.09	−0.53	−0.78	+0.81	85.51	—	—
2	+0.48	+0.63	−0.42	−0.40	11.06	—	—
3	−0.77	+0.47	−0.14	+0.25	1.83	—	—
4	+0.02	+0.29	−0.32	+0.01	1.33	—	—
5	+0.05	+0.02	+0.15	−0.13	0.14	—	—
6	−0.25	+0.02	+0.11	+0.07	0.07	—	—
Standardised:							
1	+0.42	+0.88	−0.01	−0.74	—	63.86	7.22
2	−0.63	+0.35	+0.65	−0.21	—	22.43	2.54
3	−0.50	+0.30	−0.72	+0.53	—	12.04	1.36
4	−0.13	−0.02	+0.04	+0.06	—	0.98	0.11
5	−0.27	+0.02	−0.03	+0.16	—	0.28	0.03
6	−0.11	−0.01	−0.16	+0.16	—	0.12	0.01

Fig. 5. First six principal components for the standardised data

weights that cause the correlations between scores and the concentrations of these constituents to be positive. Similarly, the negative correlations (r_{cs}) with benzoic acid and filler are caused by the negative weights associated with their absorbance effects.

The remaining four components together account for 3.37% of the original spectral variation and in each, effects relating to the absorbing constituents can clearly be observed. If a constituent is positively correlated with a component (r_{cs}) then these effects will be observed as local maxima, if negatively correlated as local minima.

Standardised spectra

The first six principal components are shown in Fig. 5. The percentage variations and correlations (r_{cs}) are included in Table 1. The variation for each component is expressed as a percentage of the total variation both before and after standardisation. Thus, for example, the first standardised component accounts for 63.86% of the remaining variation after standardisation, equivalent to 7.22% of the variation in the raw spectra. Together these components account for 99.71% of the variation in the data after standardisation, corresponding to 11.31% of the original spectral variation.

Comparison of the graphs in Figs. 4 and 5 shows that the standardisation algorithm has removed the raw principal component associated with particle size. Principal components derived from standardised data can often be directly related to specific components for raw data. For these samples, the first standardised and second raw and the second standardised and third raw components are closely related. Features observed in raw components can be identified in the remaining standardised components and these features match absorption effects of constituents.

There is a close correspondence between the shape of the first standardised component and the spectrum of sucrose and this is reflected in the correlation (r_{cs} = 0.88) between scores on this component and the concentration of sucrose. In this component the high negative correlation between scores and the amount of filler confirms the relationship between sucrose and sodium hydrogen carbonate already observed in their raw correlation graphs.

The fourth, fifth and sixth components together express only 1.38% of the spectral variation and no constituent correlates (r_{cs}) highly with these components. Effects relating to each constituent can, however, be found in each component, but the number of effects that cannot be directly associated with individual constituents increases. Inevitably, these higher components will begin to be dominated by artifacts generated by the optical system and care should be taken in their interpretation.

Discussion

If we consider the information presented by all the graphs used to interpret the spectral structure, only those graphs which represent some function of the variation give any clear indication of composition. By examining the patterns of spectral variation instead of the actual spectral values, clearly defined patterns emerge, which, from a purely visual assessment, indicate the presence of and interactions between constituents. Further, absorption effects specific to a constituent of interest always result in local maxima in the corresponding correlation graph, while in principal components the sign of the correlation (r_{cs}) between scores and the concentration of a constituent determines whether absorbance effects will appear as local maxima or minima.

Standard deviation, correlation and principal component graphs each provide a different way of representing spectral variation. Standard deviation graphs are of limited value in that they indicate only the number of absorbance bands that influence the spectra. Correlation graphs present a picture of how the spectral variation relates to a specific constituent.

One drawback in their use is that errors associated with reference analytical values can distort the shape of the graph. For the samples considered in this paper such errors are likely to be minimal, although errors associated with sampling the mixtures will still remain. One advantage of principal components is that their shapes are derived purely from spectral data and errors associated with analytical values will affect only the correlation (r_{cs}) between the component scores and the constituents.

In these spectra, as for most NIR spectra, the dominant effect is particle size. Particle size is usually a function of the milling process used to prepare the samples and reflects, only indirectly, influences of the sample constituents. The particle size effect for these samples, however, is related directly to the particle size of the four constituents.

Using a Quantimet 900 Image Analyser, a brief examination was carried out of the particle size distribution in each constituent. For all four constituents the particle sizes, as measured by the areas of the particle images, fell into two distinct categories. The first, which accounted for between 39 and 50% of each constituent, consisted of small particles of less than 3.2 μm^2. The second included particles that ranged in size from 4.6 μm^2 to greater than 2048.0 μm^2. When the medians for these larger particles were ranked, their order was as follows: benzoic acid (22.4); arginine hydrochloride (29.8); sodium hydrogen carbonate (34.0); and sucrose (45.0). This order corresponded with the ranking order of the general levels of absorbance for the constituents (Fig. 1).

Standardisation of the data did not change the form of any of the graphs but seemed to enhance the effects due to absorbance bands. This is almost entirely due to the removal of particle size influences. Irrespective of its use in regression modelling, standardisation does appear to be useful in interpreting the effects of constituents. However, the samples used in this experiment are unusual in that their spectra are approximately linear and are therefore ideally suited to the application of Murray's algorithm. In our experience, the algorithm can be used with samples of biological origin but because of the non-linear nature of such spectra the results are likely to be less predictable.

In the interpretation of the graphical displays it is important to realise that in each instance the wavelengths quoted were identified by examining the actual data from which the graphs were produced together with the graphs themselves. It is reassuring that, when considering any of the graphical representations of the variation, the wavelengths at which effects are most pronounced either match exactly (within the limits of accuracy of the instrument) the absorbance bands detected in a constituent, or are shifted by a factor consistent with the interference effects of overlapping absorbance bands. It is also important to realise that, when comparing the shapes of different graphs, the scales used were larger than those presented in this paper, thus enabling detailed and accurate comparisons to be made.

In any NIR experiment, the statistical design should, wherever possible, be carefully controlled to provide adequate representation of the levels of variation normally associated with the sampled population. In this experiment, by limiting the number of factors likely to influence the results and by controlling the levels of these factors to avoid any confounding of the main effects, the relationship between the spectra of constituents and of the samples can be exposed with a clarity seldom possible with agricultural products. The results presented in this paper suggest two important guidelines for future experiments. Firstly, examination of variation is the best method of determining the composition of samples. This enables the effects of particle size to be distinguished from those due to absorbance bands. Secondly, the interpretation of all summary graphs is greatly simplified if spectra of known constituents are available as references. In this experiment such spectra were obtained using commercially produced pure chemical samples. In other experiments where it may be impossible to obtain the constituents in such a form, it would still be worthwhile preparing tissue fractions with high concentrations of a constituent and using these fractions to obtain reference spectra.

References

1. Norris, K. H., and Hart, J. R., in "Proceedings of the International Symposium on Humidity and Moisture, Principles and Methods of Measuring Moisture in Liquids and Solids," Volume 4, Reinhold, New York, 1968, pp. 19–25.
2. Williams, P. C., *Cereal Chem.*, 1975, **52**, 561.
3. Tkachuk, R. J., *J. Am. Oil Chem. Soc.*, 1981, **58**, 819.
4. Lanza, E. J., *J. Food Sci.*, 1983, **48**, 471.
5. Whetsel, K. B., Robinson, W. E., and Krell, M. W., *Anal. Chem.*, 1958, **30**, 98.
6. Goddu, R. F., and Delker, D. A., *Anal. Chem.*, 1960, **32**, 140.
7. Hruschka, W. R., and Norris, K. H., *Appl. Spectrosc.*, 1982, **36**, 261.
8. Mardia, K. V., Kent, J. T., and Bibby, J. M., "Multivariate Analysis," Academic Press, London, 1979.
9. Cowe, I. A., and McNicol, J. W., *Appl. Spectrosc.*, 1985, **39**, 257.
10. Murray, I., and Hall, P. A., *Anal. Proc.*, 1983, **20**, 75.

A Designed Experiment for the Examination of Techniques Used in the Analysis of Near-infrared Spectra

Part 2.* Derivation and Testing of Regression Models

Ian A. Cowe, James W. McNicol and D. Clifford Cuthbertson
Scottish Crop Research Institute, Pentlandfield, Roslin, Midlothian EH25 9RF, UK

Using mixtures of four pure chemicals, the predictive abilities of wavelength regression models produced by three different selection strategies are compared with models based on principal components. While both types of model predicted composition equally well, component models were less likely, based on calibration data, to produce an overoptimistic impression of predictive performance. No single wavelength selection strategy consistently produced better models. While wavelength models tended to be difficult to interpret in terms of absorbance bands, consistent patterns analogous to measurements of derivatives could be identified.

Keywords: *Near-infrared reflectance; regression analysis; principal components*

The use of multiple linear regression[1] to relate changes in apparent absorption at several points in the near-infrared (NIR) spectrum to the concentration of one of a number of constituents has been the basis of almost all published NIR results.[2] There are, however, problems associated with the use of regression on NIR data. The strong inter-correlation between absorption measurements at each wavelength has tended to produce regression models for which there is no satisfactory spectroscopic interpretation. It is also possible to identify many combinations of wavelengths, which for calibration samples predict composition with equal accuracy but whose performances on other sample sets differ considerably.

While the derivation of a single regression model is relatively simple, the necessity to test a large number of alternative combinations to identify the best sub-set of wavelengths from the entire NIR spectrum has led several workers to try fitting models based on Fourier analysis[3,4] or principal components.[5] These approaches have the advantage of providing very simple procedures for determining which terms should be included in the models. Further, each term is a function of the apparent absorption values at every wavelength.

In Part 1,[6] a set of spectra were examined to see how effectively various statistical techniques could reveal the known composition of the samples. In this part, the same set of calibration spectra were used to compare various methods for deriving regression models to predict the concentration of the sample constituents. The predictive ability of the models was compared using two further sets of samples of known concentration, one using the same factorial design as the calibration samples, the other with concentration varying in a less controlled manner.

Materials and Methods

Samples

Data from three sets of samples are considered here. The first, or calibration, set (sample set A) consisted of 64 samples that included all possible combinations at each of four concentration levels, 1.0, 2.0, 3.0 and 4.0 g of three constituents, AnalaR sucrose, arginine hydrochloride and benzoic acid, added to a filler, sodium hydrogen carbonate. Each sample

was made up to a constant mass of 40 g resulting in an amount of filler ranging from 28.0 to 37.0 g. Sodium hydrogen carbonate was therefore the major ingredient of each sample. The design of this set of samples has been considered in detail in Part 1. Two further sets (sample sets B and C), used to validate the regression models derived from the calibration set, were created in a similar manner. For the 32 samples in set B, the distribution of concentrations for each of the constituents was approximately uniform within the range 0.5 to 4.5 g, rather than fixed at one of four pre-determined levels. Some attempt was made to achieve low correlations among the constituents (see Table 1) by avoiding any obvious linear trends between the levels of each pair of constituents. The total mass of each sample was again made up to 40 g using sodium hydrogen carbonate as a filler. Although this design, when compared with the factorial design used in set A, makes it more difficult to distinguish between effects related to each constituent, it is inherently closer to the experimental situation that occurs in most applications of NIR. For the last of the sets (sample set C), the factorial design used for the calibration samples was repeated producing 64 samples that included all possible combinations of the three constituents at each of the four concentration levels.

Methods

Both sets of samples were scanned using the same Neotec 6350 Research Composition Analyser used to scan the calibration samples. Spectra were again recorded as log $1/R$ (where R is the reflectance) at 2-nm intervals from 1100 to 2500 nm and, after smoothing, only wavelengths within the range 1120 to 2480 nm were considered. As in Part 1, the modified version of Murray and Hall's algorithm[7] was applied to standardise all the sample spectra, and results for both raw and standardised data are presented.

Table 1. Inter-correlation for constituents in sample set B. V_1 = arginine hydrochloride; V_2 = sucrose; V_3 = benzoic acid; and V_4 = sodium hydrogen carbonate

	V_1	V_2	V_3	V_4
V_1	1.0000	—	—	—
V_2	0.1766	1.0000	—	—
V_3	0.2516	0.4713	1.0000	—
V_4	−0.6526	−0.7554	−0.7784	1.0000

In the statistical definitions listed in Part 1, subscripts were used to distinguish between various correlation coefficients. Using the same notation: r_{ce} is defined as the correlation between constituent concentrations and energy values (log $1/R$) at a single wavelength; r_{cc} is defined as the correlation between constituent concentrations; and r_{cs} is defined as the correlation between constituent concentrations and the scores on a principal component.

In addition to these correlations, the multiple correlation coefficient, R', is used as a measure of the fit of a regression model to calibration samples. It can be defined as the correlation between the actual determinations y, and the fitted determinations $\hat{y}$, thus

$$R' = \sqrt{\frac{\Sigma(y_i - \bar{y})(\hat{y}_i - \bar{\hat{y}})}{\Sigma(y_i - \bar{y})^2 \Sigma(\hat{y}_i - \bar{\hat{y}})^2}}$$

where $\bar{y} = 1/n\Sigma y_i$ and $\bar{\hat{y}} = 1/n\Sigma\hat{y}_i$. Values of R' for prediction samples have been calculated in the same way, except that the estimated determinations, $\hat{y}_i$, are calculated from the regression model derived from the corresponding calibration samples.

The standard error of calibration (SEC) and standard error of prediction (SEP) have been used to assess the ability of a model to estimate actual constituent levels. The SEC is defined as

$$SEC = \sqrt{\frac{\Sigma(y_i - \hat{y}_i)^2}{n - p - 1}}$$

where y_i and $\hat{y}_i$ are defined as above, n denotes the number of samples and p the number of independent variables in the model. The SEC is therefore a measure of the accuracy with which the model fits the data from which it was derived. The SEP is defined in the same way as the SEC, but measures how well the model fits other sets of samples and is therefore a measure of the predictive ability of the model.

Four further diagnostic statistics are quoted in the tables, namely bias, slope, intercept and adjusted SEP. The bias refers to prediction samples only and is defined as the mean of the actual determinations less the mean of the corresponding fitted values, i.e., $\bar{y} - \bar{\hat{y}}$. The slope and intercept refer to the regression of the estimated determination values on the actual values. A good model will produce slope and intercept values of approximately 1.0 and 0.0, respectively. Deviations from these values can give some indication of the manner in which the model is inadequate. The adjusted SEP is quoted because, for agricultural products, established calibration models used with sets of samples derived from different sites or grown in different seasons often produce slope values close to 1.0 but intercepts considerably different from 0.0. In such instances, there is a convention of adjusting the estimates to account for this bias.[5] The adjusted SEP is then used as a measure of the predictive ability of the model and is defined as follows:

$$SEP = \sqrt{\frac{\Sigma[y_i + (\hat{y}_i + bias)]^2}{n - p - 1}}$$

In Tables 2, 3 and 4, R' has been used as the summary measure of the fit of the regression models. This has been carried out to allow comparison with other published results, although R' itself is a slightly inadequate measure of fit as it does not take into account the number of independent variables in the regression model. On the other hand, the statistics used to measure predictive ability, namely SEC and SEP, do take into account the number of independent variables in the model.

Model Selection

NIR spectra typically consist of several hundred data points and given this number of potential independent variables it is impractical, even with the largest computers, to consider testing for predictive ability all possible sub-sets of up to five

or six wavelengths. It becomes necessary, therefore, to adopt a selection strategy that rapidly identifies one or several combinations of wavelengths whose values for R' are as high as possible.

In this paper we have reported results using three different strategies that have proved successful with previous sets of data. We also consider models based on principal components. Such models incorporate the energy values at every wavelength in the spectrum.

Selection strategies for wavelength regression models

Forward regression. This strategy is inherently the simplest in that it produces, for either raw or standardised data, a single solution. The wavelength with the highest modulus correlation between energy values and concentration (r_{ce}) is chosen as the initial term in a multiple regression equation. The second term is the wavelength that, in combination with the initial wavelength, has the highest multiple correlation (R') with concentration. Subsequent terms are the wavelengths that in turn maximise R'. When the inclusion of additional terms does not reduce the standard error of calibration (SEC), or leads to an increase in the standard error of prediction (SEP) for a set of test samples, then the model is considered complete. In practice, increasing the number of regression terms above three or four often leads to models that overfit the data.

Forward regression is generally successful when the constituent of interest is one of the major constituents of the sample, for example, protein. Where a more complex character is being estimated, such as forage digestibility, which can be considered as a function of several constituents, this method is often less successful.

Regardless of the ability of the forward regression strategy to produce a model that fits the calibration data, it does provide a reference set of results against which results obtained using other strategies may be compared.

Correlation pair selection. This strategy identifies a sub-set of wavelengths by examining the graph of correlation values (r_{ce}). Local maxima or minima in these graphs represent points in the spectrum where effects relating to absorbance bands from constituents can be most easily detected against a background effect from particle size. Local maxima match absorbance effects relating to either the constituent of interest, or to another constituent positively correlated (r_{cc}) with the constituent of interest. Local minima relate to absorbance bands from constituents other than the constituent of interest.

Having identified a sub-set of wavelengths (typically up to 40) that relate absorbance effects from both the constituent of interest and other major constituents, it is relatively easy to test, for values of R', all possible pair combinations from this sub-set. When likely pairs have been selected, an optimisation procedure is then applied to determine whether an alternative combination of closely related wavelengths would exhibit a higher value for R'. This iterative procedure attempts to compensate for the interference effects of overlapping absorbance bands. Where two or more bands overlap, selecting a wavelength on the shoulder of a band relating to the constituent of interest, rather than on the apex, may give better results. This occurs because such a wavelength, is further from the source of the interference effect, although the signal is weaker.

To illustrate how this optimisation procedure operates, consider an example for a selected pair of wavelengths w_1 and w_2. The initial stage of any cycle is the calculation of values for R' for combinations of w_1 with all wavelengths within 20 nm of w_2. The wavelength within 20 nm of w_2 at which R' is maximised, say w_{2a}, is selected as the second wavelength in the regression model. It is possible that $w_{2a} = w_2$.

The second half of the cycle involves fixing w_2 or w_{2a} and calculating R' for all combinations using this wavelength with

all wavelengths within 20 nm of w_1. The wavelength within 20 nm of w_1 at which R' is maximised, say w_{1a}, is selected as the initial wavelength in the regression model. Again w_{1a} can equal w_1.

If w_1 has been substituted, then a second cycle is initiated with w_{1a} replacing w_1. The process continues through as many cycles as necessary until no substitution occurs. The wavelengths that result from this optimisation procedure are then used as the initial two terms in a forward regression strategy.

Our experience, having analysed many different types of data, is that this strategy generates a number of models, whose predictive ability is comparable to, or better than, the solution derived from forward regression. In addition, models using wavelengths in the lower half of the spectrum where absorbance bands relate to first or second overtones can be compared with models using wavelengths above 2000 nm where combination bands are more important.

Selection from constituent spectra. A similar strategy to the correlation pair selection process can be adopted by examining the spectra of constituents rather than correlation graphs. Constituent spectra present a clear picture of the wavelengths at which absorbance bands occur. These wavelengths, which are known to relate to specific constitutents, can then be tested in models. Using this strategy, a sub-set of wavelengths is chosen to represent the absorbance bands from both the constituent of interest and the other major constituents. All possible pairs from this sub-set are then tested, and after the same optimisation process described previously, suitable pairs are used as the initial terms in forward regression.

This strategy can also produce models whose predictive ability is comparable to, or better than, the solution derived from forward regression. In particular, it can succeed in situations where there are only a few dominant absorption effects and where the interactions between these effects are relatively simple.

Principal component strategy

The selection of principal components to be included in a regression model to predict composition is straightforward because of the uncorrelated nature of the components. This causes the multiple correlation R' for any combination of

components to be the square root of the sum of the squares of correlations (r_{cs}) for individual components. Thus for the model using standardised data, which includes the first, second, third and fifth principal components for arginine hydrochloride (Model 4 in Table 2)

$$R' = \sqrt{(0.42)^2 + (0.63)^2 + (-0.50)^2 + (-0.27)^2}$$
$$= 0.943$$

The simple nature of this procedure provides an uncomplicated selection strategy where components with the highest values of r_{cs} are included in the model. As a consequence, few combinations of components need be tested, and such testing is aimed largely at determining whether the model is over-fitting the data, rather than whether the model is intrinsically sound.

Results

Summary regression results relating to all component and wavelength models for arginine hydrochloride, sucrose and benzoic acid are given in Tables 2, 3 and 4, respectively. Although the results for both prediction sets of samples were calculated only those for set B are included in the tables in order to save space. Discussion of these results has been restricted mainly to set B because of the more natural distribution of constituent values and because the results for set C are in broad agreement. Regression coefficients for all component models are given in Table 5 and for all wavelength models in Table 6.

The tables discussed summarise results using regression models selected by the three strategies previously described.[6] The criteria used for including models in the tables were as follows.

1. Principal component models that include the first six components. These models incorporate almost all the variation found in the sample spectra.

2. Principal component models using only those components shown to correlate highly with the constituent of interest.

3. Forward regression wavelength models. These provide a reference against which other selection strategies are compared.

Table 2. Summary of statistics for arginine hydrochloride regression models. Table headings are as defined in the text: RPC = principal components for raw data; SPC = principal components for standardised data; RW = raw wavelengths; SW = standardised wavelengths; FR = forward regression strategy; CP = correlation pairs strategy; SP = constituent spectra strategy; A = sample set A (calibration samples); and B = sample set B

Model for arginine hydrochloride	Sample set	R'	SEC	SEP (raw)	SEP (adjusted)	Bias	Intercept	Slope
1. RPC 1, 2, 3, 4, 5 and 6	A	0.943	0.395	—	—	—	0.28	0.89
	B	0.905	—	0.636	0.609	−0.16	0.42	0.89
2. RPC 2 and 3	A	0.903	0.493	—	—	—	0.46	0.82
	B	0.973	—	0·369	0·305	0.20	−0.02	0.92
3. SPC 1, 2, 3, 4, 5 and 6	A	0.959	0.336	—	—	—	0.20	0.92
	B	0.948	—	0.577	0.449	−0.32	0.51	0.92
4. SPC 1, 2, 3 and 5	A	0.943	0.386	—	—	—	0.28	0.89
	B	0.948	—	0.432	0.432	0.02	0.14	0.93
5. SPC 1, 2 and 3	A	0.903	0.496	—	—	—	0.46	0.82
	B	0.971	—	0.412	0.317	0.25	−0.17	0.97
6. RW 1540, 1590, 1240 and 1356; FR	A	0.972	0.272	—	—	—	0.14	0.95
	B	0.950	—	1.015	0.441	−0.84	0.85	0.99
7. RW 1240, 1394 and 1356; CP ..	A	0.970	0.281	—	—	—	0.15	0.94
	B	0.959	—	0.759	0.397	−0.61	0.57	1.02
8. SW 1540, 1302, 2282 and 1242; FR	A	0.973	0.269	—	—	—	0.13	0.95
	B	0.946	—	0.669	0.463	−0.44	0.45	1.00
9. SW 1242, 1848, 1172 and 2282; CP	A	0.977	0.248	—	—	—	0.11	0.96
	B	0.948	—	0.475	0.453	−0.13	0.15	0.99
10. SW 1242, 1908, 1172 and 2288; CP	A	0.976	0.252	—	—	—	0.12	0.95
	B	0.945	—	0.483	0.470	−0.10	0.10	1.00
11. SW 1304, 1552, 1612 and 2276; CP	A	0.957	0.337	—	—	—	0.21	0.92
	B	0.950	—	0.659	0.433	−0.46	0.52	0.97

Table 3. Summary statistics for sucrose regression models. Abbreviations as in Table 2

	Model for sucrose	Sample set	R'	SEC	SEP (raw)	SEP (adjusted)	Bias	Intercept	Slope
1.	RPC 1, 2, 3, 4, 5 and 6	A	0.995	0.117	—	—	—	0.02	0.99
		B	0.993	—	0.206	0.190	0.07	−0.22	1.06
2.	RPC 1, 2, 3 and 4	A	0.995	0.120	—	—	—	0.03	0.99
		B	0.991	—	0.276	0.201	0.17	−0.29	1.05
3.	SPC 1, 2, 3, 4, 5 and 6	A	0.995	0.116	—	—	—	0.02	0.99
		B	0.993	—	0.185	0.180	0.04	−0.15	1.05
4.	SPC 1, 2 and 3	A	0.995	0.118	—	—	—	0.03	0.99
		B	0.993	—	0.184	0.172	0.06	−0.18	1.05
5.	RW 1438, 1462 and 1698; FR ..	A	0.992	0.143	—	—	—	0.04	0.99
		B	0.990	—	0.202	0.195	0.05	−0.04	1.04
6.	RW 2070, 2226, 2312; CP	A	0.994	0.130	—	—	—	0.03	0.99
		B	0.991	—	0.310	0.191	−0.23	0.13	1.04
7.	RW 1476, 1706, 1300, 1178; CP ..	A	0.994	0.126	—	—	—	0.03	0.99
		B	0.988	—	0.232	0.218	0.07	−0.16	1.04
8.	RW 1440, 1704, 1310; CP	A	0.994	0.126	—	—	—	0.03	0.99
		B	0.990	—	0.199	0.195	0.04	−0.11	1.03
9.	RW 1442, 1462, 1492; CP	A	0.992	0.144	—	—	—	0.04	0.98
		B	0.985	—	0.241	0.240	−0.01	−0.08	1.04
10.	RW 2068 and 2194; SP	A	0.995	0.116	—	—	—	0.03	0.99
		B	0.996	—	0.209	0.153	0.14	−0.32	1.08
11.	RW 2076 and 2190; SP	A	0.996	0.108	—	—	—	0.02	0.99
		B	0.996	—	0.247	0.150	0.19	−0.37	1.08
12.	SW 1482, 1474, 1444, 2190; FR ..	A	0.994	0.123	—	—	—	0.03	0.99
		B	0.992	—	0.217	0.174	0.12	−0.19	1.03
13.	SW 1204, 1456 and 1494; CP ..	A	0.994	0.129	—	—	—	0.03	0.99
		B	0.989	—	0.223	0.209	0.07	−0.16	1.04
14.	SW 1442, 2092 and 2430; CP ..	A	0.995	0.112	—	—	—	0.02	0.99
		B	0.996	—	0.160	0.158	0.02	−0.20	1.07
15.	SW 2086, 2212, 1212 and 2046; CP	A	0.996	0.107	—	—	—	0.02	0.99
		B	0.994	—	0.223	0.174	−0.13	−0.02	1.06
16.	SW 2076, 2444 and 2462; CP ..	A	0.996	0.105	—	—	—	0.02	0.99
		B	0.992	—	0.202	0.199	−0.03	−0.16	1.08

4. Wavelength models derived by either the correlation pair strategy or by the selection from constituent spectra strategy, where the results are comparable to, or better than, those for forward regression. If these strategies produce much better results than forward regression, then only the best of these models are included.

For reasons of space, scatter diagrams of fitted against actual concentration values are not shown for all models presented in Tables 2, 3 and 4. Fig. 1, however, shows scatter diagrams for two representative models from each constituent.

Arginine Hydrochloride

Regression results are given in Table 2. Using principal components, the best models (Models 2 and 5) were obtained by restricting the number of components to two or three, rather than including all six. Although the calibration standard errors (SECs) were much higher for these two models than for Models 1 and 3, their standard errors of prediction (SEPs) were much lower. It would appear therefore that, for both raw and standardised data, the inclusion of components four, five and six overfits the data. The best component models (Models 2 and 5) were able to predict the amount of arginine hydrochloride in test samples with SEPs close to 0.3.

Both the raw and standardised wavelength models produced consistently lower SECs than models based on principal components. However, for the test samples this situation was reversed, with the two best component models (Models 2 and 5) having much lower SEPs, both before and after correction for bias. In addition, the number of wavelength models with SEP (after correction for bias) less than 0.50 was very small; the correlation pair strategy yielded only one raw and three standardised combinations, while the strategy based on constituent spectra did not produce a single model to this specification.

Examination of the regression diagnostic statistics showed that the regression slopes for wavelength models were better (closer to 1.0) than those for components, but their bias values were higher. While no single wavelength model was considerably better than any other, the forward regression solution for raw data showed a high bias figure (−0.84) and for this reason would normally be discarded.

Of all the absorbance bands found in the spectrum of arginine hydrochloride, only those at 1540 and 2288 nm were included in any of the wavelength models. None of the other wavelengths appear to relate to clear absorption effects from arginine hydrochloride or to bands from the other constituents. The forward regression strategy (Models 6 and 8) produced models based on the very weak band at 1540 nm. The remaining models were all dominated by wavelengths from the lower half of the spectrum. While for raw data these selections are consistent with the information presented in the correlation graph [see Part 1, Fig. 2(a)], no explanation can be offered for the higher correlations for those weaker bands, when compared with the correlations for the strong absorbance bands at 2000 and 2288 nm. Standardised models also rely more on wavelengths from the lower half of the spectrum, even though standardisation does increase considerably correlation values for bands in the upper half.

Although all these models appear to predict the amount of arginine hydrochloride reasonably well, it would appear that no single model, whether based on components or wavelengths, matches all three desirable characteristics of consistently low SEC and SEP, low bias and a regression slope of 1.0.

Sucrose

Regression results are given in Table 3. Because there were a large number of models for which R' approached 1.0, only those for which the calibration value of R' exceeded 0.994 were tested.

Table 4. Summary statistics for benzoic acid regression models. Abbreviations as in Table 2

	Model for benzoic acid	Sample set	R'	SEC	SEP (raw)	SEP (adjusted)	Bias	Intercept	Slope
1.	RPC 1, 2, 3, 4, 5 and 6	A	0.970	0.289	—	—	—	0.15	0.94
		B	0.979	—	0.282	0.271	0.68	−0.02	0.98
2.	RPC 1, 2 and 4	A	0.943	0.385	—	—	—	0.28	0.89
		B	0.930	—	0.779	0.480	0.58	−0.51	0.97
3.	SPC 1, 2, 3, 4, 5 and 6	A	0.984	0.208	—	—	—	0.08	0.97
		B	0.971	—	0.320	0.318	−0.03	0.29	0.90
4.	SPC 2, 3 and 6	A	0.983	0.210	—	—	—	0.08	0.97
		B	0.966	—	0.353	0.328	−0.12	0.43	0.88
5.	SPC 2, 3	A	0.970	0.278	—	—	—	0.15	0.94
		B	0.977	—	0.358	0.260	−0.23	0.40	0.93
6.	RW 2076, 1668, 1698 and 1748; FR	A	0.974	0.264	—	—	—	0.13	0.95
		B	0.987	—	0.437	0.223	0.35	−0.45	1.04
7.	RW 1676, 1696 and 1752; CP	A	0.973	0.265	—	—	—	0.13	0.95
		B	0.987	—	0.422	0.215	0.34	−0.43	1.04
8.	RW 1668, 2088, 1698 and 1748; CP	A	0.974	0.264	—	—	—	0.13	0.95
		B	0.987	—	0.444	0.222	0.35	−0.46	1.04
9.	RW 2064, 2458, 2424 and 2472; CP	A	0.982	0.223	—	—	—	0.09	0.96
		B	0.962	—	0.352	0.347	0.06	0.14	0.92
10.	RW 2426, 2456 and 1976; CP	A	0.981	0.223	—	—	—	0.09	0.96
		B	0.969	—	0.317	0.312	−0.05	0.22	0.89
11.	RW 1436, 2250, 2136 and 2188; SP	A	0.976	0.252	—	—	—	0.12	0.95
		B	0.969	—	0.631	0.387	0.46	−0.74	1.11
12.	RW 2164, 2308, 1724 and 2198; SP	A	0.982	0.221	—	—	—	0.09	0.96
		B	0.972	—	1.080	0.443	0.91	−1.40	1.20
13.	RW 2210, 2310, 2458 and 2422; SP	A	0.981	0.225	—	—	—	0.09	0.96
		B	0.964	—	0.349	0.341	0.07	0.21	0.89
14.	SW 1662, 2462 and 2430; FR	A	0.981	0.227	—	—	—	0.10	0.96
		B	0.968	—	0.313	0.310	−0.04	0.21	0.93
15.	SW 1390, 1662, 2458 and 1376; CP	A	0.979	0.239	—	—	—	0.11	0.96
		B	0.977	—	0.335	0.269	−0.18	0.26	0.97
16.	SW 1450, 1662 and 2462; CP	A	0.974	0.261	—	—	—	0.13	0.95
		B	0.981	—	0.268	0.243	−0.11	0.27	0.93
17.	SW 1442, 2458 and 1168; CP	A	0.980	0.232	—	—	—	0.10	0.96
		B	0.979	—	0.316	0.256	−0.17	0.35	0.93
18.	SW 1656, 2438 and 2170; CP	A	0.973	0.268	—	—	—	0.14	0.95
		B	0.970	—	0.357	0.335	0.12	−0.24	1.05
19.	SW 1662, 2462, 2430 and 1334; CP	A	0.981	0.228	—	—	—	0.10	0.96
		B	0.970	—	0.313	0.309	−0.05	0.25	0.92
20.	SW 2424, 2458, 1390 and 1382; CP	A	0.982	0.222	—	—	—	0.09	0.97
		B	0.959	—	0.390	0.366	−0.12	0.47	0.86
21.	SW 2380, 2156, 2140 and 1136; SP	A	0.956	0.342	—	—	—	0.22	0.91
		B	0.965	—	0.659	0.334	−0.52	0.59	0.98

Table 5. Regression coefficients for the principal component models shown in Tables 2, 3 and 4. A = arginine hydrochloride; S = sucrose; B = benzoic acid

	Model	Intercept	Component					
			1	2	3	4	5	6
A	Raw	2.50	−0.21	−3.18	−12.57	0.30	3.05	−20.92
	Standardised	2.50	3.43	8.71	−9.54	8.82	−34.01	−21.01
S	Raw	2.50	−1.28	−4.22	7.66	5.64	1.44	1.59
	Standardised	2.50	7.26	−4.90	5.79	1.07	2.86	−1.91
B	Raw	2.50	−1.87	2.83	−2.24	−6.22	8.71	8.99
	Standardised	2.50	−0.11	−8.99	−13.77	−2.49	−3.13	−30.94

While both raw component models (Models 1 and 2) had similar SEPs, the inclusion of components four, five and six marginally improved the SEP and reduced the bias. For the standardised models, inclusion of these components had the opposite effect. Models 1 and 4 would therefore appear to be the better choices.

All three wavelength strategies produced combinations for which the SEP was low, with no single equation being outstanding. The levels of error for both component and wavelength models were almost identical (SEP < 0.20) and the diagnostic statistics confirmed the accuracy of the models. All regression slopes were close to 45° (slope = 1.0) with very low bias values.

Most models relate either to several overlapping absorbance bands in the region 1400–1600 nm, or to the band at 2076 nm. With the exception of Model 14, which included terms from both areas, the selection of an initial term from either part of the spectrum appeared to cause subsequent terms to be selected from nearby parts of the spectrum only.

For this constituent, wavelength models tended to relate solely to its own absorbance bands, and neither of the other two constituents appeared to contribute to any great extent in any of the models derived using any of the three strategies.

Benzoic Acid

Regression results for this constituent are shown in Table 4. As with sucrose, the best raw component model (Model 1) included all six components; for standardised data Model 5, which included only components two and three, gave the best

Table 6. Regression coefficients (and corresponding wavelengths, nm) for wavelength models shown in Tables 2, 3 and 4

Model No.	Intercept	Term			
		1st	2nd	3rd	4th
Arginine hydrochloride:					
6	11.61	−44.70 (1540)	60.60 (1590)	466.70 (1240)	−467.60 (1356)
7	11.38	356.40 (1240)	33.40 (1394)	−375.90 (1356)	—
8	138.60	148.49 (1540)	174.40 (1302)	−231.30 (2282)	235.20 (1242)
9	86.30	580.80 (1242)	−30.56 (1848)	−364.30 (1172)	−106.30 (2282)
10	91.20	589.40 (1242)	−35.30 (1908)	−357.10 (1172)	−107.80 (2288)
11	81.00	407.20 (1304)	266.40 (1552)	−191.80 (1612)	−128.80 (2276)
Sucrose:					
5	5.01	121.50 (1438)	−92.00 (1462)	−19.95 (1698)	—
6	−0.19	75.65 (2070)	−136.00 (2226)	67.10 (23.12)	—
7	5.67	73.90 (1476)	−31.62 (1706)	−92.70 (1300)	51.90 (1178)
8	5.43	60.33 (1440)	−28.58 (1704)	−27.30 (1310)	—
9	0.39	230.36 (1442)	−269.70 (1462)	42.40 (1494)	—
10	7.07	98.15 (2068)	−98.24 (2194)	—	—
11	7.50	93.28 (2076)	−95.12 (2190)	—	—
12	9.30	402.90 (1482)	−414.00 (1474)	77.40 (1444)	−24.90 (2190)
13	−10.55	13.20 (1204)	71.80 (1456)	38.20 (1494)	—
14	−86.10	32.11 (1442)	80.40 (2092)	43.93 (2430)	—
15	12.20	130.82 (2086)	−103.10 (2212)	59.90 (1212)	−35.00 (2046)
16	−102.54	123.19 (2076)	6.23 (2444)	27.55 (2462)	—
Benzoic acid:					
6	7.52	−4.93 (2076)	188.50 (1668)	−295.20 (1698)	99.30 (1748)
7	6.60	244.50 (1676)	−313.70 (1696)	56.80 (1752)	—
8	7.67	187.90 (1668)	−5.90 (2088)	−294.00 (1698)	100.00 (1748)
9	0.97	8.51 (2064)	138.30 (2458)	−111.20 (2424)	−38.20 (2472)
10	5.96	−137.45 (2426)	114.06 (2456)	17.48 (1976)	—
11	4.30	−28.58 (1436)	−93.50 (2250)	199.70 (2136)	−91.30 (2188)
12	3.59	381.40 (2164)	−202.55 (2308)	−84.20 (1724)	−104.00 (2198)
13	4.73	22.60 (2210)	−12.10 (2310)	114.60 (2458)	−132.60 (2422)
14	−20.29	55.52 (1662)	99.70 (2462)	−96.00 (2430)	—
15	−64.25	536.00 (1390)	39.10 (1662)	71.76 (2458)	−639.00 (1376)
16	−61.20	−14.01 (1450)	63.50 (1662)	57.11 (2462)	—
17	−73.23	−50.32 (1442)	98.80 (2458)	−87.20 (1168)	—
18	−182.90	56.10 (1656)	88.90 (2438)	151.80 (2170)	—
19	−22.49	51.15 (1662)	101.70 (2462)	−94.30 (2430)	14.20 (1334)
20	5.34	−133.00 (2424)	121.56 (2458)	338.00 (1390)	−340.00 (1382)
21	−172.00	185.60 (2380)	−228.00 (2156)	−284.10 (2140)	30.09 (1136)

results. However, for benzoic acid the derivation of a standardised component model was more complicated than for the other constituents. When compared with Model 3, the omission of components one, four and five (Model 4) did in fact increase the SEPs for the two sets of test samples by approximately 0.01, but when component six was also omitted (Model 5) the SEPs, corrected for bias, were respectively 0.05 and 0.02 lower than those for Model 3. This indicates that inclusion of component six may have caused overfitting of the data.

All three wavelength strategies produced acceptable combinations, with the forward regression and correlation pair strategies producing marginally better results than selection from constituent spectra. In general, regression slopes for wavelength models were closer to 1.0 than component models but there was considerable variation in the slopes for both types. Three wavelength models (Models 11, 12 and 21) exhibited considerable bias effects and could not be recommended for this reason. Most models related to one of two strong benzoic acid absorbance bands (1664 and 2456 nm), but two models were based on the band at 2156 nm (Models 12 and 21).

The forward regression solution for raw data (Model 6) was interesting in that 2076 nm, the initial term, related not to benzoic acid but to sucrose. This, however, is consistent with the interpretation of the raw benzoic acid correlation graph proposed in Part 1. The high negative correlation of benzoic acid with particle size produces a negative base line effect upon which are superimposed local maxima and local minima relating to absorbance bands from other constituents. As

effects due to the constituent of interest (in this instance benzoic acid) always result in local maxima, then a consequence of this negative base line is that the highest modulus correlation will always relate to one of the other constituents. The second term (1668 nm) does, however, relate to benzoic acid and for this reason the model is probably sound.

For both raw and standardised data, many of the models included one wavelength that relates to one of the other constituents (1438, 2422 and 2076 nm for sucrose and 2426 and 1744 nm for arginine hydrochloride). Standardisation excluded wavelengths relating to arginine hydrochloride from the models, but those relating to sucrose were still evident.

Discussion

Unlike samples of biological origin where the accuracy of the reference analytical method for each constituent may differ, in these samples all three constituents were measured with the same degree of accuracy (±2 mg). Despite this, the accuracy by which the constituents were predicted varied considerably. The variation in SEP between models for any one constituent was less than the variation between models for different constituents. For sucrose almost all models tested had, after correction for bias, values for SEP of less than 0.20. For benzoic acid, the best models had values of between 0.25 and 0.30 while for arginine hydrochloride only two models had SEPs of less than 0.40.

Two possible explanations can be offered. Firstly, when the samples were prepared it was easier to mix the filler with sucrose than with benzoic acid, which tended to form
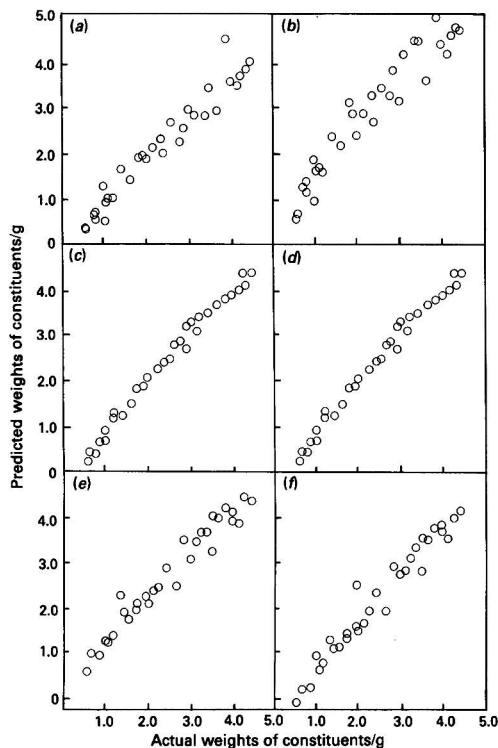
Fig. 1. Scatter diagrams of actual values *versus* predicted values for three constituents. (*a*) Arginine hydrochloride (Model 2); (*b*) arginine hydrochloride (Model 7); (*c*) sucrose (Model 1); (*d*) sucrose (Model 14); (*e*) benzoic acid (Model 5); and (*f*) benzoic acid (Model 7)

aggregates. Secondly, sucrose absorbs strongly while the bands chosen by the wavelength models for arginine hydrochloride and benzoic acid are much weaker and lie in an area of the spectrum where interference from sucrose is greatest. In particular, the band at 1540 nm, which correlates most highly with arginine hydrochloride is very poorly defined and is likely to be most affected by this interference.

The ranking of the constituents, in terms of the accuracy of prediction, was matched by the ease with which suitable wavelength models could be identified. For sucrose a very large number of models could be identified where, for calibration data, $R' > 0.99$; for benzoic acid the best model had a correlation of 0.98 with only 12 alternatives having values where $R' > 0.975$, while for arginine hydrochloride $R' = 0.977$ was the highest calibration correlation for any wavelength model and only five other models approached this value.

The constituents also showed differences in the stability of the regression slopes. For sucrose, almost perfect values of 1.00 were obtained; for benzoic acid the slopes tended to be lower and more variable, while for arginine hydrochloride this tendency to increased variability and low regression slope was most pronounced with slopes varying between 0.83 and 1.00.

For some constituents there was evidence that, particularly with standardised data, inclusion of the fourth, fifth or sixth components tended to overfit the data with a consequent increase in SEP. These components could be affected either by numerical accuracy during calculation of the components or by instrumental factors such as temperature drift during the period in which the samples were scanned.

For principal component models, the coefficients are shown in Table 5. Whereas regression coefficients for wavelength models vary in magnitude as terms are either added to or are removed from the developing model, those for component models are fixed regardless of how many terms are included in the model.

Examination of the form of the wavelength models reveals at least two different ways in which regression models relate absorbance bands to the concentration of a constituent. In the first of these, each of several absorbance bands is characterised by a single wavelength, and at least one band must relate to the constituent of interest. In the second, several wavelengths describe a single absorbance band, which again must relate to the constituent of interest. In both instances, additional wavelengths are usually found that do not relate to any specific absorbance band. It may be that these terms are included in the model to compensate for some general effect. The obvious candidate in this respect would be particle size.

The first category includes most of the models for arginine hydrochloride and, among others, Models 7 and 14 for sucrose and Models 11 and 21 for benzoic acid. The predicted values produced by this type of model can be considered as a comparison of the effects caused by a number of sources of variation. Coefficients (see Table 6) for this type of model do not form any set pattern of either magnitude or sign, and an interpretation of this type of model can often be difficult.

Almost all models for sucrose can be considered as being of the second type, as could Model 6 for arginine hydrochloride and Models 7 and 20 for benzoic acid. For this type of model, coefficients do conform to a definite pattern (see Table 6). Where two wavelengths are involved, they characterise the slope of one side of an absorbance band. The coefficients are of opposite sign and one wavelength lies near the apex of the band. This arrangement can be expressed as a function of the first derivative of the spectrum. Model 8 for arginine hydrochloride illustrates this point. Where three wavelengths are involved, the shape of part of the NIR spectrum is described. The highest and lowest wavelengths have coefficients of the same sign; the intermediate wavelength has a coefficient of the opposite sign. This arrangement is equivalent to a function of a second derivative. Model 15 for sucrose illustrates this pattern. The correspondence between this type of model with first- or second-derivative transformations of the data supports the use of derivative models as suggested by Norris et al.[9]

Conclusions

The results reported in this paper illustrate the performance and properties of two types of regression model, the first based on wavelengths, the second on principal components. Both types of model were used to predict the levels of three constituents. The accuracy of the predictions appeared to be a function of the nature of the constituents rather than the type of model used.

For wavelength models it was difficult to tell from calibration results how well any model would perform. As a general rule, the standard error of calibration tended to give an overoptimistic impression of the ability of the model to predict other sets of data. Wavelength models were also difficult to interpret in terms of composition and several different wavelength strategies were required to identify the best models.

On the other hand, the performance of component models appeared to be more stable in that the standard error of calibration was usually closer in value to the standard error of prediction. Also, the number of combinations of components that needed to be tested was relatively small, with overfitting being the only problem.

Although the amount of computation involved in the derivation of a given wavelength model was much less than that involved in the derivation of a component model, the total amount of computation could be greater as the number of alternative combinations that had to be tested was very much larger.

It would appear, therefore, that the use of principal components in near-infrared analysis has the advantage of combining analysis of spectral structure as described in Part 1 with a simple and dependable regression strategy.

References

1. Draper, N. R., and Smith, H., "Applied Regression Analysis," Wiley, New York, 1981.

2. Williams, P. C., and Cordeiro, H. M., *J. Agric. Sci. Camb.*, 1985, **104**, 113.
3. Giesbrecht, F. G., McClure, W. F., and Hamid, A., *Appl. Spectrosc.*, 1981, **35**, 210.
4. McClure, W. F., Hamid, A., Giesbrecht, F. G., and Weeks, W. W., *Appl. Spectrosc.*, 1981, **38**, 301.
5. Cowe, I. A., and McNicol, J. W., *Appl. Spectrosc.*, 1985, **39**, 257.
6. Cowe, I. A., McNicol, J. W., and Cuthbertson, D. C., *Analyst*, 1985, **110**, 1227.
7. Murray, I., and Hall, P. A., *Anal. Proc.*, 1983, **20**, 75.
8. Lanza, E., *J. Food Sci.*, 1983, **48**, 471.
9. Norris, K. H., Barnes, R. F., Moore, J. E., and Shenk, J. S., *J. Anim. Sci.*, 1976, **43**, 889.

Note—Reference 6 is to Part 1 of this series.

Extraction - Spectrophotometric Determination of Palladium(II) with 3,5-Dichlorosalicylaldehyde-4-phenyl-3-thiosemicarbazone

Shigeroku Yamaguchi* and Katsuya Uesugi

Laboratory of Analytical Chemistry, Himeji Institute of Technology, 2167, Shosha, Himeji-shi, Hyogo, Japan

A method for the extraction - spectrophotometric determination of palladium with 3,5-dichlorosalicyl-aldehyde-4-phenyl-3-thiosemicarbazone (CSAPS) is described. The method is based on the formation of an insoluble palladium(II) - CSAPS complex, which is extractable into chloroform from an aqueous solution at pH 0. The absorbance is measured at 410 nm and the molar absorptivity is 14300 l mol^{-1} cm^{-1}. The complex system conforms to Beer's law for up to 8 p.p.m. of palladium(II). The method has been applied successfully to the determination of palladium in standard palladium carbon powder (palladium catalyst).

Keywords: *Palladium(II) determination; spectrophotometry; 3,5-dichlorosalicylaldehyde-4-phenyl-3-thiosemicarbazone; palladium carbon powder analysis*

Thiosemicarbazides and thiosemicarbazones have been widely used as spectrophotometric reagents.[1] Recently, several phenylthiosemicarbazones with phenyl radicals at the end of the thiosemicarbazide molecule have been studied as spectrophotometric reagents for the determination of metal ions.[2-5] It has been found that these reagents react sensitively with metal ions to form complexes, which are easily extracted[2-4]; however, phenylthiosemicarbazones of salicylaldehyde have been little used as analytical reagents. Phenylthiosemicarbazones of salicylaldehyde have three donor atoms, N, O and S, and may coordinate to a number of metal ions. In this work, a new compound, 3,5-dichlorosalicylaldehyde-4-phenyl-3-thiosemicarbazone (CSAPS), has been used as a spectrophotometric reagent for the determination of palladium(II).

Experimental

Apparatus

Absorption spectra and absorbance values were measured with a Hitachi Model 624 automatic recording digital spectrophotometer using quartz cells of 10-mm path length. A Hitachi-Horiba Model F7LC pH meter equipped with a combined glass electrode was used for pH measurements.

Reagents

All chemicals used were of analytical-reagent grade unless stated otherwise.

3,5-Dichlorosalicylaldehyde-4-phenyl-3-thiosemicarbazone (CSAPS). Prepared by refluxing equimolar amounts of 3,5-dichlorosalicylaldehyde and 4-phenyl-3-thiosemi-carbazide in 100 ml of ethanol for 1 h. The crude compound obtained on cooling was recrystallised twice from ethanol (found: C 49.38, H 3.25, N 12.32, S 9.37; $C_{14}H_{12}Cl_2N_4O_3S$ requires C 49.42, H 3.26, N 12.35, S 9.42%). The compound was soluble in alkaline solutions and very soluble in most organic solvents. A 2.5 × 10^{-4} mol l^{-1} solution was prepared in chloroform and stored in the dark. The solution was stable for several weeks.

Standard Pd(II) solution, 1 mg ml^{-1}. Prepared by dissolving 1 g of pure palladium (99.99%) in 12 ml of hydrochloric acid and 4 ml of concentrated nitric acid. Chlorine was removed by adding, repeatedly, 10-ml portions of concentrated nitric acid

and evaporating. The mixture was diluted to 1 l, keeping the nitric acid concentration at approximately 1 + 10. This solution was further diluted as required.

Procedure

Transfer the sample solution containing up to 80 μg of palladium(II) into a 50-ml separating funnel. Add 5 ml of 3 M sulphuric acid. Dilute to 30 ml with distilled water, add 10 ml of the CSAPS in chloroform solution and shake the mixture for 7 min. Filter the organic phase through a dry filter-paper. Measure the absorbance of the organic phase at 410 nm against a reagent blank.

Results and Discussion

Absorption Spectra

The absorption spectra of the light yellow complex formed between palladium(II) and CSAPS in a chloroform medium and the reagent blank are shown in Fig. 1. The palladium complex and reagent have absorption maxima at 398 nm and 345 nm, respectively, and these spectra overlap at 398 nm as shown in Fig. 1. In order to minimise the effect of the reagent blank, the absorbance of the complex is measured at 410 nm, as the absorbance of the reagent is lower at this wavelength.
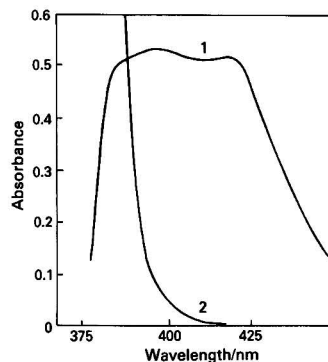

Fig. 1. Absorption spectra of Pd(II) - CSAPS complex in chloroform. Conditions as follows: CSAPS, 2.5 × 10^{-4} M; pH 0; 1, 4 p.p.m. of palladium(II) extracted into chloroform *vs.* reagent blank; and 2, reagent blank *vs.* chloroform

Effect of pH

The above procedure was used to examine the effect of pH. The final pH of each aqueous solution was measured after extraction. Palladium(II) was extracted quantitatively into chloroform at pH -0.3 to 6.5. In more acidic or alkaline solutions, the absorbance decreased because of the incomplete complex formation and hydrolysis of the complex, respectively. In this work, the pH was adjusted to 0 with sulphuric acid. This reduced the number of potentially interfering ions as many metal complexes are only extracted from weakly acidic solutions.

Effect of CSAPS Concentration

The absorbances of a series of solutions containing 40 µg of palladium(II) and various concentrations of CSAPS (2.5×10^{-5}–7.5×10^{-4} M), were measured. Other variables were kept constant, except that a shaking time of 20 min was used.
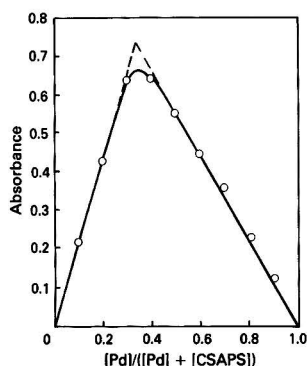
Fig. 2. Continuous variations graph. Conditions as follows: [Pd] + [CSAPS] $= 1.5 \times 10^{-4}$ M; pH, 0; and measured wavelength, 410 nm

Table 1. Effect of organic solvent on the molar absorptivity (ε) of palladium(II) - CSAPS

Solvent	λ_{max}/nm	$\varepsilon \times 10^{-4}$/l mol^{-1} cm^{-1} Pd(II) complex	CSAPS
Chloroform	398	1.45	0.018
	410*	1.43	0.002
1,2-Dichloroethane ..	410	1.36	0.022
Benzene	415	1.32	0.003
Toluene	415	1.35	0.006
Carbon tetrachloride ..	398	1.33	0.029

* Adopted wavelength in this method.

It was found that 10 ml of 1.2×10^{-4} M CSAPS sufficed for 40 µg of palladium(II). Hence, 10 ml of 2.5×10^{-4} M CSAPS solution were used in further studies.

Shaking Time and Stability

The shaking time for the extraction was varied from 0.25 to 20 min. Other variables were kept constant. The minimum shaking time for complete extraction of 40 µg of palladium with chloroform was found to be 5 min at room temperature. The absorbance at 410 nm was then stable for at least 2 h. Therefore, a 7-min shaking time was adopted in further studies.

Calibration, Sensitivity and Precision

The colour system obeyed Beer's law over the range 0–8.0 p.p.m. of palladium(II). The molar absorptivity and Sandell's sensitivity for log $I/I_0 = 0.001$ were 1.43×10^4 l mol^{-1} cm^{-1} and 7.5×10^{-3} µg cm^{-2}, respectively. The coefficient of variation of the absorbance for 4 p.p.m. of palladium(II) was 0.41% (determined from five measurements).

Composition of the Complex

The combining ratio of palladium(II) with CSAPS was investigated by the continuous variations method. The results obtained are shown in Fig. 2. The molar fraction of palladium(II) was 0.336, and therefore it can be deduced that palladium(II) forms a 1:2 complex with CSAPS.

Choice of Solvent

Five solvents (chloroform, 1,2-dichloroethane, benzene, toluene and carbon tetrachloride) were studied for the extraction system (Table 1). Although, there was no significant difference in the molar absorptivities in these solvents, chloroform was selected for its sensitivity and convenience.

This method, using CSAPS, was compared with a method using salicylaldehyde-4-phenyl-3-thiosemicarbazone and two other derivatives. From the absorption characteristics of their palladium(II) complexes presented in Table 2, it can be seen that the proposed reagent has advantages in sensitivity and low absorbance of the reagent blank and thus is the most suitable for the determination of palladium(II).

Effect of Diverse Ions

The effect of diverse ions on the determination of palladium was examined. Scandium(III) and tin(II) caused a negative error, while copper(II), gold(III), mercury(II), silver(I) and vanadium(V) gave a positive error. In particular, copper(II), gold(III), silver(I) and mercury(II) interfered seriously, even when present in equal amounts to palladium(II). However, these ions except for gold(III), can be masked effectively with

Table 2. Absorption characteristics of palladium(II) - salicylaldehyde-4-phenyl-3-thiosemicarbazone (SAPS) complexes, in chloroform

Reagent	λ/nm	$\varepsilon \times 10^{-4}$/l mol^{-1} cm^{-1} Pd complex	Reagent	pH
SAPS	375*	1.73	0.200	2–6
	400	1.38	0.007	
5-Chloro-SAPS	385*	1.40	0.168	0–6
	410	1.09	0.022	
3,5-Dichloro-SAPS (CSAPS) ..	398*	1.45	0.018	0–6
	410	1.43	0.002	
2-Hydroxy-1-naphthaldehyde-PS ..	413*	1.40	0.130	0–6
	435	0.97	0.029	

* Absorption maximum.

potassium thiocyanate. The results are summarised in Table 3, where the tolerance limit is set to ±3% for a palladium(II) recovery of 40 µg.

Application of the Method to Real Samples

In order to confirm the usefulness of the proposed method, it was applied to the determination of palladium in a standard palladium carbon powder sample for which the palladium content was certified. A recovery experiment was carried out by adding standard palladium(II) to the palladium carbon powder sample. The procedure for the preparation of the sample solutions was as follows.

A 0.1-g mass of the palladium carbon sample was accurately weighed into a silica combustion boat of a plasma asher (Plasma Reaction Model PR-151, Yamato Co., Japan). After ashing the carbon for 8 h, the sample was treated with 5 ml of formic acid (1 + 4) and dried by heating on a hot-plate. The resulting compound was dissolved in 6 ml of hydrochloric acid and 2 ml of nitric acid and diluted with water to 500 ml. An aliquot of this solution was taken and the proposed procedure

followed. Good recoveries were obtained after adding known amounts of palladium(II) to the sample. The results are shown in Table 4.

Conclusion

There are numerous methods for the photometric determination of palladium using chelating agents, but the use of phenylthiosemicarbazones of salicylaldehydes has not previously been investigated. These newly synthesised phenyl-thiosemicarbazones of salicylaldehyde have been studied as photometric reagents for palladium. The absorption spectra of their palladium complexes overlapped considerably with the reagent blank for all of the reagents examined except for CSAPS, which was concluded to be the most suitable reagent for palladium. The proposed method is similar in sensitivity to the method using 1-(2-pyridylazo)-2-naphthol[6] but offers the advantages of greater simplicity, rapidity, accuracy and reasonable selectivity for the determination of palladium.

Table 3. Effect of diverse ions in the presence of potassium thiocyanate. Amount of Pd(II) taken, 40 µg; tolerable error, ±3%

Interferent	Tolerance limit/µg
Ag(I),* Cd(II), Co(II), Cr(III), Cu(II),* Fe(III), Ir(III), Mn(II), Mo(VI), Ni(II), Os(IV), Pb(II), Rh(III), Ru(III), Sc(III),* Ti(IV), V(V)*, Zn(II), Sn(II),* Hg(II)*	500
Au(III)*	100

*3 ml of 2.5×10^{-2} M KSCN were added as a masking agent; after extraction the organic phase was washed with 10 ml of 3 M H_2SO_4.

References

1. Sandell, E. B., and Onishi, H., "Photometric Determination of Traces of Metals," Fourth Edition, Wiley, New York, 1978, p. 542.
2. Cano, J. M., and Pino, F., *Talanta*, 1972, **19**, 1959.
3. Asuero, A. G., and Cano, J. M., *Analyst*, 1978, **103**, 140.
4. Cano, J. M., and Pino, F., *Anal. Chim. Acta*, 1975, **75**, 335.
5. Kato, T., and Hasegawa, A., *Bunseki Kagaku*, 1982, **31**, 580.
6. Sawada, T., and Kato, S., *Bunseki Kagaku*, 1962, **11**, 544.

Table 4. Determination of palladium(II) in palladium carbon powder

Sample*	Sample volume/ml	Pd(II) Found/ µg	C.v,† %	Found, %	Recovery, %
0.1 g in 500 ml	3	29.88	0.17 (n = 5)	4.98 ± 0.005	
0.1 g + 2 mg of Pd in 500 ml ..	3	41.87	0.30 (n = 5)		99.2

* Standard 5% palladium carbon powder, Nippon Engelhard Co. (Japan).
† C.v. = coefficient of variation.

Reaction of Yttrium with *p*-Nitrochlorophosphonazo and the Spectrophotometric Determination of Yttrium in Nickel-base Alloys in the Presence of Cerium Sub-group Rare Earths

Chung-Gin Hsu and Jiao-Mai Pan

Department of Chemistry, East China Normal University, 3663 Chung-Shan Road (N), Shanghai, People's Republic of China

Yttrium reacts with *p*-nitrochlorophosphonazo to form a 1 : 3 β-type complex, having an absorption maximum at 731 nm. The complex formation was complete within 10 min in a small volume of 0.2–0.5 M perchloric acid and the resulting complex was stable for at least 4 h after dilution. Under the conditions employed, the molar absorptivity was found to be 8.49×10^4 l mol^{-1} cm^{-1} at 731 nm. The determination range was 0–6 μg of yttrium in 25 ml of solution and was obtained using a standard addition - deduction method. Using this procedure yttrium can be determined in the presence of a 10-fold amount of lanthanum or cerium without separation. A selective and sensitive procedure for the determination of microamounts of yttrium in nickel alloys is described. The precision and recovery are both satisfactory.

Keywords: *Yttrium determination; spectrophotometry; p-nitrochlorophosphonazo; nickel-base alloy*

Microamounts of rare earths added as minor constituents to nickel-base alloys can remove oxygen and other gases, and increase the resistance of the alloys towards oxidation; the presence of the cerium sub-group rare earths and yttrium in nickel-base alloys further improves the properties of the materials. However, because of their similar behaviour, the independent determination of cerium sub-group rare earths and yttrium when they are present simultaneously is a difficult problem in analytical chemistry and metallurgical analysis.

Conventionally, chlorophosphonazo III has been widely used as a chromogenic reagent for the determination of the total rare earths,[1-3] and *m*-nitrochlorophosphonazo,[4,5] an unsymmetric bisazo derivative of chromotropic acid with one *o*-phosphono-*o*'-hydroxyazo functional group, has been employed to determine cerium sub-group rare earths. We now propose the use of its isomer, *p*-nitrochlorophosphonazo (PNCP)[6,7] (I) as a reagent for yttrium.

I
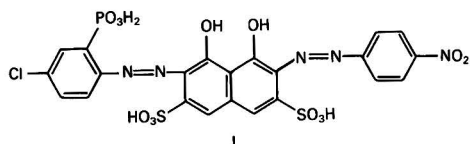
However, this method suffers the following disadvantages: microamounts of rare earths interfere with the reaction, the complex formation requires a longer time and the complex obtained is unstable; hence gelatine has been introduced as a stabilising agent.[7]

In this work, the conditions for the complex formation were studied in detail. The complex formed more rapidly in a small volume of solution before dilution with water, and was stable for a longer period. Microamounts of yttrium were determined in the presence of 10-fold amounts of lanthanum or cerium by using a standard addition - deduction method.

The composition of the Y - PNCP complex was also studied and a method for the determination of yttrium in a nickel-base alloy is described. The method is accurate, sensitive and can easily be applied to routine analysis.

Experimental

Apparatus

Absorbances and absorption spectra were measured on a Beckman DU-7 spectrophotometer with 1-cm cells. A Model pHS-3 pH meter (Shanghai Third Analytical Instruments Factory) was used to measure the pH values of the solutions.

Reagents

Unless otherwise stated all reagents were of analytical-reagent grade. Stock solutions of yttrium and other rare earths were prepared as described previously[4] and standardised complexometrically with xylenol orange as the indicator. The working solutions (10 p.p.m.) were prepared by dilution with perchloric acid (1 + 200).

PNCP solution, 0.03%. Prepared by dissolving 0.03 g of PNCP in 100 ml of water.

Diethylenetriaminepentaacetic acid (DTPA) solution, 0.05 M. Prepared by dissolving 2 g of DTPA in 90 ml of water, adjusting the pH to approximately 4 with sodium hydroxide, warming if necessary and diluting to 100 ml with water.

Perchloric acid, 2 M.

Oxalic acid, 3%.

Synthesis of PNCP

PNCP was synthesised and purified using a procedure described previously for *m*-nitrochlorophosphonazo, except that *p*-nitroaniline was used instead of *m*-nitroaniline. After drying at 80 °C, the reagent was found to contain 5 mol of water, a result that was determined by thermogravimetry (calculated, H_2O 11.58; found, H_2O 11.51%). Elemental analysis confirmed the purity (calculated, N 9.00, P 3.98, Cl 4.56; found, N 8.97, P 3.96, Cl 4.33%) The pure product, a dark brown powder, which decomposes at 200 °C, is stable both in the solid state and in aqueous solution. In 0.1 M hydrochloric acid PNCP is purple - red, having an absorption maximum at 555 nm with a molar absorptivity of 4.4×10^4 l mol^{-1} cm^{-1}.

Recommended Procedures

Procedure for studying the reaction (procedure A)

To an aliquot containing 8.0–10.0 μg of yttrium, in a 25-ml calibrated flask, add 1 ml of 2 M perchloric acid and adjust the volume to 6 ml using distilled water. Next, add 2 ml of 0.03% PNCP solution and mix well. After standing for 10 min, dilute to the mark with water. Measure the absorbance at 731 nm in a 1-cm cell against water.

Procedure for the determination of yttrium (procedure B)

To a test solution containing not more than 6.0 µg of yttrium in a 25-ml calibrated flask, add 8.0 µg of yttrium, 1 ml of 2 M perchloric acid, 1 ml of 3% oxalic acid, 1 ml of 0.05 M DTPA solution and make up to 6 ml with distilled water. Next, add 2 ml of 0.03% PNCP solution and mix well. After standing for 10 min, dilute to the mark with water. Measure the absorbance as described above.

Procedure for the determination of yttrium in nickel-base alloys (procedure C)

To 0.2 g of the sample, add 8 ml of aqua regia (more if necessary), heat to decompose the sample and evaporate nearly to dryness. After cooling to room temperature, dissolve the residue with water, filter if necessary to remove silicic acid, transfer the solution into a 100-ml calibrated flask and dilute to the mark with water. Place 2.0 ml (or another appropriate aliquot) of the resultant solution in a 25-ml calibrated flask and follow procedure B for the determination of yttrium.

Results and Discussion

Absorption Spectra

As shown in Fig. 1, the cerium - PNCP complex, and those of other rare earths, gave two absorption maxima at 614 and 677 nm, respectively (graph 2), while the yttrium complex had a characteristic absorption peak at 731 nm (graph 3). The complex, defined as a β-type complex,[8,9] was formed in the
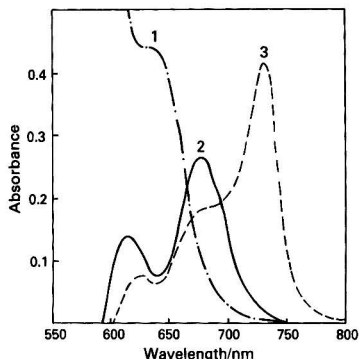
presence of an excess of reagent; none of the other rare earths produced this reaction. The absorption of PNCP at the denoted wavelength (graph 1) was negligible, hence water was used as a reference solution for the determination of yttrium.

Effect of Standing Time on the Colour Development

Under the conditions employed, 8.0 µg of yttrium in 25 ml of solution formed a complex that was stable for more than 5 h. If the reaction was performed in a smaller volume, it proceeded more rapidly. For convenience, a volume of 8 ml was chosen for the colour development before dilution to 25 ml with water.

The standing time for colour development was examined from 5 to 40 min. It was found that full colour was developed within 10 min and the absorbance remained constant for at least 4 h. On prolonging the standing time from 10 to 30 min, it was found that the absorbance of the final solution increased by 6.7%. However, after dilution to 25 ml, the absorbance decreased gradually to a stable value that was almost identical with that of the solution obtained on standing for 10 min.

Because the β-type complex probably exists in micellar form in solution,[8] the rate of formation and dissolution of this type of complex is relatively slow as compared with an α-type complex. In a small volume of solution, the reaction rate is accelerated owing to the higher concentrations of the reactants, and more particles of micellae are formed, but, after dilution, a small part of micellae will be slowly dissolved in the solution. In order to save time and obtain a maximum and constant absorbance, a standing time of 10 min was considered suitable.
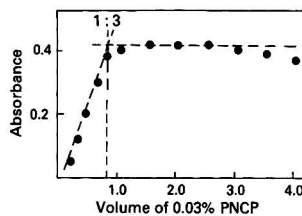

Fig. 1. Absorption spectra of PNCP complexes of Ce and Y. 1, PNCP against water; 2, Ce - PNCP against reagent blank; 3, Y - PNCP against reagent blank. Ce, 10.0 µg; Y, 10.0 µg; 2 M HClO₄, 1.0 ml; 0.03% PNCP, 2.0 ml

Fig. 2. Absorption spectra of Y - PNCP at various acidities. pH of final solutions: 1, 2.44; 2, 1.78; 3, 1.27; other conditions as in Fig. 1

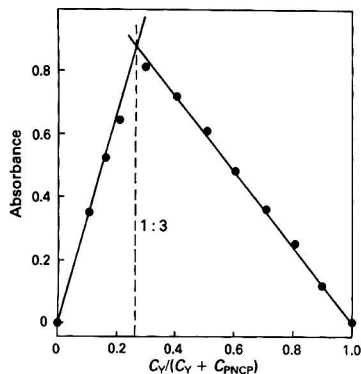**Fig. 3.** Effect of amount of PNCP on the formation of Y - PNCP. Wavelength, 731 nm; other conditions as in Fig. 1

Fig. 4. Determination of the molar ratio of Y to PNCP using the method of continuous variations. $C_Y + C_{PNCP} = 3.6 \times 10^{-5}$ M; 2 M HClO₄, 1.0 ml; wavelength, 731 nm

Effect of Acidity

As shown in Fig. 2, when the pH value of the final solution was 2.44, the complex was present in the α-form with two absorption maxima at 611 and 676 nm, respectively (graph 1). As the acidity increased, a mixture of α-type and β-type complexes were present in the solution (graph 2). The β-type complex formed completely in 0.19–0.5 M perchloric acid (graph 3) and gave a maximum and constant absorbance at 731 nm. At acidities of greater than 0.75 M perchloric acid, the precipitation of PNCP will occur. Therefore, 1 ml of 2 M perchloric acid was introduced in 8 ml of solution during colour development, which corresponds to 0.25 M perchloric acid and a final pH of *ca.* 1.3.

Effect of Amount of PNCP

A 1.5–3.0-ml volume of 0.03% PNCP solution was required to obtain a maximum and constant absorbance for 10.0 μg of yttrium (Fig. 3), hence 2.0 ml of PNCP solution were used in all subsequent work.

Composition of the Complex

The molar composition of the yttrium - PNCP complex formed under the conditions described, was ascertained by the molar-ratio method (Fig. 3) and Job's method of continuous variations (Fig. 4). Both methods indicated that the metal to ligand ratio was 1 : 3.

Effect of Other Reagents

A mixture of oxalic acid and DTPA was added to mask, partly, nickel and other foreign ions that combine with PNCP and reduce the excess concentrations of PNCP appreciably. More than 3 ml of 3% oxalic acid or 2 ml of 0.05 M DTPA solution depressed slightly the absorbance of the yttrium complex. Therefore, an addition of 1.0 ml of each reagent solution is recommended.

Calibration Graph and Standard Addition - Deduction Method

A calibration graph was constructed by introducing various amounts of yttrium in 25-ml calibrated flasks, adding the reagents and developing the colour according to procedure B. The calibration graph was linear for 0.0–6.0 μg of yttrium in 25 ml of solution, which corresponds to a total amount of 8.0–14.0 μg of yttrium in the solution.

For sample analysis, 8.0 μg of yttrium were also added to each of the test solutions for colour development, and the yttrium content was found from the calibration graph (from which 8.0 μg of yttrium had previously been deducted). Microamounts of yttrium can thus be determined using the standard addition - deduction method.

Sensitivity and Precision

The molar absorptivity and Sandell's sensitivity calculated from increments on the slope of the calibration graph, were 8.49×10^4 l mol^{-1} cm^{-1} and 1.05 ng cm^{-2} of yttrium (for an absorbance of 0.001), respectively, at 731 nm. Ten replicate analyses of a test solution containing 2.0 μg of yttrium by procedure B gave a mean absorbance of 0.417 with a standard deviation of 0.0022 and a relative standard deviation of 0.5%.

Effect of Foreign Ions

Solutions containing 2.0 μg of yttrium and various amounts of foreign ions (including rare earths) were prepared according to procedure B. The tolerance limits are shown in Table 1.

The same procedure was used to determine yttrium in the presence of various amounts of rare earth ions and the tolerance limits for errors of up to 10% in the determination of 1.0 μg of yttrium are listed in Table 2.

It was observed that in the absence of yttrium, all the other rare earth (RE) complexes (of the α-type) gave negligible absorption at 731 nm, the wavelength used for the determination of yttrium. However, in the presence of yttrium, the absorbance at this wavelength increased by an appreciable amount. This behaviour may be considered as a "co-

Table 1. Tolerance limits for foreign ions in the determination of 2.0 μg of yttrium

Foreign ion	Tolerance limit/μg	Foreign ion	Tolerance limit/mg
Ni(II)	5000	Oxalate	7
Mn(II)	3000	Citrate	20
Co(II)	2000	Tartrate	20
Cu(II)	1000	Fluoride	0.5
Fe(III), Al(III) . .	500	Phosphate	2
Mo(VI)	400	EDTA	4
Mg(II), W(VI), V(V)	100	DTPA*	4
Ti(IV)	30		
Ca(II)	20		
Zr(IV)	8		

* Diethylenetriamine pentaacetate.

Table 2. Tolerance limits for rare earth ions in the determination of 1.0 μg of yttrium

Rare earth ion [M(III)]	Tolerance limit/μg
La	10.0
Ce	10.0
Pr	5.0
Nd	5.0
Sm	5.0
Eu	2.0
Gd, Tb, Dy, Ho, Er, Tm, Yb, Lu	1.0

Table 3. Determination of yttrium in nickel-base alloys

Sample No.	Reference value, %		Y found, %	Mean, %	Relative standard deviation, %
	Ce*	Y			
NBA-1	0.16	—	0.0161, 0.0160, 0.0164, 0.0167, 0.0153	0.0161	3.2
NBA-2	0.10	0.047	0.0482, 0.0485, 0.0482, 0.0445, 0.0482	0.0475	3.6
NBA-3	0.04	—	0.0120, 0.0135, 0.0130, 0.0139, 0.0140	0.0133	6.1
NBA-4	0.19	0.17	0.176, 0.173, 0.171, 0.177, 0.171	0.174	1.6

* Cerium sub-group rare earths.

Table 4. Recoveries of yttrium in spiked samples

Sample No.	Y added/µg	Y found/µg*	Recovery, %
NBA-1	2.00	2.05	102.5
NBA-2	2.00	1.97	98.4
NBA-3	2.00	1.92	96.0
NBA-4	2.00	2.01	100.5

* Mean of five determinations.

colouration effect" and is probably due to the formation of a ternary complex such as Y - RE - PNCP.

In our experiments, it was found that the co-colouration effect was enhanced as the atomic number of the rare earths increased, so that the tolerance limits gradually decreased from lanthanum to the heavier rare earths. However, the cerium sub-group rare earths had higher tolerance limits, which allowed the determination of microamounts of yttrium in their presence.

Determination of Yttrium in Nickel-base Alloys

Using procedure C described above, yttrium was determined in four samples of nickel-base alloy. The results obtained (Table 3) indicate that the method is reliable. The recoveries

of the spiked samples were between 96.0 and 102.5% (Table 4).

References

1. O'Laughlin, J. W., and Jensen, D. F., *Talanta*, 1970, **17**, 329.
2. Taketatsu, T., Kaneko, M., and Kono, N., *Talanta*, 1974, **21**, 87.
3. Pan, J. M., Chen, Y. S., and Yan, H. T., "Chromogenic Reagents and Their Applications in Metallurgical Analysis," (in Chinese), Shanghai Publishing House of Science and Technology, Shanghai, 1981, p. 161.
4. Hsu, C. G., Hu, C. S., Jia, X. P., and Pan, J. M., *Anal. Chim. Acta*, 1981, **124**, 177.
5. Jia, X. P., Hu, C. S., Pan, J. M., and Hsu, C. G., *J. East China Normal Univ.*, 1981, **3**, 79.
6. Pan, J. M., *Huaxue Shiji*, 1981, 240.
7. Wang, W. Z., Wu, J. P., and Pan, J. M., *Fenxi Huaxue*, 1983, **11**, 913.
8. Taketatsu, T., and Kono, N., *Chem. Lett.*, 1974, 989.
9. Taketatsu, T., *Bull. Chem. Soc. Jpn.*, 1977, **50**, 1758.

Determination of Uranium in Phosphoric Acid Using 4-(2-Pyridylazo)-resorcinol and 2-(5-Bromo-2-pyridylazo)-5-diethylaminophenol Reagents

Ivan Brčić, Eugenio Polla* and Marko Radošević

INA-Research and Development, Proleterskih brigada 78, 41000 Zagreb, Croatia, Yugoslavia

An extraction - spectrophotometric procedure for the determination of uranium in phosphoric acid is described. It is based on the extraction of uranium with trioctylphosphine oxide in cyclohexane and subsequent reaction with 4-(2-pyridylazo)resorcinol or 2-(5-bromo-2-pyridylazo)-5-diethylaminophenol, both of which are highly sensitive reagents that produce stable complexes. The determination of uranium in different stages of its extraction from wet-process phosphoric acid and in phosphate rocks, gypsum and water has been successfully carried out using the described procedures and reagents.

Keywords: *Uranium determination; 4-(2-pyridylazo)resorcinol; 2-(5-bromo-2-pyridylazo)-5-diethylamino-phenol; spectrophotometry; solvent extraction*

Solvent extraction is the favoured technique for recovering uranium from wet phosphoric acid and the di(2-ethylhexyl)phosphoric acid - trioctylphosphine oxide (DEHPA - TOPO) process[1,2] has been successfully demonstrated in pilot and full-scale plant operations. However, in the two-cycle solvent-extraction DEHPA - TOPO process there is a lack of methods for the determination of uranium in different media in real systems, *i.e.*, in fresh feed, loaded and raffinate phosphoric acid, organic solvents (kerosene and organophosphorus extractants) and aqueous ammonium carbonate.

Many reagents have been proposed for the spectrophotometric determination of uranium but only 4-(2-pyridylazo)resorcinol (PAR)[3] and 2-(5-bromo-2-pyridylazo)-5-diethylaminophenol (bromo-PADAP)[4] meet the requirements with respect to sensitivity and enable accurate results to be obtained.

In this work, two combined extraction - spectrophotometric procedures have been developed for the determination of uranium in phosphoric acid, each using one of the highly sensitive chromogenic reagents PAR and bromo-PADAP. This method has been in use in our laboratory for three years, and has proved reliable, accurate and versatile.

Experimental

Apparatus

A Pye Unicam SP 8–10 and 6–550 UV - visible spectrophotometer in conjunction with a 1-cm optical path quartz cell was used. A Iskra MA 5705 pH meter with a combined glass - calomel electrode was also used.

Reagents

All reagents used were of analytical-reagent grade unless otherwise specified, and doubly de-ionised water was used for preparing the solutions. All volumes were dispensed using pipettes with disposable polyethylene tips.

Ascorbic acid solution, 5% *m/V*.

Sodium fluoride solution, 2% *m/V*.

Sodium hydroxide solution, 40% *m/V*.

PAR solution, 0.2% *m/V*. Dissolve 237.2 mg of the sodium salt of PAR in 100 ml of water.

Bromo-PADAP solution, 0.05% *m/V*. Dissolve 0.05 g of bromo-PADAP in 100 ml of absolute ethanol. Prepare a sufficient amount to last only 1 week.

Buffer solution, pH 8.00. Dissolve 149 g of triethanolamine in 800 ml of water, neutralise to pH 8.00 with hydrochloric acid and dilute to 1 l.

Buffer solution, pH 8.35. Dissolve 149 g of triethanolamine in 800 ml of water and neutralise to pH 8.35 using perchloric acid. The pH should first be adjusted to about 8.5–8.6 and the solution left to stand for 24 h before making the final adjustment.

Complexing solution (PAR method). Dissolve 50 g of *trans*-1,2-diaminocyclohexane-*N,N,N,N*-tetraacetic acid, 5 g of sodium fluoride and 65 g of sulphosalicylic acid in 800 ml of water, neutralise to pH 8 with 40% *m/V* sodium hydroxide solution and make up to 1 l.

Complexing solution (bromo-PADAP method). Dissolve 25 g of *trans*-1,2-diaminocyclohexane-*N,N,N,N*-tetraacetic acid, 5 g of sodium fluoride and 65 g of sulphosalicylic acid in 800 ml of water. Neutralise to pH 7.85 with 40% *m/V* sodium hydroxide solution and make up to 1 l.

Complexing solution, dilute (bromo-PADAP method). Dilute one volume of complexing solution with one volume of water and neutralise to pH 8.35 with 40% *m/V* sodium hydroxide solution.

TOPO solution, 0.1 M. Dissolve 19.3 g of trioctylphosphine oxide in cyclohexane and make up to 500 ml with cyclohexane.

Nitric acid, 2 M.

Phosphorus pentoxide (P_2O_5) solution, 30% *m/V*.

Procedures

Preparation of the stock solution and calibration standards, PAR method

The standard uranium solution was prepared as follows. Dissolve 400 mg of $UO_2(NO_3)_2.6H_2O$ in 30% P_2O_5 solution and make up with the same solution to 1 l. This is a stock standard solution containing 189.60 μg ml^{-1}.

Because of the effect of the degree of dilution of the phosphoric acid sample and the large range of uranium concentrations in real system samples it is necessary to use different calibration graphs. Three series of calibration standards each consisting of five or six different concentrations of uranium in 30% P_2O_5 solution were prepared using the stock standard solution. Each series was appropriately diluted with 2 M HNO$_3$.

The first series (A) was prepared as follows. Transfer 2, 4, 8, 10, 15 and 20 ml of the prepared stock standard solution into 100-ml calibrated flasks, add to each 50 ml of 2 M HNO$_3$ and make up to volume with 30% P_2O_5 solution.

The second series (B) was prepared by transferring 4, 8, 15, 20, 30 and 40 ml of the stock standard solution into 50-ml calibrated flasks and diluting to volume with 30% P_2O_5 solution. Transfer 25 ml of each previously prepared solution into 100-ml calibrated flasks and make up to volume with 2 M HNO$_3$.

The third series (C) was prepared according the following procedure. Transfer 10, 20, 30 and 40 ml of the stock standard solution into 50-ml calibrated flasks and make up to volume with 30% P_2O_5 solution. Transfer 10 ml of each previously prepared solution into 100-ml calibrated flasks and make up to volume with 2 M HNO_3. The fifth calibration standard in the third series was prepared by transferring, directly, 10 ml of the stock standard solution into a 100-ml calibrated flask and diluting to volume with 2 M HNO_3.

Three different calibration graphs were obtained by transferring 20 ml of each of the previously prepared calibration standard solutions (three series) into 100-ml separating funnels and following the general procedure for the PAR method. When the degree of dilution was as in series C or higher an identical calibration graph was obtained.

PAR method, general procedure

Each acid sample should be diluted with 30% P_2O_5 solution to give a maximum uranium content according to the calibration graph. Dilute the sample to the appropriate concentration with 2 M HNO_3, which also serves as an oxidant and converts the eventually present U(IV) into U(VI), and leave to stand for 1 h before carrying out the extraction step.

Transfer into a 100-ml separating funnel a 20-ml volume of sample and add 30 ml of 2 M HNO_3. Add, in order, 5 ml of sodium fluoride solution, 5 ml of ascorbic acid solution and 5 ml of 0.1 M TOPO solution. Shake the funnel for 3 min and allow the phases to separate. Run off and discard the aqueous phase. Pipette 2 ml of the organic phase into a dry 25-ml calibrated flask. Add 2 ml of buffer solution (pH 8.00), 2 ml of complexing solution and 1 ml of PAR solution, in that order, mixing thoroughly after each addition. Make up to volume with ethanol and mix well. Measure the absorbance against a blank at 530 nm. Prepare the blank solution after transferring 50 ml of the 30% P_2O_5 solution, appropriately diluted with 2 M HNO_3, into a separating funnel and follow the same procedure without uranium.

Preparation of the stock solution and calibration standards, bromo-PADAP method

The standard uranium solution was prepared as follows. Dissolve 800 mg of $UO_2(NO_3)_2.6H_2O$ in 30% P_2O_5 solution and make up with the same solution to 1 l. This is a stock standard solution containing 379.20 of µg ml^{-1} of uranium.

Because of the effect of the degree of dilution of the phosphoric acid sample and the large range of uranium concentrations in real samples it is necessary to use different calibration graphs. Three series of calibration standards each consisting of six or seven different concentrations of uranium in 30% P_2O_5 solution were prepared using the stock standard solution. Each series was appropriately diluted with 2 M HNO_3.

The first series (A) was prepared as follows. Dilute the stock standard solution 2.5-fold with 30% P_2O_5 solution. Next, transfer 2, 4, 8, 10, 15 and 20 ml of the diluted stock standard solution into 200-ml calibrated flasks, add to each 160 ml of 2 M HNO_3 and dilute to volume with 30% P_2O_5 solution.

The second series (B) was prepared by transferring 4, 8, 15, 20, 30 and 40 ml of the stock standard solution into 100-ml calibrated flasks and making up to volume with 30% P_2O_5 solution. Transfer 10 ml of each of the previously prepared solutions into 100-ml calibrated flasks and make up to volume with 2 M HNO_3.

The third series (C) was prepared according to the following procedure. Transfer 10, 20, 30, 40, 50 and 80 ml of the stock standard solution into 100-ml calibrated flasks and dilute to volume with 30% P_2O_5 solution. Then transfer 4 ml of each previously prepared solution into 100-ml calibrated flasks and make up to volume with 2 M HNO_3. The seventh calibration

standard was prepared by transferring, directly, 4 ml of stock standard solution into a 100 ml calibrated flask and making up to volume with 2 M HNO_3 solution.

Three different calibration graphs were obtained by transferring 20 ml of each previously prepared calibration standard solution (three series) into 100-ml separating funnels and following the general procedure for the bromo-PADAP method. When the degree of dilution was as in series C or higher, an identical calibration graph was obtained.

Bromo-PADAP method, general procedure

Each acid sample should be diluted with 30% P_2O_5 solution to give a maximum uranium content according to the calibration graph. Dilute the sample to the appropriate concentration with 2 M HNO_3, which also serves as an oxidant and converts the eventually present U(IV) into U(VI), and allow to stand for 1 h before carrying out the extraction step.

Into a 100-ml separating funnel transfer a sample, usually 20 ml, and add a volume of 2 M HNO_3 to give a total volume of 50 ml. Add, in order, 5 ml of sodium fluoride solution, 2 ml of ascorbic acid solution and 5 ml of 0.1 M TOPO solution and shake the funnel for 3 min. Allow the phases to separate. Run off and discard the aqueous phase and pipette 2 ml of the organic phase into a dry 25-ml calibrated flask. Add, in order, 1 ml of buffer solution (pH 8.35), 1 ml of dilute complexing solution and 4 ml of bromo-PADAP solution, mixing thoroughly after each addition. Stopper the flask and allow to stand for 15 min. Add 1 ml of water of make up to volume with ethanol and mix well. Measure the absorbance against a blank at 574 nm. The blank solution is prepared by transferring 50 ml of the 30% P_2O_5 solution, appropriately diluted with 2 M HNO_3, into a separating funnel and following the same procedure, but without uranium.

Results and Discussion

Absorption Spectra and Nature of Complexes

Uranium(VI) with PAR and bromo-PADAP forms orange and red complexes, respectively. The absorption spectra of the uranyl - PAR and bromo-PADAP complexes in aqueous ethanolic solution were recorded and are shown in Figs. 1 and 2. The uranyl - PAR and bromo-PADAP complexes exhibited absorbance maxima at 530 and 574 nm, with molar absorptivities of 2.10×10^4 and 6.33×10^4 l mol^{-1} cm^{-1}, respectively. The empirical formulae of the uranyl - PAR and bromo-PADAP complexes by continuous variations and molar-ratio
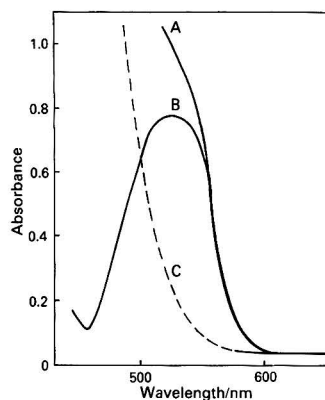

Fig. 1. Absorption spectra of PAR and its uranyl complex. A, Uranyl - PAR complex against water; B, uranyl - PAR complex against reagent blank; and C, reagent blank against water. Conditions: U, 223.6 µg per 25 ml of final solution; complexing solution (pH 8.00), 5 ml; buffer solution (pH 8.00), 2 ml; 0.2% m/V PAR solution, 1 ml; ethanol, 15 ml; and λ_{max}, 530 nm
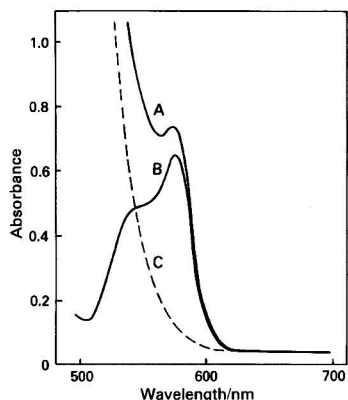
Fig. 2. Absorption spectra of bromo-PADAP and its uranyl complex. A, Uranyl - bromo-PADAP complex against water; B, uranyl - bromo-PADAP complex against reagent blank; and C, reagent blank against water. Conditions: U, 60.68 µg per 25 ml of final solution; dilute complexing solution, 1 ml; buffer solution (pH 8.35), 1 ml; 0.05% m/V bromo-PADAP solution, 4 ml; water, 1 ml; ethanol, 16 ml; and $\lambda_{max.}$, 574 nm
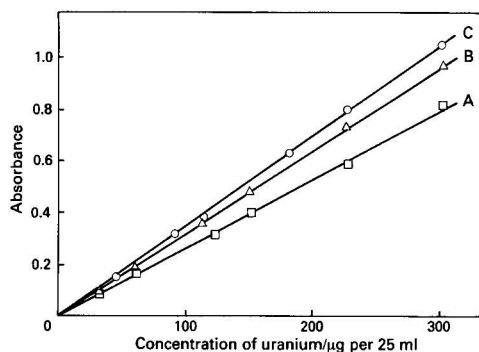

Fig. 3. Calibration graphs obtained with PAR reagent at 530 nm for three different degrees of dilution. A, B and C correspond to equations (1), (2) and (3), respectively
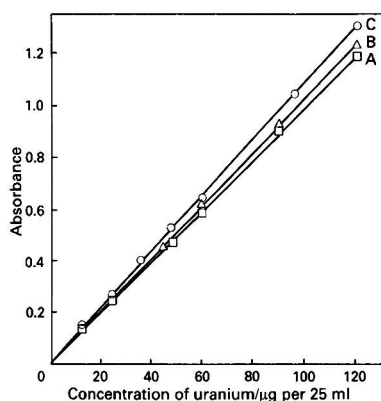
Fig. 4. Calibration graphs obtained with bromo-PADAP reagent at 574 nm for three different degrees of dilution. A, B and C correspond to equations (4), (5) and (6), respectively

methods have been reported.[3,4] It was found that 1:1 (UO_2^{2+} : reagent) complexes were formed.

Effect of Shaking Time and Other Variables in the Extraction

A solution of TOPO in cyclohexane, as extractant, completely extracts the uranium from 0.5–6 M HNO_3 (log $E > 2$).[5] Therefore 2 M HNO_3, as a diluent for 30% P_2O_5 solution and also an oxidant, was used in order to convert the eventually present U(IV) into U(VI).

Variation of the shaking time from 1 to 10 min revealed that 3 min were sufficient for the complete extraction of the uranium. The extraction of uranium was reproducible and more than 99% of that present in the aqueous acid solution was extracted by a single extraction. The extraction efficiency changed when the organic to aqueous phase ratio was varied, the optimum ratio being 10:1, $i.e.$, 50 ml of aqueous solution to 5 ml of organic solvent.

Effect of Reagent, pH and Diverse Ions

A 2-ml aliquot of organic phase was used in both methods, as that volume gave the optimum ratio between the complexing and buffer solution, ethanol and organic phase in order to maintain a homogeneous solution for colour development. Various amounts of both chromogenic reagents were examined. The absorbance, using both reagents separately, remained constant when volumes of the reagent solution between 0.5 and 5.0 ml were used. Therefore, 2.0 ml of 0.2% m/V PAR solution and 4.0 ml of 0.05% m/V bromo-PADAP solution were preferred throughout the experiments.

The effect of pH on the uranyl - PAR and bromo-PADAP complexes was similar to that found previously.[3,4] The absorbance of the uranyl - PAR and bromo-PADAP complexes was almost constant in the pH range 7.0–8.5 and, when triethanolamine buffer solutions of pH 8.00 and 8.35 were used, maximum values were achieved, respectively.

A study of the stability of the uranyl - PAR and uranyl - bromo-PADAP complexes with time was carried out; both complexes were stable and gave a constant absorbance, even after 24 h.

The influence of diverse ions on the direct determination of uranium by PAR and bromo-PADAP methods has previously been reported.[3,4] Using the TOPO extraction procedure, uranium was extracted from dilute phosphoric acid - 2 M HNO_3, containing sodium fluoride and ascorbic acid as mixed masking agent, without any interference being observed for either method.

Calibration Graphs, Sensitivity and Precision

The results obey Beer's law for 0–304 and 0–122 µg of uranium per 25 ml of final solution using PAR and bromo-PADAP reagent, respectively. Although straight-line calibration graphs were obtained, distinct differences in the calibration graphs were observed for particular degrees of phosphoric acid dilution (series A, B and C). Three calibration graphs were necessary for both methods. The linear regression equations obtained by a least-squares treatment are as follows (Figs. 3 and 4).

PAR method at 530 nm ($r = 0.999$):

$$A = 2.622 \times 10^{-3}[U] - 4.037 \times 10^{-4} \quad .. \quad .. \quad (1)$$
$$A = 3.182 \times 10^{-3}[U] - 2.689 \times 10^{-3} \quad .. \quad .. \quad (2)$$
$$A = 3.511 \times 10^{-3}[U] - 5.111 \times 10^{-3} \quad .. \quad .. \quad (3)$$

Bromo-PADAP method at 574 nm ($r = 0.999$):

$$A = 9.726 \times 10^{-3}[U] + 6.237 \times 10^{-3} \quad .. \quad .. \quad (4)$$
$$A = 1.022 \times 10^{-2}[U] - 2.590 \times 10^{-3} \quad .. \quad .. \quad (5)$$
$$A = 1.065 \times 10^{-2}[U] + 5.753 \times 10^{-3} \quad .. \quad .. \quad (6)$$

When the degree of dilution of P_2O_5 solution is higher than in series C [equations (3) and (6)] the calibration graphs for the PAR and bromo-PADAP methods can be represented by equations (3) and (6), respectively.

The fact that the calibration graph depends on the degree of dilution of the phosphoric sample does not reduce the value of the methods and their applicability. Sandell sensitivities (based on an absorbance of 0.001 unit) and molar absorptivities, calculated from equations (3) and (6), were 1.13×10^{-2} $\mu g\ cm^{-2}$ and $2.10 \times 10^4\ l\ mol^{-1}\ cm^{-1}$ for the PAR method and $3.80 \times 10^{-3}\ \mu g\ cm^{-2}$ and $6.33 \times 10^4\ l\ mol^{-1}\ cm^{-1}$ for the bromo-PADAP method.

Four series of ten standard solutions each containing 121.2 and 227.5 μg of uranium per 25 ml of final solution for the PAR method, and 24.3 and 91.0 μg of uranium per 25 ml of final solution for the bromo-PADAP method, were analysed by the recommended procedures. The results gave relative standard deviations of 0.42 and 0.94 and 0.59 and 0.61% for the PAR and bromo-PADAP methods, respectively.

Applications

The PAR and bromo-PADAP methods have been successfully applied to the determination of uranium in different stages of its extraction from wet-process phosphoric acid (fresh feed, loaded and raffinate phosphoric acid), rocks, gypsum and water. The pre-treatments of all mentioned samples were performed using 2 N HNO_3 solution and each determination was carried out according to the recommended extraction - spectrophotometric procedures.

Conclusion

4-(2-Pyridylazo)resorcinol and 2-(5-bromo-2-pyridylazo)-5-diethylaminophenol have been used, as chromogenic reagents, in the combined extraction - spectrophotometric procedure for the determination of uranium in phosphoric acid. The calibration graphs for PAR and bromo-PADAP reagents were linear over the range 0–304 and 0–120 μg of uranium per 25 ml of final solution and the molar absorptivities were 2.10×10^4 and $6.33 \times 10^4\ l\ mol^{-1}\ cm^{-1}$ at 530 and 574 nm, respectively.

These methods are accurate and precise, and have been successfully used for the analysis of samples from laboratory and pilot plant evaluations and as process control methods in the extraction process from wet-process phosphoric acid (phosphate rocks; fresh feed, loaded and raffinate phosphoric acid; gypsum and water).

References

1. Hurst, F. J., Crouse, D. J., and Brown, K. B., *Ind. Eng. Chem., Process Des. Dev.*, 1972, **11**, 122.
2. Hurst, F. J., Arnold, W. D., and Ryon, A. D., *Chem. Eng.*, 1977, **84**, 56.
3. Florence, T. M., and Farrar, Y., *Anal. Chem.*, 1963, **35**, 1613.
4. Johnson, D. A., and Florence, T. M., *Anal. Chim. Acta*, 1971, **53**, 73.
5. Sandell, E. B., and Onishi, H., "Photometric Determination of Traces of Metals," Volume 3, Part I, Fourth Edition, Wiley-Interscience, New York, 1978.
6. Pakalns, P., *Mikrochim. Acta*, 1980, **I**, 339.

Photometric Determination of Nickel by Means of Photochemically Generated (Z)-2-Thiophenaldehyde 2-Pyridylhydrazone

Francisco García Sánchez* and Miguel Hernández López

Department of Analytical Chemistry, Faculty of Sciences, University of Málaga, Málaga-4, Spain

The photochemical isomerisation of 2-thiophenaldehyde 2-pyridylhydrazone (TAPH) in ethanolic solution was investigated and the E/Z ratio in the photostationary state was determined. (E)-TAPH scarcely reacted or did not react with metal ions whereas, after irradiation, (Z)-TAPH gave sensitive reactions with several metal ions. A photometric method was developed for the determination of nickel (0.017–0.9 µg ml⁻¹) in aqueous ethanolic medium (50% V/V) at pH 10.7 with a detection limit of 0.005 µg ml⁻¹ and a relative standard deviation of 1.03%. By considering the E/Z ratio in the photostationary state, the corrected stoicheiometry of the chelate was found to be 3:1 (ligand to metal). Applications of the method to the determination of nickel in special steels and environmental fume samples are described.

Keywords: *Nickel determination; anti-2-thiophenaldehyde 2-pyridylhydrazone; photochemical isomerisation; spectrophotometry*

In spite of the development of techniques such as atomic-absorption spectrometry, with improved analytical performance, spectrophotometry remains widely employed in routine analyses of both organic and inorganic analytes. In inorganic analysis, the formation of a metal chelate with an organic ligand is usually a prerequisite for the photometric determination of metallic ions. The considerable development of coordination chemistry during the past three decades has made possible the recognition of the factors that determine the analytical selectivity of complexation reactions, and more analytical problems can be solved via complexation.

Of the great variety of organic reagents that are in common use today, hydrazones, *i.e.*, azomethines characterised by the grouping >C=N–N< , in particular are used extensively in the detection and determination of various metal ions.[1,2] Many hydrazones are now commercially available. This type of ligand often undergoes photochemical transformations,[3–14] leading to instability and poor precision of the analytical measurements.[15–19] Although this effect can be alleviated by employing reduced slit widths in the apparatus or keeping the samples in the dark, studies of the mechanism and the variables that affect the photolability of the ligand may be advisable in order to improve the analytical characteristics of photometric and fluorimetric methods.

Although, to some extent, the technique is complicated by the irradiation of the ligand, the advantages obtained in the analytical performance of the method can be valuable. Side-reactions that may lead to transformations of the ligand and prevent it from acting in its own right are avoided, favouring conditions of high stability for the chelate and the ligand.

The technique described in this paper is very simple and compares favourably in terms of precision and sensitivity (detection limit) with emission spectrometry (arc, spark, plasma), flame emission and atomic-absorption spectrometry, X-ray fluorescence, polarography and activation analysis.[20] As the main interferences have been masked, the selectivity is good.

Light-induced reactions of compounds with a carbon–nitrogen double bond may lead to isomerisation, phototropy, rearrangement, cycloaddition, oxidation, hydrolysis, cyclisation, photoreduction or photoalkylation.[21] However, although radiationless paths that maintain molecular geometry are important to some extent, E–Z isomerisation provides the major route for deactivation of the excited imine state.[22]

Because of the low thermal barrier[23] between the two isomers, the photochemically induced shift in the isomeric equilibrium is frequently followed by rapid thermal relaxation, which re-establishes the initial configurational equilibrium.[21,24] This feature impedes the isolation of the isomers and complicates photoisomerisation studies. However, in the hydrazone derivatives of aromatic aldehydes and ketones the thermal barrier is sufficient to prevent thermal interconversion.[23]

This paper reports the light-induced transformation of 2-thiophenaldehyde 2-pyridylhydrazone (TAPH) to the Z-isomer, which permits its use as a complexing agent in the photometric determination of nickel at trace levels. The nature of the photoproducts of TAPH is discussed in order to elucidate their photochemical behaviour.

It must be pointed out that this type of ligand is frequently cited as not being a chromogenic reagent for metal ions, probably as a consequence of the E–Z transformation. In this context, the quinolyl analogue of TAPH shows similar behaviour.[25,26]

Experimental

Apparatus

A Shimadzu UV-240 Graphicord spectrophotometer was used for recording spectra and a Beckman DU-2 instrument was used for measurements at fixed wavelengths, with matched 1.00-cm quartz cells. IR spectra were recorded on KBr disks with a Beckman IR-4240 spectrophotometer. NMR spectra were run on solutions in dimethyl sulphoxide using a Hitachi Perkin-Elmer R-24b spectrometer. Tetramethylsilane was used as an internal reference.

The light source used for irradiation was an Atom-70 vapour lamp, the strongest line being at 365 nm. The irradiation equipment consisted of a black box equipped with an Hg lamp, and the reaction cells were calibrated flasks made of Pyrex glass (lower limit of transparency 300 nm). The distance between the radiation source and the sample was 10 cm and constant agitation was maintained during irradiation.

Reagents

(E)-2-Thiophenaldehyde 2-pyridylhydrazone was synthesised in the usual way for hydrazones[27] by heating equimolar amounts of 2-hydrazinopyridine and doubly distilled thiophenaldehyde. The compound was characterised by IR and

---

* To whom correspondence should be addressed.

NMR spectroscopy and the purity was confirmed by elemental analysis: required for $C_{10}H_9N_3S$, C 59.11, H 4.43, N 20.67; found, C 59.04, H 4.45, N 20.55%.

The Z-isomer was prepared starting from a 1×10^{-3} M ethanolic solution of the E-isomer by direct irradiation for 6 h at 365 nm. It was isolated by silica gel high-performance thin-layer chromatography (HPTLC) using chloroform - diethyl ether $(1 + 1)$ as the eluent. The melting-point of the E-isomer is 153–154 °C and that of the Z-isomer is 52–53 °C. Silica gel HPTLC gave R_F values for the E- and Z-isomers of 0.49 and 0.63, respectively. Characterisation was performed by UV, IR and NMR spectroscopy. A 1×10^{-3} M solution of (E)-TAPH in absolute ethanol was prepared daily and stored in the dark.

A 0.1 M nickel stock solution was prepared from nickel sulphate hexahydrate and standardised gravimetrically with dimethylglyoxime. Working solutions were prepared by appropriate dilution with de-ionised, distilled water.

A pH 9.40 buffer solution was prepared from 0.1 M boric acid and 0.1 M sodium hydroxide solution.

Procedures

Direct photoisomerisation

For direct photoisomerisation of the pure E-isomer, 2×10^{-5} and 1×10^{-3} M ethanolic solutions were irradiated in calibrated flasks. The reaction was followed by measuring the spectral changes at regular time intervals between 250 and 450 nm. The photostationary state was considered to be attained when subsequent irradiation did not alter the electronic spectra. The constant isosbestic point and chromatographic analysis indicated that only one product was formed by irradiation and no-side reactions could be detected.

Spectrophotometric determination of nickel

Into a 25-ml calibrated flask transfer a volume of solution containing 0.4–2.2 µg of nickel, add 6 ml of 1×10^{-3} M irradiated TAPH ethanolic solution, 11.5 ml of ethanol and 5 ml of pH 9.40 buffer solution and dilute to the mark with de-ionised water. Measure the absorbance at 427 nm against a reagent blank. Use a suitable calibration blank and an empirical equation to convert absorbance into concentration.

Procedure for a special steel

To a 0.25-g sample in a 50-ml Erlenmeyer flask, add 15 ml of 1 + 1 hydrochloric acid and warm gently until complete decomposition. Add carefully 10 ml of 1 + 1 nitric acid and boil the solution until evolution of brown vapour ceases. Dilute to 250 ml with de-ionised water, take an aliquot and proceed as above for the determination of nickel.

Procedure for environmental fume samples

Fume samples were collected in workshop environments according to the NIOSH Manual[28] as described previously.[26]

An aliquot of this solution was then subjected to the photometric procedure.

Results and Discussion

The Ligand: Absorption Spectra and pH Effects

The UV spectra of the E- and Z-isomers of TAPH in seven different organic solvents are reported in Table 1. The spectra of (E)-TAPH exhibit a high-intensity long-wavelength absorption, as expected for substituted hydrazones,[29] in which the unshared electron pair orbital of the nitrogen atom is parallel to and overlaps with the π orbitals of the C=N bond.

In the UV spectra of the Z-isomer the long-wavelength band undergoes a blue shift and a decrease in intensity (hypsochromic - hypochromic shift). This shift is related to the non-bonded repulsion between the aryl groups, which leads to the lone pair of the amine nitrogen being almost orthogonal to the π orbital of the azomethine group. Table 1 shows that the time of irradiation needed to attain the photostationary state is independent of the nature of the solvent.

The spectral changes that TAPH suffers on irradiation are shown in Fig. 1. (E)-TAPH has an absorption maximum at 340 nm ($\varepsilon = 2.60 \times 10^4$ l mol^{-1} cm^{-1}), which shifts to 332 nm ($\varepsilon = 2.10 \times 10^4$ l mol^{-1} cm^{-1}) in the photostationary state, showing an isosbestic point at 320 nm.

The pH of the TAPH solution before irradiation has a minor effect on the spectral characteristics of the Z-isomer. At pH greater than 6 the Z-isomer shows a blue shift of 5 nm and $\Delta\varepsilon = -2500$ l mol^{-1} cm^{-1} respect to (E)-TAPH. At lower pH the spectral shapes are identical for both isomers, which can be explained by the formation of an intramolecular hydrogen bond between the free electron pair of the exocyclic nitrogen and the protonated ring nitrogen.

The NMR spectra of the Z- and E-isomers were examined at 60 MHz, and no difference could be detected.

In the IR spectra, the shift of the NH stretching vibration in the E-isomer towards lower frequencies in the anti-isomer (3200 to 3160 cm^{-1}), showing a broad band, suggests the formation of weak N–H–S hydrogen bonds, which modifies by a parallel effect the CNH bending, which shifts to lower frequencies (1520 to 1510 cm^{-1}). On the other hand, the alteration of the thiophene ring vibrations provides evidence for the E and Z configurations (stretching, 1550 to 1560 cm^{-1}, with the appearance of a new band at 1410 cm^{-1}).

The effect of pH on the UV spectra of 2×10^{-5} M aqueous ethanolic $(1 + 1)$ solutions of (E)-TAPH (Fig. 2) shows that the two main absorption bands (240 and 340 nm) are involved in the prototropic behaviour. The invariance of the spectra at low pH suggests that at pH below 3.9 they correspond to the protonated species of TAPH, and at pH above 8.3 to anionic TAPH. Hypsochromic shifts corresponding to the transformation from the cationic to the neutral species occur in slightly alkaline solution, leading to shifts in the maximum absorption bands from 280 and 360 nm to 240 and 340 nm, respectively.

Table 1. UV spectroscopic data for (E)- and (Z)-TAPH

Solvent	E band maxima		$t_{p.s.}$*/ min	Z band maxima†	
	λ/nm	ε/l mol^{-1} cm$^{-1} \times 10^4$		λ/nm	ε/l mol^{-1} cm$^{-1} \times 10^4$
Benzene	342	2.42	15	338	2.07
Dioxane	342	2.50	15	337	2.10
Chloroform	340	2.47	15	336	2.12
Diethyl ether	340	2.80	15	334	2.30
Propanol	340	2.65	15	332	2.15
Ethanol	340	2.62	15	333	2.12
Methanol	340	2.65	15	333	2.12

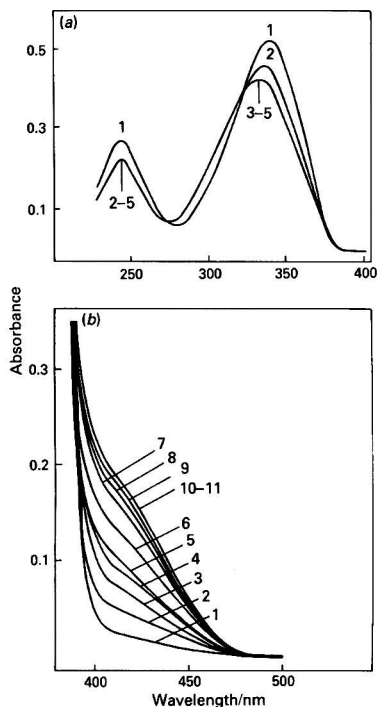* Time to attain the photostationary state.
† In the photostationary state.

Fig. 1. Spectral changes of TAPH on irradiation. (*a*) [TAPH] = 2 × 10⁻⁵ M. Irradiation time for curves 1–5: 0, 5, 15, 30 and 60 min, respectively (*b*) [TAPH] = 1 × 10⁻³ M. Irradiation times for curves 1–11: 0, 15, 30, 45, 60, 90, 135, 180, 240, 300 and 360 min, respectively
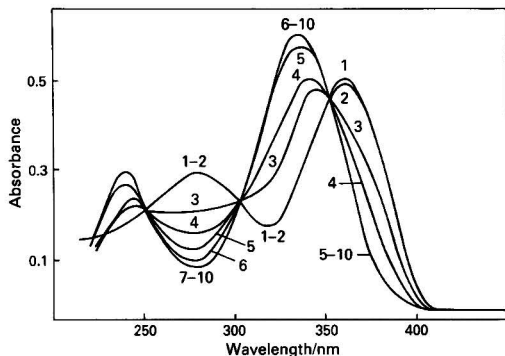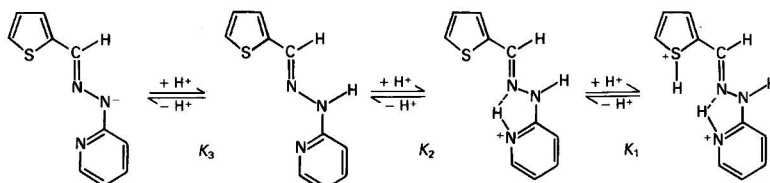

Fig. 2. Absorption spectra of 2 × 10⁻⁵ M solutions of (*E*)-TAPH at several pH values and an ethanol concentration of 50% *V*/*V*. pH: 1, 1.83; 2, 3.92; 3, 5.03; 4, 5.53; 5, 6.62; 6, 8.31; 7, 9.60; 8, 11.30; 9, 11.63; and 10, 12.32

The ionisation constant in aqueous ethanolic (1 + 1) medium at an ionic strength of 0.1 was determined from the variation of absorbance with pH.[30] As is apparent from its structure (Scheme 1), TAPH is dibasic and has a dissociable imino hydrogen in the molecule. Hence the reagent exists in solution in any of the forms shown, depending on the pH.

Spectrophotometrically, the prototropic equilibria can be followed only for K_2. The first deprotonation takes place in fairly acidic solution below pH 1, whereas the final deprotonation of the uncharged molecule (K_3) does not occur below pH 12.3. As the electron pair of the azomethine nitrogen is involved in the hydrogen bonding with the pyridine ring, the first deprotonation has been assigned to the sulphur heteroatom.

The spectra below pH 4 are identical because the protonation of heterocyclic sulphur hardly affects the electron distribution in the whole molecule.

As expected for a nitrogen heterocycle, the protonation of the free base causes a red shift that can be attributed to intramolecular hydrogen bonding between the azomethine nitrogen and the pyridine NH arrangement, which increases the electron migration and molecular rigidity. The yellow fluorescence that appears in acidic solution gives additional support to this hypothesis.

From the absorptiometric study, the pK_2 value for protonated TAPH was calculated to be 5.5 ± 0.1, obtained from five points from photometric titration at 325 and 375 nm.

Determination of the *E*/*Z* Ratio in the Photostationary State

After irradiation, (*E*)- and (*Z*)-TAPH were separated from the mixture by silica gel column chromatography using chloroform - diethyl ether (1 + 1) as the eluent. From UV data for the isolated isomers the composition of the mixture in the photostationary state was calculated to be (*E*)-TAPH = 48.9%, (*Z*)-TAPH = 51.1%.

Metal Complexes

TAPH appears to be a bi- or tridentate ligand with a convenient steric arrangement of its donor groups, and contains a conjugated system of π electrons connected with the donor system.

The reaction of both isomers of TAPH with 45 cations at various pH values was investigated quantitatively. The absorption spectra of the complexes were obtained (Fig. 3), and the analytical characteristics are summarised in Table 2. No fluorigenic reactions were detected with either isomer.

In alkaline media, (*E*)-TAPH reacts with nickel(II) to form an orange complex and with zinc(II) to form a yellow complex, both of which fade rapidly.

From these data, the most relevant observation is that the *Z*-isomer forms five new stable chelates with Zn, Cd, Hg, Ni and Co. On the other hand, it was found that the introduction of the thiophene sulphur atom into the coordinating system causes a decrease in the molar absorptivities of the chelates compared with the pyridine analogue. As expected, the introduction of a group of small complexing capacity in the coordinating system provided better selectivity.

Scheme 1
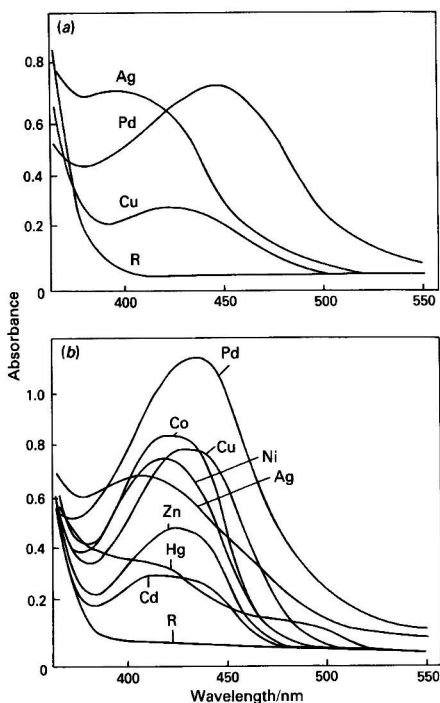
Fig. 3. Absorption spectra of TAPH chelates in water - ethanol (1 + 1) solutions at an apparent pH of 10.70. (*a*) (*Z*)-TAPH; (*b*) (*E*)-TAPH. $C_R = C_M = 8 \times 10^{-5}$ M
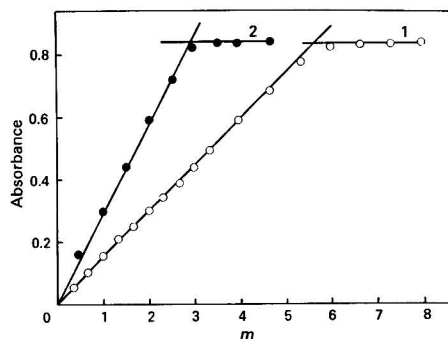

Fig. 4. Composition of the (*E*)-TAPH - Ni complex by the molar-ratio method. $C_M = 1.5 \times 10^{-5}$ M; $\lambda = 427$ nm. 1, (*E*)-TAPH - (*Z*)-TAPH mixture in the photostationary state; 2, corrected concentration of (*E*)-TAPH

Table 3. Characteristics of the analytical method

Parameter			Value
Calibration sensitivity, $S_C = m/A\,\mu g^{-1}$ ml	..	..	0.9179
Analytical sensitivity, $S_A = m/s_S/\mu g^{-1}$ ml	..	..	148
$1/S_A/\mu g$ ml^{-1}	..	..	0.007
C_L ($k = 3$)/μg ml^{-1}	..	..	0.005
C_O ($k = 10$)/μg ml^{-1}	..	..	0.017
Linear dynamic range/μg ml^{-1}	..	..	0.017–0.9

Table 4. Tolerance to foreign ions and other species

Ion added					Tolerance ratio (ion to Ni)
Urea, thiourea, triethylamine	..	..	..	..	35 000
I$^-$, acetate ..	..	..	..	..	25 000
Thiocyanate	..	..	..	..	4 000
F$^-$, NH$_3$, ethylene glycol	..	..	..	..	300
S$_2$O$_3{}^{2-}$, tartrate ..	..	..	..	..	150
Cd(II),* H$_2$O$_2$	..	..	..	..	50
Cu(II),† Zn(II),‡ Al(III),§ Fe(III)§	..	..	..	25
Ca(II), Cr(III), oxalate, ascorbic acid	..	..	..	10
Pb(II), Mn(II)	..	..	..	..	5
Co(II)‡	..	..	..	..	2
Hg(II)	..	..	..	..	1
EDTA, citrate	..	..	..	..	0.2

* Thiocyanate, 2400 p.p.m.
† Thiourea, 20 000 p.p.m.
‡ NH$_3$, 200 p.p.m.
§ Triethanolamine, 20 000 p.p.m.

Study of the (Z)-TAPH - Ni(II) Complex

Spectral behaviour of the complex

A pH study of the complexation of (*Z*)-TAPH with nickel(II) showed that the yellow complex ($\lambda_{max.}$ = 427 nm) gives a constant absorbance in the pH range 11.0–12.0. For complete complexation, a 10 M excess of TAPH is sufficient. The complex is quickly formed and the colour remains stable for at least 4 h. Slight variations in absorbance can be found by modifying the concentration of ethanol in the medium. Optimum results are obtained in ethanol - water (7 + 3). The pH can be adequately adjusted to apparent pH 11.5 by the addition of 5 ml of pH 9.4 borate buffer solution, when the samples are of moderate acidity (pH > 4). No changes in absorbance were observed when the order of addition of the reagents was modified.

Stoicheiometry

The metal to ligand ratio in the complex was studied under the established working conditions by the molar-ratio method. The method was applied to a series of solutions containing nickel at a fixed concentration of 1.5×10^{-5} M, the

Table 2. Spectral data for the chelates formed by (*E*)- and (*Z*)-TAPH

			(*E*)-TAPH		(*Z*)-TAPH	
Ion			$\lambda_{max.}$/nm	$\varepsilon_{max.}$/l mol^{-1} cm$^{-1} \times 10^3$	$\lambda_{max.}$/nm	$\varepsilon_{max.}$/l mol^{-1} cm$^{-1} \times 10^3$
Pd(II)	..	..	445	9.2	437	14.2
Ag(I)	..	..	400	9.2	412	8.5
Cu(II)	..	..	425	3.5	435	9.7
Co(II)	..	..	—	—	435	11.0
Ni(II)	..	..	—	—	427	10.0
Zn(II)	..	..	—	—	427	6.0
Hg(II)	..	..	—	—	412	4.2
Cd(II)	..	..	—	—	425	3.5

(*E*)-TAPH could act as potentially tridentate because the linear arrangement of the thiophenic sulphur, pyridine nitrogen and azomethine nitrogen gives rise to two five-membered chelate rings. In the *Z*-position, the torsion around the C=N bond impedes the participation of the sulphur atom as a donor owing to steric considerations, thus giving rise to a five-membered chelate ring between the azomethine and pyridine nitrogens.

In (*E*)-TAPH the distortion caused by the bulky sulphur atom in the tridentate chelate as a consequence of its weakly basic character and the great delocalisation of the unshared heterocyclic electron pair makes the chelate very unstable. In (*Z*)-TAPH, the thiophene sulphur does not participate as a donor atom and undistorted chelates are formed. Consequently, the stability increases on going from chelates with two five-membered rings to one five-membered ring.

Table 5. Determination of nickel in special steels and environmental fume samples

Sample	Nickel present/ $\mu g\ ml^{-1}$	Nickel found/ $\mu g\ ml^{-1}$	Nominal composition, %
Steel BAS 22b	0.60	0.59$_7$	Ni, 3.04
Steel F-156.IHA . .	0.60	0.59$_5$	Mn, 0.58; Si, 0.29; Cr, 1.04; Ni, 3.874; Mo, 0.490
Steel F-122.IHA . .	0.60	0.59$_9$	Mn, 0.572; Si, 0.26; Cr, 1.186; Ni, 4.176
Fume sample 1	0.20*	0.19$_7$	—
Fume sample 2	0.24*	0.23$_6$	—
Fume sample 3	0.28*	0.28$_1$	—

* By atomic-absorption spectrometry.

concentration of irradiated TAPH being varied. A graph of absorbance *versus* molar ratio of TAPH to nickel showed a break at a ratio of 1 : 5.9 (Fig. 4). If it is assumed that absorbing species are formed by (Z)-TAPH, the true stoicheiometric ratio of metal to ligand can be obtained by multiplying the TAPH molar concentration by a factor that converts the real concentration of (Z)-TAPH in the solutions employed. As we employed irradiated TAPH at the photostationary equilibria, where the proportion of the Z-form is 51.1%, the corrected stoicheiometry leads to a metal to ligand ratio of 1 : 3. This finding was expected on the basis of the bidentate character of (Z)-TAPH, as discussed above, and the octahedral hexacoordinate nature of the nickel ion.

Spectrophotometric Determination of Nickel with (Z)-TAPH

The relationship between concentration and absorbance obeyed Beer's law in the range 0–1.2 $\mu g\ ml^{-1}$ of nickel, the graph obtained being a straight line that passed through the origin ($A = 0.9179c + 0.009$; $r = 0.997$). The molar absorptivity at $\lambda_{max.} = 427$ nm was $\varepsilon = 5.52 \times 10^4$ l mol^{-1} cm^{-1}). The Ringbom plot showed that the optimum range for accurate determination was 0.2–0.9 $\mu g\ ml^{-1}$ of nickel.

The precision of the method was determined by measuring the absorbance of eleven separate samples each containing 0.6 $\mu g\ ml^{-1}$ of nickel; a relative error ($P = 0.05$) of 0.74% and a relative standard deviation of 1.03% were obtained. A negligible contribution of between-batch variation to the precision of the determination was found. To determine the between-day variation, triplicate determinations were made on each of ten days; all absorbances were within the range 0.555–0.565 (0.6 $\mu g\ ml^{-1}$ of nickel).

Sensitivity and Limit of Detection

The sensitivity of the method is reported as the calibration sensitivity,[31] $S_C = m$ (m = slope of the calibration graph), and analytical sensitivity,[32] $S_A = m/s_s$. As deduced from the equation for its definition, S_A is inversely related to the ability to distinguish a concentration difference, and therefore the inverse relationship $1/S_A$ is also included.

The limit of detection, C_L, is reported as defined by IUPAC.[33] The limit of quantitation,[32] C_Q, is employed to establish the inferior limit of the linear dynamic range. The results obtained are presented in Table 3.

Interference Study

The effect of various potentially interfering ions on the determination of 0.6 $\mu g\ ml^{-1}$ of nickel was examined over a wide range of interferent concentrations. The criterion for interference was a relative error in the absorbance of ±2%. Elimination of the main interferences was performed by using several common masking agents. The results obtained are shown in Table 4.

Application to Real Samples

The recommended procedure for the determination of nickel was applied to special steels and environmental fume samples to evaluate its effectiveness. The results obtained are summarised in Table 5.

References

1. Katyal, M., and Dutt, Y., *Talanta*, 1975, **22**, 151.
2. Zatka, V., Abraham, J., Holzbecher, J., and Ryan, D. E., *Anal. Chim. Acta*, 1971, **54**, 65.
3. Schulte-Frohlinde, D., *Justus Liebigs Ann. Chem.*, 1959, **47**, 622.
4. Hausser, I. D., *Naturwissenschaften*, 1949, **36**, 313.
5. Hausser, I. D., Jerchel, D., and Khun, R., *Chem. Ber.*, 1949, **82**, 515.
6. Khun, R., and Weitz, H. M., *Chem. Ber.*, 1953, **86**, 1199.
7. Wong, J. L., and Zady, M. F., *J. Org. Chem.*, 1975, **40**, 2512.
8. Condorelli, G., and Costanzo, L., *Boll. Accad. Gioenia Sci. Nat.*, 1966, **8**, 753.
9. Condorelli, G., and Costanzo, L. *Boll. Accad. Gioenia Sci. Nat.*, 1967, **9**, 126.
10. Condorelli, G., Costanzo, L., Pistara, S., and Giuffrida, S., *Z. Phys. Chem., N.F.*, 1974, **90**, 58.
11. Condorelli, G., Costanzo, L., Pistara, S., and Giuffrida, S., *Z. Phys. Chem., N.F.*, 1975, **96**, 97.
12. Fischer, E., Kaganowich, M., *Bull. Res Counc. Isr., Sect. A*, 1961, **10**, 138.
13. Costanzo, L., Chiacchio, U., Giuffrida, S., and Condorelli, G., *J. Photochem.*, 1980, **13**, 83.
14. Costanzo, L., Chiacchio, U., Giuffrida, S., and Condorelli, G., *J. Photochem.*, 1980, **14**, 125.
15. Laserna, J. J., Navas, A., and García Sánchez, F., *Anal. Chim. Acta*, 1980, **121**, 295.
16. Laserna, J. J., Navas, A., and García Sánchez, F., *Anal. Lett.*, 1981, **14A**, 833.
17. Ishii, H., Odashima, T., and Imamura, T., *Analyst*, 1982, **107**, 885.
18. Singhal, S. P., and Ryan, D. E., *Anal. Chim. Acta*, 1967, **37**, 91.
19. Santiago, M., Navas, A., Laserna, J. J., and García Sánchez, F., *Mikrochim. Acta*, 1983, **2**, 197.
20. Pinta, M., "Modern Methods for Trace Element Analysis," Ann Arbor Science Publishers, Ann Arbor, MI, 1978.
21. Padwa, A., *Chem. Rev.*, 1977, **77**, 37.
22. Herkstroeter, W. G., *J. Am. Chem. Soc.*, 1976, **98**, 330.
23. Izawa, H., de Mayo, P., and Tabata, T., *Can. J. Chem.*, 1969, **47**, 51.
24. Costanzo, L., Giuffrida, S., Chiacchio, U., and Condorelli, G., *J. Photochem.*, 1979, **11**, 39.
25. Hernández López, M., and García Sánchez, F., unpublished work.
26. Martinez de la Barrena, M. R., Laserna, J. J., and García Sánchez, F., *Anal. Chim. Acta*, 1983, **147**, 303.
27. Geldard, J. S., and Lions, S., *Inorg. Chem.*, 1963, **2**, 270.
28. "Manual of Sampling Data Sheets," National Institute of Safety and Hygiene, Cincinnati, 1976.
29. Iffland, D. C., McAneny, M. D., and Weber, D. J., *J. Chem. Soc.*, 1969, 1703.
30. Stenstrom, W., and Goldsmith, N., *J. Phys. Chem.*, 1926, **30**, 1683.
31. "Nomenclature, Symbols, Units and Their Usage in Spectrochemical Analysis—II," *Spectrochim. Acta, Part B*, 1978, **33**, 242.
32. "Guidelines for Data Acquisition and Data Quality Evaluation in Environmental Chemistry," *Anal. Chem.*, 1980, **52**, 2242.
33. Long, G. L., and Winefordner, J. D., *Anal. Chem.*, 1983, **55**, 712A.

Sensitive Method for the Spectrophotometric Determination of Boron in Plants and Waters Using Crystal Violet

Ignacio López García, Manuel Hernández Córdoba and Concepción Sánchez-Pedreño*
Department of Analytical Chemistry, Faculty of Chemistry, University of Murcia, Murcia, Spain

A sensitive and rapid spectrophotometric method for the determination of boron is described, which is based on the formation of a blue complex at pH 1–2 between the anionic complex of boric acid with 2,6-dihydroxybenzoic acid and crystal violet; the colour is stabilised with poly(vinyl alcohol). At 600 nm the calibration graph is linear in the range 0.3–4.5 µg of boron per 25 ml of final solution with a relative standard deviation of $\pm 2.6\%$ for 0.069 µg ml^{-1} of boron. The molar absorptivity is 3.75×10^4 l mol^{-1} cm^{-1}. The method has been applied to the determination of boron in plants and natural waters.

Keywords: *Boron determination; crystal violet; 2,6-dihydroxybenzoic acid; spectrophotometry; plant and natural water analysis*

The development of more sensitive and selective methods for the spectrophotometric determination of boron has been considered by many workers.[1,2] Most of the recent papers are based on the extraction of ion pairs[3–11] formed between boron complex anions and large, coloured cations using Ducret's method.[12] The procedures described so far are both sensitive and selective but, generally, back-washing with different solutions is required in order to remove the excess of reagent that is extracted with the boron complex. This is a major disadvantage and a more simple and sensitive method for the routine determination of boron is therefore desirable.

The classical work of Dagnall and West[13,14] demonstrated that some dyes show a change in their absorption spectra when forming ion-association compounds. If this occurs, the solvent extraction step can be avoided and the spectrophotometric method can be carried out with the minimum of manipulation. In this way, the interaction between the complex anion, boron - 2,6-dihydroxybenzoic acid, and several basic dyes has been studied with the aim of developing a rapid method for the spectrophotometric determination of boron, without extraction.

The results obtained using crystal violet are presented. The method has been applied to the determination of boron in both plants and natural waters.

Experimental

Apparatus

Absorbance measurements were made with a Pye Unicam SP8-200 spectrophotometer using glass cells of 10-mm path length. The pH values were measured with a Radiometer PHM62 pH meter.

Reagents

All inorganic chemicals were of analytical-reagent grade and were used without further purification. All reagent solutions were kept in polyethylene bottles and doubly distilled water was used throughout.

Standard boron solution, 1000 µg ml^{-1}. Prepared from dried boric acid.

Crystal violet solution, 10^{-3} M.

Poly(vinyl alcohol)(PVA) solution, 1% *m/V*.

2,6-Dihydroxybenzoic acid (DHBA) solution, 0.2 M. Prepared from the commercial product (Merck) by dissolving 6.16 g in 200 ml of water containing 3.28 g of sodium acetate.

Preparation of Reagent Solution

The reagent solution was prepared by mixing 200 ml of 10^{-3} M crystal violet solution, 200 ml of 1% *m/V* PVA solution and 2 ml of 1 N sulphuric acid and allowing the mixture to stand for 2 h.

General Procedure

Transfer up to 20 ml of the sample solution containing no more than 4.5 µg of boron into a 25-ml calibrated flask and dilute to 20 ml with water, if necessary. Add 1 ml of 0.2 M DHBA solution and 1 ml of 1 N sulphuric acid. Set aside for 20 min, add 2 ml of reagent solution and dilute to the mark with water. Mix thoroughly and measure the absorbance at 600 nm after 15 min, against a reagent blank. Beer's law is obeyed over the concentration range 0.3–4.5 µg of boron in 25 ml of solution (12–180 ng ml^{-1}).

Procedure for the Determination of Boron in Plants

Dry the plant tissues in a silica dish at 60 °C, weigh accurately 0.2–1.0 g (depending on the boron content) of the finely ground sample and add 0.1 g of calcium hydroxide. Ash in a muffle furnace at 400 °C for 4 h and leave to cool inside the furnace. Add 5 ml of 1 N sulphuric acid and heat the mixture carefully to 80 °C on a hot-plate. Cool to room temperature, filter into a 25-ml calibrated flask, wash with water, neutralise with 1 N sodium hydroxide solution to the colour change of methyl orange and dilute to 25 ml. Take a suitable aliquot and determine the boron content as described under General Procedure.

Procedure for the Determination of Boron in Waters

Acidify the samples with sulphuric acid to pH 2–3, filter if necessary through a membrane filter (0.5 µm) and store in a polyethylene bottle. Take a suitable aliquot, neutralise as described above and determine the boron content as described under General Procedure.

Results and Discussion

The reaction of boric acid with 2,6-dihydroxybenzoic acid (DHBA) to produce an anionic complex that can be associated with cationic dyes has been previously reported.[15] Consequently, several extraction - spectrophotometric[8,15] methods for the determination of boron have been described. With the aim of developing a method without extraction, the interaction between the anionic complex of boron and several basic dyes (malachite green, methyl violet, ethyl violet, crystal

---
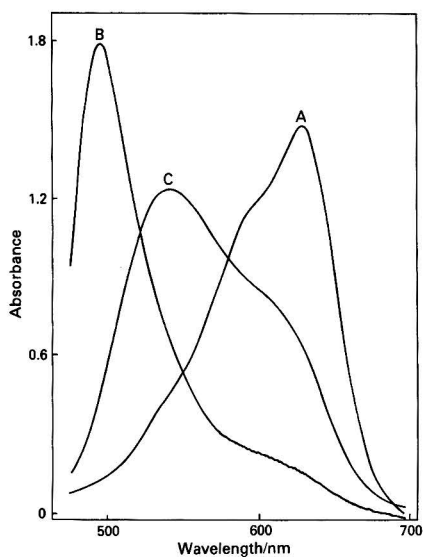
Fig. 1. Absorption spectra of A, crystal violet (4×10^{-5} M) with PVA (0.04%) at pH 1.5; B, as A but with DHBA (8×10^{-3} M); and C, as B but with 4.5 µg of boron
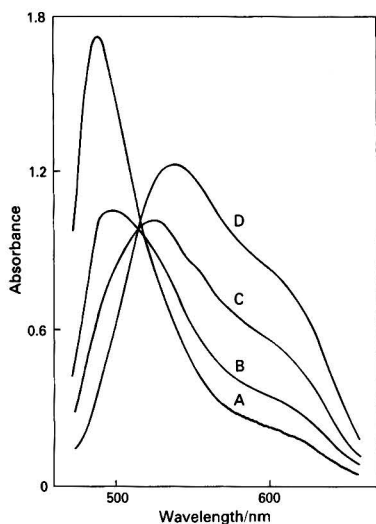

Fig. 2. Absorption spectra of A, reagent blank (reference water); and B, C and D with 0.9, 2.4 and 4.5 µg of boron, respectively (reference, water)

violet, Rhodamines B, S and 6G, victoria blue and brilliant green) was examined for a shift in the spectral characteristics of the dye. The most appropriate cationic dye was found to be crystal violet.

As can be seen in Fig. 1 when DHBA is added to an acidified solution of crystal violet the colour changes to red. If the anionic DHBA - boron complex is present, a considerable bathochromic shift occurs. Fig. 2 shows the absorption spectra obtained for crystal violet solutions with different amounts of boron in the presence of an excess of DHBA. All absorbance measurements were carried out at 600 nm.

The blue ternary complex formed by the addition of the dye to the aqueous solution of boric acid containing DHBA was unstable and a gradual precipitation on standing was ob-
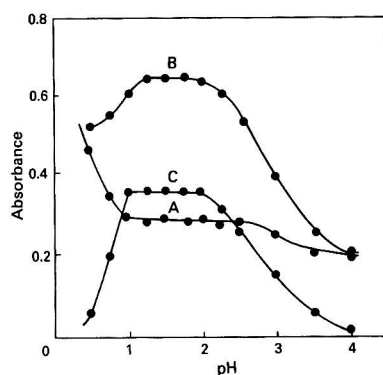
Fig. 3. Effect of pH on absorbance. A, Reagent blank (reference, water); and B and C, with 2.6 µg of boron (B, reference, water; and C, reference, reagent blank)
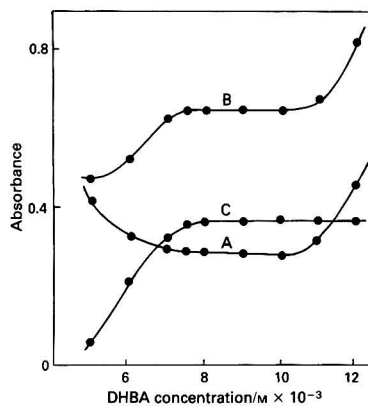
Fig. 4. Effect of DHBA concentration. A, Reagent blank (reference, water); and B and C, with 2.6 µg of boron (B, reference, water; and C, reference, reagent blank)
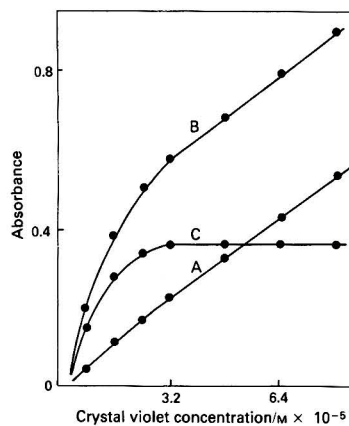
Fig. 5. Effect of crystal violet concentration. A, Reagent blank (reference, water); B and C, with 2.6 µg of boron (B, reference, water; and C, reference, reagent blank)

served. Stabilisation was achieved by the addition of PVA or gelatine as protective colloids, which successfully retarded precipitation of the complex. The use of PVA is recommended because the reproducibility was higher, although a standing time of about 15 min is required for stabilisation. The best results were obtained when the PVA was added together with the acidified dye, so the absorbance due to boron was almost constant for at least 4 h.

Effect of pH

The effect of the acidity was examined by varying the sulphuric acid concentration in the final solution and the results are shown in Fig. 3. Maximum and constant absorbance values were obtained over the pH range 1–2 when the reagent blank solution was used as a reference. Outside this pH range the absorbance decreased rapidly. Experimentally, it was found that better reproducibility and faster develop-

ment of the colour were achieved when the dye solution was previously acidified to pH 2–3 as described under Experimental.

Effect of DHBA Concentration

The effect of DHBA concentration on the absorbance at 600 nm is shown in Fig. 4. In the range 0.006–0.01 M in the final solution the absorbance of the reagent blank was not high and the coloration was maximum. Consequently, the concentration of DHBA was adjusted to 8×10^{-3} M.

Effect of Crystal Violet Concentration

Fig. 5 shows the effect of crystal violet. At levels above 3×10^{-5} M in the final solution, the highest constant absorbance was obtained. In this study, the concentration of crystal violet was adjusted to 8×10^{-5} M, that is, the concentration of the reagent solution was fixed at 5×10^{-4} M.

Stoicheiometry of the Complex

The stoicheiometry of the ternary complex was investigated by the method of continuous variations. The results showed that a species with a crystal violet to boron molar ratio of 1 : 1 was formed.

Calibration Graph and Reproducibility

Under the recommended conditions, the calibration graph was linear over the range 0.3–4.5 µg of boron in a final volume of 25 ml. The molar absorptivity calculated from the slope of the graph was 3.75×10^4 l mol^{-1} cm^{-1} at 600 nm with a Sandell's sensitivity of 2.8×10^{-3} µg cm^{-2} and was not affected by temperature over the range 15–25 °C. Ten replicate determinations on a standard solution that contained 68 ng ml^{-1} of boron showed a relative standard deviation of 2.6%. Several tests showed that the use of a glass calibrated flask did not affect the absorbance values of the reagent blank, even on standing for 1 h.

Table 1. Effect of different ions on the determination of boron. Boron taken, 1.7 µg

Ion added			Molar ratio of [ion added] to [boron]
NO$_3$$^-$, Br$^-$, Cl$^-$, Ca(II), Mg(II), NH$_4$$^+$	..	..	20 000*
EDTA†	..	..	6 250
ClO$_4$$^-$, Al(III), Co(II), Cr(III), Cu(II) ..	..	..	2 000
PO$_4$$^{3-}$, SCN$^-$, F$^-$, Mn(II), Cd(II), Ni(II),			
Fe(III)‡	..	..	1 000
I$^-$, Hg(II)‡, Ag(I)	..	..	500
SiO$_3$$^{2-}$, Bi(III)‡	..	..	200
Fe(III)	..	..	10
Hg(II), W(VI), V(V)	..	..	3
Bi(III)	..	..	<1

* Maximum molar ratio tested.

† Higher amounts are suitable but pH control is necessary.

‡ Limiting ratio tolerated in the presence of 4×10^{-3} M EDTA solution.

Table 2. Determination of boron in waters and recovery of boron

				Boron found*/ µg l^{-1}	Recovery test			
					Boron/µg		Recovery, %	Reference method‡
Sample					Taken†	Found		
Spring water 1	..	..	..	148 ± 1	1.48	3.07	99.7	150
Spring water 2	..	..	..	62 ± 2	1.24	2.90	102.1	60
Tap water 1	..	..	..	100 ± 1	1.00	2.65	101.9	102
Tap water 2	..	..	..	117 ± 2	1.17	2.70	97.5	116
Pozo	..	..	..	423 ± 1	1.27	1.74	95.4	420

* Mean boron content ± standard deviation for three determinations.

† Amount of boron added to each aliquot, 1.6 µg; results are the means of three determinations.

‡ The results were obtained using a solvent extraction method.[8]

Table 3. Determination of boron in plant samples

				Boron found*/ µg g^{-1}	Recovery test			
					Boron/µg		Recovery, %	Reference method‡
Sample					Taken†	Found		
Pirus malus	..	..	..	22 ± 2	0.89	2.49	100.5	22
Pirus communis	..	..	..	12 ± 2	1.00	2.76	98.3	11
Vitis vinifera ..	..	..	..	39 ± 1	1.56	3.12	97.5	39
Morus alba	..	..	..	121 ± 1	0.97	1.96	102.2	125
Citrus limonum 1	..	..	..	575 ± 1	1.15	2.77	101.4	574
Citrus limonum 2	..	..	..	356 ± 1	1.42	3.02	99.8	354

* Mean boron content ± standard deviation for three determinations.

† Amount of boron added to each aliquot, 1.6 µg; results are means of three determinations.

‡ Results obtained using the quinalizarin method.[16]

Effect of Different Ions

The effect of different ions on the determination of 1.7 µg of boron was studied and the results are summarised in Table 1. The limiting value of the concentration of foreign ion was taken as that value which caused an error of not more than ±5% in the absorbance value. In the presence of 0.004 M EDTA solution the interference from Hg(II), Bi(III) and Fe(III) was overcome. When fluoride was present at amounts higher than 1000-fold that of boron, a negative error resulted. Large amounts of silicate were eliminated by acidification of the sample solution followed by filtration through a membrane filter.

Determination of Boron in Natural Waters and Plant Tissues

As can be seen from the results presented in Table 1 most of the ions normally present in natural waters do not interfere with the determination of boron. The proposed method was applied to the determination of boron in several waters from Murcia (Spain) and the results are shown in Table 2 together with those obtained by a sensitive solvent-extraction method.[8] Moreover, in order to detect any losses of boron, the standard additions method was also used.

The proposed method was also applied to the determination of boron in plant samples and the results, shown in Table 3, have been compared with those obtained using the established quinalizarin method.[16] Again, recovery tests for boron, using standard additions, have been included. Note the very high content of boron in *Citrus limonum* leaves; the trees from which these leaves were obtained had been irrigated with water with a high concentration of boron named Pozo.

Conclusion

The reaction between crystal violet and the complex of boric acid with 2,6-dihydroxybenzoic acid provides a reliable means for boron determination. The boron complex is formed in aqueous solution, the sensitivity and selectivity for boron are very high and the method does not involve an extractive separation, so that the proposed method is simple and rapid. Finally, the complex-forming reagent and the counter cation (basic dye) are commercially available.

References

1. Snell, F. D., "Photometric and Fluorometric Methods of Analysis. Nonmetals." Wiley, New York, 1981, p. 163.
2. Marczenko, Z., "Spectrophotometric Determination of Elements," Ellis Horwood, Chichester, 1976.
3. Vasilevskaya, A. E., *Nauchn. Tr. Inst. Miner. Resur. (Ukr. SSR)*, 1971, 22; *Anal. Abstr.*, 1973, **24**, 55.
4. Bassett, J., and Matthews, P. J., *Analyst*, 1974, **99**, 1.
5. Korenaga, T., Motomizu, S., and Tôei, K., *Anal. Chim. Acta*, 1980, **120**, 321.
6. Sato, S., and Uchikawa, S., *Anal. Chim. Acta*, 1982, **143**, 283.
7. Sato, S., *Anal. Chim. Acta*, 1983, **151**, 465.
8. Sánchez-Pedreño, C., Hernández Córdoba, M., and López García, I., *Anal. Quim. Ser. B*, 1984, **80**, 252.
9. Sato, S., and Uchikawa, S., *Bunseki Kagaku*, 1984, **33**, 87.
10. Tôei, K., Motomizu, S., Oshima, M., and Watari, H., *Analyst*, 1981, **106**, 776.
11. Oshima, M., Motomizu, S., and Tôei, K., *Anal. Chem.*, 1984, **56**, 948.
12. Ducret, L., *Anal. Chim. Acta*, 1957, **17**, 213.
13. Dagnall, R. M., and West, T. S., *Talanta*, 1961, **8**, 711.
14. Dagnall, R. M., and West, T. S., *Talanta*, 1964, **11**, 1533.
15. Oshima, S., Fujimoto, K., Shoji, M., and Tôei, K., *Anal. Chim. Acta*, 1982, **134**, 73.
16. Johnson, E. J., and Toogood, M. J., *Analyst*, 1954, **79**, 493.

SHORT PAPERS

High-performance Liquid Chromatographic Determination of Pyrrolizine Isopropyl Carbamate

L. Malspeis and Mohamed H. Abdel-Hay*
Pharmaceutical Chemistry Department, Ohio State University, Columbus, OH 43210, USA
and Abdel-Aziz M. Wahbi†
Faculty of Pharmacy, Alexandria University, Alexandria, Egypt

A rapid, sensitive and precise HPLC method for the determination of pyrrolizine isopropyl carbamate in an emulsion formulation is presented. Mean recoveries for amounts ranging from 100 to 1500 ng were between 98.1 and 102.1%. The coefficient of variation was less than 2%. The determination was achieved using the dimethoxy derivative as an internal standard.

Keywords: *Pyrrolizine isopropyl carbamate determination; high-performance liquid chromatography*

Pyrrolizine isopropyl carbamate[1,2] (I), 2,3-dihydro-5-(3,4-dichlorophenyl)-6,7-bis(hydroxymethyl)-1*H*-pyrrolizine bis-*N*-(2-propyl)carbamate, is a new compound that is active against leukaemia[3] is still undergoing testing in animals. It undergoes extensive degradation in aqueous media and methanol, but it is stable in non-hydroxylic solvents such as chloroform, dichloromethane and various ethers and esters. Moreover, it is soluble in soybean oil, and for this reason it is normally formulated as an emulsion.
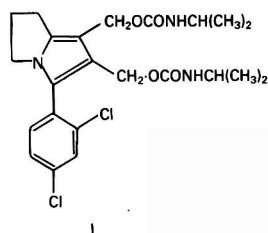
In the absence of any published method for its determination, some methods could be proposed on the basis of the groups present. Thus, a distinctly basic tertiary amino group gives a red - violet colour with citric acid in acetic anhydride.[4] A chloroform solution may give a charge-transfer complex with iodine in chloroform with an absorption maximum in the ultraviolet region.[5–7] The oxygen-flask combustion method[8] can be used to determine the chlorine content of this compound. Unsaturated pyrrolizidines containing a Δ^3-pyrroline ring have been determined spectrophotometrically after oxidation to the *N*-oxide followed by coupling with 4-dimethylaminobenzaldehyde.[9]

This paper describes a sensitive, accurate and precise high-performance liquid chromatographic (HPLC) method for the determination of the intact molecule in pharmaceutical preparations, with future promising applications to tissues and biological fluids. The method has been applied to an emulsion formulation of this compound.

---

* Present address: King Fahd Medical Research Centre, Jeddah, Saudi Arabia.

† To whom correspondence should be addressed. Present address: College of Pharmacy, King Saud University, P.O. Box 2457, Riyadh 11451, Saudi Arabia.

Experimental

The analysis was achieved with an Altex HPLC system with a radial compression separation system (Waters). The latter is a liquid chromatographic column system that uses radial compression to form a non-voiding, homogeneous chromatographic bed. It consists of two components: a Radial-Pak cartridge (Waters) containing reversed-phase C_{18} packing material, and an RCM-100 module, which is a self-contained, manually operated device that compresses the Radial-Pak cartridge. The mobile phase [acetonitrile - water (7 + 3)] was degassed prior to use and maintained at a flow-rate of 2 ml min^{-1}. Analytes were detected by ultraviolet absorption at 307 nm.

Chemicals and Reagents

Pyrrolizine isopropyl carbamate. Supplied by the National Cancer Institute (Bethesda, MD, USA).

Dimethoxy derivative of pyrrolizine isopropyl carbamate. Supplied by the Pharmaceutical Chemistry Department, Ohio State University (Columbus, OH, USA).

Intralipid-10%. Supplied by Cutter Medical Labs., Berkeley, CA, USA. It is a fat emulsion made up of 10% soybean oil, 1.2% egg yolk phospholipids, 2.25% glycerine and water for injection. It was used for preparation of the emulsion formulation of pyrrolizine isopropyl carbamate.

Solvents. All solvents were of analytical-reagent grade. Dichloromethane, acetonitrile and methanol were obtained from Omni MCB (Deerfield, IL, USA) and dimethylacetamide from Aldrich (Milwaukee, WI, USA).

Glassware

All glassware was cleaned and silanised prior to use. All reactions and extractions were carried out in 15 × 125 mm test-tubes (Pyrex 9826) with PTFE-lined screw-caps.

Procedure for the Preparation of the Emulsion Formulation

The emulsion formulation was prepared by slowly adding 100 µl of a dimethylacetamide solution of pyrrolizine isopropyl carbamate (10 mg ml^{-1}) to 9.9 ml of Intralipid-10% while stirring with a magnetic stirrer. The final concentration of the compound was 1 mg per 10 ml of emulsion.

Calibration Graph

Prepare the calibration graph by using 5, 20, 30, 50, 60, 85 and 100 µl of an acetonitrile solution of pyrrolizine isopropyl

carbamate (20 μg ml⁻¹) and 50 μl of the internal standard in acetonitrile (20 μg ml⁻¹). Evaporate the series of solutions to dryness under nitrogen, dissolve in 200 μl of acetonitrile and then inject 50 μl on to the HPLC column. Determine the ratio of the peak height of pyrrolizine isopropyl carbamate to that of the internal standard and plot it against the concentration of pyrrolizine isopropyl carbamate to obtain the calibration graph.

Procedure for the Assay of Pyrrolizine Isopropyl Carbamate in an Emulsion Formulation

Place the appropriate amount of the internal standard in a clean, dry, silanised test-tube with a PTFE-lined cap. Add a volume of the emulsion formulation containing pyrrolizine isopropyl carbamate in the range 100–2000 ng and then extract both compounds into 6 ml of dichloromethane by vortexing for 5 min. Centrifuge for 10 min, transfer 5.5 ml of the dichloromethane solution into another clean, dry test-tube and evaporate to dryness under nitrogen. Dissolve the residue into 200 μl of acetonitrile and inject 50 μl of the acetonitrile solution on to the HPLC column.

Results and Discussion

Under the conditions described, the retention times were 5 min for pyrrolizine isopropyl carbamate and 7.65 min for the internal standard, with corresponding capacity factors, k', of 4 and 6.65, respectively.

The calibration graph was constructed with seven points using a series of concentrations of pyrrolizine isopropyl carbamate. Regression analysis on the standards indicated a linear relationship between peak-height ratio (pyrrolizine isopropyl carbamate to internal standard) and concentration of pyrrolizine isopropyl carbamate. For the range 100–2000 ng, the slope (change in peak-height ratio per unit change in concentration) was $9.88 \times 10^{-4} \pm 8.92 \times 10^{-6}$ (standard deviation), $Y = 4.31 \times 10^{-4} \pm 1.06 \times 10^{-2}$ (standard deviation) (where Y is the intercept on the ordinate of the least-squares regression line, in peak-height ratio units), the correlation coefficient $r = 0.9998$ and $t(0.95) = 0.041$ (2.571), where the value in parentheses is the theoretical significant level. The value of the intercept was shown to be not significantly different from zero according to the t-test.

Recovery

The relative recoveries of pyrrolizine isopropyl carbamate from the emulsion formulation were determined at different concentrations by comparing the relative amounts recovered from each extracted emulsion sample with the linear regression obtained from the calibration graph. The results are presented in Table 1.

The over-all mean relative recovery was found to be 100.2%, which is excellent. Table 1 shows that the relative recovery depends on the amount of drug, and the reduced recovery at high levels should be allowed for.

Table 1. Precision and recovery in the determination of pyrrolizine isopropyl carbamate in an emulsion form

Amount of pyrrolizine isopropyl carbamate/ng	Mean amount recovered/ng	Precision (CV), %	Relative recovery, %
1500	1489.1	0.42	99.3
1100	1079.1	0.83	98.1
600	597.7	1.29	99.7
200	204.0	0.54	102.0
100	102.1	1.73	102.1

Precision

The precision of the method for the determination of pyrrolizine isopropyl carbamate in emulsion formulations is indicated by the coefficient of variation (CV, %) of the mean amount recovered from extracted emulsion samples repeated on five occasions (Table 1). The coefficient of variation was less than 2%, which indicates excellent precision of the method.

Analytical studies indicate that extracts from the blank Intralipid-10% that was used for preparation of the emulsion do not show peaks that interfere in the quantitative determination of pyrrolizine isopropyl carbamate. In addition, the whole assay was performed in less than 2 h. Hence the proposed technique is fast, reproducible and accurate enough for the determination of pyrrolizine isopropyl carbamate in the emulsion form.

References

1. Prous, J. R., *Editor*, "Annual Drug Data Report," Volume 4, International Publishers, Provenza, Barcelona, 1982, p. 62.
2. Anderson, W. K., New, J. S., and Corey, P. F., *Arzneim.-Forsch.*, 1980, **30**, 765.
3. Anderson, W. K., New, J. S., and Corey, P. F., *Cancer Treat. Rep.*, 1982, **66**, 91.
4. Kalnin, P., *Helv. Chim. Acta*, 1928, **11**, 977.
5. Popov, A. I., and Rugg, R. H., *J. Am. Chem. Soc.*, 1957, **79**, 4622.
6. Taha, A. M., Ahmed, A. K. S., Gomaa, C. S., and El-Fatatry, H., *J. Pharm. Sci.*, 1974, **63**, 1853.
7. Henry, S. I. T., Eric, D. G., and Anthony, S. D., *J. Pharm. Sci.*, 1977, **66**, 767.
8. "British Pharmacopoeia 1980," HM Stationery Office, London, 1980, p. A89.
9. Mattocks, A. R., *Anal. Chem.*, 1967, **39**, 443.

Iodimetric Determination of Iodine or Bromine in Organic Compounds Using a 126-Fold Amplification Method

Abdel-Fattah B. Farag, Hassan N. A. Hassan,* Abdel-Galil M. Khalil and Abdel-Aziz F. Abdel-Aziz
Department of Chemistry, Faculty of Science, Mansoura University, Mansoura, Egypt

A method is described for the iodimetric micro-determination of iodine or bromine in organic compounds based on combustion in an oxygen flask using bromine or hypochlorite as absorbents to convert the combustion products of iodine or bromine into iodate and bromate ions, respectively. An excess of potassium iodide is added to the solution and the separation of the liberated iodine is performed on a polyurethane foam column. The collected iodine is then oxidised to iodate using an excess of periodate solution. Iodate in the effluent solution is then titrated iodimetrically after masking the excess of unreacted periodate with molybdate. The method is simple, rapid and can be employed for determination at sub-microgram levels.

Keywords: *Iodine determination; bromine determination; iodimetry; oxygen-flask combustion; organic compounds*

The oxygen-flask method is well suited to the determination of various elements in a wide variety of organic compounds.[1] Indeed, probably the most attractive method for the determination of iodine and bromine in organic compounds is that based on oxygen-flask combustion followed by oxidation of the combustion products with bromine[2,3] or hypochlorite,[3-5] respectively, to produce a six-fold amplification reaction.[6]

A two-step amplification method has been described[7] for the determination of trace amounts of iodine based on the oxidation of iodine to iodate, the liberation of iodine followed by its extraction into a carbon tetrachloride solution and finally the re-oxidation to iodate after its back-extraction into sodium hydrogen sulphite solution. This method gives a 36-fold amplification. However, at least three extraction processes are required to ensure the complete transfer of iodine from aqueous solution into the carbon tetrachloride. The loss of even trace amounts of iodine during extraction will cause a serious error.

In this study a new amplification method is described for the iodimetric micro-determination of iodine and bromine in organic compounds. The method depends upon the selective separation of iodine, produced from the oxygen-flask combustion of iodine- and bromine-containing organic compounds after suitable absorption and oxidation, on a normal or pulsed polyurethane foam column.[8] The oxidation of the iodine retained on the foam column to a washable iodate ion is carried out using an excess of potassium periodate solution and the iodimetric determination of iodate in the effluent is carried out after masking the excess of unreacted periodate with molybdate.[9] This method produces a 126-fold amplification.

Experimental

Reagents and Materials

Unless otherwise specified all reagents were of analytical-reagent grade. Polyurethane foam, an open-cell type polyether of bulk density 30 kg m^{-3}, was supplied by Greiner KG (Schaumstoff-Werk-Kremsmunster, Austria). The foam material was washed and treated as previously described.[8]

Ammonium molybdate solution, 25%. Aqueous solution of the tetrahydrate [(NH$_4$)$_6$Mo$_7$O$_{24}$.4H$_2$O].

Buffer solution, pH 2.2–2.5. Prepared by mixing 80 ml of sodium acetate solution and 200 ml of glacial acetic acid.

Potassium periodate solution. Prepared by dissolving 1.75 g of the recrystallised solid reagent in 500 ml of distilled water containing 3 ml of saturated disodium tetraborate solution. This was kept in an amber bottle.

Sodium thiosulphate solutions, 0.002 *and* 0.02 M. Standardised against potassium iodate solutions.

Apparatus

Water-jacketed glass columns 15 mm in diameter and 15 cm long were used in the dynamic experiments.

The foam columns were packed with 2.0 g of dried foam cubes using the vacuum method of foam column packing described previously.[10,11]

A medical syringe of 10-ml capacity packed with 0.3 g of dried foam cubes was used as the pulsed column.[12]

Procedure

Weigh exactly 3–6 mg of the organic compound containing iodine or bromine and wrap it as usual for the oxygen-flask technique.[1] To the flask add 10 ml of saturated bromine water or 10 ml of potassium dihydrogen phosphate (10%), 4 ml of freshly prepared 0.4 N sodium hypochlorite solution and 2 ml of 2 N sodium hydroxide solution. Light the paper fuse, insert the stopper rapidly and invert the flask, holding the stopper firmly on. When the combustion is complete shake for 5 min. Open the flask and rinse down the stopper and gauze with about 10 ml of distilled water. When using bromine as the absorbent, the excess of bromine is eliminated by boiling. However, when using sodium hypochlorite, the excess is eliminated by adding 5 ml of 40 g l^{-1} oxalic acid solution. In both instances, the iodate or bromate remaining is diluted to 50 ml with distilled water and a 5-ml aliquot of this solution is allowed to react with an excess of iodide in acidic medium in order to liberate the iodine, which is then collected on a normal or pulsed foam column[8] at room temperature.

When using a normal foam column, sorption of iodine occurs at a flow-rate of 1–2 ml min^{-1}. A 15-ml volume of 1 M hydrochloric acid is then passed through the column at a flow-rate of 5 ml min^{-1} to wash out the excess of iodide. Freshly prepared potassium periodate solution (5 ml) and 5 ml of borate buffer (pH 7) are then added to the upper separating funnel of the column while its tap is closed. Water, thermostated at 80 °C, is then circulated through the external jacket of the column for about 5 min, and the periodate solution is

Table 1. Iodimetric micro-determination of iodine or bromine in organic compounds using the 126-fold amplification method

Compound	Iodine or bromine present, %	Average value of iodine or bromine found,* %	Average absolute error, %	Standard deviation, %
p-Iodobenzoic acid	51.17	51.41	+0.24	0.389
Iodoform	96.69	96.54	−0.15	0.329
3,5-Diiodo-1-tyrosine	56.28	56.40	+0.12	0.338
Phenyltrimethylammonium iodide	48.23	48.45	+0.22	0.226
7-Iodo-8-hydroxyquinoline-5-sulphonic acid ..	36.14	35.75	−0.39	0.267
p-Bromobenzoic acid	39.75	39.71	−0.04	0.216

* Results are the averages of four determinations.

allowed to pass through the foam column at a flow-rate of 1–2 ml min⁻¹. Another 5 ml of periodate - borate buffer are then passed through the column at the same flow-rate followed by 50 ml of distilled water at a flow-rate of 5 ml min⁻¹ to wash out the iodate.

The effluents and washings are collected in a conical flask and cooled with tap water. Acetate buffer (5 ml) is then added followed by 5 ml of ammonium molybdate solution in the presence of an excess of potassium iodide.

For a pulsed foam column, sorption of iodine takes place by pressing and releasing the plunger of the syringe several times while keeping its tip in the aqueous iodine solution; 10–15 pulses are usually employed. Hydrochloric acid (1 M, 15 ml) is then used to wash the column bed by employing 3–5 pulses. Oxidation of the absorbed iodine is carried out by making several pulses with the pulsed column in the periodate solution and disodium tetraborate buffer mixture (at *ca.* 80 °C). The pulsed column is then washed with 50 ml of distilled water and 5 ml of the acetate buffer solution are added. The iodate produced is then titrated as usual with a standard thiosulphate solution after masking the excess of unreacted periodate with ammonium molybdate.

Results and Discussion

Polyurethane foam, an open-cell type polyether, has proved to be very efficient for the absorption of iodine in aqueous[8] and gaseous[13] media. The presence of relatively high amounts of iodide, bromide and chloride ions in aqueous solution has no effect on the absorption of iodine.[8] Oxidation of the iodine retained on the foam column with periodate at 80 °C produces iodate, which is easily and quantitatively washed from the foam column with distilled water. This process offers a 21-fold amplification according to equation (1)[9]:

$$I_2 + 5IO_4^- + H_2O \rightarrow 7IO_3^- + 2H^+ \qquad .. \quad (1)$$
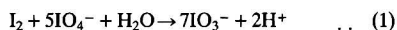
The method described for the iodimetric determination of iodine and bromine in organic compounds is based on the combustion of the organic compound by the oxygen-flask method using bromine water or hypochlorite solution as absorbents to produce iodate or bromate, respectively. Liberation of iodine occurs by the addition of an excess of iodide ion in the presence of an acid according to equation (2) or (3)[6]:

$$IO_3^- + 5I^- + 6H^+ \rightarrow 3I_2 + 3H_2O \qquad .. \quad (2)$$

$$BrO_3^- + 6I^- + 6H^+ \rightarrow 3I_2 + 3H_2O + Br^- \quad .. \quad (3)$$
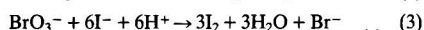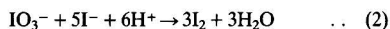
This step produces a six-fold amplification of the iodine or bromine originally present in the organic compound.

Iodine produced in this step is allowed to percolate through a normal or a pulsed foam column[8] at room temperature in order to separate it from the excess of iodide normally present in the reaction medium. Iodine retained on the foam column is then oxidised to iodate using periodate solution at pH 7 according to equation (1). This step produces a 21-fold amplification of the iodine produced in the previous step, producing, overall, a 126-fold amplification with respect to the iodine or bromine originally present in the organic compound, which is very favourable.

It is worth noting that a reasonably large amount of iodine is produced (at the milligram level) and, consequently, it is advisable to dilute the iodate or bromate solution produced in the first step to 50 ml with distilled water and subjecting only 5 ml of this solution to the foam amplification method. The foam amplification step is simple, rapid and accurate and has implications for use at submicrogram levels or for the determination of iodine and bromine in organic macromolecules that contain very low percentages of these elements. The results obtained for the analysis of a representative series of iodoorganic compounds are accurate and reproducible (Table 1). The percentages of iodine present in these compounds range between 36 and 96%.

The blank values for distilled water taken through the whole procedure using freshly prepared periodate and molybdate solutions ranged between 0.2 and 0.3 ml of 0.002 M thiosulphate solution.

In addition, analysis of *p*-bromobenzoic acid by the proposed method gave very satisfactory results for the determination of bromine (Table 1) with an average absolute error of ±0.04% and a standard deviation of 0.216%.

The proposed method can be employed for the determination of other elements and functional groups that liberate iodine during their determination.

References

1. Macdonald, A. M. G., *Analyst*, 1961, **86**, 3.
2. Belcher, R., Macdonald, A. M. G., and Nutten, A. J., *Mikrochim. Acta*, 1954, 104.
3. Schöniger, W., *Mikrochim. Acta*, 1955, 123; 1956, 869.
4. Kolthoff, I. M., and Yutzy, H., *Ind. Eng. Chem., Anal. Ed.*, 1937, **9**, 75.
5. El-Wakil, A. M., and Farag, A. B., *Fresenius Z. Anal. Chem.*, 1981, **309**, 126.
6. Belcher, R., *Talanta*, 1968, **15**, 357.
7. Gel'man, W., and Bartlingck, H., *Mikrochemie*, 1942, **30**, 217.
8. Farag, A. B., El-Wakil, A. M., Hassan, H. N. A., and Abdel-Aziz, A. F., *Indian J. Chem.*, in the press.
9. Belcher, R., Hamya, J. W., and Townshend, A., *Anal. Chim. Acta*, 1970, **49**, 570.
10. Braun, T., and Farag, A. B., *Anal. Chim. Acta*, 1972, **62**, 476.
11. Braun, T., and Farag, A. B., *Anal. Chim. Acta*, 1972, **61**, 265.
12. Braun, T., and Palagyi, S., *Anal. Chem.*, 1979, **51**, 1697.
13. Farag, A. B., Attia, M. E., and Hassan, H. N. A., *Indian J. Chem.*, 1981, **20B**, 693.

Thermogravimetric Determination of Solvents in Certain Polymeric Additives

Dhoaib Al-Sammerrai, Hazim Al-Najjar and Wejdan Selim
Petroleum Research Centre, P.O. Box 10039, Jadiriyah, Baghdad, Iraq

A thermoanalytical method is described for the determination of solvents in certain polymeric additives used as four-point depressants and flow improvers. The method is potentially useful for the rapid determination of solvents in polymeric compositions made up of components with widely differing volatiles.

Keywords: *Solvent determination; thermogravimetry; polymeric additives*

In recent years,[1] efficient pour-point depressants and flow improvers have been developed for petroleum products of various types and many of these additives are already being produced commercially. These additives are characteristically polymers of polyethylene or copolymers of ethylene with vinyl acetate,[2] which are added in concentrations between 0.01 and 1.0% by mass in order to reduce the pour-point or improve the flow properties of petroleum products.[3] These polymers are usually blended in the form of concentrates in aromatic hydrocarbon solvents or kerosene, rendering them more soluble in these products.

Common methods for determining the amount of solvent present are distillation, precipitation and various analytical techniques,[4] which are time consuming. Recently, however,[5,6] thermoanalytical methods, such as differential thermal analysis (DTA) and thermogravimetric analysis (TGA), have been used extensively for the rapid and accurate determination of different organic compositions. As these polymeric concentrates are susceptible to physical transformations such as solvent evaporation or phase separation during long periods of storage, it would be of practical and economical importance to determine their exact composition quantitatively prior to their incorporation in very small concentrations in petroleum products.

In this paper, a rapid and simple thermogravimetric (TG) technique is described for the quantitative determination of solvents in these polymeric additives.

Experimental

Thermogravimetric measurements were carried out on a Heraeus TA 500 thermal analyser.

The polymeric solutions were prepared at 60–70 °C by dissolving the appropriate polymer or copolymer in petroleum-derived kerosene (b.p. 140–275 °C) with thorough mixing to ensure homogeneity of the solution. The polymer input ranged between 25 and 50% by mass. The samples were shaken prior to TG determinations.

TG and differential thermogravimetric (DTG) curves were recorded simultaneously by placing a sample weighing 10–15 mg in a platinum crucible and heating at a rate of 50 or 20 °C min^{-1} in an atmosphere of nitrogen gas flowing at 15 cm^3 min^{-1}.

All measurements were performed in duplicate.

Results and Discussion

Fig. 1 (*a*) and (*b*) show representative TG and DTG traces obtained between room temperature and 600 °C for the polymeric solutions using heating rates of 50 and 20 °C min^{-1}, respectively. The mass losses recorded in the inert atmosphere of nitrogen gas correspond mainly to volatilisation of the polymeric composite.

At a heating rate of 50 °C min^{-1}, three major mass loss steps were identified. The first corresponds to the volatilisation of
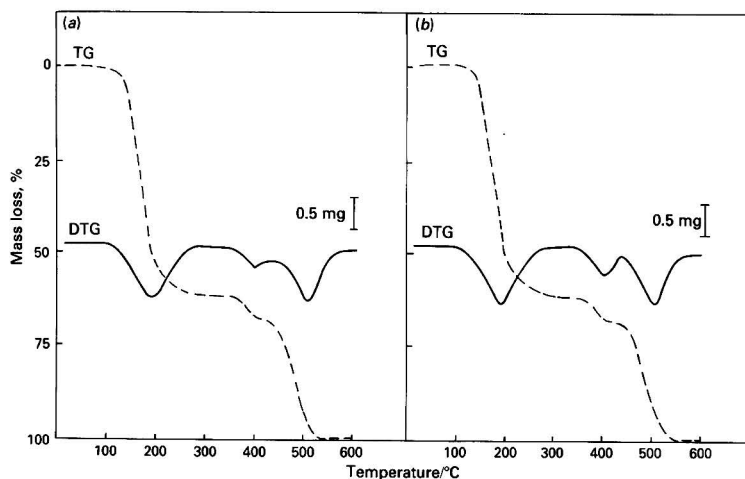
Fig. 1. Typical TG and DTG thermograms for a polymeric additive obtained at a heating rate of (*a*) 50 °C min^{-1} and (*b*) 20 °C min^{-1}

the solvent with an initial, maximum and final temperature transitions (from the DTG trace) of 135, 190 and 275 °C, respectively. The remaining two steps, which proceeded at about 80 °C higher, are related to degradative volatilisation of the polymeric constituent with initial and final transition temperatures of 350 and 560 °C, respectively. The mass losses and transition temperatures were obtained on evaluation of the thermogram when the determinations were performed at a slower heating rate of 20 °C min^{-1}; however, the doublet transition, related to degradative volatilisation, showed discontinuity at *ca.* 430 °C. No residual matters remained at the end of the temperature programmes.

Results of the duplicate measurements for the samples studied at the two different heating rates showed estimated repeatability limits of within ± 0.5%.

It should be pointed out that the present technique is applicable to compositions made up of components of widely differing volatilities. This difference in volatilities will ensure that interferences from effects such as thermal stability and molecular association are avoided.

By use of this technique, a sample can be assayed in about 15 min when choosing the faster heating rate. Further, on neglecting the transitions following the solvent volatilisation, the experimental running time can be reduced by a further 6 min.

Factors weighing heavily in favour of using thermogravimetry are shorter time, higher accuracy, smaller sample size and simplicity of the technique. Also, the thermograms obtained can be used to study other properties of polymeric compositions, *e.g.*, thermal stability.

References

1. Esso Research and Engineering, *Br. Pat.*, 1 003 314, 1965.
2. Esso Research and Engineering, *Br. Pat.*, 1 147 904, 1969.
3. British Petroleum, *Br. Pat.*, 1 197 813, 1970.
4. Finar, I. L., "Organic Chemistry," Volume I, Longman, London, 1973, Chapter 1.
5. Al-Sammerrai, D., *Analyst*, 1985, **110**, 219.
6. Slade, P. E., and Jenkins, L. T., "Thermal Characterisation Techniques," Edward Arnold, London, 1970.

COMMUNICATIONS

Determination of Ultra-trace Levels of Selenite and Selenate in Water Using High-performance Liquid Chromatography with Automated Fluorimetric Detection and an On-line Reduction System

Yasuyuki Shibata,* Masatoshi Morita and Keiichiro Fuwa
National Institute for Environmental Studies, Onogawa 16-2, Yatabe, Tsukuba, Ibaraki 305, Japan

Speciation of selenium in natural and polluted waters has been attracting much attention in recent years.[1,2] As the biological effects of selenium are known to depend on the chemical form, it is important to elucidate the amount of each selenium species in the environment. Theoretical treatment predicts selenite [Se(IV)] as the predominant state, but there are a number of observations that give somewhat contradictory reports on the various ratios of Se(IV) and Se(VI) in different types of waters.[2]

Several analytical methods have been reported for differentiation and quantification of both species. Se(IV) and Se(VI) can be separated by coprecipitation, chemical treatment or liquid chromatography, followed by detection using GC with electron capture, atomic-absorption spectrometry, ICP-AES, spectrofluorimetry and XRF. These methods, however, are intricate, time consuming or are not sensitive enough to deal with environmental samples.

In this paper we report a sensitive method for determining Se(IV) and Se(VI). The method employs ion-exchange chromatography for the separation and spectrofluorimetry for post-column detection using 2,3-diaminonaphthalene (DAN) as a derivatiser. To minimise peak broadening during the post-column derivatisation procedure, we employed an air-segmented continuous flow AutoAnalyzer system connected to the HPLC outlet. As DAN reacts with Se(IV) and not with Se(VI), we devised an on-line reduction system to reduce Se(VI) to Se(IV) and to facilitate the detection of both Se(VI) and Se(IV) in the effluent from the column.

Experimental

Apparatus

A Waters HPLC system (Model 6000A) equipped with an anion-exchange column, Nucleosil 5SB (Gasukuro Kogyo Inc., Tokyo; 4.6 × 300 mm, quaternary ammonium group), was used. The selenium detection system was constructed based on a Technicon AutoAnalyzer II combined with a Hitachi F1000 spectrofluorimeter. The excitation and emission wavelengths were 380 and 520 nm, respectively. The cell volume was 12 µl.

Reagents

DAN was purchased from Dojindo Laboratories, Kumamoto. All other reagents were of analytical-reagent grade. The Se(VI) standard solution (1000 p.p.m.) was prepared by dissolving an appropriate amount of sodium selenate (Nakarai Chemicals Ltd., Kyoto) in water, and was further diluted appropriately just before use. Se(IV) standard solution was prepared from a 1000 p.p.m. standard solution for atomic-absorption spectrometry (Kanto Chemical Co., Tokyo; selenious acid solution). Doubly distilled water, from an all-quartz glass still, was used throughout.

Procedure

Elution conditions

The optimum conditions for the separation of Se(IV) and Se(VI) were determined by HPLC with ICP-AES detection. The elution buffer selected was 0.075 M ammonium phosphate solution (pH 7.2, adjusted with ammonia solution), and the flow-rate was 1 ml min^{-1}.

AutoAnalyzer detection system

The final conditions for the determination of Se(IV) and Se(VI) are summarised in Fig. 1.

Results and Discussion

Spectrofluorimetry using DAN[3] is one of the most frequently used methods for determining selenium.[2] Brown and Watkinson[4] constructed an AutoAnalyzer system based on this process. In total selenium determination, it is necessary to convert Se(VI) into Se(IV) because Se(VI) does not give an Se - DAN complex. A hydrochloric acid concentration of 4–6 N has frequently been used for this purpose.[2] The reduction is usually performed at a high temperature (*ca.* 120 °C) for about 10 min. However, these reduction conditions appeared to be too severe for incorporation into a continuous flow system. We therefore looked for an alternative reductant for use at a lower acidity, lower temperature and with a shorter reaction time. Of the reductants tested, only HBr was as efficient as HCl. Almost quantitative reduction to Se(IV) was performed at 70 °C with 4 N HBr for 5 min, at 87 °C with 3 N HBr for 5 min and at 100 °C with 1.8 N HBr for 5 min. Because a pH

---

* To whom correspondence should be addressed.
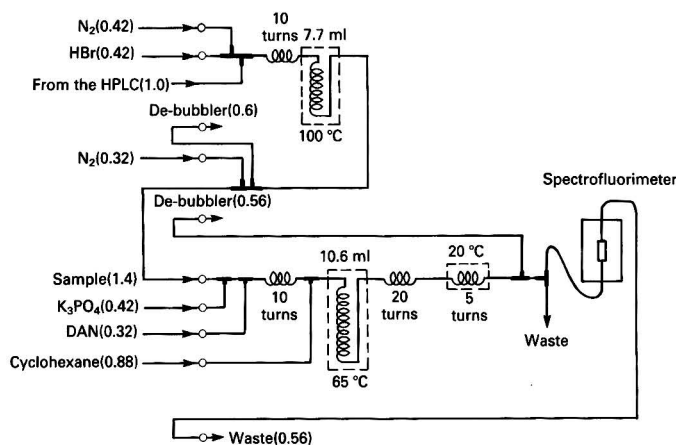
Fig. 1. Flow diagram of the AutoAnalyzer-based selenium detection system. The numbers in parentheses are the flow-rates for each line (ml min^{-1}). The concentrations of the stock solutions are: HBr, 6 N; K_3PO_4, 2 M; DAN, 0.2% m/V in 0.05 N HCl. See text for the elution conditions for HPLC
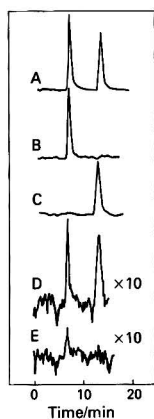
Fig. 2. Chromatograms of some solutions and a tap water. The injected samples (200 µl) are: A, mixture of Se(IV) and Se(VI), 5 µg l^{-1} of each; B, Se(IV), 5 µg l^{-1}; C, Se(VI), 5 µg l^{-1}; D, a mixture of Se(IV) and Se(VI), 0.5 µg l^{-1} of each; and E, tap water. The sensitivity of the F1000 is raised 10-fold for D and E

appropriate amounts of K_3PO_4. The final pH (pH of a sample of waste solution separated just before the spectrofluorimeter, see Fig. 1) was *ca.* 1.5 and any variation was small.

Chromatograms of solutions containing Se(IV) and/or Se(VI) are shown in Fig. 2. Se(IV) and Se(VI) are detected as separate peaks, with retention times of 6.4 and 12.8 min, respectively. The delay time by the post-column derivatisation procedure was 9.3 min.

The detection limits are good. When 200 µl of a mixed solution of Se(IV) and Se(VI) are injected, the peaks of both species can be clearly detected at a low level, 0.5 µg l^{-1} of Se (Fig. 2). Fig. 2 also demonstrates the detection of Se(IV) in tap water at the level of 0.17 µg l^{-1}; Se(VI) is not detected.

The proposed method is simple and very sensitive. The detection limits may be improved further by increasing the injection volume. A column head concentration technique[6] may also be applicable for river or lake water samples. In the spectrofluorimetric determination of selenium using DAN, some chemical species, including NO_2^-, Pd^{2+}, Sn^{4+}, Zr^{4+}, V^{5+} and W^{6+}, are known to interfere.[4,7] These interferents are removed by HPLC, hence the proposed method will give an accurate result. Attempts to establish a suitable protocol for the analysis of environmental waters are now being undertaken in this laboratory.

adjustment procedure is necessary before the reaction with DAN, a low HBr concentration was preferred. Therefore, 1.8 N HBr at 100 °C was employed and an on-line reduction system was constructed as a closed system (see Fig. 1). The reduction efficiency was finally checked by injecting equal amounts of Se(IV) and Se(VI) directly into the line, with the chromatographic column disconnected. The Se(VI) to Se(IV) peak-height ratio obtained was 0.98, and no sign of further reduction was obtained.

Coupling of Se(IV) and DAN is known to proceed efficiently at *ca.* pH 1.5.[3,5] In order to adjust the pH after reduction, we used an $H_2PO_4^-$ - H_3PO_4 buffer, by adding

References

1. Shamberger, R. J., *Sci. Total Environ.*, 1981, **17**, 59.
2. Robberecht, H., and Van Grieken, R., *Talanta*, 1982, **29**, 823.
3. Parker, C. A., and Harvey, L. G., *Analyst*, 1962, **87**, 558.
4. Brown, M. W., and Watkinson, J. H., *Anal. Chim. Acta*, 1977, **89**, 29.
5. Cukor, P., and Lott, P. F., *J. Phys. Chem.*, 1965, **69**, 3232.
6. Morita, M., and Uehiro, T., *Anal. Chem.*, 1981, **53**, 1997.
7. Lott, P. F., Cukor, P., Moriber, G., and Solga, J., *Anal. Chem.*, 1963, **35**, 1159.

Application of Gradient Flow Injection Analysis to Studies of Drug - Protein Binding

G. L. Abdullahi and James N. Miller
Department of Chemistry, Loughborough University of Technology, Loughborough, Leicestershire LE11 3TU, UK

Keywords: *Drug - protein binding; high-dispersion flow injection analysis; fluorescence probes*

Drug - protein binding interactions and other non-covalent equilibria between small molecules and proteins are of great importance in analytical chemistry, immunochemistry, pharmacology and related fields.[1] They are best investigated by measuring changes in spectroscopic or other properties that accompany the binding reaction. Such "homogeneous" methods avoid the need to separate bound and unbound drug molecules once equilibrium is established, and are thus conveniently automated. In the authors' laboratory, merging zone flow injection analysis (FIA) with fluorescence detection was applied to investigations of the protein binding of acidic and basic drugs[2,3]: the detector monitored the enhanced fluorescence of probe molecules competing with the drugs for protein binding sites. These studies used medium-dispersion FIA, the required range of drug to protein concentration ratios being obtained by separate injections of drug and protein solutions of different concentrations.

Applications of high-dispersion FIA have recently received close scrutiny.[4-6] Such methods allow the formation of large concentration gradients in the flowing system, with the possibility that a complete drug - protein binding titration, and the determination of the binding parameters (the association constant, K_A, and the number of binding sites on each protein molecule, n) might be achieved in a single rapid experiment. This paper describes the results of such experiments, and demonstrates that the approach is of wide validity.

Experimental

FIA was performed at room temperature using polyethylene tubing (0.50–1.02 mm i.d.), the flowing stream being impelled at 2 ml min^{-1} by a peristaltic pump (Ismatec). Samples (30–100 µl) were injected through a loop injection valve (Rheodyne). Mixing chambers (volumes 0.4–7.0 ml) were made of glass and contained miniature magnetic stirrer bars. The inlet was positioned in the cylindrical lower portion of each chamber, with the outlet in the domed upper portion. "Mixing chambers" with volumes below 0.6 ml were also produced using extended coils of flow tubing. The fluorescence detector was a Perkin-Elmer Model 1000 fluorescence spectrometer fitted with a glass 45-µl flow cell (1 mm i.d.) and connected to a chart recorder (Bryans Model 27000). Excitation and emission wavelengths, selected by interference filters, were 346 and 525 nm, respectively, for studies of basic drugs and 370 and 470 nm for acidic drugs.

Protein binding of acidic and basic drugs was studied in Tris - HCl buffer (pH 7.4, 0.1 M) using 1-anilinonaphthalene-8-sulphonic acid (ANS) and DL-*N*-[2-hydroxy-3-(1-naphthyloxy)propyl]-*N'*-dansylethylenediamine (DAPN), respectively, as fluorescence probes. The proteins used were albumin and α_1-acid glycoprotein, respectively. All these materials were obtained from Sigma, except for DAPN, which was purchased from Molecular Probes Inc. (Oregon, USA). All other materials were of the purest quality obtainable.

Several distinct experimental setups were used. In the first, a drug concentration gradient, produced in a mixing chamber, was subsequently merged at a Y-junction with a pre-formed protein - probe complex. Mixing of the solutions thus occurred in the tubing (<100 cm) between the junction and the detector. Secondly, in a single-channel method, the mixing chamber was equilibrated with one solution and the second solution was then injected into the chamber as a concentration step. The concentrations of both solutions thus varied simultaneously and mixing occurred throughout the FIA manifold. The third technique was a variant of the second, in which a large bolus of drug solution was injected immediately before a small mixing chamber, made of coiled tubing and containing the protein - probe complex. Mixing of the drug with the complex thus occurred at both ends of the bolus, although the trailing end phenomenon was used in this work. The association constant of each binding interaction and the number of binding sites per protein molecule were determined by combining the equations describing mixing chamber behaviour[7] with those describing ligand - protein interactions at different concentrations.[8] These calculations will be described in detail in a subsequent paper.

Results

The behaviour of the mixing chambers was entirely satisfactory: in each instance the correlation coefficient of the linear equation describing chamber behaviour exceeded 0.9996 and the apparent chamber volumes were close to their physical volumes. In the experimental conditions concentration gradients could be generated over periods ranging from 25 s for a 260-µl chamber to 300 s for a 7-ml chamber. The smaller chambers were economical in the consumption of materials, but the precision of their results was inevitably lower because of the relatively greater timing errors.

Preliminary studies using single-channel and merging methods with mixing tanks of various volumes gave K_A and n values of 1.8×10^6–2.3×10^6 l mol^{-1} and 0.80–0.90, respectively, for the albumin - ANS interaction. These values compared favourably with values of 2.1×10^6 l mol^{-1} and 0.93, respectively, obtained by static fluorimetry. The standard deviation of the FIA determinations of K_A was *ca.* 0.17×10^6 l mol^{-1}, compared with a standard deviation of 0.20×10^6 l mol^{-1} in the static method. When flufenamic acid displaced ANS from the albumin molecule, the calculations gave a K_A value of $(1.2 \pm 0.20) \times 10^6$ l mol^{-1} in a 7-ml mixing chamber used in the single-channel mode, compared with a static fluorimetry value of $(1.08 \pm 0.22) \times 10^6$ l mol^{-1}.

Application of the method to basic drug binding produced the results shown in Table 1. In every instance the results of the FIA method were in good agreement with those from static measurements, and the precision of the FIA measurements was superior overall.

Table 1. Gradient FIA—binding of ligands to α_1-acid glycoprotein. Protein concentration, 1.04 (experiment 1) and 1.25 μM; DAPN concentration (experiments 2–4), 7.5 μM; mixing chamber volume in merging FIA experiments, 260 μl

Experiment	Ligand	Method	n	$K_A/l\,mol^{-1} \times 10^{-6}$
1	DAPN	FIA	1.06	3.0 ± 0.4
		Static	1.10	2.9 ± 0.7
2	Chlorpromazine	FIA	—	0.40 ± 0.032
		Static	—	0.42 ± 0.045
3	Imipramine	FIA	—	0.12 ± 0.03
		Static	—	0.11 ± 0.03
4	Propranolol	FIA	—	0.057 ± 0.08
		Static	—	0.053 ± 0.10

Discussion

The application of gradient FIA to these examples of molecular interactions show that FIA is well suited to such studies. A complete titration curve can be obtained within a few seconds or minutes, and the results show excellent accuracy and precision. The equipment is simple to use, and the results from the fluorescence spectrometer can be output to a microcomputer to expedite the binding calculations. The latter facility will be highly desirable when there is more than one protein binding site, with two or more different affinity constants. The approach can be extended to any system in which the fluorescence properties of a ligand change on binding to a macromolecule, and can thus be applied to, *e.g.*,

fluorescence enhancement, quenching and polarisation immunoassays. Stopped flow periods could readily be introduced when the ligand binding is not rapid.[3] The gradient FIA technique thus offers a substantial advance in the study of several types of interacting biochemical systems.

References

1. Bridges, J. W., and Wilson, A. E. G., *in* Bridges, J. W., and Chasseaud, L. F., *Editors*, "Progress in Drug Metabolism," Volume 1, Wiley, London, 1976.
2. Miller, J. N., *Anal. Proc.*, 1981, **18**, 227.
3. Abdullahi, G. L., Miller, J. N., Sturley, H. N., and Bridges, J. W., *Anal. Chim. Acta*, 1983, **145**, 109.
4. Olsen, S., Růžička, J. R., and Hansen, E. H., *Anal. Chim. Acta*, 1982, **136**, 101.
5. Janata, J., and Růžička, J. R., *Anal. Chim. Acta*, 1982, **139**, 105.
6. Růžička, J. R., and Hansen, E. H., *Anal. Chim. Acta*, 1983, **145**, 1.
7. Tyson, J. F., Appleton, J. M. H., and Idris, A. B., *Anal. Chim. Acta*, 1983, **145**, 159.
8. Gutfreund, H., "Enzymes: Physical Principles," Wiley-Interscience, New York, 1972.

SOFTWARE REVIEW

From time to time, *The Analyst* will publish reviews of computer software packages designed for analytical applications. Commercial and other suppliers of such packages are invited to submit analytical software for review; full technical specifications should be included.

BALANCE

D. L. Massart, M. P. Derde, Y. Michotte and L. Kaufman. Elsevier Scientific Software. 1984. Price $150; Dfl420; £105; manual only $27.50; Dfl77; £19.25. Technical specifications:

Computer:	Apple II, II+, IIe, IIc
Language:	Applesoft Basic
Operating system:	DOS 3.3
Required peripherals:	One 140K 5¼ in diskette drive
Minimum memory:	48K RAM
Storage medium:	One 5¼ in diskette
Order Ref. No.:	ISBN 0 444 42316 8
Computer:	IBM-PC, IBM-PC AT
Language:	PC-Basic
Operating system:	PC-DOS 2.0 or higher
Required peripherals:	One 180K or 360K 5¼ in diskette drive
Minimum memory:	128K RAM
Storage medium:	One 5¼ in diskette
Order Ref. No.:	ISBN 0 444 42317 6

Textbooks on statistics, with a few notable exceptions, usually concentrate on providing the reader with the theoretical background to the subject. Examples of the application of statistical tests are often chosen to illustrate the test itself rather than the reason for selecting it. In analytical chemistry, statistical evaluation of experimental data is of great importance, but unfortunately, practical aspects of the subject are often obscured in the mathematical treatment given in textbooks. Microcomputers now provide a convenient means of data handling in the laboratory. However, whilst statistics programs are available for most microcomputers, the majority of these anticipate that the user is fully conversant with the assumptions made and the limitations of the tests employed.

BALANCE is a statistical program designed specifically for application in analytical chemistry. Versions of the program are available for Apple and IBM PC microcomputers. The program is provided on disk and is supplied with a comprehensive manual. It is intended to be used in the comparison of two series of measurements, *e.g.*, of reference and new methods of analysis. The user is guided to the appropriate statistical test

via a menu-driven program that requires a minimum of user knowledge. A range of options, including the calculation of means and standard deviations, independent and paired tests, one and two tailed tests, Students *t*- and Cochran tests, *F*-test, Wilcoxon matched-pairs signed rank test, Mann - Whitney *U*-test and a histogram display, are available to the user. The manual provides clear instructions concerning the operation of the program. Examples of all menus and screen displays generated during a run are given, allowing the user to become familiar with the format and also verify the correct operation of the program.

Data can be input via the keyboard or from disk and consist of two groups which are to be compared. Full editing of each data group is possible, allowing additions or correction of erroneous entries prior to statistical analysis, an option that in practice is most helpful. The program is also protected against the most likely erroneous user inputs on the menu options. Data are stored on a sequential file on disk, and in principle this will facilitate on-line data handling. Once the data file has been read, or all keyboard entries made, the program calculates the mean and standard deviation of each data group. Other options may then be selected as required, usually in consultation with the appropriate section of the manual that gives the relevant background to the statistical test. The size of each data group is restricted by default to 100 entries, but this can be increased if required by altering the Basic program. A full listing of the BALANCE program is supplied in an easily readable form in the manual. The actual program on disk is compressed by comparison, but it should be possible to modify or extend the package should this be desirable. The results may be displayed on the computer screen or on a printer if this is available. The display is well set out, and includes a comment as to whether a significant difference exists between the results.

It is important that programs that are intended for non-specialist users are supplied with documentation at an appropriate level. In this respect, the BALANCE manual can be highly recommended. The documentation consists of a 43-page user guide to the software, a 49-page section on statistical tests with worked examples, a selected bibliography (8 references), a program flow chart and a 21-page Basic program listing. The program and accompanying documentation have been designed to be user-friendly and the authors have succeeded in this regard with this implementation.

The program is likely to find application, within the remit of the tests provided, in routine laboratory situations in which the acquisition of a commercial package such as this is more cost-effective than in-house development.

J. Marshall

BOOK REVIEWS

Statistics for Analytical Chemistry
J. C. Miller and J. N. Miller. Pp. 202. Ellis Horwood. 1984. Price £18.50. ISBN 0 85312 662 3 (Library Edition); 0 85312 655 0 (Student Edition); 0 470 20128 2 (Halsted Press).

Twenty years ago at a staff meeting, I awoke from a dream to hear, "as an analytical chemist he knows all about statistics," and to find that responsibility for teaching the statistics course had been thus assigned. Only resignation from the University relieved me of the duty. Were that course still going, the Millers' book would be the one adopted.

The style is set in the Preface, ". . . many highly competent scientists are woefully ignorant of even the most elementary statistical methods. It is even more astonishing that analytical chemists, who practise one of the most quantitative of all sciences, are no more immune than others to this dangerous,

but entirely curable, affliction." The book is the sugar-coated pill to effect the cure.

All of the basic statistical methods that are likely to be of use to the analyst are dealt with clearly, succinctly and with the aid of a relevant example. Parametric and non-parametric methods are described and there is a chapter on experimental design, optimisation and pattern recognition to give the flavour to these more advanced methods.

This will surely be a popular book with students and a convenient refresher and reference for practising chemists. The only cavil is the brevity of the theory. The classic book of Davies, which was based on the experience of ICI, dealt with the problem by first showing how to do the calculations and then describing their rationale in an appendix. It could have been added to the general bibliography for those in search of the complete cure. Otherwise the authors' taste in statistics books is catholic, and shows a strong preference for those that are readable and useful.

D. Betteridge

Laboratory Raman Spectroscopy
Dennis P. Strommen and Kazuo Nakamoto. Pp. viii + 138. Wiley–Interscience. 1984. Price £36.20. ISBN 0 471 81323 0.

During recent years there has been a slow but steady increase in the utilisation of Raman spectroscopy, both for analytical work and in other areas. Some of those involved will have learned the craft while working in centres of excellence, but there are others, trained primarily in allied techniques such as infrared spectroscopy, who, in isolation, had to become proficient in a technique which, by common consent, requires a considerable degree of experimental skill in addition to scientific ability. This book must be judged in the context of how well it succeeds in helping such neophytes.

Unquestionably, it will provide them with ample information and advice on the principal components of a Raman spectrometer. For example, the instructions on the operation and maintenance of gas lasers are very detailed, to the point of providing an operations sequence for the preparation of the various solutions used in tunable dye lasers. Similarly, the operation of signal processing systems is considered in depth. Amid this welter of detail it is refreshing to find some cardinal general points emphasised. The authors stress that only by investing the time to align the instrument properly can quality Raman data be obtained and, noting that the wavenumber or wavelength reading on a spectrometer is not to be trusted, they recommend that the instrument be calibrated at the time any spectrum is taken. There is also a very pragmatic account of intensity calibration.

The authors' enthusiasm for detail wanes somewhat, unfortunately, on topics where it would have been of particular value. Surely, those new to the technique could have benefited from the inclusion of worked examples in the more unfamiliar areas such as the measurement of excitation profiles, depolarisation ratios and temperatures from the intensity ratio of Stokes and anti-Stokes lines. Similarly, the discussion on sampling methods could have been brought into sharper perspective by considering how best to obtain good spectra from, say, a 1 mm square green single crystal, or a pale yellow organic liquid boiling at -20 °C. Hence, to summarise, this text will prove useful but the neophyte will not be able to turn to it for answers to all of his practical problems.

The price, rather than these minor shortcomings, will surely limit the sale of this book, and in this respect the publishers have adopted a curious format that must have added to the cost. It appears to have been reproduced from a double-spaced typescript and about 20% of the pages are not completely filled. Had a more conventional layout and method of production been employed the page size, 28 × 21 cm, which many users will find inconveniently large, could have been reduced to more typical proportions.

W. F. Maddams

Microcomputers and Laboratory Instrumentation
David J. Malcolme-Lawes. Pp. x + 246. Plenum. 1984. Price $35. ISBN 0 306 41668 9.

This book is based on courses given by the author to undergraduate and postgraduate students at King's College, London. It is aimed, however, at practising scientists rather than students, and in this it succeeds. The original source material was obviously associated with practical work to be carried out in the laboratory, which has resulted in a book with a welcome practical bias that is enhanced by an ordered structure with the subject being tackled in a logical and progressive manner.

The book opens with a brief introduction to the subject, which is followed by a useful chapter on the nature of signals that places due emphasis on the need for impedance matching; it also examines the problems of noise and interference and covers the practical aspects of making connections for data acquisition and control purposes.

Two chapters on analogue and digital signal handling follow. The former provides a good survey of operational amplifiers and their applications to integration and filtering, the latter looks at the action of logic gates and the application of TTL devices to counters, timers, latches, comparators and analogue to digital interconversion.

A chapter on microcomputers starts with the usual discussion of bits and bytes, RAM and ROM, etc., followed by an explanation of high-level languages, assemblers, compilers, interpreters and operating systems—a subject that often causes much confusion to the beginner. Hardware aspects are dealt with by a discussion of peripheral equipment followed by useful information on busses and visual displays. This very readable chapter concludes with sections on bit manipulation, the use of interrupts and finally a brief review of the advantages of 16-bit processors.

A chapter that describes the basic principles of interfacing microcomputers and instruments is followed by one on standard interfaces. This is practically oriented with descriptions of connectors and pin-outs and a useful discussion of the pitfalls of interfacing.

A final chapter on system design adopts a sensible and logical approach using a case study of a liquid chromatographic system to take the reader step by step through the process of developing a complete system.

A short bibliography lists a number of fairly inexpensive books and data sources, much, however, 6502/PET based.

The book has been prepared from the author's word-processed copy, which has reproduced very well, but a few spelling errors have remained uncorrected and the use of the same size typeface for the text and the captions to diagrams sometimes causes confusion. This has been aggravated by some badly executed pagination. The book deserves a better index. In spite of these criticisms, this is a book that can be warmly recommended.

D. G. Porter

Spectroscopy of Biological Molecules. Theory and Applications—Chemistry, Physics, Biology and Medicine.
Edited by Camille Sandorfy and Theophile Theophanides. NATO ASI Series, Volume 139. D. Reidel. 1984. Price £58.50; Dfl 230; $89. ISBN 90 277 1849 0.

The book contains written versions of the papers presented at the 1983 NATO Advanced Study Institute on The Spectroscopy of Biological Molecules. The Institute focused on the structure and dynamics of DNA, proteins, visual pigments and plant pigments. There are 32 chapters with over 1000 literature references devoted to applications using a range of spectroscopic techniques including: nuclear magnetic resonance (^{13}C, ^{15}N, ^{31}P); Fourier transform infrared; resonance and surface-enhanced Raman; Raman microscopy and microprobing; and kinetic and static IR difference spectroscopy. Specific topics include: conformation and dynamics of nucleic acids and proteins; Raman and FTIR spectroscopy of drug - biological target interactions; Raman spectroscopy of biomaterials acting as bone prostheses; studies of visual pigments and related systems—rhodopsin and bacteriorhodopsin; spectroscopy of plant tetrapyrroles *in vitro* and *in vivo*; *in situ* monitoring of membrane-bound reactions by kinetic light scattering; molecular structure of the gramicidin transmembrane channel; and a review of the Fourier transform near-infrared spectrometer.

There is such a wealth of information included in the book that it is difficult to cite individual contributions for particular attention. However, the two chapters by Hadzi on "Hydrogen

bonding—theoretical and spectroscopic" and "Hydrogen bonds in biological structure and mechanism" are particularly impressive and provide an excellent, comprehensive, readable overview of the topic. On the other hand, the chapter on "Teaching the new NMR: a computer aided introduction to the density matrix formalism of multipulse sequences" seemed out of place in a book devoted to applications.

The attempt to economise by using the authors' original submissions without editing or reformatting leads to variable quality of typeface and printing of both diagrams and text. Also, the number of grammatical and typographical errors is surprising.

Despite the minor criticisms, this book will provide a useful acquisition for all entering or working in this challenging and rapidly changing field. The detailed subject and author indexes are invaluable.

In summary, the book provides an excellent overview of the "Spectroscopy of Biological Molecules," which encompasses parts of chemistry, physics, biochemistry and medicine.

D. P. Leworthy

Auger Electron Spectroscopy

Michael Thompson, Mark D. Baker, Alec Christie and Julian F. Tyson. *Chemical Analysis Series Volume 74.* Pp. viii + 394. Wiley–Interscience. 1985. Price £95. ISBN 0 471 04377 X.

Auger spectroscopy had to wait for almost 50 years from its discovery by Pierre Auger for a full appreciation of its analytical potential. As with photoelectron spectroscopy, this delay was due to a lack of commercially available equipment to measure the kinetic energies of low-energy electrons. Now a range of suitable spectrometers, thoroughly described in this book, can be purchased. All are designed to work under conditions of high vacuum as the Auger electrons that are most commonly studied have energies of a 1000 V or less. The escape depths of such electrons from solids are of the order of nanometres; Auger spectroscopy for such samples is therefore nothing if not a technique for surface analysis. This aspect of Auger spectroscopy in metallurgy and materials science is extensively and thoroughly reviewed in this book. Methods for probing the nature and thickness of surface films and coatings, of oxide layers and of surface enrichment zones are all discussed. The chemically destructive nature of ion-etching procedures for depth profiling is also frankly considered. This occupies about one third of the book and provides a comprehensive review of the uses and applications in analysis up to about 1981.

The remainder of the book is devoted to an introduction to the nature and electronic origins of the Auger effect (and in common with almost all other books fails to provide an explanation for the transition to the $KL_{2,3}L_{2,3}$ ^3P state, being forbidden other than as an enigmatic reference to parity), a useful section on instrumentation and a very long and detailed chapter on Auger electron spectra from gaseous molecules. Whilst fascinating reading for academic spectroscopists, this chapter can have little value for practising analysts.

The book is nicely produced, although Fig. 6.5 referred to on p. 277 would appear to have become lost somewhere between manuscript and final printed version (it is not Fig. 6.5 on p. 273 and it is not Fig. 6.6 either)—maybe relative intensities of LMM peaks from transition metals do not really matter. It is also unfortunate that a long time seems to have elapsed in getting into print. The latest references, and they are very few, are to 1982 publications, but for some chapters the most recent work mentioned is 6 years old. Not an up-to-date review, then, but still a useful introduction to all aspects of Auger spectroscopy.

D. S. Urch

Small Bore Liquid Chromatography Columns: Their Properties and Uses

Edited by Raymond P. W. Scott. *Chemical Analysis, Volume 72.* Pp. xiii + 271. Wiley–Interscience. 1984. Price £49.60. ISBN 0 471 80052 X.

Although HPLC is now a well established analytical technique, it is only recently that the importance of column diameter has been fully realised. The use of small or micro-bore columns, with internal diameters of typically 1–2 mm, can lead to a number of advantages when compared with the currently standard column of 4–5 mm i.d. There are, however, some difficulties associated with using these columns, not least of which is the need for specially designed instrumentation. A considerable amount of work has now been published on the preparation and use of these smaller columns and a number of instrument manufacturers are now producing the necessary equipment. The authors of this book have chosen this opportune moment to review progress in this field. They have concentrated almost exclusively on columns of 1–2 mm i.d. and the use of capillary columns with inner diameters of 100 μm or less is not covered.

The eleven chapters of this book cover both the theory and practice of smaller bore columns. The advantages and disadvantages are clearly and fairly explained and the greater importance of extra-column dispersion is emphasised. Apparatus, detectors and packing procedures are generally well dealt with. Occasionally, however, as with mass spectrometry, the treatment would have benefited from some expansion. The particularly important use of small-bore columns in high-speed separations is detailed and some practical examples are given. The latter half of the book reviews particular applications of the technique, including trace and biological analysis.

In general this book is written in a very readable style. Whilst not prolifically illustrated, those illustrations which are given are clear and concise. References are given up to 1983 and are fairly comprehensive. A particularly nice feature is the synopsis given at the end of each chapter.

In conclusion, this book is a useful addition to the library of any analyst who requires a handy and compact volume covering the use of 1–2 mm i.d. columns for HPLC.

C. R. Loscombe

Analytical Measurement and Information. Advances in the Information Theoretic Approach to Chemical Analysis

K. Eckschlager and V. Štěpánek. Pp. xii +140. 1985. Research Studies Press; distributed by Wiley. Price £25. ISBN 0 86380 021 1 (Research Studies Press); 0 471 90652 2 (Wiley).

The authors are much more reliable than the writer of the blurb, who states, "The application of information theory is a topic likely to increase in importance in the future, and this book will be of interest to analytical chemists in general . . ."

Compared with other chemometric methods, the applications of and enthusiasm for information theory in analytical chemistry have been rather minimal. It is to be regretted that this book will not do much to reverse the trend, for it is very doubtful whether the "analytical chemist in general" will manage to proceed beyond the first few pages. It assumes a familiarity with an earlier work (itself heavy going) and uses, with a minimum of definition, mathematical expressions that will be unfamiliar to many readers. The specialist will cope, but the demands made on the average reader are excessive and the rewards are meagre. Information theory may have a place in analytical chemistry, but on the evidence presented here it is a fairly minor one.

D. Betteridge

Vibrational Spectroscopy at High External Pressures. The Diamond Anvil Cell
John R. Ferraro. Pp. xiv + 264. Academic Press. 1984. Price £41.50; $59. ISBN 0 12 254160 X.

It must be said clearly at the outset, to catch the eye of the casual reader, that this book will be of value to many chemists and physicists using the term in a very broad sense, and is not simply a specialist compilation for the coterie of vibrational spectroscopists engaged in background studies using high pressures. Dr. Ferraro has written a book of considerable utility simply because, contrary to what the title might imply, the text is concerned with far more than a description of the diamond anvil cell as a convenient means for making measurements at elevated pressures. Three quarters of the book are devoted to a detailed survey of the published work of pressure on the vibrational spectra of both inorganic and organic compounds, together with a discussion of some specific technological problems where high-pressure studies are very relevant, and herein lies its wide potential value.

Following a brief introductory chapter, where the author outlines the effects of pressure on vibrational spectra, and usefully tabulates the various units of pressure that may be encountered, he moves on to instrumentation in the following chapter. Here, he gives a lucid account of the principles and construction of high-pressure cells, concentrating largely on the diamond anvil cell. This chapter, like the book as a whole, contains a very liberal ration of tables and detailed diagrams. Indeed, such is the enthusiasm of the author for these aids that the text occasionally becomes seriously out of step with them. The third and final experimental chapter concentrates on methods of pressure calibration, and it will be very useful for newcomers to the technique.

The remainder of the text is essentially a detailed and reasonably critical survey of the published work on measurements, mostly involving vibrational spectroscopy, at high pressures. However, it is more than this as it highlights areas, such as co-ordination compound chemistry, where there is ample scope for additional work. The chapter devoted to special applications should prove useful to a wide range of readers. Here, the author considers what has been done in the fields of geochemistry and geophysics, electrical conductors and lubrication studies. The first of these topics is particularly fascinating for the non-specialist, as high-pressure studies in the laboratory are shedding considerable light on the chemical nature of the compounds likely to be present in the transition zone and the lower mantle of the earth's crust.

The book concludes with a brief chapter on miscellaneous applications, where the author considers the somewhat controversial published work on the existence of metallic hydrogen, metallic xenon and superconducting copper(I) chloride at very high pressures. In the last of these there is strong evidence that disproportionation reactions occur, leading to the formation of metallic copper, and the author's final sentences, aptly, stress the dangers involved in subjecting materials to high pressures, and the need to interpret the results cautiously.

W. F. Maddams

Electrochemical Detectors. Fundamental Aspects and Analytical Applications
Edited by T. H. Ryan. Pp. vii + 172. Plenum. 1984. Price £39.50. ISBN 0 306 41727 8.

The Editor has prefaced that he has aimed at producing a text that would be valuable to analysts who use or might consider using electrochemical detectors to monitor separations performed by HPLC. To provide the fundamental aspects and applications of electrochemical detection, eleven papers presented in 1981 at the Fifth Anglo-Czech Symposium in Electrochemistry were chosen and used in compiling this book.

The first of these papers, "New Electroanalytical Techniques Applied to Medicine and Biology," details three applications of eletrochemical detection but only one of these, the identification and determination of proteins with a ring-disc electrode, involves any chromatographic separation. The other two applications are the use of membrane sensors for the measurement of CO_2, N_2O_5 and halothane, and the *in vivo* detection of catecholamines. Unfortunately, another three papers giving details of electrochemical techniques that are not compatible with solute detection in flowing solutions are also included, namely, "Tensammetry in Combination with Adsorptive Accumulation," "Applications in Immiscible Electrolyte Interfaces" and "Impedance of Small Li - CuO Primary Cells."

The remaining seven papers can be divided broadly into two categories; three cover theoretical aspects and four present applications and some background knowledge.

The theoretical papers impart a good basic knowledge of such aspects as the design of voltammetric detectors, renewable electrode surfaces and voltammetry at solid electrodes. This last topic is particularly useful as it presents electrode reactions that occur at solid electrode surfaces.

Analyses of organic acids, sterols, non-ionic surfactants, plasma catecholamines and gingerols and related compounds in ginger are given as examples of application of electrochemical detection techniques used in conjunction with HPLC.

The book is produced in camera-ready form and there are several instances where reading comes to a halt while trying to locate tables and figures, which are sometimes misplaced by up to four pages from the relevant text. The format of using papers from a meeting has resulted in a text that is disjointed, and the reader with little knowledge of the subject will experience difficulties in trying to grasp the fundamental details. With the considerable interest in electrochemical detection techniques that has developed during recent years, the experienced analyst will not find this book a particularly useful addition to the bookshelf, as most of the references are at least 4 years old. If the papers had been grouped together as the "Proceedings" of the meeting, this book would have been more acceptable as it could have been published earlier, and many of the above comments would have been irrelevant. In its current form it is difficult to recommend as it fails to meet the requirements of either the experienced or non-experienced analyst.

P. C. White

Recent Developments in the History of Chemistry

Edited by C. A. Russell

This book is intended primarily to inform chemists of recent progress in the history of chemistry. It originated from an initiative of the Historical Group of the Royal Society of Chemistry who for some considerable time had been aware of a rising surge of interest amongst chemists in the history of their subject. Yet there was also considerable frustration in obtaining reliable and up-to-date information, in understanding recent trends and in perceiving the relevance specific problems of some of the less obviously 'chemical' writing of the last few years. Those with whom the Group was in touch included chemistry teachers wishing to introduce—perhaps only occasionally—historical elements into their school curricula. Others who expressed both interest and frustration were members of university and polytechnic chemistry departments, chemists in industrial research and those who had taken early or normal retirement. These are the readers for whom this book has been published, although it is hoped that professional historians of science may also find it to be of interest and value in its general surveys of the literature.

Brief Contents:
Introduction;
Chemical Biographies;
Chemical Education and Chemical Institutions;
Chemistry to 1800;
General and Inorganic Chemistry;
Organic Chemistry;
Physical Chemistry;
Analytical Chemistry;
Biochemistry;
Instruments and Apparatus;
Industrial Chemistry;
Chemistry by Location in Western and Central Europe;
Appendix I Periodicals for the History of Chemistry;
Appendix II Some Useful Addresses; Author Index; Subject Index: People; Subject Index: Themes.
Hardcover 344pp. ISBN 0 85186 917 3
Price £27.50 ($36.00) RSC Members £12.00

FOLD HERE

THE ANALYST READER ENQUIRY SERVICE   OCT'85

For further information about any of the products featured in the advertisements in this issue, please write the appropriate number in one of the boxes below.
Postage paid if posted in the British Isles but overseas readers must affix a stamp.

PLEASE USE BLOCK CAPITALS LEAVING A SPACE BETWEEN WORDS   *Valid 12 months*

1 NAME

2 COMPANY

PLEASE GIVE YOUR BUSINESS ADDRESS IF POSSIBLE. IF NOT, PLEASE TICK HERE ☐

3 STREET

4 TOWN

5 COUNTY
  POST CODE

6 COUNTRY

7 DEPARTMENT/
  DIVISION

8 YOUR JOB TITLE/
  POSITION

9 TELEPHONE NO.

OFFICE USE ONLY   REC'D   PROC'D

FOLD HERE

Postage
will be
paid by
Licensee

Do not affix Postage Stamps if posted in Gt. Britain,
Channel Islands, N. Ireland or the Isle of Man

2

BUSINESS REPLY SERVICE
Licence No. WD 106

Reader Enquiry Service
The Analyst
The Royal Society of Chemistry
Burlington House, Piccadilly
LONDON
W1E 6WF
England

The Analyst

The Analytical Journal of The Royal Society of Chemistry

CONTENTS